



**Investigations of the Innate Immune Defences in the
Urogenital Tract**

Marcelo Lanz

Thesis submitted for the degree of Doctor of Philosophy

**Institute for Cell and Molecular Biosciences,
Newcastle University, UK
September 2013**

DECLARATION

I certify that this thesis is my own work, except where stated, and has not been previously submitted for a degree or any other qualification at this university.

**Marcelo Lanz,
September 2013**

Abstract

The urinary tract (UT) is a sterile environment despite being constantly challenged by pathogens from its surrounding environment. Protection of the uroepithelium from microbial assault involves the innate immune system, but still, to date, little is known of the actual mechanisms that function in such defences. The focus of the research presented in this thesis, which used RT4 and VK-2 E6/E7 *in vitro* cell systems to model the bladder and vaginal epithelia respectively, was to interrogate the mechanisms by which these epithelia recognise and respond to microbial assault.

The RNA of bladder RT4 cells challenged with motile and non-motile *Escherichia coli* strains was analysed via a TLR related gene array. The data supported upregulation of the NF- κ B dependent cytokine IL-8 and thus NF- κ B signalling was used to measure the uroepithelial response to microbial infection. Flagellin, recognised by TLR-5, and responsible for bacterial motility, induced a significant ($p < 0.001$), 44.9 ± 1.7 fold increase, in RT4 NF- κ B signalling within 4h of challenge and with use of TLR-5 blocking antibody was identified as the key activating PAMP in the UT. Other bacterial cell wall components, namely LPS and peptidoglycan, failed to induce comparable NF- κ B activation (maximum 10.7 ± 0.8 and 6.3 ± 0.6 fold increase at 16 hours post challenge).

These data led to the hypothesis that strains associated with urinary tract infection (UTI) have reduced or no motility. However, 12/24 clinical strains associated with UTI were motile and induced a NF- κ B signalling response. Variability in the responses (3.4 ± 0.3 to 40.3 ± 1.8 fold at 8 hours post challenge), could not be explained by flagellin, suggesting that other factors, host and bacterial, may also contribute to the intensity of the response. Analysing UPEC strains isolated from the urine of patients carrying a C1174T SNP encoding a truncated TLR-5 revealed such strains to induce normal NF- κ B signalling (39.5 ± 0.3 fold) in RT4 cells. These data emphasised the importance of TLR-5 and bacterial motility in the innate response of the host to a UTI.

Human (h) β D-2, a member of the Defensin family with microbial killing properties, is important in the innate defences of the uroepithelium. To identify agents that could be used therapeutically to enhance the innate defences of the UT, a reporter construct (ph β D-2-Luc), containing 2 kbp of h β D-2 5'UTR sequence, was transfected into RT4 and VK-2 E6/E7 vaginal cells. Reporter activity (fold increase) was significantly increased with calcitriol (VitD, 10 nM), or 17 β -oestradiol (17 β -oes, 4 nM), treatments when challenging VK-2 E6/E7 with either flagellin (68.1 ± 8.5 vs. 196.3 ± 28.3 for VitD, $p < 0.001$, or vs. 199.5 ± 37.7 for 17 β -oes, $p < 0.01$) or *E. coli* NCTC 10418 (19.9 ± 3.8 vs. 40.1 ± 4.3 for VitD, $p < 0.01$) or vs. 40.2 ± 6.6 for 17 β -oes, $p < 0.05$). The h β D-2 reporter data also revealed Zymosan (50 μ g/ml) enhancing reporter activity in both cell lines (RT4 34.8 ± 5.0 and VK-2 E6/E7 27.2 ± 2.9 , both $p < 0.001$) and had a synergistic effect to flagellin increasing reporter activity by more than 60 % ($p < 0.05$). These data suggested that Zymosan, vitamin D as well as oestrogen regulate the h β D-2 gene.

The expression of h β D-3, another member of the Defensin family with microbial killing properties, was identified in human bladder biopsies so its expression was further investigated *in vitro*. While no h β D-3 expression was measured in the RT4 cells, constitutive and inducible expression was identified in VK-2 E6/E7 cells. Human β D-3 expression was enhanced at 8 hours following challenge of the cells (PBS 70.5 ± 13.4) with *E. coli* NCTC 10418 (1094.5 ± 293.8 , $p < 0.001$), flagellin (518 ± 139.2 , $p < 0.01$) and Zymosan (280.8 ± 65.7 , $p < 0.01$). Induction was also observed with LPS but at 16 hours (27.0 ± 8.1 (PBS), 612.2 ± 260.8 , $p < 0.001$) but not with peptidoglycan (32.2 ± 12.3 , $p > 0.05$). These data suggested that h β D-3 functions in the defence of urogenital tract and as its expression was inducible, a potential target for therapeutic strategies.

The fungal cell wall β 1,3-glucan, Zymosan, induced NF- κ B signalling as well as h β D-2 in the RT4 and VK-2 E6/E7 cells, and h β D-3 expression and secretion in VK-2 E6/E7 cells. Molecular analysis of the cell RNA identified the expression of three isoforms (417, 330, 211 bp) of the Dectin-1 (CLEC7A) receptor and immunocytochemistry identified the receptor protein localised to the cell membrane. Following Zymosan challenge of VK-2 E6/E7 cells, receptor clustering and the phosphorylation of a Dectin-1 signalling protein, SYK was observed supporting the presence of functional receptors. Induction of NF- κ B signalling by Zymosan was inhibited by blocking TLR-5 (4.2 ± 0.4 vs 2.8 ± 0.1 , $p < 0.01$) suggesting functional interactions between Dectin-1 and TLR-5. These data provide support for the presence of Dectin-1 receptor in the urogenital tract.

In conclusion, the data presented in this thesis confirms the importance of TLR-5 in the defence of the urogenital tissues. Investigations of h β D-2 and h β D-3 expression and their enhancement in the UT have led to the discovery of a role for the Dectin-1 receptor. This receptor represents a target for future therapeutic strategies to enhance the innate response.

For my Wife and Family, who gave without asking during my journey...

Acknowledgements

Firstly, I would like to thank my excellent supervisors, *Dr Judith Hall* and *Prof. Robert Pickard* for their enormous help, great advice, patience, guidance and support throughout this project. I would like to acknowledge the *Dr William Edmund Harker Foundation*, for giving me the opportunity to have this incredible and exciting experience. Additionally, I would also like to thank the members of the research group, *Dr Ased Ali*, who more than a co-worker became a friend and a companion in our journey through the realms of the urinary tract infections. *Dr Claire Townes*, for the invaluable help during my first steps in the laboratory and introducing me to the *champion mackem* dialect as well as my colleagues *Ms Anna Stanton*, *Sherko Subhat*, *Kevin Cadwell* and *Dr Catherine Mowbray* for carrying on this research with enthusiasm and passion. My sincere gratitude goes to *Dr Phillip Aldridge* and his amazing team for helping me with my bacterial experiments and for their vast knowledge about the world of motile bacteria. Special thanks go to the *Epithelia Research Group* (*pseudo* and *real* science) for their, not always, scientific advice, stimulating discussion in the coffee room and for introducing me to the British way of life. In particular, my endless thanks go to *Mr Git Chung*, for his immeasurable help and incomparable friendship.

For their love and support, I give my special thanks to my parents, *Helza & Ralf* and *Ricarda & Wilfried*, my sister, *Daniela*, and my godson, *Gabriel*, for understanding my need for this long expedition away from you.

Above all, I want to express my gratitude to my wife, *Larissa Ledig-Lanz*, for her support, understanding, encouragement and unconditional love and for giving me *meinen kleinen Mann*, *George*.

Abbreviations

5'UTR	5 prime untranslated region
A.U.	Arbitrary units
ABU	Asymptomatic bacteriuria
AP-1	Activator protein 1
APC	Antigen presenting cells
B-cells	Bone marrow derived cells
BCR	Bone marrow cell receptor
BLAST	Basic Local Alignment Search Tool
bp	Base pair
BSA	Bovine serum albumin
C3a	Complement component 3a
C3b	Complement component 3b
C5a	Complement component 5a
C3H/HeJ	Mouse strain
CAMP	Cationic antimicrobial peptides
CCL	Chemokine (C-C motif) ligand
CCR	C-C motif receptor
CD-4/CD-8	Cluster of differentiation-4 or 8
cDNA	Complementary DNA
CFT 073	UPEC isolated from a patient suffering pyelonephritis
CFU/ml	Colony forming units per milli litre
CLEC7A	C-type lectin 7a (Dectin-1)
CLR	C-type lectin receptors
CMV	Cytomegalo virus promoter
cmv-luc	CMV attached to the firefly luciferase gene
CpG-DNA	Cytosine connected to a guanine through phosphodiester link
C _q	Quantitation cycle used to quantitate gene expression
CRD	Carbohydrate recognition domain
CXCL	Chemokine (C-X-C motif) ligand
DEFB 4	hβD-2 gene
DH5α	<i>E. coli</i> strain used for transformation
DMSO	Dimethyl sulfoxide
DNA	Deoxyribonucleic acid
DNase	Enzyme used to digest genomic DNA

dNTPs	Deoxyribonucleotide
dsRNA	Double stranded RNA
<i>E. coli</i>	<i>Escherichia coli</i>
EAU	European Association of Urology
EcoRI	restriction enzyme isolated from <i>E. coli</i>
ECV	Bladder uroepithelium cell line derived from T24
EDTA	Ethylenediaminetetraacetic acid
EGFR	Epithelial growth factor receptor
ELISA	Enzyme-Linked Immunosorbent Assay
ER- α	Oestrogen receptor alpha
FCS	Fetal calf serum
FimA	Fimbriae A
FimH	Fimbriae H
FliC	Structural unit of Flagellum. Recognised by TLR-5
GFP	Green fluorescent protein
H&E	Hematoxylin and eosin
hCAP-18	Propeptide of cathelicidin
HD-5	Human α -Defensin 5
HEPES	<i>4-(2-hydroxyethyl)-1-piperazineethanesulfonic acid</i>
HindIII	Restriction enzyme isolated from <i>Haemophilus influenzae</i>
HLA	Human Leukocyte Antigen
HRP	Horseradish peroxidase
h β D	Human β -Defensin
IBC	Intracellular bacterial colonies
ICaMB	Institute of Cell and Molecular Biology
iE-DAP	D-glutamyl-meso-diaminopimelic acid
IFN- γ	Interferon gamma
IgG	Immunoglobulin G
I κ B	Inhibitor of kappa light polypeptide gene enhancer in B-cells
IL	Interleukin
IPTG	Isopropyl β -D-1-thiogalactopyranoside
IRAK	Interleukin-1 receptor-associated kinase
IroN	Iron transporter found in <i>E. coli</i>
K-12	Laboratory <i>E. coli</i> strain
kbp	1000 base pairs
kDa	1000 Dalton

KOD	<i>Thermococcus kodakaraensis</i>
KpnI	Restriction enzyme isolated from <i>Klebsiella pneumoniae</i>
LB-Agar	Lysogenic Broth supplemented with agar
LB-Agar-XGal	Lysogenic Broth supplemented with agar and X-Gal
LB-media	Lysogenic Broth
LL-37	Cathelicidin (mature peptide)
LPS	Lipopolysaccharide
LY86	Lymphocyte antigen 86
MAPk	Mitogen-activated protein kinases
MD2	Myeloid differentiation factor-2
MDA-MB 231	Breast cancer cell line
MDP	Muramyl dipeptide
MHC	Major histocompatibility complex
MIQE	Minimum information for publication of quantitative real-time PCR experiments.
MPBST	5 % non-fat dry milk dissolved in PBS containing 0.1 % Tween 20
MRes	Master of Research
mRNA	Messenger RNA
MuLV-RT	Reverse transcriptase isolated from the murine leukemia virus
MyD88	Myeloid differentiation primary response gene 88
NCTC 10418	Laboratory motile E. coli strain
NF-kB	Nuclear factor kappa B
NK-cells	Natural killer cells
NLR	NOD like receptor
NOD	Nucleotide-binding oligomerisation domain
NU14	UPEC isolated from a patient suffering cystitis
OD ₆₀₀	Optical density measured at 600 nm
Opti-MEM	Medium used for transfection
p	Probability
PAMP	Pathogen associated molecular patterns
PapG	P pilus adhesion G
PASivE	Pathogen-specific, antigenic, surface-exposed, and <i>in vivo</i> expressed
PBS	Phosphate buffer saline
PBSE	Phosphate buffer saline supplemented with EDTA
PBS-PSA	Phosphate buffer saline supplemented with Penicillin-Streptomycin-Amphotericin B

PCR	Polymerase chain reaction
PFA	Paraformaldehyde
PG	Peptidoglycan
pGLOW TOPO	Reporter vector containing GFP
ph β D-2-GFP	h β D-2 reporter gene construct using GFP
ph β D-2-Luc	h β D-2 reporter gene construct using luciferase
PI	Propidium Iodide
PK2 E6/E7	Immortalised postmenopausal vaginal epithelium cell line
PMN	Polymorphonuclear leukocytes
PROMO software	Transcription factor binding site software
PRR	Pattern recognition receptors
PSI	Pounds per square inch (measuring pressure)
qPCR	Quantitative real time PCR
RAR	Retinoic acid receptor
REC	Research Ethics Committee
RefSeq	Reference sequence (collection of nucleotidesequences (DNA, RNA) and their protein products)
RIG	Retinoic acid inducible gene
RIN	RNA integrity number
RIPA-Buffer	Radioimmunoprecipitation assay buffer
RLB	Reporter lysis buffer
RLR	RIG like receptor
RNA	Ribonucleic acid
RNase	Enzyme used to digest RNA
RPMI	Roswell Park Memorial Institute
rRNA	Ribosomal RNA
RT4	Bladder uroepithelium cell line
RT-qPCR	Reverse transcriptated quantitative real time PCR
rUTIs	Recurrent urinary tract infection
SAHRP	Streptavidin-labelled horseradish peroxidase
SDS	Sodium dodecyl sulphate
SDS-gel	Sodium dodecyl sulphate containing gel for protein separation
SNP	Single-nucleotide polymorphism
ssRNA	Single stranded RNA
SYK	Spleen tyrosine kinase
T24	Bladder carcinoma uroepithelium cell line

TAB1-3	TGF-beta-activated kinase 1-3
TAK1	TGF-beta-activated kinase 1
<i>Taq</i>	<i>Thermus aquaticus</i>
T-cells	Thymus cells
TcpC	TIR-domain containing protein of <i>E. coli</i>
TCR	Thymus cell receptor
TEMED	Tetramethylethylenediamine
TERT-NHUC	Telomerase-immortalized normal human urothelial cell line
TF	Transcription factor
TGF- β	Transforming growth factor beta
T _H -cells	T-helper cell
THP	Tamm-Horsfall protein
TIR	toll-interleukin 1 receptor
TIRAP	toll-interleukin 1 receptor (TIR) domain containing adaptor protein
TLR	Toll-like receptor
TMB	3,3',5,5'-Tetramethylbenzidine
TNF- α	Tumour necrosis factor alpha
TRAF	TNF receptor associated factor
UP	Uroplakin
UPEC	Uropathogenic <i>Escherichia coli</i>
UT	Urinary Tract
UTI	Urinary Tract Infection
VDR	Vitamin D receptor
VK-2 E6/E7	Immortalised vaginal epithelium cell line

Contents

ABSTRACT	I
ACKNOWLEDGEMENTS	III
ABBREVIATIONS	IV
CONTENTS	IX
LIST OF FIGURES	XIV
LIST OF TABLES	XVII
1. INTRODUCTION	1
1.1. INFECTIONS OF THE UROGENITAL TRACT	2
1. Types of Urinary Tract Infections.....	2
2. Risks associated with UTI.....	3
3. Routes of infection	4
1.2. UTI ASSOCIATED PATHOGENS	6
1.3. UROPATHOGENIC <i>ESCHERICHIA COLI</i> (UPEC)	7
1. Virulence factors ASSOCIATED WITH Uropathogenic <i>Escherichia coli</i>	7
1.4. IMMUNE MECHANISMS ACTIVE IN THE UROGENITAL TRACT DURING INFECTION	10
1. Adaptive immune system in UTI.....	10
2. The innate immune system	11
1.5. THE ROLE OF THE UROGENITAL EPITHELIA DURING UTIS	13
1.6. PATTERN RECOGNITION RECEPTORS IN THE UROEPITHELIUM	14
1. Toll-like Receptors in the uroepithelium	16
2. Signalling cascade of Cell Surface TLRs	19
3. Proteins associated with TLR induced Immune Responses	21
I. Cathelicidins	21
II. Defensins	21
III. Human Beta Defensins (h β D)	22
IV. Interleukin 8 (IL-8)	24
V. Other innate factors.....	25
1.7. PATHWAYS FOR THERAPEUTIC INTERVENTION	25
1.8. BACKGROUND TO RESEARCH	28
1.9. HYPOTHESIS	29
1.10. AIMS AND OBJECTIVES	29
2. MATERIALS AND METHODS	30
2.1. CHEMICALS AND REAGENTS	31
2.2. TISSUE CULTURE	31

1. RT4 Bladder epithelium.....	31
2. VK-2 E6/E7 vaginal epithelium.....	31
3. Primary human vaginal epithelium	32
4. Ethical approval.....	32
2.3. BACTERIAL CULTURE	33
2.4. TRIZOL RNA ISOLATION.....	33
2.5. POLYMERASE CHAIN REACTION.....	34
1. DNase treatment	34
2. Reverse Transcription	34
3. POLYmerase Chain Reaction.....	35
4. Primers	35
5. <i>Taq</i> Polymerase	37
6. KOD-Polymerase	37
7. Quantitative PCR	38
8. Cloning of calibrator plasmid.....	39
2.6. SABIOSCIENCES TLR-PLATE ASSAY	39
1. RT4 challenge, RNA isolation and DNase Treatment	39
2. Agilent RNA Control assay	40
3. RT-qPCR.....	41
2.7. PCR AND PLASMID PURIFICATION.....	42
2.8. PROTEIN CONCENTRATION DETERMINATION	42
2.9. PROTEIN ANALYSIS USING SDS-PAGE.....	43
1. 10 % Tricine-gels.....	43
2. 4 %-12 % NOVEX NuPAGE®	43
2.10. FLAGELLIN PURIFICATION	44
2.11. EUKARYOTE CELL TRANSFECTION	45
1. Attractene.....	45
2. TurboFect.....	45
2.12. PROMOTER REPORTER CONSTRUCT	46
1. Bioinformatics.....	46
2. Cloning using pGLOW TOPO vector.....	46
3. Cloning using pGL4.10.....	47
2.13. REPORTER GENE ASSAY	47
1. Luciferase based reporter	48
2. Green fluorescent protein based reporter	48
2.14. HUMAN UROGENITAL EPITHELIA CHALLENGE EXPERIMENTS....	49
1. Escherichia coli strains.....	49
2. PAMPs.....	50
3. Blocking of TLR using monoclonal antibody	51
4. Motility determination of <i>E. coli</i> strains.....	51

2.15. PROTEIN IDENTIFICATION USING WESTERN BLOTTING	51
2.16. ELISA.....	53
1. Indirect ELISA	54
2. Sandwich ELISA.....	55
3. Interleukin-8.....	56
2.17. FLOW CYTOMETRY	57
2.18. IMMUNOCYTOCHEMISTRY AND CONFOCAL MICROSCOPY	57
1. Preparation of Mowiol	59
2. investigating Specificity of Mab 1859.....	59
2.19. BIOINFORMATICS.....	60
1. PROMO Transcription binding factor search tool.....	60
3. UROEPITHELIAL INNATE IMMUNE RESPONSES TO UROPATHOGENIC <i>ESCHERICHIA COLI</i>	61
3.1. INTRODUCTION.....	62
3.2. EARLY INNATE IMMUNE RESPONSE TO <i>E. COLI</i> LABORATORY STRAINS	63
1. RNA Quality Control	63
2. TLR-related Gene Array	65
3.3. NF-KB ACTIVATION BY LABORATORY <i>E. COLI</i> STRAINS.....	68
3.4. DETERMINATION OF MOTILITY OF THE LABORATORY STRAINS ..	71
3.5. FLAGELLIN ISOLATION FROM <i>E. COLI</i> NCTC 10418.....	72
3.6. INNATE IMMUNE RESPONSE OF THE URO-EPITHELIUM TO COMPONENTS OF THE BACTERIAL CELL WALL	74
1. Flagellin	74
2. Inhibition of NF- κ B activation by TLR-5 blocking	78
3. Lipopolysaccharides	80
4. Peptidoglycan	83
3.7. NF-KB AND IL-8 RESPONSE TO CLINICAL ISOLATES.	85
1. Determining the motility of clinical isolates of UPEC strains.....	85
2. Innate immune response of the uro-epithelium to clinical isolates of UPEC.....	86
3. Innate immune response to flagellin isolated from clinical strains	89
3.8. INNATE IMMUNE RESPONSE TO CLINICAL STRAINS ISOLATED OF PATIENTS CARRYING TLR-5(C1174T) SNP	90
1. Innate Immune Response of RT4-NF- κ B to bacteria isolated from Urine of TLR-5(C1174T) carriers	91
2. Inhibition of innate immune response by TLR-5 blocking	92
3. IL-8 response in Urine of Patients with a Urinary Tract Infection	93
3.9. DISCUSSION	95

4. HUMAN B-DEFENSIN 2 REPORTER.....	100
4.1. INTRODUCTION.....	101
4.2. TRANSCRIPTION FACTOR BINDING SITES IN THE 5' UTR OF HBD-2	102
4.3. CONSTRUCTION OF REPORTER PLASMID USING GFP REPORTER	105
1. Transfection optimisation of RT4 and VK-2 E6/E7 cells	108
4.4. VALIDATION OF PHBD2-GFP REPORTER GENE	110
4.5. CONSTRUCTION OF REPORTER PLASMID USING LUCIFERASE REPORTER VECTOR	113
4.6. CHALLENGING RT4 CELLS TRANSFECTED WITH PHBD-2-LUC	116
4.7. INVESTIGATING THE PHBD-2-LUC REPORTER RESPONSE OF RT4 CELLS USING THE MOTILE NCTC 10418 AND BACTERIAL COMPONENTS	117
4.8. ENHANCING PHBD-2-LUC REPORTER RESPONSE USING IMMUNOMODULATORY TREATMENT IN RT4 CELLS	118
1. Zymosan Enhances ph β D-2-Luc reporter activity.....	118
2. Further enhancement of h β D-2 reporter activity using Calcitriol	119
3. Cytotoxic effect of oestrogen or resveratrol treatment on RT4 cells.....	121
4.9. INVESTIGATING PHBD-2-LUC REPORTER RESPONSE IN VK-2 E6/E7 VAGINAL EPITHELIUM.....	122
1. Zymosan Enhances of ph β D-2-Luc Reporter response in VK-2 E6/E7	123
2. Further Enhancement of ph β D-2-Luc response upon calcitriol treatment	124
3. Enhancement of ph β D-2-Luc Reporter Response through Oestrogen Treatment	126
4. Resveratrol has an ambivalent effect on the ph β D-2-Luc activity	127
4.10. COMPARISON OF THE PHBD-2-LUC REPORTER ACTIVITY WITH THE HBD-2 PROTEIN SECRETION USING AN ELISA	128
4.11. DISCUSSION	130
5. INVESTIGATING HUMAN B-DEFENSIN 3 IN THE UROGENITAL TRACT	137
5.1. INTRODUCTION.....	138
5.2. DETECTION OF HBD-3 EXPRESSION IN THE UROGENITAL TRACT	138
5.3. DEVELOPMENT OF HBD-3 ASSAYS.....	140
1. Quantitative Gene expression measurements using a PCR assay	140
I. Engineering a h β D-3 Calibrator Plasmid	140
II. Establishing a Working Standard Curve	142
2. Development of a h β D-3 ELISA	147
I. Indirect ELISA specific for h β D-3.....	147
II. Development of a sandwich ELISA specific for h β D-3	148
5.4. RT4 HBD-3 RESPONSE TO <i>E. COLI</i> CHALLENGE.....	150

5.5. VK-2 E6/E7 HBD-3 RESPONSE TO <i>E. COLI</i> CHALLENGE	154
5.6.....HBD-3 REGULATION IN VK-2 E6/E7 CHALLENGED WITH COMPOUNDS OF THE BACTERIAL CELL WALL.....	159
1. Flagellin	159
2. Lipopolysaccharides (LPS)	161
3. Peptidoglycan	163
5.7. ALTERNATIVE ACTIVATION OF HBD-3 USING FUNGAL CELL WALL COMPONENT ZYMOSAN.....	165
5.8. DISCUSSION	167
6. THE DECTIN-1 RECEPTOR IN THE UROGENITAL TRACT	171
6.1. INTRODUCTION.....	172
6.2. THE NF-KB RESPONSE TO FUNGAL ZYMOSAN.....	173
1. Zymosan induces NF-κB activation in RT4 and VK-2 E6/E7.....	173
2. Zymosan induces IL-8 secretion in RT4 and VK-2 E6/E7	175
6.3.....INVESTIGATING THE ROLE OF TLR-2 IN THE RECOG-NITION OF ZYMOSAN	176
6.4. DETECTION OF MULTIPLE ISOFORMS OF DECTIN-1 IN RT4 AND VK-2 E6/E7	177
6.5. DECTIN-1 DETECTION USING FLOW CYTOMETRY.....	181
6.6. DETECTION OF DECTIN-1 IN UROGENITAL CELL LINES USING IMMUNOCYTOCHEMISTRY	185
6.7. LOCALISATION OF DECTIN-1 USING CONFOCAL MICROSCOPY	186
6.8. ACTIVATION OF THE DECTIN-1 RECEPTOR IN VAGINAL EPITHELIA	188
6.9. PHOSPHORYLATION OF SYK ADAPTOR PROTEIN.....	190
6.10. DECTIN-1 IN PRIMARY VAGINAL EPITHELIA.....	191
6.11. DECTIN-1 ACTIVITY IN THE ABSENCE OF TLR-5.....	194
6.12. COLOCALISATION OF TLR-5 AND DECTIN-1 USING IMMUNOCYTOCHEMISTRY	195
6.13. DISCUSSION	197
7. FINAL DISCUSSION.....	202
7.1. LIMITATIONS OF THE INVESTIGATION	203
7.2.FUTURE WORK	204
REFERENCES	210
APPENDIX.....	I
A.1. PUBLISHED ABSTRACTS	I
A.2. PRESENTATIONS	II

List of Figures

	Page
Figure 1.1 Routes of infection in the Urinary Tract.	5
Figure 1.2 Uropathogenic <i>Escherichia coli</i> with its virulence factor.	7
Figure 1.3 Uroepithelium and asymmetric unit membrane	13
Figure 1.4 Extracellular TLRs and their ligands	17
Figure 1.5 MyD88- dependent TLR-signalling	20
Figure 2.1 Principle of an Enzyme-Linked ImmunoSorbent Assay(ELISA)	53
Figure 3.1 Analysis of RNA quality using Agilent RNA 6000 Nano kit	64
Figure 3.2 NF- κ B Response of RT-4 to different laboratory <i>E. coli</i> strains	70
Figure 3.3 Assessing <i>E. coli</i> 's motility using a soft agar assay.	71
Figure 3.4 Isolation of flagellin from NCTC 10418	73
Figure 3.5 NF- κ B and IL-8 response of RT4 uroepithelium to Flagellin isolated from <i>E. coli</i> .	75
Figure 3.6 NF- κ B and IL-8 response of RT4 to different concentrations of flagellin	77
Figure 3.7 Inhibition of innate response to flagellin through TLR-5 blocking in RT4 cells.	79
Figure 3.8 Innate immune response of RT4 cells to three different types of <i>E. coli</i> 's LPS.	82
Figure 3.9 Expression of TLR6 in RT4.	83
Figure 3.10 Innate immune response of RT4 cells to 10 μ g/ml of <i>E. coli</i> 's peptidoglycan.	84
Figure 3.11 Motility of the clinical UPEC Strains.	86
Figure 3.12 Innate Immune Response of RT4 to clinical UPEC isolates	88
Figure 3.13 Isolation of flagellin from clinical isolates and NF- κ B response of RT4 cells to purified flagellin	90
Figure 3.14 NF- κ B response of RT4 cells to bacteria isolated from Patients carrying TLR-C1174T.	92
Figure 3.15 Inhibition of innate immune response to SNP-Bacteria by blocking TLR-5	93
Figure 3.16 Measurement of IL-8 concentration in Urine from patients suffering a UTI.	94
Figure 4.1 Transcription factor binding site search using the Bioinformatics software PROMO.	103
Figure 4.2 Amplification of a 2030 bp region 5'UTR of the DEFB4 gene.	105
Figure 4.3 Engineering ph β D-2-GFP Reporter.	106
Figure 4.4 Confirmation of engineered ph β D-2-GFP Reporter by sequencing and alignment.	107
Figure 4.5 Optimisation of transfection using CMV-Luciferase reporter plasmid	109

Figure 4.6	Validation of ph β D-2-GFP using fluorescent microscopy	111
Figure 4.7	ph β D-2-GFP reporter activity in challenged RT4 cells.	112
Figure 4.8	ph β D-2-GFP reporter activities in challenged RT4 cells maintained in PBS.	113
Figure 4.9	Engineering of the ph β D-2-Luc reporter.	114
Figure 4.10	Confirmation of engineered ph β D-2-Luc reporter by sequencing and alignment	115
Figure 4.11	Validating ph β D-2-Luc reporter activity in RT4.	116
Figure 4.12	ph β D-2-Luc response to <i>E. coli</i> strain NCTC 10418 or bacterial PAMPs.	117
Figure 4.13	Enhancing h β D-2 Response from RT4 cells to Flagellin using Zymosan	119
Figure 4.14	ph β D-2-Luc Response enhancement in RT4 cells by the presence of calcitriol	120
Figure 4.15	Cytotoxic effect of 17 β -oestradiol..	121
Figure 4.16	ph β D-2-Luc response in VK-2 E6/E7 challenged with <i>E. coli</i> NCTC 10418 or bacterial PAMPs.	123
Figure 4.17	Enhancing the h β D-2 response in VK-2 E6/E7 to flagellin with Zymosan	124
Figure 4.18	h β D-2 response enhancement in VK-2 E6/E7 to <i>E. coli</i> NCTC 10418 and PAMPs after calcitriol treatment.	125
Figure 4.19	Enhancing the h β D-2 response in VK-2 E6/E7 to flagellin using 17 β -oestradiol.	126
Figure 4.20	h β D-2 response in VK-2 E6/E7 to <i>E. coli</i> NCTC 10418 and PAMPs after resveratrol treatment.	127
Figure 4.21	Enhancement of h β D-2 peptide secretion in VK-2 E6/E7	129
Figure 5.1	Detection of h β D-3 expression in VK-2 E6/E7 vagina and RT4 bladder epithelium.	139
Figure 5.2	Engineering a pGem-T-easy plasmid containing part of the h β D-3 gene.	141
Figure 5.3	First trial for a standard curve determination.	143
Figure 5.4	Second trial for a standard curve determination.	145
Figure 5.5	Determination of an h β D-3 peptide standard curve using indirect ELISA.	147
Figure 5.6	Determination of a h β D-3 peptide specific standard curve using a sandwich ELISA.	149
Figure 5.7	Expression of h β D-3 in RT4 challenged with <i>E. coli</i> strains.	151
Figure 5.8	Expression of h β D-3 in RT4 cells challenged with flagellin.	153
Figure 5.9	Expression of h β D-3 in VK-2 E6/E7 challenged with <i>E. coli</i> strains.	155
Figure 5.10	h β D-3 secretion of VK-2 E6/E7 upon challenge with <i>E. coli</i> strains.	157
Figure 5.11	h β D-3 response of VK-2 E6/E7 cells to flagellin	160
Figure 5.12	h β D-3 response of VK-2 E6/E7 cells challenged with LPS	162
Figure 5.13	h β D-3 response to Peptidoglycan in VK-2 E6/E7.	164
Figure 5.14	h β D-3 response in VK-2 E6/E7 challenged with Zymosan.	166

Figure 6.1	Reporter construct used to measure NF-κB activity in VK-2 E6/E7.	173
Figure 6.2	NF-κB activity of RT4 or VK-2 E6/E7 challenged with Zymosan.	174
Figure 6.3	IL-8 secretion of urogenital epithelial cell lines when challenged with of Zymosan.	175
Figure 6.4	NF-κB activation in RT4 cells challenged with Zymosan after blocking TLR-2	176
Figure 6.5	The Dectin-1 gene with its different known and predicted isoforms.	177
Figure 6.6	Expression of Dectin-1 in urogenital epithelial cell lines.	178
Figure 6.7	Sequencing and BLAST results for the bands from the Dectin-1 PCR, performed using RT4 mRNA.	179-180
Figure 6.8	Determining the cell surface presence and concentration of Dectin-1 using flow cytometry.	182
Figure 6.9	Repetition of the cell surface concentration determination of Dectin-1 using flow cytometry.	184
Figure 6.10	Detection of Dectin-1 in the urogenital tract using fluorescent microscopy	185
Figure 6.11	Dectin-1 Antibody specificity control using recombinant Dectin-1.	186
Figure 6.12	Cellular localisation of Dectin-1 using confocal microscopy.	187
Figure 6.13	Clustering of Dectin-1 in VK-2 E6/E7 when challenged with Zymosan	189
Figure 6.14	Detection of SYK and phosphorylated SYK by Western Blot	190
Figure 6.15	Primary vaginal epithelium.	191
Figure 6.16	Control for epithelial cell marker cytokeratin using C11- antibody	192
Figure 6.17	Control for unspecific binding in the primary vaginal cultures	193
Figure 6.18	Immunostaining of Dectin-1 in Primary Vaginal Epithelia.	194
Figure 6.19	Inhibition of Zymosan induced NF-κB activation by blocking TLR-5	195
Figure 6.20	Dual immunostaining VK-2 E6/E7 for TLR-5 and Dectin-1.	196

List of Tables

	Page
Table 1.1 Risk factors for uncomplicated cystitis	4
Table 1.2 Toll like receptors and their ligands.	16
Table 2.1 List of primers used in endpoint and quantitative PCR	36
Table 2.2 <i>Escherichia coli</i> strains	49
Table 2.3 PAMPs used to challenge RT4 and VK-2 E6/E7 cells	51
Table 2.4 List of primary antibodies used in immunocytochemistry	58
Table 3.1 Results of TLR-associated genes array	67
Table 3.2 Motility of clinical UPEC strains	86
Table 4.1 Concentration of DNA-Transfection Reagent Mixture	108
Table 5.1 Linear regression analysis of the standard curve determined by indirect ELISA	147
Table 5.2 Linear regression analysis of the standard curve determined by a sandwich ELISA	149

CHAPTER ONE

Introduction

1.1. INFECTIONS OF THE UROGENITAL TRACT

The urinary tract is considered to be normally a sterile environment. However, it is frequently the site of clinical infection, urinary tract infection (UTI), resulting in symptoms, need for treatment and secondary health problems. In the UK for example, urinary tract infections are responsible for 1-3 % of all GP visits¹, affecting mainly sexually active women and are defined by the presence of $\geq 10^4$ CFU/ml of a single organisms or $\geq 10^5$ CFU/ml in mixed cultures obtained from a midstream urine sample. In fact, between a half and three-quarters of all women will develop a urinary tract infection at least once in their lifetime². Of these, 20 % to 50 % will experience recurrent UTI, defined as having two or more incidents of UTI in six months or three or more in 12 months^{3,4}. Analysis of UTIs among female university students revealed an incident rate of 0.7 UTIs per person per year⁵. In a more general cohort the incident rate was 0.5 UTIs per person per year⁵. This high prevalence and the fact that it affects a productive age group mean that UTI has a significant socio-economic impact as well as causing personal distress to sufferers. In the United States for example it is estimated that US\$1.6 billion are spent directly and indirectly for the treatment of UTIs⁶.

1. TYPES OF URINARY TRACT INFECTIONS

Urinary tract infections are classified according to the area of occurrence, urgency of treatment and the need of post-treatment evaluation, as well as by the presence or absence of symptoms. The most common variant is named uncomplicated lower UTI or acute cystitis and occurs in the bladder. The symptoms of cystitis vary from dysuria (painful micturition), haematuria (visible blood in the urine), suprapubic pain, frequency and urgency to urinate, causing great distress for the patients, and which last for an average of 6 days if left untreated⁷. Pyelonephritis is the infection of a kidney and relatively rare when compared to cystitis with around 12-13 cases of pyelonephritis per

10,000 population⁸. It causes symptoms of nausea, vomiting, fever and a typical flank pain sometimes preceded by symptoms of lower UTI⁹.

Complicated cystitis and pyelonephritis are defined by the European Association of Urology (EAU) as UTI events combined with factors that raise the need for different treatment and an evaluation of patients before and after the treatment¹⁰. Such factors are: the environment where the infection was acquired, *e.g.* hospital-acquired UTI, the cause of infection, *e.g.* catheterisation, anatomical (vesicoureteric reflux) and functional (urine flow obstruction by renal stones) abnormalities, as well as the presence of pathological conditions predisposing to UTI, such as diabetes mellitus and the immunocompromised patient¹¹. Occurrence of UTI in the elderly population often fulfils the criteria of complicated UTI and the mortality among elderly UTI patients can be up to 33 %¹².

Infections of urinary tract can also occur in the absence of symptoms. These infections are named asymptomatic bacteriuria (ABU). Hooton *et al.* (2000) showed that the risk factors associated with ABU are the same associated with symptomatic UTI, that ABUs are present in 5 % of women and that they increase the risk of developing a symptomatic bacteriuria¹³. In the UK, 17 % of elderly women were detected with an ABU^{14,15}.

2. RISKS ASSOCIATED WITH UTI

The main population group affected by UTI is sexually active women, with an increased risk for diaphragm and spermicide users or women after the menopause⁴. Although sexually active women are the cohort with the highest risk, UTIs occur at all life stages and in both genders. In children, genetic factors and anatomical abnormalities are the major cause for infections¹⁶. In the elderly, the main risk for infection is incomplete

bladder emptying and greater use of urinary catheterisation¹⁷. Established risk factors for simple cystitis are listed in Table 1.1:

Table 1.1 Risk factors for uncomplicated cystitis

Risk Factor	Cause
Sexual activity	Increased inoculation
Urinary incontinence	
Faecal incontinence or constipation	
Spermicide	Increased binding
Oestrogen depletion	
Antimicrobial agents	Decreased commensal 'healthy' flora of the vagina
Inadequate fluid uptake (dehydration)	Decreased urinary flow
Diabetes mellitus	Enhanced medium for bacterial growth

3. ROUTES OF INFECTION

Infections of the urinary tract originate from a variety of routes (Figure 1.1). In the bladder, the most common infection route is through the urethra by bowel commensals which develop pathogenicity when they colonise the urinary tract. The inoculation is often strengthened during sexual intercourse. Interestingly, the uropathogenic strain is commonly found in the bowel reservoir of the sexual partner as well, indicating a possible source for re-infection¹⁸.

Pathogens can also be introduced into the sterile urinary environment through urinary catheterisation, a particular risk for patients requiring long term indwelling or intermittent catheterisation and those requiring catheter urinary drainage as part of intensive care¹⁷.

The most common route of infection of the kidney is believed to originate from bacteria ascending from the bladder up along the ureters¹⁹. Recently, the role of bacterial ascension of uropathogenic bacteria to the kidneys has been questioned. While some investigators conclude that the ascending migration of uropathogens from the bladder is possible, the same authors view that this event is uncommon^{20,21}. An alternative route of kidney infection is from the blood stream to the kidney through the glomerulus. This route of infection can occur during surgical procedures although it is quite rare due to the sterile operating environments.

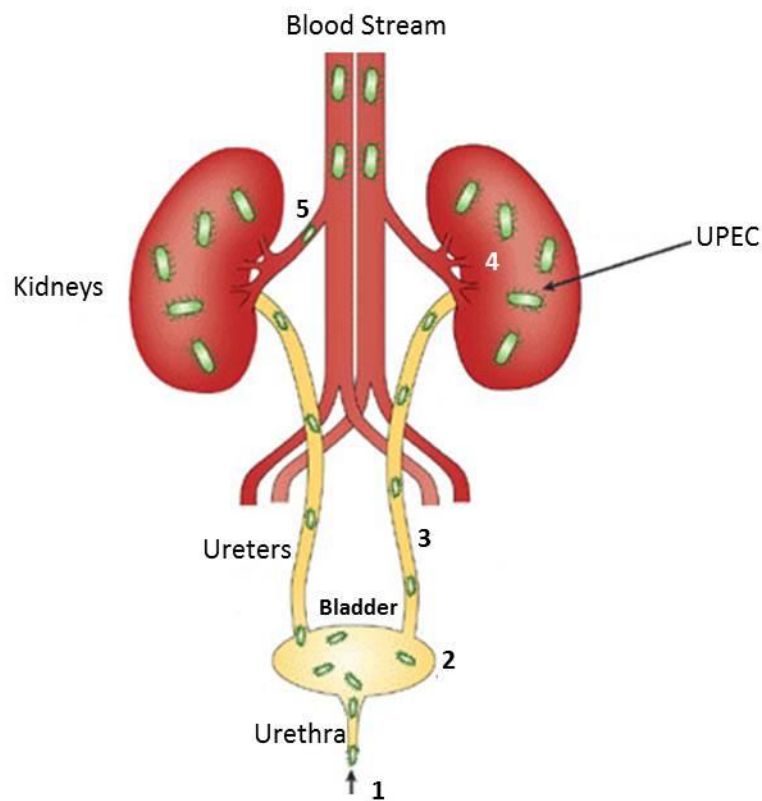


Figure 1.1 Routes of infection in the Urinary Tract. (1) Uropathogenic *Escherichia coli* entering the urinary tract by ascending the urethra. (2) Cystitis (infection of the bladder). (3) UPEC ascending the ureter to infect the kidneys causing (4) pyelonephritis. (5) Descending pyelonephritis caused by Sepsis. Diagram extracted from Kaper *et al.*(2004)¹⁹.

1.2. UTI ASSOCIATED PATHOGENS

Many pathogenic microorganisms are able to infect the urinary tract, e.g. viruses, bacteria and fungi, although viral and fungal infections are very rare and mainly found in immunocompromised or kidney transplant patients⁸.

Bacterial infection can be caused either by Gram-positive species, e.g. *Enterococcus faecalis* and *Staphylococcus saprophyticus* (responsible for 5-15 % of all UTI infections and mainly found events of cystitis)^{6,22}, or more commonly Gram-negatives, e.g. *Pseudomonas aeruginosa* and Enterobacter species, such as *Klebsiella* spp., *Proteus mirabilis*, *Serratia marcescens* and *Escherichia coli* (*E. coli*). The bowel commensal *E. coli* is responsible for the vast majority of occurrences of UTI accounting for between 70 % in dependent care environments such as hospitals and nursing homes and 95 % in the case of community-acquired infections in young women. Because of this preponderance, the investigation carried out and described in this thesis will focus on the main pathogen *E. coli*.

1.3. UROPATHOGENIC *ESCHERICHIA COLI* (UPEC)

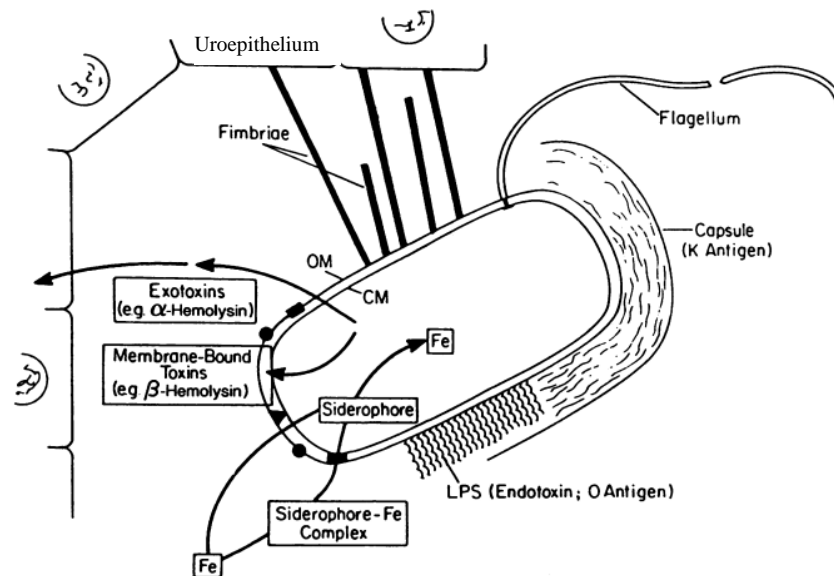


Figure 1.2 Uropathogenic *Escherichia coli* with its virulence factor. *E. coli* shown in the centre of the image. Host tissue represents the uroepithelium. The four groups of virulence factors are shown: 1) Adherence proteins attach to molecules present in the plasma membrane of the uroepithelium. 2) Toxins (α -haemolysin, cytotoxic necrotising factor). 3) Siderophore (aerobactin, enterobactin). 4) Membrane changing complexes (capsule and LPS manipulating proteins, control of flagellin production). Diagram extracted from Johnson (1991)²³.

The main source of *E. coli* infection of the urinary tract is the host's own bowel flora or infection from the bowel flora of a sexual partner²⁴. Nonetheless, certain virulence factors are necessary for a bowel derived commensal *E. coli* to become an uropathogenic *E. coli* (UPEC, Fig. 1.2). Investigations comparing the genome of faecal originated *E. coli* and UPECs show several differences, including absence of a type 3 secretion system and the presence of genes encoding urinary tract virulence factors²⁵.

1. VIRULENCE FACTORS ASSOCIATED WITH UROPATHOGENIC *ESCHERICHIA COLI*

Four classes of virulence factors are found to be necessary for a wild type and bowel derived *E. coli* to become a UPEC, able to colonise the urinary tract and cause symptomatic infection.

The first one is the acquisition of iron by the uptake of siderophores, which extract free or protein-bound iron from the urine and the uroepithelium, or through the uptake of haem moieties. Both iron acquisition mechanisms enhance absorption of iron by the bacteria through outer membrane transporters²⁶. Examples of functional siderophores are aerobactin, enterobactin and its glucosylated form salmochelin, and yersiniabactin²⁶. The latter two are more common among UPECs when compared to commensal *E. coli* strains isolated from faeces²⁷.

The second type of virulence factor postulated as essential for UPEC colonisation of the urinary tract is the presence of adherence proteins named pili or fimbriae²³. They are involved in the attachment of the bacteria to the uroepithelium²³. The two major pili investigated in UTI are P-fimbriae and Type 1 fimbriae^{23,28,29}. It has been noticed that Type P fimbriae mainly contribute to UPEC attachment to the renal rather than bladder epithelium³⁰. In clinical isolates from cystitis patients, the genes involved in the P-fimbriae production were only present in 33 % of the isolates³¹. In the lower urinary tract, Type 1 fimbriae are necessary for attachment³². Type 1 fimbriae are helical rods of repeating FimA subunits with a FimH subunit at the distal tip which when they adhere to recognition molecules on the uroepithelial cell surface cause exfoliation of the umbrella cells which form the luminal uroepithelial surface³³. An explanation for this differential attachment according to anatomical location could be the localisation of ligands of the adherence proteins on the host cell surface. While type 1 fimbriae mainly bind to the uroplakins Ia and Ib found in umbrella cells of the uroepithelium in the bladder, the PapG adherence molecule of P-fimbriae recognises α -D-galactopyranosyl-(1-4)- β -D-galactopyranoside, a major glycolipid found in renal epithelium³⁴.

The third class of virulence factor for the infection of the urinary tract is secretion of toxins by the bacteria, *e.g.* α -hemolysin, cytotoxic necrotising factor 1 and 2, and

secreted autotransporter toxin (sat). Alpha-hemolysin is responsible for Ca⁺ oscillation across the renal epithelial cells resulting in cell lysis in a concentration dependent manner³⁵.

The fourth class of virulence factors consists of methods of circumventing and inhibiting immune protective responses activated by the host. At present, two mechanisms are known: First, it has been demonstrated that the laboratory standard UPEC strain NU14 can modify the composition of its cell surface. Using the genes *ampG* and *waaL*, it can change the structure of the peptidoglycan and lipopolysaccharide (LPS) membrane, avoiding recognition by the host receptors on luminal uroepithelial cells³⁶. Secondly, another laboratory UPEC strain, CFT 073 has been shown to produce a protein that mimics the activation domain of a host adaptor protein involved in the recognition of the pathogen (see section 1.4), thereby inhibiting initiation of a host immune response³⁷.

Additionally, intracellular bacterial colonies (IBC) have been reported in mice. UPEC binds to umbrella cells of the bladder and is engulfed by the uroepithelial cell. In humans, preliminary findings suggest that such IBC cultures can be detected in exfoliated epithelia cells³.

Controversy remains about the actual and relative importance of the described virulence factors: There is evidence that the adherence through P-fimbriae or type 1 fimbriae is not necessary for a UPEC infection of the bladder or the kidney³⁸. It was shown that the gene for α -hemolysin was present in only 25-35 % of isolates from urinary tract infections^{31,39}. Of these, some strains did not express functional haemolytic activity even if the gene was present³⁹.

More intriguingly, in a study detecting main virulence present on 550 *E. coli* clinical isolates from people suffering infections of the urinary tract, and 318 strains isolated from the surroundings of the urethra and from faeces of the same patients, found that around 50 % of the UPEC strains had none or only one of the virulence genes⁴⁰. The majority of the *E. coli* isolated from the bowel and from cystitis had one of the Fim genes, which form the fimbriae. Hence, the presence and particular combination of virulence factors alone does not explain a successful infection of the bladder⁴⁰.

Other research has shown that untreated UTIs have a spontaneous cure rate of 37 % after 5-7 weeks⁴¹, suggesting that bacteria can be eradicated by the host defence mechanisms. The ways in which the host may eliminate urinary pathogens and hence avert or resolve symptomatic infection will be discussed next.

1.4. IMMUNE MECHANISMS ACTIVE IN THE UROGENITAL TRACT DURING INFECTION

The immune system has been classically divided into two types: the evolutionary older one being named the innate immune system, which is non-specific. In contrast, the evolutionary later adaptive immune system present in vertebrates is specific due to the recognition of a single processed antigen.

1. ADAPTIVE IMMUNE SYSTEM IN UTI

The adaptive immune system is composed of two different types of lymphocytes. Both cell types have their progenitor in the bone marrow and depending on the location of maturation they are classified as bone marrow cells (B-cells) or thymus cells (T-cells). T-cells are characterised by the presence of the T- cell receptor (TCR). Additionally, the function of the T-cell is determined by the presence of the receptors CD-8 or CD-4. The sub-type CD-8+ T-cells are called killer T-cells and are responsible for the cell

mediated immune response. The sub-type CD-4+ cells can be differentiated into helper T-cell variants; Th1, Th2, and Th17. T-helper cells are involved in the maturation of killer T-cells and of B-cells.

The activation of B-cells is dependent on the recognition of an antigen by the B-cell receptor (BCR) and the co-stimulation of a helper T-cell. Upon activation, the B-cells are induced to proliferate and differentiate into plasma cells, which secrete specific antibodies into the local tissue or blood stream, or into long-lived memory B-cells. B-cells are therefore responsible for the humoral immune response.

The presence of activated lymphocytes and antibodies has been detected during urinary tract infection^{42,43}. However, our knowledge about the role of lymphocytes during urinary tract infections is limited and mainly obtained using mice models. Hence, their role can only be estimated. A strong indicator of a required role is the finding that nude mice are unable to clear a urinary tract infection⁴⁴.

2. THE INNATE IMMUNE SYSTEM

For maturation of lymphocytes it is essential that an antigen is processed and presented. The presentation of the antigen is conducted by several different types of cells, named accordingly as antigen presenting cells (APC). These cells link the adaptive and the innate immune systems. They present the antigen using the major histocompatibility complex (MHC)-type 1 and 2^a. MHC-1 is expressed by all nucleated cells while MHC-2 is only expressed by certain cells. Examples of APCs are dendritic cells, mast cells, macrophages and B-cells. The infiltration of dendritic cells and macrophages into urinary tissues during UTI has been shown previously⁴² and investigations showed that dendritic cells not only uptake UPEC, but also release nitric oxide⁴⁵. The same group

^a The MHC molecules are named Human Leukocyte Antigen (HLA) in humans

later showed that monocytes migrated to the bladder, through a CCR2 mediated mechanism during UTI⁴⁶. Nonetheless, these investigators concluded that neither dendritic cells nor monocytes are necessary for clearance of bacteria causing UTI^{45,46}. Macrophages, together with other phagocytes such as neutrophils, can in addition to their antigen presenting function engulf bacteria via phagocytosis.

Some lymphoid cells are considered part of the innate immunity and are termed natural killer cells (NK-cells). Although NK-cells have the same progenitor as the other lymphocytes (B- and T-cells), they lack their characteristic BCR and TCR. Nonetheless, they have the ability to kill many different types of cells. It has been shown that they can be activated by bacteria FimH through the cell surface pattern-recognition molecule, Toll-like receptor-4 (TLR-4)⁴⁷.

Neutrophils^b are granulocytes or polymorphonuclear leukocytes (PMN) and the first dedicated innate immune cell type to infiltrate the bladder wall and the urine upon bacterial infection. They are attracted by cytokines such as interleukin-8 (IL-8) secreted by the uroepithelium following contact adherence by colonising bacteria⁴⁸⁻⁵⁰. In contrast to the APCs, the PMN cell types are deemed to be essential for effective clearance of bacteria causing UTI⁵¹.

Upon activation, PMN granulocytes degranulate to release a mixture of different antimicrobial peptides and reactive oxygen species⁵². The relative density of neutrophil migration during UTI is much higher in the human than in mice. This may be linked to the finding that 70 % of leukocytes in human blood are PMNs compared to 30 % in mice⁵³.

^b Neutrophils are defined as neutral because of their staining properties, using hematoxylin and eosin (H&E) staining, where the granules are stained by both stains resulting in a purple colour.

As mentioned before, migration and activation of neutrophils require the presence of chemo-attractants secreted by the urothelium. It therefore follows that the uroepithelium plays a pivotal crucial role in the early host immune response to UPEC infections.

1.5. THE ROLE OF THE UROGENITAL EPITHELIA DURING UTIS

The epithelium forms a cell layer covering organs and tissues. It is the first line of contact with the external environment (although often internal to the body), and hence it is constantly under challenge from external attack. Epithelia have diverse functions, depending on location, *i.e.* barrier, secretion, absorption and sensing functions⁵⁴. In recent years, the epithelium has been recognised as a highly effective part of the immune system, not only by providing passive barrier function, but also by the active recognition and direct killing of pathogens, as well as inducing innate and adaptive immune responses^{55,56}.

The uroepithelium that lines the inner luminal surface of the urinary bladder originates from the endoderm⁵⁷ and includes three different layers (Fig. 1.3):

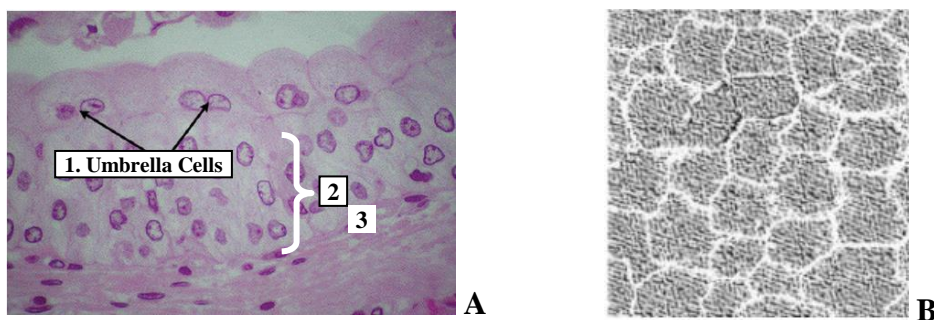


Figure 1.3 Uroepithelium and asymmetric unit membrane. (A) The three layers of Uroepithelium. 1. Umbrella cells with multiple nuclei. 2. Intermediate uroepithelium and 3. Basal cell layer. Image adapted from http://www.dartmouth.edu/~anatomy/Histo/lab_5/renal/DMS154/50.gif. (B) Asymmetric unit membrane formed by uroplakins. Image extracted from Lewis (2000)⁵⁸.

An apical layer of cells directed to the lumen of the bladder named umbrella cells due to their shape, a pear-shaped intermediate layer composed of one to several layers of transitional epithelial cells and a basal layer with a monolayer of small (10 µm) progenitor cells (Fig. 1.3)^{54,59}. The outermost epithelial umbrella cells are large (25-250 µm) in comparison to the intermediate and basal cells and multinucleated⁵⁹. Depending on the filling state of the bladder, the shape of the apical and intermediate cells varies from cuboidal shape (empty bladder) to squamous cells (filled bladder), hence the name transitional⁵⁴.

The barrier function of the umbrella cells is provided by inter-cellular tight junctions formed by occludins and claudins⁶⁰. Claudins-3, -4, -5, -7, -8 and -12 are expressed in human uroepithelium⁶⁰. They inhibit the influx of urine and its constituents into the bladder epithelium and the invasion of pathogens^{58,61,62}. A unique set of proteins are located on the luminal surface of the umbrella cell surface, termed uroplakins. These structural proteins form hexagonal plaques named the asymmetric unit membrane, and composed of uroplakin (UP) dimers; UP Ia-UP III dimers and UP Ib-UP II dimers⁶⁰. Another particular aspect of the umbrella cells is their high lipid composition with high concentrations of phosphatidyl choline, cholesterol and cerebroside⁵⁹.

1.6. PATTERN RECOGNITION RECEPTORS IN THE UROEPITHELIUM

The sentinel function of the uroepithelium is provided by a group of intracellular and cell-surface receptors with the common function of recognising pathogen associated molecular patterns (PAMPs) which are present on the cell surface and within the cell. Accordingly, they are named pattern recognition receptors (PRRs). Recent research has mainly focussed on four families of PRRs, *i.e.* the intracellular retinoic acid inducible (RIG)-I gene like receptor (RLR) and nucleotide-binding oligomerisation domain

(NOD) like receptor (NLR), the cell-surface C-type lectin receptors (CLR), and the intra- and cell-surface receptor family of TOLL-like receptors (TLR)⁶³.

RIG-I is expressed in the uroepithelium when induced by inflammatory cells or interferon gamma (IFN- γ)⁶⁴. The RLR recognise viral double stranded DNA and they induce the release of type 1 interferon (IFN-I) when activated⁶⁵. They do not participate in an immune response during a bacterial urinary tract infection.

The second group of PRR are the intracellular NOD-like receptor (NLR). Although some NLR recognise viral PAMPs, the majority of them recognise microbial motifs. The best characterised NLRs are NOD-1 and NOD-2. They recognise part of peptidoglycans, *g*-D-glutamyl-meso-diaminopimelic acid (iE-DAP) and muramyl dipeptide (MDP), respectively. iE-DAP is present on Gram negative bacilli and some Gram positive species such as *Bacillus subtilis*, while MDP is present on all cell walls^{63,66,67}.

CLRs are receptors which detect fungal infections or endogenous ligands⁶⁸. The best characterised is the Dectin-1 receptor (CLEC7A), a Ca⁺-independent CLR that recognises β -1,3-glucans, *e.g.* Zymosan, found on the membrane surface of fungi, *e.g.* *saccharomyces*, *candida* and *aspergillus*^{69,70}. Dectin-1 was first discovered in dendritic cells and shown to be the principle receptor for fungal recognition by macrophages⁷¹⁻⁷³.

Recent investigations have demonstrated the expression of Dectin-1 in pulmonary epithelial cells and keratinocytes^{74,75}. Dectin-1 recognises β -1,3-glucans through its N-terminal expressed carbohydrate recognition domain (CRD). Upon binding to β -1,3-glucans, Dectin-1 starts a signalling cascade through spleen tyrosine kinase (SYK), resulting in the translocation of the proinflammatory transcription factor NF- κ B to the

nucleus, hence promoting an immunological response⁷⁶. Interestingly, interactions with TLR-2 have been reported⁷⁷.

1. TOLL-LIKE RECEPTORS IN THE UROEPITHELIUM

TLR-2 is part of the TLR-family composed of 11 receptors (TLR-1 to -12; murine TLR-7 is homologous to human TLR-8) in mammals⁶⁵. TLRs were among the first discovered and best characterised PRRs and are present in the epithelia of many different tissues⁷⁸. TLRs may be located intracellularly (TLR-3, -8, -9, -10), or in the plasma membrane (TLR-1, -2, -4, -5, -6) or in both locations (TLR-4) and are able to recognise PAMPs from a variety of microorganisms, such as bacteria, parasites, fungi, protozoa as well as viruses and endogenous ligands⁷⁹. Table 1.2 summarises the known TLRs and their ligands:

Table 1.2 Toll like receptors and their ligands. Receptors in brackets are only found in mice.

Cell-surface	Ligand
TLR-2/TLR-1 TLR-2/TLR-6	Peptidoglycans
TLR-4	LPS, among others
TLR-5	Flagellin
(TLR-11)	unknown UPEC ligand and Profilin

Intracellular	Ligand
TLR-3	dsRNA
TLR-8 (TLR-7)	ssRNA
TLR-9	CpG-DNA
(TLR10*)	unknown

They are homologues of the original Toll-receptor found in 1985 in *Drosophila melanogaster*, where a mutation in the gene changed embryogenesis⁸⁰. Eleven years later, protection of fungal infection was associated with the Toll-gene and since then the role of TLRs as the principal family of pattern recognition receptors in mammals has been established⁶⁵. The investigation described in this thesis will focus on the role of extracellular TLRs in the human uroepithelium. Hence, the next part will describe the cell-surface TLR's structure and signalling (Figure 1.4):

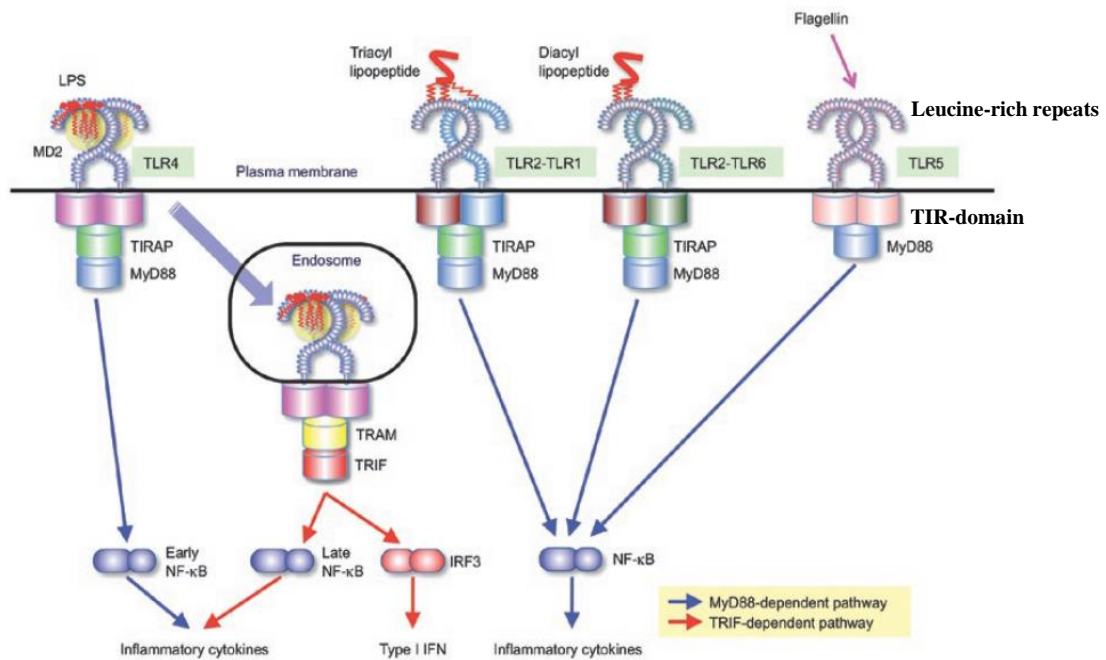


Figure 1.4 Extracellular TLRs and their ligands. The cell-surface homodimers TLR-4 and TLR-5 are shown together with the heterodimer TLR-2/TLR-1 and TLR-2/TLR-6. Diagram adapted from Kawai et Akira (2010)⁶⁵.

Structurally, TLRs have a characteristic extracellular leucine-rich repeat at the N-terminal and an intracellular TOLL/IL-1R homology domain (TIR) responsible for ligand induced signalling. Upon recognition of their respective ligands some TLRs form homodimers (TLR-4 and -5) or heterodimers (TLR-2/-1, TLR-2/-6) with each other.

TLRs have been described as having a role in the detection of bacterial UTI. Previous research has mainly focussed on mice as an animal model and in particular the role of TLR-4. TLR-4^{-/-} mice and C3H/HeJ mice with a mutated TLR-4 gene fail to resolve UPEC infections^{81,82}. A human correlate of these experimental studies is that a genetic mutation in the TLR-4 gene (substitution A→C at position 896) found in humans increases the risk of recurrent UTIs in childhood⁸³. Additionally, children with syndromes associated with reduced TLR-4 expression tend to have persistent asymptomatic bacteriurea⁸⁴. However, the importance of TLR-4 in human UTI remains controversial. TLR-4 is exclusively expressed on superficial umbrella cells which exfoliate upon recognition of UPECs⁸⁵⁻⁸⁷ and its cofactor CD14 is only found in the bladder submucosa⁸⁸. In the human, Hawn *et al.* (2009) showed that a TLR-4 polymorphism, which results in a LPS-hyporesponsive TLR-4, protects adult women from recurrent UTI⁸⁹ and other studies have established that TLR-4 independent mechanisms can result in UPEC clearing⁹⁰.

In mice, TLR-2 does not appear to play a role in UPEC clearance⁹¹. In humans, however, a SNP in the TLR-2 gene (2251 G→A mutation resulting in a Arg753Gln) is associated with a higher risk for recurrent UTI and asymptomatic UTI in children⁹². In contrast, the investigation of Hawn *et al.* (2009) showed no significant effect of the polymorphism in adult women⁸⁹, although a significantly higher number of ABU was noticed⁹³. Interestingly, a polymorphism in the TLR-2 associated TLR-1 gene was shown to have a protective effect for pyelonephritis⁸⁹.

The final cell surface TLR characterised in humans is TLR-5. It recognises flagellin (FliC), a subunit of the flagellum apparatus responsible for bacterial motility⁹⁴. The role of TLR-5 in UTI is not clearly defined. UPEC seems to be able not only to sense the presence of TLR-5 but also to switch off its flagella and turn on the FimH production,

suggesting no role for TLR-5 in UTI in mice^{20,21}. However, TLR-5^{-/-} mice were highly prone to UTIs⁹⁵ and in adult humans, the only gene polymorphism associated with a higher incidence of recurrent UTI involved the TLR-5 gene⁸⁹. Hence the role of TLR-5 in the human urinary tract is a legitimate target for further investigation.

It is important to note that murine TLR-11, a cell surface TLR closely related to TLR-5, seems to be important for clearing UPEC infections in mice⁹⁰. In humans however, the gene for TLR-11 is truncated and hence not expressed⁹⁰, indicating again problems with using mice as a model organism for human UTI.

In conclusion, the role of cell surface TLRs remains controversial and needs to be better defined in the human uroepithelium, as the relevance of findings in the mice model to the human situation is compromised by the many structural, molecular and genetic differences between murine and human uroepithelium. Hence, the definition of the role of each cell-surface TLR in a human model system will be one of the major aims of this investigation.

2. SIGNALLING CASCADE OF CELL SURFACE TLRs

Activation of TLRs starts a signalling cascade, which leads to the upregulation of many genes. Different signalling pathways have been described for specific TLRs and broadly defined as MyD88 dependent or independent. All TLRs, except TLR-3, start a signalling cascade using the MyD88 pathway, although TLR-4 was shown to use at least two MyD88 independent signalling pathways^{56,65,96}. The research described in this thesis will focus on MyD88 dependent TLRs as shown in Figure 1.5:

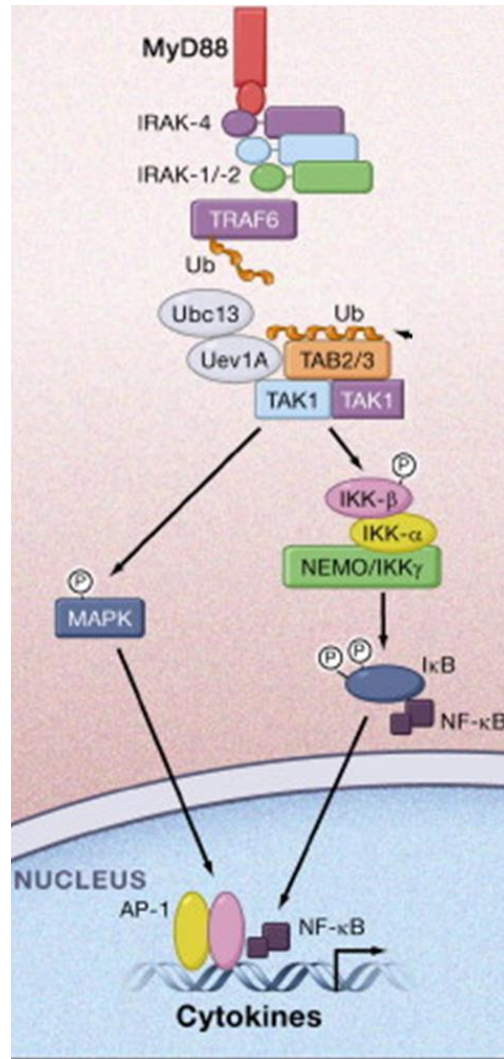


Figure 1.5. MyD88- dependent TLR-signalling. TLR-5 binds directly to its signalling adaptor protein MyD88, while TLR-4 and the TLR-2 heterodimers need TIRAP. Diagram extracted from Takeuchi et Akira (2010)⁷⁹.

Upon ligand-binding, TLR-5 directly, and TLR-2/TLR-1, TLR-2/TLR6 heterodimers and TLR-4 through TIRAP, activate MyD88 which subsequently binds to IRAK-4 through its death domain. The complex binds then to IRAK-1 and IRAK-2 releasing the IRAK complex from the MyD88. The IRAK-complex then unites with TRAF-6, ubc13 and Uev1A, resulting in an unconjugated free lysine 63 polyubiquitin chain which forms a complex with TAK1, TAB1, TAB2 and TAB3. This complex then phosphorylates the inhibitor of NF-κB (IκB), causing its degradation. NF-κB translocates to the nucleus where it acts as a transcription factor for a series of immune-active genes, such as those encoding antimicrobial peptides and cytokines.

3. PROTEINS ASSOCIATED WITH TLR INDUCED IMMUNE RESPONSES

Studies suggest that cationic anti-microbial peptides (CAMP) such as human β -Defensin 1 (hBD-1), human α -Defensin 5 (HD-5) and the cathelicidin, LL-37, are important for urogenital epithelial defence⁹⁷.

I. CATHELICIDINS

The cathelicidin family is a group of peptides synthesised in mammals and with antimicrobial as well as chemo-attractive properties⁹⁸. Although other mammals *e.g.* sheep and mice, have more than one cathelicidin gene^{12,99} only one has been found to be expressed in humans; that encoding LL-37¹⁰⁰, being synthesised as a propeptide and cleaved extra-cellularly into cathelin and the C-terminal peptide also known as LL-37⁹⁸. Interestingly, both peptides have antimicrobial activity and interact with FimH suggesting that cathelicidin plays a key role in the protection of the UT against bacterial (*E. coli*) infection, although whether the peptide originates from the kidney or the lower urinary tract urothelium is undetermined^{100,101}.

II. DEFENSINS

Another family of CAMPs are the Defensins. They were first characterised in humans in skin tissue where these cationic peptides show a broad spectrum of activity¹⁰². They are active against gram-negative as well as gram-positive bacteria, fungi, some parasites and enveloped viruses.

All Defensins are cationic, due to their high number of lysine and arginine residues^{103,104}. In humans, six highly conserved cysteines form three disulfide bridges. Based on the order of this disulfide bridges, the Defensins are subdivided into α or β -Defensins¹⁰⁵. The order of cysteine forming disulfide bridges is 1–6, 2–4 and 3–5 for α -Defensins and

1–5, 2–4 and 3–6 for β -Defensins¹⁰⁵. Human α -Defensins and β -Defensin (h β D) originate from a common β -Defensin ancestor, hence show a similar secondary structure of three β -sheets and one α -helix, have hydrophobic and hydrophilic parts and are therefore amphipathic^{103,106}.

The mechanisms by which the Defensins kill microbes are not yet completely understood. There are three widely described models: the carpet model, the pore model and the inhibition of DNA, RNA and protein synthesis¹⁰⁵. The carpet model compares the β -Defensins to classic detergents, where they bind at high concentration to the phospholipid head forming a “carpet” layer, neutralising the negatively charged membrane and thereby destroying the transmembrane action potential¹⁰³. The second model makes use of h β D amphiphilic properties. First, the positively charged β -Defensin attaches to the negatively charged bacterial membrane due to the lipid composition, then it fuses with the membrane because of hydrophobic interactions between the lipid core and β -Defensin molecules and finally, oligomerizes with other β -Defensins forming a multimeric channel¹⁰⁵. The third model was based on observations that Defensins inhibit the synthesis of DNA, RNA and proteins¹⁰⁷. To date, none of the models have been conclusively proven experimentally but it is probable that the killing mechanism *in vivo* is a combination of all three.

III. HUMAN BETA DEFENSINS (h β D)

Human β -Defensin 1 (h β D-1) is ubiquitously expressed by human epithelia, but when its killing activities are compared to other Defensins, *i.e.* h β D-2 & 3, it has only weak killing capacity. Mice, which lack *defb1* (the gene encoding h β D-1) have a higher risk of developing bacteriuria¹⁰⁸. Recent work by Schroeder *et al.* (2011) has shown that in reducing environments such as those found in the gastro-intestinal tract, the disulphide-bridges of h β D-1 are broken¹⁰⁹. Following reduction the peptide has increased killing

properties against the fungus *Candida albicans* (an opportunistic pathogen in the urogenital tract) and anaerobic, Gram-positive commensals including *Bifidobacterium* and *Lactobacillus* species. The results of this study are novel and exciting as they suggest that reduced h β D-1 exists *in vivo* and helps to protect the healthy epithelium against colonisation by commensal bacteria and opportunistic fungi. This in turn indicates an important interaction between redox-regulation and the epithelial innate immune defences.

The human β -Defensin 2 (h β D-2, *DEFB 4*) gene (238 base pairs; bp) is located in the Defensin gene cluster on chromosome 8p23.1-p22. The gene contains two exons: the first exon (81 bp) encodes the signal peptide and the proform; the second exon encodes the mature peptide. The expression of the h β D-2 peptide is induced by many different signals, including, for example, presence of cytokines such as interleukin-1 α ; -1 β ; tumour necrosis factor alpha (TNF- α); IFN- γ . PAMPs, including flagellin and lipopolysaccharide (LPS) can induce h β D-2 via Toll-like-receptors, as well¹¹⁰.

The gene for h β D-3 (*DEFB103*) is located 13 kbp upstream of h β D-2¹⁰⁵. It is composed of two exons and encodes a 67 amino acid propeptide that is cleaved into a 45 amino acid active peptide¹⁰². It has a primary amino acid sequence that is dissimilar to the other h β Ds and its charged amino acids are asymmetrically distributed with most clustered towards the C-terminus¹⁰². H β D-3 molecules are amphipathic and can form symmetrical dimers although dimerisation does not seem to be involved in its antimicrobial activity¹⁰².

Regarding the β -Defensins, the main research focus has been related to investigations of their antimicrobial activity^{111,112}. Beta-Defensins are able to inhibit growth or kill bacteria, fungi and even viruses^{109,110}. Human β D-2 was reported to have a strong

killing activity against Gram-negative bacteria primarily and some fungi, while hBD-3 is a strong inhibitor of both Gram-negative and Gram-positive bacteria, as well as yeast¹¹⁰. Both Defensins are more effective against aerobic than anaerobic bacteria. Interestingly, the activity of hBD-2 is strongly inhibited by sodium chloride at physiological concentrations¹¹³, whilst the antimicrobial activity of hBD-3 is not¹⁰³.

Previous research has also shown that β -Defensins have other functions; hBD-2 has chemotactic properties for different cell types, including T-cells and immature dendritic cells, as well as keratinocytes^{110,114}. Human β D-2 also has the ability to activate macrophages, which provides a link to the adaptive immune system through the activities of T_H-cells. In turn, T_H-cells can signal the production of hBD-2 through releasing different cytokines¹¹⁵, supporting a self-perpetuating innate defence system. This loop can be turned off by the immunosuppressive activity of hBD-3¹¹⁶ highlighting potential interactions between the different antimicrobial peptides.

IV. INTERLEUKIN 8 (IL-8)

As mentioned earlier, NF- κ B translocation to the nucleus results in expression and secretion of cytokines. The most important cytokine involved in UTI is interleukin-8 (IL-8). It is part of the interleukin family and responsible for the chemo-attraction of neutrophils. It is well known that the urogenital tract epithelia secrete IL-8 in response to pathogens such as UPEC^{117,118}. The secretion of IL-8 induces a strong infiltration of neutrophils into the urinary bladder⁴⁸. Other cytokines and chemokines induced in the bladder by UPEC are CCL2, CCL4, CCL5, CXCL, β IL12P40 and IL17, although only analysed in bladder rather than elsewhere in the urogenital tract¹¹⁹. In humans, IL-6 has also been found to be secreted in response to bacterial infection although these data come from analysis of the whole bladder¹²⁰ or from cell lines derived from a bladder carcinoma¹²¹ with no specific localisation to the uroepithelium. A further study showed

that IL-6 was only found in carcinomatous or inflamed (interstitial cystitis) uroepithelium¹¹⁷. Other cytokines, such as transforming growth factor beta (TGF- β) and IL-4 were present in normal tissue or only in carcinomatous uroepithelial cells, respectively¹¹⁷.

V. OTHER INNATE FACTORS

Other important urinary innate defence factors are Tamm-Horsfall protein (THP), a glycoprotein synthesised by the kidney and which functions to prevent bacterial attachment and colonisation of the uroepithelium, together with lactoferrin and lysozyme⁵⁵.

In addition, the complement system is also thought to play a key role during UTI¹²². This involves pathogens being opsonised by C3b which facilitates their recognition, and with other factors such as C3a and C5a facilitating clearance by phagocytes. However, the consequences of complement activation may be negative in UTI since complement activation can lead to the internalisation of bacteria, potentially leading to subsequent recurrent infection when the initial inflammatory response subsides¹²². A reduction of the complement response also reduces any damage to infected tissue, shown in the kidney¹²². Interestingly, the complete absence of complement inhibits UPEC moving from the bladder upwards to the kidneys¹²³.

1.7. PATHWAYS FOR THERAPEUTIC INTERVENTION

The main, and generally very successful, therapy for UTI is the use of antibiotic medication. Unfortunately, several unwanted affects may arise from this treatment. First, *E. coli* is possibly able to form intracellular colonies and biofilms circumventing urinary antibiotic activity. Second, antibiotic resistance among UPEC strains is

increasing and overuse of antibiotics for many mild self-limiting infections such as cystitis and upper respiratory tract infection is increasing this problem^{8,124,125}. Hence alternative routes urgently need to be investigated.

The finding that adaptive immunity may play a role in defence against UTI encouraged many researches to focus on the development of vaccines using a number of different approaches. The first approach was the delivery of antigens normally found in UPEC strains. Some target proteins were the proteins involved in LPS synthesis, P-fimbriae, Type 1 Fimbriae and α -haemolysin¹²⁶⁻¹²⁸. Each vaccine only showed moderate success and none have entered routine practice. There are different causes for this failure. As mentioned earlier, UPEC are able to change their LPS structure, thereby avoiding tagging by specific antibodies. Additionally, although a P-fimbriae vaccine might be specific to the rarer pyelonephritis, it will not be of use in the far more common condition of simple cystitis where the role of P-fimbriae appears limited. Type 1 fimbriae expression is phase variant meaning that the gene is turned on or off depending on presence of particular transcription factors. It is also, together with α -haemolysin, not a suitable antigen as many of the commensal gut *E. coli* strains express it. Vaccination using specific antigens only could therefore be ineffective and potentially dangerous due to its specificity for non-UPEC strains such as the one present in the normal gut flora. To avoid these problems, Sivick *et al.* (2009) screened for proteins only expressed in UPECs and found that outer membrane proteins involved in iron uptake were fulfilling the pathogen-specific, antigenic, surface-exposed, and *in vivo* expressed (PASivE) requirements¹²⁹. IroN has been used before to immunise mice and it reduced the risk of pyelonephritis¹³⁰. Nonetheless, the number and bacterial load of the bladder remained constant, maybe indicating a more important role for the innate rather than adaptive immunity in bladder infection.

Vaccination using whole UPEC organisms has also been investigated. However, side effects due to the unspecific antigenic response could be dangerous. Indeed, studies using a vaccine composed of 18 UPEC strains showed severe side effects¹³⁰.

Interestingly, one of the most effective approaches is the inoculation of ABU strains. In 2001, Darouiche *et al.* inoculated patients with spinal cord injuries with the ABU strain 83972 and showed a significant reduction of recurrent UTI compared to the control group¹³¹. In 2006, Roos *et al.*, showed that ABU strain 83972 is able to outcompete many UPECs, among them the previously discussed CFT 073 and NU14 strains, in urine and in a murine UTI model¹³². It was later shown that ABU 83972 was better in forming bio-films when growing in urine¹³³.

Another therapy angle is the modulation of the innate immunity. It is believed that the consumption of cranberry juice is able to increase the resistance to recurrent UTI although this practice is controversial¹³⁴⁻¹³⁶.

1.8. BACKGROUND TO RESEARCH

Pilot work towards this thesis carried out and described in an MRes dissertation (unpublished data available from the Author) resulted in the production of an uroepithelial cell line (RT4) stably transfected with a NF- κ B-Luciferase reporter gene construct¹³⁷. This allowed the investigation of NF- κ B signalling response of uroepithelial cells to bacteria and PAMPs. Flagellin, but not LPS, was identified through this work as being a NF- κ B activator. In addition, TLR-2, 4 and 5 were all identified as being expressed by RT4 uroepithelial cells. Analysis of human tissue samples from different levels in the urinary tract using quantitative PCR showed TLR-5 expression was predominant in ureter and bladder biopsies and TLR4 in the kidney.

Data from *in vitro* experiments carried out in our laboratory have shown that RT4 cells, used as an *in vitro* model of the urothelium, when challenged with flagellin originating from *Salmonella typhimurium* secrete the Defensin h β D-2 (Mr Ased Ali, PhD Thesis, Newcastle University).

Little is known about the mechanisms by which the urinary tract, despite being challenged continuously by potential pathogens, is able to maintain its sterility. Thus this PhD project has a broad aim to increase our understanding of the interactions between urinary pathogens and the host epithelium, particularly in relation to the cell-surface TLRs and Defensin family.

1.9. HYPOTHESIS

The hypothesis that I wished to investigate was:

Innate Immune Response in the Urinary Tract is dependent on Host Recognition of bacterial motility and can be enhanced by Immunomodulatory Compounds.

1.10. AIMS AND OBJECTIVES

Protection of the urogenital tract from infection is mediated primarily through the innate immune system, but still, to date, little is known of the host mechanisms that function in such defences. The focus of the research presented in this thesis, which used RT4 and VK-2 E6/E7 *in vitro* cell systems to model the bladder and vaginal epithelia respectively, was to interrogate the mechanisms by which these epithelia recognise and respond to microbial assault.

The first aim was to explore the NF- κ B signalling response of bladder cells challenged with *E. coli* UTI strains, as well as bacterial PAMPs, with the objectives of defining the hierarchy of the uroepithelial TLR response and identifying the importance of bacterial motility in urinary tract infections.

The second aim was to explore the mechanisms, in addition to NF- κ B, involved in regulating the expression and synthesis of host epithelial defence factors with microbial killing properties, specifically h β D-2 and h β D-3, with the objective of identifying agents that could be used therapeutically to enhance the innate defences of the urogenital tract.

CHAPTER 2

Materials and Methods

2.1. CHEMICALS AND REAGENTS

All chemicals and reagents were purchased from Sigma-Aldrich (St Louis, USA) unless otherwise stated. Bacteriological media and agar were bought from Oxoid (Basingstoke, Hampshire, UK).

2.2. TISSUE CULTURE

The cell lines used were RT4 (ATCC-HTB-2, LGC Standards, UK), a bladder uro-epithelium isolated from a transitional cell papilloma and VK-2 E6/E7 (ATCC-CRL2616), a vaginal epithelial cell line immortalised using the human papilloma virus¹³⁸. Additionally, a protocol for growing primary human vaginal epithelia from vaginal biopsy clinical samples was established. All cell lines were cultured in 5 % CO₂ at 37 °C.

1. RT4 BLADDER EPITHELIUM

RT4 cells were cultured in Corning 75 cm culture flasks (Corning, UK) using RPMI growth media (modified by addition of 2.5 % of HEPES buffer), supplemented with 2 mM L-glutamine and 10 % FCS. The medium was changed twice per week and cells passaged weekly. For passaging cells were collected following trypsinisation (5 minutes at 37 °C and 5 % CO₂) and seeded at a ratio of 1:50.

For the stably transfected RT4–NF-κB reporter cells the media was supplemented with the eukaryotic antibiotic G418 [0.5 mg/ml].

2. VK-2 E6/E7 VAGINAL EPITHELIUM

VK-2 E6/E7 cells were cultured using Keratinocyte Serum free media supplemented with 0.05 ng/ml recombinant human epithelial growth factor, 0.05 mg/ml bovine

pituitary extract and 0.4 mM CaCl₂. Medium was changed twice weekly. Cells were passaged weekly; for passaging, cells were collected following trypsinisation (5 minutes at 37 °C and 5 % CO₂) and split at a ratio of 1:20.

3. PRIMARY HUMAN VAGINAL EPITHELIUM

Vaginal biopsies were collected in PBS from the Royal Victoria Infirmary, Newcastle upon Tyne, UK. The tissue was dissected of excess fatty tissue or stroma and washed three times using PBS supplemented with Penicillin-Streptomycin-Amphotericin B (Lonza, Walkersville, USA) (PBS-PSA). The epithelial cells were detached from the connective tissue by incubating the tissue in Dispase [1U/ml], diluted in 10 ml of PBS-PSA for 24 h at 4 °C. The epithelial layer was removed from the connective tissue using a forceps and incubated in prewarmed trypsin for 10 minutes at 37 °C with occasional shaking. The trypsin was neutralised by the addition of RPMI medium containing 10 % FCS and the cells collected by centrifugation at 1500 x G for 5 minutes. The supernatant was decanted off and the cell pellet resuspended in two ml Epilife medium (Life Technologies, Carlsbad, USA) without supplements; one ml was used to seed each well of a six well plate. The medium was changed after 24 hours, the cells washed twice with PBS-PSA 72 hours after seeding and every other day afterwards. Using this protocol cells were maintained for up to 8 weeks (5 passages). Experiments were performed between passage 3 and 4.

4. ETHICAL APPROVAL

The use of vaginal tissue was approved by the Newcastle and North Tyneside Research Ethics Committee (REC reference 2003/11). Surgical specimens of the human vaginal tissue were collected after receiving informed consent. Samples were obtained from patients undergoing surgical removal of vaginal prolapses.

2.3. BACTERIAL CULTURE

All compounds for bacteriological media and agar were purchased from Oxoid (Basingstoke, UK). Bacteria were grown in LB-media composed of 10 % (w/v) Bacto-tryptone, 10 % (w/v) sodium chloride and 5 % (w/v) Bacto-yeast extract diluted in deionised water. The pH of the LB-medium was set to 7.4 by the addition of 5M NaOH and sterilised at 121 °C for 20 minutes at 15 PSI. For LB-Agar, the above described LB-medium was supplemented by 3 % (w/v) of Agar before being sterilised.

E. coli DH5 α competent cells were mixed with plasmid, incubated 30 minutes at 4 °C, 40 seconds at 42 °C and further 30 minutes at 4 °C before plating on LB-Agar-XGal-(5-bromo-4-chloro-3-indoyl-beta-galactopyranoside dissolved in DMSO) Ampicillin plates (X-Gal and ampicillin working concentrations were 50 μ g/ml and 0.1 mg/plate, respectively). Transformed colonies were further multiplied in LB-Amp medium with a working concentration of 0.1 mg/ml of ampicillin and the plasmid isolated as described in section 2.7.

2.4. TRIZOL RNA ISOLATION

The isolation of mRNA was performed using TRIzol (Invitrogen, Carlsbad, USA). Briefly, the medium bathing the eukaryote cells was removed and the cells were washed twice using PBS. The cells were incubated for 5 minutes at room temperature in one ml TRIzol (Invitrogen, Carlsbad, USA) per well of a six well plate and 200 μ l per well of a 96 wells plate. The phase separation was initialised by adding 20 % of chloroform of the initial TRIzol volume and gently shaking the tubes for 15 seconds. The mixture was incubated for 3 minutes at room temperature and the aqueous phase separated from the organic phase by centrifugation at 12000 x G for 15 minutes at 4 °C. The aqueous phase was collected and the RNA precipitated in 500 μ l isopropanol for 16 hours at -80 °C.

The RNA was collected by centrifugation at 12000 x g for 10 minutes at 4 °C and washed using one ml of 75 % ethanol. The supernatant was discarded and the RNA pellet was resuspended in 20 µl MilliQ H₂O. The dissolved RNA was incubated for 10 minutes at 65 °C and stored at -80 °C.

2.5. POLYMERASE CHAIN REACTION

1. DNASE TREATMENT

To reduce genomic DNA contamination, purified RNA was DNase treated (Promega kit Southampton, UK), as shown below.

4.5 µg	RNA
4.5 µl	DNase [1 U/µl]
2.0 µl	10 x Reaction Buffer (400mM Tris-HCL, pH 8.0, 100mM MgSO ₄ , 10mM CaCl ₂)
<hr/>	
20 µl	reaction volume (adjusted using MilliQ water depending on the RNA concentration)

After 30 minutes at 37 °C the reaction was stopped by adding 4 µl DNase Stop solution (Promega, Southampton, UK) and incubating at 65 °C for 10 minutes.

2. REVERSE TRANSCRIPTION

The DNase treated RNA was transcribed to cDNA by incubation with a reverse transcriptase isolated from a murine leukaemia retrovirus (MuLV, Applied Biosystems, UK) at 42 °C for one hour. The reaction contained:

10 µl	DNased RNA (1.875 µg)
3.2 µl	MgCl ₂ [25 mM] (Applied Biosystems, UK)
4 µl	10 x NH ₄ Buffer (Applied Biosystems, UK)
16 µl	dNTPs [10mM] (Bioline, UK)
2 µl	Oligo dT [15mM] (Promega, Southampton, UK)
1 µl	MuLV Reverse Transcriptase (Applied Biosystems, UK)
1 µl	RNase inhibitor (Promega, UK)
2.8 µl	MilliQ water
<hr/>	
40 µl	reaction volume

The reaction was stopped by increasing the temperature to 95 °C for five minutes. The cDNA was used for PCR experiments, including endpoint and qPCR.

3. POLYMERASE CHAIN REACTION

DNA amplification was conducted using a modified method of the technique developed by Mullis *et al.*(1986)¹³⁹. The amplification was performed using two different polymerases. For general gene expression a type A polymerase isolated from *Thermus aquaticus* (*Taq*) was used. It exhibits 5'→3' synthesis and 5'→3' exonuclease activity¹⁴⁰. For products used in cloning, a modified type B polymerase was used isolated from *Thermococcus kodakaraensis* (KOD). It exhibits 5'→3' synthesis and a 3'→5' proofreading exonuclease activity^{141,142}. The quantitation of gene expression was performed using a LightCycler SYBR Green I Master (Roche, Mannheim, Germany), which uses a modified version of the before mentioned *Taq*-polymerase.

4. PRIMERS

Primers were specifically designed for each gene using the NCBI Primer-Blast design tool¹⁴³. A prerequisite for the primers was that they were located in two different exons or spanning over an exon-exon junction. The retrieved primers were further analysed for hetero- and homodimer formation, as well as hairpin formation using Netprimer Software (<http://www.premierbiosoft.com/netprimer/>). The optimal temperature for each set of gene primers was detected using a temperature gradient and analysing the product using Gel-electrophoresis for endpoint PCR and/or melting curve analysis when using qPCR. The sequences of the primers used are listed in Table 2.1:

Table 2.1 List of primers used in endpoint and quantitative PCR. Small letters in bold show the restriction sites for HindIII and KpnI normal small letters show additional nucleic bases to maintain the reading frame.

Primers used in qPCR assays:

Gene	Direction	Sequence	T _m /°C	Product size
h-βD-3 qPCR Marcelo Lanz	Forward	CTTTGCTCTTCCTGTTTTGG	57	134 bp
	Reverse	CGATCTGTTCTCCTTTGG		
h-βD-3 qPCR Kalus <i>et al.</i>	Forward	GTGAAGCCTAGCAGCTATGAGGAT	60	89 bp
	Reverse	TGATTCTCCATGACCTGGAA		
GAPDH	premixed	unknown (commercial primer)	60	unknown

Primers used in Endpoint-PCR assay:

Gene	Direction	Sequence	T _m /°C	Product size
h-βD-3	Forward	CAGCGTGGGGTGAAGCCTA	65	224 bp
	Reverse	CTTTCTTCGGCAGCATTTTCGG		
TLR-6	Forward	GGGACTTTTCTGGTTGTCTTAG	55	777 bp
	Reverse	CATTATCTGGCTGACCTCTTG		
Dectin-1	Forward	GACAATGCTGGCAACTGGGC	61	330* bp
	Reverse	CTCTCCTTCTCCACCCTTCCTC		

* expected size for isoform 1

Primers used in cloning assays:

Gene	Direction	Sequence	T _m /°C	Product size
promoter h-βD-2 2000 bp	Forward	CTGGACACTGGTCTCATCTG	55	2000 bp
promoter h-βD-2	Reverse	CTGGGGAGGACATCAAGC		
promoter h-βD-2 2000 bp – KPNI	Forward	tttggtaccCTGGACACTGGTCTCATCTG	61	2020 bp
promoter h-βD-2 - HindIII	Reverse	ttaagcttttCTGGGGAGGACATCAAGC		

5. *TAQ* POLYMERASE

PCR using *Taq* polymerase was used to amplify plasmid DNA or cDNA. 10 μ l of cDNA and 1.2 ng/ml of plasmid DNA were used. All reactions used 35 cycles of amplification unless stated otherwise. The following volumes of reagents were used:

0.8	μ l	MgCl ₂ [50 mM] (Bioline, UK)
4	μ l	10 x NH ₄ Buffer (Bioline, UK)
0.5	μ l	<i>Taq</i> Polymerase (Bioline, UK)
4	μ l	Primer (2 μ l of forward and 2 μ l reverse primer (both 10 μ M); IDT DNA, UK)
8	μ l	dNTPS [10mM](Bioline, UK)
40	μ l	reaction volume adjusted using MilliQ H ₂ O

The PCR conditions were:

Polymerase activation	95 °C	2 min	
Denaturation	95 °C	30 sec	} 35 cycles
Annealing	T _m	30 sec	
Extension	72 °C	30 sec	
Final extension	72 °C	12 min	

DNA bands were visualised by agarose-gel electrophoresis.

6. *KOD*-POLYMERASE

A modified *Kod*-hotstart polymerase (Novagen, Darmstadt, Germany) was utilised according to the manufacturer's recommendation. Each reaction was set up as follows:

5	μ l	10 x Buffer
3	μ l	MgSO ₄
5	μ l	dNTP
31.5	μ l	PCR grade H ₂ O
3	μ l	Primer (2 μ l of forward and 2 μ l reverse primer (both 10 μ M); IDT DNA, UK)
0.5	μ l	<i>KOD</i>
2	μ l	DNA
50	μ l	reaction volume

The PCR conditions were dependent on the product's size:

Polymerase activation	95 °C	2 min	
Denaturation	95 °C	20 sec	} 30 cycles
Annealing	Tm	10 sec	
Extension	68 °C	25 sec	

cDNA bands were either visualised by agarose gel electrophoresis, purified for DNA cloning or sequenced.

7. QUANTITATIVE PCR

The quantitation of gene expression was performed using a LightCycler 480 (Roche, UK). The reaction was conducted using LightCycler 480 SYBR Green I Master mix. SYBR green is a chemical compound that intercalates with double stranded DNA and is excited at 486 nm and emits light at 521 nm. The amount of fluorescence is directly dependable to the amount of double stranded DNA, since there is a surplus of SYBR green in the reaction. Therefore the concentration of double stranded DNA can be quantitated.

Each reaction was set up as follows:

5	µl	qPCR SYBR Green I Mastermix
2.5	µl	cDNA or Plasmid
1.5	µl	MilliQ H ₂ O
1	µl	Primer
10	µl	Reaction volume

The protocol for the reaction was:

Preincubation	95 °C	10:00	
Amplification	95 °C	00:10	} 40 cycles
	60 °C	00:30	
	72 °C	00:10	
Melting curve	95 °C	00:05	
	70 °C	00:01	
Cooling	4 °C	00:10	

After each run, the amplification curves were analysed using the LightCycler 480 software (Roche, UK) to determine a C_q -(*quantitation cycle*) value and the amplification of a single product was verified by analysis of the melting curves¹⁴⁴.

8. CLONING OF CALIBRATOR PLASMID

The MIQE guidelines state that determination of the PCR efficiency is pivotal for accurate quantitation of RNA¹⁴⁴. Hence, the efficiency was determined using a calibration curve created from a serially diluted cloned PCR product (see section 5.3.I for details). A 224 bp PCR product of the h β D-3 gene was cloned into pGem-T Easy (Promega, Southampton, UK) following the manufacturer's recommendations. Briefly, the DNA was isolated using the MinElute Gel Extraction kit (Qiagen, Hilden, Germany) and 30ng of the isolated DNA were ligated into 50 ng of pGem-T easy by the addition of 3 Weiss units of T4 DNA ligase and 5 μ l Rapid ligation buffer (both Promega, Southampton, UK). The ligation was performed for 16 hours at 4 °C, before being transformed into competent *E. coli* DH5 α , as described in section 2.3.

2.6. SABIOSCIENCES TLR-PLATE ASSAY

1. RT4 CHALLENGE, RNA ISOLATION AND DNASE TREATMENT

The expression of 84 genes associated with TLRs was determined using a gene array plate (SABiosciences, Qiagen, Hilden, Germany). RT4 cells were challenged with

5×10^4 CFU/ml for four hours with the *E. coli* strains K-12, NU14, NCTC 10418 and PBS. The RNA was collected using TRIzol, purified using the method described in section 2.4, and further purified using RNeasy columns (QIAGEN, Hilden, Germany), to increase the purity and perform an on-the-column DNase treatment, as recommended by the TLR-gene array manufacturer. Briefly, the RNA was diluted in 100 μ l MilliQ H₂O, mixed with 350 μ l RLT buffer and precipitated by adding 250 μ l of ethanol. The mixture was added to a RNeasy column and centrifuged at 8000 x g for 15 seconds at room temperature. The on column DNase digestion was performed by adding 350 μ l of RW1 buffer to the column followed by a centrifugation at 8000 x g for 15 seconds at room temperature. A mixture of 10 μ l of DNase in 70 μ l of RDD buffer was added to the column and incubated for 15 minutes at room temperature. The DNase was washed off the column by adding 350 μ l of RW1 buffer and centrifuging at 8000 x g for 15 seconds at room temperature. The column was washed twice with 500 μ l of RPE buffer followed by centrifugation at 8000 g for two minutes. The RNA was eluted from the column using 30 μ l of MilliQ H₂O and further analysed using Agilent® Bioanalyzer. The concentration was determined by a NanoDrop 2000 (Thermo Scientific, Waltham, USA)

2. AGILENT RNA CONTROL ASSAY

The integrity of the RNA was assessed using the Agilent RNA 6000 Nano Kit according to the manufacturer's protocol. The RNA chip was prepared by adding 550 μ l of gel to a spin filter and centrifuging at 1500 x g for 10 minutes. 65 μ l of the flow through were mixed with one μ l of RNA 6000 Nano dye and centrifuged at 13000 x g for 10 minutes. Gel-dye mix (27 μ l) was added to the RNA Nano chip followed by the RNA 6000 Nano marker which was then followed by the loading marker.

The ladder and the RNA samples were denatured at 70 °C for 2 minutes and one µl of each was loaded onto the chip, vortexed at 2400 rpm using the Vortex Mixer MS2-S8 (IKA Works, Staufen, Germany) for 1 minute and loaded on an Agilent 2100 Bioanalyzer. The experiment was performed and analysed using the Agilent 2100 software. A RIN (RNA integrity number) above a threshold of 7 was required for downstream applications.

3. RT-QPCR

Once RIN values indicated good quality nucleic acid the RNA was reverse transcribed and gene expression quantitated using a LightCycler 480, and primers available on the pre-coated 96 wells plates. For reverse transcription a RT² first strand kit (SABiosciences, QIAGEN, Hilden, Germany) was used and the procedure performed according to the manufacturer's instructions. The RT-sample was diluted in 1350 µl of H₂O and mixed with 1350 µl of 2x RT² SYBR Green Mastermix. 25 µl of the mix was added to each well of the plate and expression was measured with the LightCycler 480 (Roche diagnostics), using the following setup:

Polymerase activation	95 °C	10 min	
Denaturation	95 °C	15 sec	} 45 cycles
Annealing	60 °C	1 min	

The C_qs were calculated using the LightCycler 480 software and analysed using the SABioscience predesigned Microsoft Excel spread sheet.

2.7. PCR AND PLASMID PURIFICATION

PCR products used for cloning were purified using MiniElute PCR purification kit (Qiagen, Hilden, Germany). DNA bands visualised on agarose gels were purified using the QIAquick gel extraction kit (Qiagen, Hilden, Germany). Plasmids of transformed DH5 α strains were isolated using the Plasmid Mini kit (Qiagen, Hilden, Germany). All purifications were performed according to the manufacturer's recommendations.

2.8. PROTEIN CONCENTRATION DETERMINATION

Protein concentrations were determined using a 660 nm Protein Assay or Bradford assay (both Pierce Protein, Thermo Fisher Scientific, Waltham, USA). For the 660 nm protein assay, a calibration curve was established using BSA concentrations ranging from 50 $\mu\text{g/ml}$ to 2000 $\mu\text{g/ml}$. 10 μl of the standard, sample or blank (H_2O or PBS) was added in triplicate to a 96 wells plate and 150 μl of 660 nm assay reagent added. The plate was covered, shaken gently for one minute and incubated for five minutes at room temperature before reading the absorbance at 660 nm using a FluoStar Omega plate reader (BMG Labtech, Ortenberg, Germany). The sample concentration was calculated using the standards as calibrators.

The Bradford assay was performed in a 96 wells plate and the same range of standards was used as for the 660 nm protein assay. Five μl of standard, sample or blank were added to 250 μl of comassie blue reagent (Pierce, Thermo Fisher Scientific, Waltham, USA), the plate was shaken for 30 seconds and incubated for 10 minutes at room temperature. The absorbance at 595nm was read using a FluoStar Omega plate reader (BMG Labtech, Ortenberg, Germany). All measurements were made in triplicate. The sample concentration was calculated using the standards as calibrators.

2.9. PROTEIN ANALYSIS USING SDS-PAGE

1. 10 % TRICINE-GELS

Proteins were separated using electrophoresis according to Schagger and von Jagow¹⁴⁵. Briefly, Tricine separation gel (10 % Total acrylamide concentration, with 3 % crosslinking) was prepared by mixing 4.7 ml of 40 % acrylamide/bis-acrylamide (mix ratio 19:1), with 9.4 ml of separation gel buffer [0.75 M Tris, 0.2 % SDS, pH 8.8], 4.6 ml H₂O, 90 µl of APS (10 %) and 30 µl of TEMED. The mixture was poured gently into a gel tank and the stacking gel was prepared while the separation gel polymerised. For a 4 % stacking gel, a volume of 380 µl of acrylamide/bis-acrylamide (40 % total acrylamide concentration, 3 % crosslinking) was mixed with 1.5 ml H₂O and 1.9 ml of stacking gel buffer [0.25M Tris, 0.2 % SDS-buffer, pH 6.8]. The polymerisation of the stacking gel was initiated by adding 30 µl of APS (10 %) and 10 µl of TEMED. Protein samples (10.4 µl) were denatured in 1.6 µl SDS reducing buffer containing 4 µl of loading buffer and following incubation at 37 °C for 15 minutes. Ten µl of the reduced protein sample were loaded onto the stacking gel and electrophoresed for 2 hours at 200V.

2. 4 %-12 % NOVEX NUPAGE®

For western blots, the commercially available NOVEX® NuPAGE® (life technologies Carlsbad, USA) precast gels were used according to the manufacturer's recommendation. Briefly, 6.5 µl of protein sample was treated with 2.5 µl of NuPAGE LDS sample buffer, 1 µl of NuPAGE reducing agent and incubated at 70 °C for 10 minutes. After loading onto the gel the protein samples were electrophoresed for 40 minutes at 200 V. Gels were either stained using coomassie brilliant blue G250 (Pierce, Thermo Scientific, Waltham, USA) or used for western blotting.

2.10. FLAGELLIN PURIFICATION

Flagellin isolation was performed in collaboration with Dr Phillip Aldridge and using *E. coli* NCTC 10418. The method of flagellin was adapted from Smith *et al.*¹⁴⁶. Briefly, the *E. coli* strain NCTC 10480 was grown overnight on LB-Agar (3 %), one colony selected and grown for 16 h at 37 °C, with shaking. The overnight culture was diluted 10 fold and the OD₆₀₀ measured. The following equation was used to calculate the volume of bacteria required to inoculate 1 L of LB at a starting OD₆₀₀ of 0.05:

$$\frac{10 * OD_{600nm}}{0.05} = \text{dilution factor} \rightarrow \frac{\text{final culture volume}}{\text{dilution factor}} \\ = \text{volume of overnight culture needed}$$

The one litre bacterial culture was grown until an OD_{600nm} of 0.6. The cells were harvested at 5000 g min at 4 °C, washed twice in 30 ml ice-cold phosphate-buffered saline (PBS) and resuspended in 30 ml ice cold PBS. The flagellin was twice separated from the cells by shearing using a blending stick at 13500 rpm for 1 min with an ice cooling step in between. The cell suspension was re-centrifuged for 15 min at 6000 x g, the supernatant decanted into a 50 ml ultraclear ultracentrifugation tube and centrifuged at 100000 x g for one hour at 4 °C. The supernatant was decanted off, the pellet washed twice with ice cold PBS, resuspended in 1 ml ice cold PBS, left for 16 h at 4 °C to dissolve completely and stored at -20 °C. The flagellin was further purified by depolymerisation at 70 °C for 15 min, filtration through a 0.22 µm filter and size exclusion. Three batches were prepared. Protein concentration was measured using the Bradford Assay.

2.11. EUKARYOTE CELL TRANSFECTION

NF- κ B reporter constructs and promoter constructs were transfected transiently into the RT4 and VK-2 E6/E7 cell lines. Two different transfection technologies to maximise cell survival rate and transfection efficiency were utilised.

1. ATTRACTENE

Attractene (QIAGEN, Hilden, Germany) is a lipid based transfection reagent, which binds DNA in liposomes and fuses with the cell membrane introducing the DNA into the cell. The transfection was optimised using the manufacturer's recommended Attractene-DNA ratio. Attractene was used to transfect the VK-2 E6/E7 cells and was the transfection method utilised in the h β D-2 promoter study (Chapter 4). The optimised transfection conditions for VK-2 E6/E7 cells were:

135 ng of plasmid DNA were diluted in 50 μ l TE Buffer together with 0.5 μ l of Attractene reagent. The Attractene-DNA sample was mixed and stored for 15 minutes at room temperature. During the incubation period, VK-2 E6/E7 cells were trypsinised, resuspended to 5×10^4 cells per 150 μ l of media and added to each well of a 96 wells plate. The Attractene-DNA mix was added to the cells and the well contents gently mixed. The cells were incubated for 16 hours before the challenge experiments.

2. TURBOFECT

The second transfection reagent used was TurboFect (Thermo Fisher Scientific, Waltham, USA), a cationic polymer which binds DNA and is uptaken by cells via endocytosis. TurboFect was used to transfect RT4 cells. The transfection was optimised using the manufacturer's recommended TurboFect-DNA ratios. The optimised concentration was used to study the h β D-2 promoter activation in RT4 cells.

150ng of plasmid DNA was resuspended in 20 μ l serum free Opti-MEM (Life Technologies, Carlsbad, USA) medium together with 0.3 μ l of TurboFect and incubated for 15 minutes at room temperature. During the incubation period RT4 cells were harvested by trypsinisation, resuspended to 5×10^4 cells per 180 μ l of media and added to each well of a 96 wells plate. 20 μ l TurboFect-DNA mix was added to each well and the well contents gently mixed. The cells were incubated for 16 hours at 37 °C, 5 % CO₂ before the challenge experiments.

2.12. PROMOTER REPORTER CONSTRUCT

1. BIOINFORMATICS

DNA sequences (2 kbp) of the 5' non-translated regions of the h- β D-2 (DEFB4) and h- β D-3 (DEFB103) genes were analysed for transcription factor binding sites using the PROMO software (http://alggen.lsi.upc.es/cgi-bin/promo_v3/promo/promoinit.cgi?dirDB=TF_8.3). Sites of interest were NF- κ B, AP-1, and those responsive to vitamin D, vitamin A, and oestrogen. The primers specific to the region were used to amplify the region of interest using KOD polymerase. The amplicons were cloned into two reporter systems utilising either GFP (pGLOW TOPO vector, Life technologies, Carlsbad, USA) or Luciferase (pGL4.10, Promega, Southampton, UK).

2. CLONING USING PGLOW TOPO VECTOR

The amplicon was cloned into the pGLOW TOPO vector (Life technologies, Carlsbad, USA) according to the manufacturer's recommendations. Briefly, following synthesis, the amplicon was treated with 0.5 units of *Taq* polymerase for 10 minutes at 72 °C in the presence of 2 mM dATP, 1x PCR buffer and 0.8 μ l of 25 mM MgCl₂, and the product purified (section 2.7). 4 μ l of the purified PCR product were mixed with 1 μ l of pGLOW TOPO vector in the presence of 1 μ l of diluted salt solution, and incubated for

20 minutes at room temperature. Competent DH5 α cells were transformed with the cloned product, and transformed bacteria selected by blue/white screening LB-agar plates, using IPTG [0.1 mM], XGal [50 μ g/ml], ampicillin [100 μ g/ml]. The white colonies were picked, each grown in 5 ml LB containing 100 μ g/ml ampicillin and plasmid isolated using a plasmid miniPrep kit (see section 2.7).

3. CLONING USING PGL4.10

The DNA amplicon was amplified using primers flanked by restriction sites and purified using a PCR purification kit (QIAGEN, Hilden, Germany). It was cleaved with appropriate restriction enzymes (HindIII and KpnI) and purified using the PCR purification kit. The cleaved amplicon was ligated into pGL4.10. The reaction was set up as follows:

pGL4.10	10 μ l
insert	2 μ l
Ligase	1 μ l
Ligase buffer	1 μ l
<hr/>	
Total reaction	14 μ l

The ligation product was transformed into DH5 α as described previously. Single white colonies were picked and further analysed (section 4.5).

2.13. REPORTER GENE ASSAY

The reporter gene assays were used to analyse the NF- κ B activity of RT4 and VK-2 E6/E7 challenged cells. Additionally, the h β D-2 promoter study was conducted using reporter vectors.

1. LUCIFERASE BASED REPORTER

RT4 cells stably transfected with RT4-NF κ B¹³⁷ were collected by trypsinisation and the cell count per ml determined using a ZM Coulter Counter (Coulter Scientific Instruments, Hialeah, USA). 5×10^4 cells/ml were seeded into each well of a white 96 wells plate, with clear bottom (#3610, Corning, Corning, USA).

For the promoter reporter assays: the RT4 or VK-2 E6/E7 cells were transfected as described in section 2.11. After 16 hours of incubation at 37 °C and 5 % CO₂, the confluent eukaryote cells were challenged with either bacterial cells or PAMPs (further details are presented in Chapter 3 and 4). Following challenge, the media bathing the cells was collected in microcentrifuge tubes and stored at -20 °C. The cells were lysed using RLB (Promega, Southampton, UK) for 16 hours at -80 °C. The luciferase concentration was measured by adding 100 μ l of luciferin (Promega, Southampton, UK) and the resulting luminescence was measured using a FluoStar Omega microplate reader (BMG Labtech, Ortenberg, Germany). The values of the PBS challenged samples were used to normalise the results and results were presented as fold increase compared to the negative control.

2. GREEN FLUORESCENT PROTEIN BASED REPORTER

The NF- κ B reporter kit Cignal NF- κ B was used for the NF- κ B activity measurements in VK-2 E6/E7 cells. Briefly, the cells were transfected with reporter DNA using TurboFect (see section 2.11) and after 16 hours at 37 °C and 5 % CO₂, challenged as described in section 2.14.

RT4 cells were transfected with the h β D-2 promoter reporter (see section 2.11). Following challenge the media bathing the cells was collected and stored at -20 °C.

Fluorescence was measured using a FluoStar Omega microplate reader (BMG Labtech, Ortenberg, Germany) with filters for 480 nm for the excitation and 530 nm for the emission filter.

2.14. HUMAN UROGENITAL EPITHELIA CHALLENGE EXPERIMENTS

1. ESCHERICHIA coli STRAINS

Four laboratory strains of *E. coli* were used. The strains are summarised in Table 2.2:

Table 2.2 *Escherichia coli* strains

Strain	Source
<i>E. coli</i> K-12	Long established strain isolated from the Gut (1922) ⁵
<i>E. coli</i> NCTC 10418	Isolated in 1947. Used for antimicrobial and disinfecting testing (personal communication Dr Ased Ali)
<i>E. coli</i> NU14	Laboratory UPEC strain isolated from a cystitis infection ²⁴
<i>E. coli</i> CFT073	Isolated from a pyelonephritis infection in 1990; genome sequenced ¹⁴⁷

The archetypal strain K-12 and the strain NCTC 10418 were kind gifts of Dr John Perry (Freeman Hospital, Newcastle). Two UPEC strains were used, CFT 073, ATCC 700928, and NU14 (a gift of Professor Neil Sheerin). Additionally, 24 UPEC strains collected from patients by Dr Kathy Walton (Freeman Hospital, Newcastle) were analysed. For the *in vitro* challenge experiments dead bacteria were used and prepared as follows: *E. coli* strains were grown in 10 ml of LB overnight, the OD₆₀₀ of the culture was determined and used to inoculate 10 ml LB to achieve an OD₆₀₀ of 0.1. The following equation was used to calculate the volume needed for 0.1 OD₆₀₀:

$$\frac{10 * OD_{600nm}}{0.1} = \text{dilution factor} \rightarrow \frac{\text{final culture volume}}{\text{dilution factor}}$$

$$= \text{volume of overnight culture needed}$$

The bacterial culture was incubated at 37 °C with shaking until an OD₆₀₀ of 0.6 was attained and then kept on ice. The culture was diluted to 10⁻⁵ to 10⁻⁸ of the original concentration and 10 µl plated onto LB-Agar plates. The actual CFU/ml was determined after incubating the plates for 16 hours at 37 °C and counting the bacterial colonies. The remaining culture was pelleted by centrifugation at 13000 x g for 10 minutes, the cells were washed twice with PBS and resuspended in one ml of PBS. The bacteria were killed by incubating for 20 minutes at 100 °C. Killing was verified by plating 10 µl of the culture diluted in PBS on a LB-agar plate and incubating overnight at 37 °C.

The dead bacterial stock was diluted to a concentration of 10⁷ CFU/ml and challenges were performed using 5 x 10⁴ CFU/ml /well. For eukaryote cell challenges the appropriate volume of the bacterial stock was diluted in 200 µl of RT4 or VK-2 E6/E7 medium.

2. PAMPS

Different PAMPs were used to activate different receptors present on the uro- and vaginal epithelial cells. The PAMPs used are described in Table 2.3:

Table 2.3: PAMPs used to challenge RT4 and VK-2 E6/E7 cells

PAMP	Source	Challenge concentration	Stock concentration	catalogue number (supplier)
LPS O55:B5	<i>E. coli</i>	10 µg/ml	1 mg/ml	L6529-1mg (Sigma-Aldrich, St Louis, USA)
LPS O26:B6	<i>E. coli</i>	10 µg/ml	1 mg/ml	L2654-1mg (Sigma-Aldrich, St Louis, USA)
LPS O111:B4	<i>E. coli</i>	10 µg/ml	1 mg/ml	L4391-1mg (Sigma-Aldrich, St Louis, USA)
Peptidoglycan	<i>E. coli</i>	10 µg/ml	2 mg/ml	PGN-EB (Invivogen, San Diego, USA)
Flagellin	<i>E. coli</i>	250 ng/ml	10 µg/ml	Own production
Zymosan	<i>S. cerevisiae</i>	50 µg/ml	1 mg/ml	Z4250-1G (Sigma-Aldrich, St Louis, USA)

3. BLOCKING OF TLR USING MONOCLONAL ANTIBODY

The activation of TLR-5 and of TLR-2 was inhibited by incubating the RT4 NF-κB cells with 5 µg/ml of mouse monoclonal TLR-5 antibody (maba2-htr5, Invivogen, San Diego, USA) and 10 µg/ml of chimeric monoclonal TLR-2 antibody (anti-hTLR2-IgA, Invivogen, San Diego, USA), 2 hours prior to the challenge with flagellin, bacteria or Zymosan.

4. MOTILITY DETERMINATION OF *E. COLI* STRAINS

The motility of *E. coli* strains was determined by Dr Phillip Aldridge (ICaMB, Newcastle University) by incubating *E. coli* strains on a reduced concentration of agar growth medium [0.3 % Agar (w/v), 1 % tryptone (w/v), 0.5 % NaCl (w/v)]. The strains were incubated at 37 °C for eight hours and the motility was detected by the identification of a halo.

2.15. PROTEIN IDENTIFICATION USING WESTERN BLOTTING

The expression and phosphorylation of SYK was assessed using the Phospho-SYK antibody sampler kit (#9905, Cell signalling, Beverly, USA). Eukaryote cells were lysed

using RIPA lysis buffer (R0278, Sigma-Aldrich, St Louis, USA). The cell lysates were analysed using 4-12 % NuPAGE precast gels (Life Technologies, Carlsbad, USA). Following electrophoresis proteins were transferred to nitrocellulose using a HEP-1 semi-dry western blot cassette system (Thermo Scientific, Waltham, USA). The setup of the western blot was as follows:

Anode (+) → 3 filter papers → nitrocellulose membrane → electrophoresed gel → 3 filter papers → cathode (-)

Prior to the blotting, the filter paper and the nitrocellulose membrane were soaked in western blot transfer buffer (25 mM Tris, 0.2 M Glycine and 20 % Methanol). The protein transfer from the gel to the membrane was performed at 10 V for 60 minutes.

The nitrocellulose membrane was blocked using 50 % blocking buffer (Li-Cor, Lincoln, USA), diluted in PBS, for one hour at room temperature. The membrane was washed, incubated with the primary antibody at a concentration of 1:1000 for SYK (#12358 for total SYK and #2711 for Phospho-SYK, both Cell Signaling) for 16 hours, at 4 °C or at 1:5000 for β -actin (SC-1616, Santa Cruz, Dallas, USA) for one hour at room temperature. The membrane was washed six times (10 minutes/wash) using PBS-Tween20 (0.1 %), incubated for 45 minutes at room temperature with an appropriate secondary reporter antibody (PN 926-32213, Li-Cor, Lincoln, USA for total SYK or Phospho-Syk and PN 926-32224 for β -actin) diluted at 1:5000, in 0.01 % SDS, 0.1 % Tween 20, 50 % blocking buffer, PBS. The membrane was finally washed six times with PBS-Tween20 for 10 minutes and then scanned using an Odyssey membrane reader (Li-Cor, Lincoln, USA).

2.16. ELISA

The enzyme-linked immunosorbent assay (ELISA) is a powerful technique to measure the concentration of an antigen in a solution. Two types of ELISA were used in this investigation. Both types are shown in Figure 2.1:

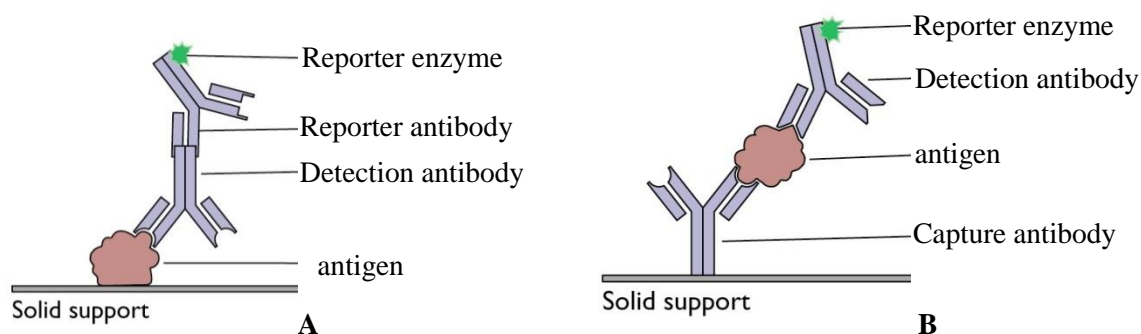


Figure 2.1. Principle of an Enzyme-Linked ImmunoSorbent Assay(ELISA). (A) indirect ELISA. where the antigen is immobilised on the solid support. (B) sandwich ELISA. The capture antibody is immobilised on the solid support. Image adapted from: <http://www.virology.ws/wp-content/uploads/2010/07/elisa.jpg>

The measurement of an antigen in an indirect ELISA is done with a single specific antibody (Fig. 2.1.A). The antigen is immobilised in a well (MaxiSorp) and detected by the antibody. The detection antibody is recognised by a reporter antibody (Fig. 2.1.A) which is linked to the enzyme horseradish peroxidase (HRP). The unbound detection and reporter antibodies are washed off by a sorbent solution. HRP reacts with its substrate (TMB) causing a change of colour to the blue spectrum. The substrate is reduced by a strong acid (1M HSO₄) changing its colour from blue to yellow. The absorbance of the substrate solution is then read at 450 nm.

The indirect ELISA is less sensitive and should only be used in the absence of two specific antibodies. A sandwich ELISA (Fig. 2.1.B) is the method of choice to detect the protein concentration. It is a modified indirect ELISA.

In addition to the detection antibody, a capture antibody is used. It ‘catches’ the antigen from the solution therefore filtering the antigen out of the solution. Assay sensitivity is therefore increased. Additionally the detection antibody is conjugated with biotin.

Biotin binds specifically to avidin or streptavidin. The HRP is linked to the streptavidin, making the use of a reporter antibody obsolete. Enzymatic reaction of the HRP-substrate and reading are the same as in the indirect ELISA.

1. INDIRECT ELISA

All ELISAs were performed using 96 wells plates MaxiSorp (Nunc, Roskilde, Denmark). A h β D-3 standard was prepared ranging from 0.1 to 1 ng/ml. One hundred μ l of the standard or media removed from challenged eukaryote cells were immobilised on a 96 wells plate (MaxiSorp Nunc, Roskilde, Denmark) for 16 hours at room temperature. The plate was washed five times using 300 μ l of PBS-Tween 20 (0.1 %), blocked using 250 μ l of 5 % non-fat dry milk dissolved in PBS containing 0.1 % Tween 20 (Sigma-Aldrich, St Louis, USA) (MPBST) for two hours at room temperature and then washed five times with 300 μ l of PBS-Tween 20 (0.1 %). For optimisation, 100 μ l of the detection antibody at different concentrations were used to detect the synthetic h β D-3 protein. After optimisation, 2 μ g/ml of detection antibody (ab109572, ABCAM, UK) diluted in MPBST were used to detect the synthetic h β D-3 and incubated for 16 hours at 4 °C. A reporter antibody (A0545-1ML, Sigma-Aldrich, St Louis, USA) was diluted in MPBST (1:2000), 100 μ l added to each well and incubated for one hour at room temperature, before washing using 300 μ l of PBS-Tween20/well. 100 μ l aliquots of TMB (T0440, Sigma-Aldrich, St Louis, USA) were added to each well and left for 25 minutes at room temperature, in the absence of light. The reaction was stopped using 100 μ l of 2 M H₂SO₄. The absorbance was read at 450 nm using a FluoStar Omega plate reader (BMG Labtech, Ortenberg, Germany).

2. SANDWICH ELISA

The secretion of hβD-3 was initially analysed via an indirect ELISA but due to its low sensitivity a sandwich ELISA was developed (see Chapter 5 for details). All reagents used, apart from the antibodies, were from the BD optEIA ELISA kit and all washing steps were carried out using 300 µl of washing buffer (BD Biosciences, Franklin Lakes, USA).

The primary or capture hβD-3 antibody (ab109572, ABCAM, Cambridge UK) was diluted to a concentration of 0.5 µg/ml in coating buffer (BD Biosciences, Franklin Lakes, USA) and 100 µl of the capture hβD-3 antibody were added to each well on a 96 wells plate. The sealed plate was incubated at 4 °C for 16 hours, the wells washed three times before being blocked with 200 µl blocking buffer (BD Biosciences, Franklin Lakes, USA) for two hours at room temperature. The wells were washed three times, the standards were prepared in cell growth media using synthetic hβD-3 (Peptide Inc., Osaka Japan), ranging from 31.25 pg/ml to 1000 pg/ml. 100 µl of standard or sample were added and the plate incubated for two hours at room temperature before being washed five times. The secondary or detection antibody (ab84234, ABCAM, Cambridge UK), conjugated with biotin and at a concentration of 0.25 µg/ml, was mixed with SA-HRP (1:250, BD Biosciences, Franklin Lakes, USA) in blocking buffer. 100 µl of detection antibody-SA-HRP mixture were added to the wells and incubated for one hour at room temperature. The plate was finally washed seven times and 100 µl of a HRP substrate solution (TMB based, Reagent A and B at a ratio of 1:1, BD Biosciences, Franklin Lakes, USA) was added to the wells. The enzymatic reaction, protected from light, occurred for 30 minutes at room temperature, before being stopped by the addition of 50 µl of Stop solution (BD Biosciences, Franklin Lakes, USA). The final result was measured by reading the absorbance at 450 nm, with a correction using

the 570nm absorbance, using a FluoStar Omega plate reader (BMG Labtech, Ortenberg, Germany). The samples were diluted if their absorbance was not in the range of the standard curve and the ELISA repeated.

3. INTERLEUKIN-8

To measure IL8 concentrations the BD optEIA IL-8 kit (BD Bioscience, Franklin Lakes, USA) was utilised. During the ELISAs the washing steps were carried out using 300 µl of washing buffer (BD Biosciences, Franklin Lakes, USA). In each case, the primary antibody was diluted 1:250 in coating buffer (BD Biosciences, Franklin Lakes, USA) and, using a 96 wells plate, 100 µl were added per well,. The sealed plate was incubated at 4 °C for 16 hours, washed three times, blocked with 200 µl blocking buffer (BD Biosciences, Franklin Lakes, USA) for two hours at room temperature and again washed three times. Standards were prepared according to the manufacturer's recommendation, ranging from 3.125 to 200 pg/ml and 100 µl of standard or sample were added to each well. Samples (dilutions ranging from 1:10 to 1:1000) were added to the wells, the plate incubated for two hours at room temperature and washed five times. A detection secondary antibody conjugated with biotin mixed with SAHRP was diluted in the blocking buffer (both 1:250, BD Biosciences, Franklin Lakes, USA) added to the wells and incubated for one hour at room temperature. The plate was finally washed seven times and the TMB based substrate solution (Reagent A and B at a ratio of 1:1, BD Biosciences, Franklin Lakes, USA), protected from light added to the plate for 30 minutes. The enzymatic reaction was stopped by the addition of 50 µl of Stop solution (BD Biosciences, Franklin Lakes, USA).The absorbance was read at 450 nm, with a wavelength correction for polystyrene absorbance or turbidities in the medium, measured at the 570 nm. All measurements were done using a FluoStar Omega plate reader (BMG Labtech, Ortenberg, Germany).

2.17. FLOW CYTOMETRY

VK-2 E6/E7 cells were trypsinised and maintained in PBS containing 5 mM EDTA (PBSE). 10^6 cells were incubated with 2.5 μ g of a primary antibody, specific for Dectin-1 (MAB1859, R & D Systems, Minneapolis, USA), for 30 minutes on ice, before being washed twice using PBSE and collected by centrifugation at 500 g for 5 minutes. Cells were then incubated with a mouse IgG specific secondary antibody conjugated with Alexa Fluor 488 (A-11059, Life technologies, Carlsbad, USA) at a concentration of 1:200, washed twice with PBSE and resuspended in 400 μ l of PBSE. Cell fluorescence was analysed using a FACSCanto II (BD Biosystems, Franklin Lakes, USA) flow cytometer (Flow cytometer core facility, Newcastle University). The results of the flow cytometry were analysed using Flowing Software (University of Turku, Sweden).

2.18. IMMUNOCYTOCHEMISTRY AND CONFOCAL MICROSCOPY

Fluorescent images were taken using a Nikon Eclipse Ti, coupled to a Photometrics Coolsnap HQ CCD camera and Nikon Plan Fluor 100x/1.30 ph3 DL lens. The system is controlled by Metamorph 7.7.8.0 (Molecular Devices, Inc., Sunnyvale, USA). Confocal images were taken at the Bioimaging unit (Newcastle University) using a Nikon A1R or a Leica TCS SP2 microscope.

RT4 cells, VK-2 E6/E7 cells and primary vaginal cells were grown on cover slips and stained using non-specific mouse monoclonal IgG (026300, Invitrogen, Carlsbad, USA), C11 mouse monoclonal antibodies (NCL-C11, Leica Biosystems, Newcastle, UK), Dectin-1 (MAB1859, R&D Systems, Minneapolis, USA) and a rabbit polyclonal TLR-5 antibody (ab37071, ABCAM, Cambridge, UK). The cover slips were sterilised by washing with 70 % ethanol, followed by washing with methanol. After drying for 20

minutes, the cover slips were placed in a six well plate and seeded with eukaryotic cells. To achieve this, 10^5 cells were diluted in 230 μ l of appropriate medium and carefully added on the coverslip, forming a meniscus. The cells were allowed to settle on the cover slips for four hours at 37 °C and 5 % CO₂, before one ml of medium was added. The cells were grown to confluence before being challenged or directly fixed. Two methods for fixation were used, methanol and paraformaldehyde (4 % PFA) fixation. 4 % PFA was prepared by dissolving 0.4 g of PFA (Sigma-Aldrich, St Louis, USA) in 10 ml PBS at 65 °C. The cells were incubated for 10 minutes at 4 °C when fixed with 100 % methanol, but 15 minutes at room temperature, when fixed with 4 % PFA. PFA-fixed cells were washed three times with 50 mM NH₄Cl for three minutes at room temperature to quench the PFA and minimise the autofluorescence. The quenched cells were washed three times with PBS and, for detection of cytokeratin using C11 antibody, further permeabilised using 0.25 % Triton X-100 followed again by three washing steps with PBS. Blocking was achieved using one ml of 1 % BSA in PBS containing 0.1 % tween (PBST) for two hours at room temperature. Incubation with primary antibody, diluted in PBST, was performed for one hour at room temperature. Table 2.4 shows the working concentration of each antibody.

Table 2.4 List of primary antibodies used in immunocytochemistry.

Target	Type	Concentration	Permeabilisation	Supplier	Catalog number
C11	mouse monoclonal IgG	1:20	yes	Leica Biosystems	NCL-C11
Dectin-1	mouse monoclonal IgG	1:200 (2.5 μ g)	no	R&D Systems	MAB1859
TLR-5	rabbit polyclonal IgG	20 μ g/ml	no	ABCAM	AB37071
IgG control	Mouse monoclonal	2.5 μ g	no	Invitrogen	026300

Following incubation with primary antibody the cells were washed three times with PBST. The appropriate secondary antibody diluted 1:500 in 1 % BSA-PBST, was

incubated with the cells for 30 minutes at room temperature. Following five x 5 minutes washes with PBST the cell nuclei were stained for one minute with Propidium iodide (Sigma-Aldrich, St Louis, USA), before washing again with PBST. The cells were washed with MilliQ H₂O and the coverslips mounted on microscope slides using 20 µl of Mowiol mounting medium (Calbiochem, Darmstadt, Germany). Mowiol solidified by incubating the slides for 16 hours in the dark and at room temperature. The slides were stored at 4 °C until images were taken.

1. PREPARATION OF MOWIOL

Mowiol is a polyvinyl alcohol used to mount the cover slips on microscopic slides. It was prepared by dissolving 2.4 g of Mowiol (Calbiochem, Darmstadt, Germany) and 6 g of glycerol in 6 ml of dH₂O for 2 hours at room temperature, followed by the addition of 12 ml of 0.2 M Tris (pH 8.5, Sigma-Aldrich, St Louis, USA). The mixture was incubated at 65 °C for 25 minutes and centrifuged at 5000 x g for 15 minutes. It was either stored at 4 °C or -20 °C depending on usage.

2. INVESTIGATING SPECIFICITY OF MAB 1859

The specificity of the antibody mab 1859 was verified by incubating the 2.5 µg of the antibody with 25 µg of recombinant Dectin-1 (1859-DC, R&D Systems, Minneapolis, USA) for one hour at room temperature. After incubation, the antibody was used to stain VK-2 E6/E7 cells as described in section 2.18.

2.19. BIOINFORMATICS

1. PROMO TRANSCRIPTION BINDING FACTOR SEARCH TOOL

A 2000 bp region preceding the transcription start was obtained from the EMBO data base. The sequence was added to the PROMO software website and analysed for transcription factor binding sites. The transcription factors binding sites added to the search were NF- κ B, retinoic acid receptor (RAR), vitamin D receptor (VDR), AP-1 and oestrogen receptor alpha (ER- α).

CHAPTER THREE

Uroepithelial Innate Immune Responses to Uropathogenic *Escherichia coli*

3.1. INTRODUCTION

In healthy women the urinary tract (UT) is maintained free of pathogens despite its anatomic localisation close to the heavily bacterial colonised anal and vaginal regions. The innate immune system is key in protecting the UT against potential uropathogens and antimicrobial peptides secreted upon activation of cell surface receptors, including Toll-like receptors (TLRs), function as part of those innate defences.

Previous research identified the expression of TLR-2, TLR-4 and TLR-5 in bladder biopsies, as well as in the RT4 cell line, an *in vitro* model of bladder epithelium¹³⁷. The research focussed on exploring the function of these TLRs in the defence of the uroepithelium via analysis of NF- κ B signalling; NF- κ B was chosen as it is generally accepted as the master regulator of innate immunity¹⁴⁸. Challenge of RT4 cells engineered to express a NF- κ B luciferase reporter with ligands for TLR-4, which is considered one of the most important TLRs in the recognition of pathogens^{81,82}, failed to significantly induce a NF- κ B response. This suggested TLR4 had a reduced function in the defence of the UT. In contrast flagellin, the TLR-5 ligand, induced significant NF- κ B signalling. Moreover, when motile bacteria strains were utilised a NF- κ B response was observed, but this was not detected with non-motile bacteria. These data suggested a pivotal role for TLR-5 in the innate response of the uroepithelium.

However, the NF- κ B signalling pathway had been chosen for study based on information assembled from the innate immune signalling literature rather than actual experimental analyses of the uroepithelial gene response to infection, and specifically TLR signalling. Thus the aim of the research reported in this Chapter was to further explore the innate response of the uroepithelium to bacterial challenge and delineate the importance of each TLR during infection.

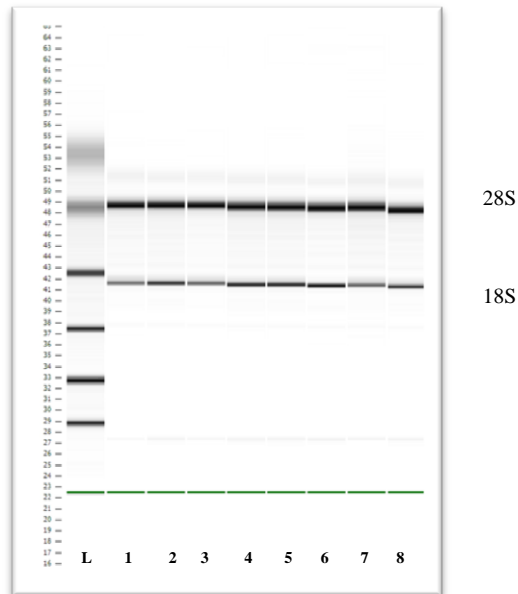
3.2. EARLY INNATE IMMUNE RESPONSE TO *E. COLI* LABORATORY STRAINS

The utilisation of gene arrays enables the simultaneous analysis of multiple genes and is therefore a useful screening tool. In this section, the early gene response in the bladder in response to infection was analysed using a commercially available pre-designed qPCR gene array with 84 genes related to TLRs.

1. RNA QUALITY CONTROL

RT4 cells were challenged for four hours with either PBS or 5×10^4 CFU/ml of the *E. coli* strains K-12, NCTC 10418 and NU14, the latter being a non-motile UPEC strain¹³⁷. Four hours was chosen based on pilot data using NCTC 10418, which indicated this time-point to reflect a maximal NF- κ B signalling response¹³⁷.

For the array experiments, it was crucial to use only high quality RNA and the RNA isolated from RT4 cells was analysed using the Agilent RNA 6000 Nano kit, according to the manufacturer's instructions. Results of the RNA quality analyses are presented in Figure 3.1:



A

1-PBS	✓	RIN:10
2-PBS	✓	RIN: 9.90
3-K12	✓	RIN:10
4-K12	✓	RIN:10
5-NU14	✓	RIN: 9.90
6-NU14	✓	RIN: 9.80
7-NCTC 10418	✓	RIN:10
8-NCTC 10418	✓	RIN:10

B

Figure 3.1 Analysis of RNA quality using Agilent RNA 6000 Nano kit. (A) RNA gel containing RNA isolated from PBS mock challenged and bacteria challenged RT4 cells. Lane L shows the marker. Lanes 1 and 2 are RNA samples of a negative control. Lanes 3 and 4 show the RNA of RT4 challenged with K-12. Lanes 5 and 6 show the RNA of RT4 challenged with NU14. Lanes 7 and 8 show the RNA of RT4 challenged with NCTC 10418. (B) RNA purity analysis performed by the Agilent program. All RNA samples showed a RIN<9.8 and were considered optimal for a TLR-Array analysis.

All lanes showed the expected two bands representing the 28S, 18S rRNA subunits (Fig. 3.1.A). Using these three bands, the Agilent software calculates the RNA integrity number (RIN). All samples showed a very high integrity by having a RIN of 9.8 or

higher (A RIN below 8.0 indicates RNA of low integrity, which cannot be utilised; Fig. 3.1.B) and were utilised for the TLR-array analysis.

2. TLR-RELATED GENE ARRAY

RT4 cells were challenged with different *E. coli* laboratory strains to analyse the early response of the urinary epithelium to *E. coli* colonisation. The strains were chosen according to their pathological background (NU14) or their motility, with NCTC 10418 being strongly motile and K-12 only having low levels of motility (Figure 3.3). The RNA was collected and gene expression analysed using a SABioscience TLR-Gene Array, according to the manufacturer's instructions (the RNA was reverse transcribed and gene expression was measured using a TLR related gene array qPCR plate (SABiosciences, Crawley, UK)). The qPCR was performed using the Lightcycler 480 (Roche, Burgess Hill, UK). The C_q-values were analysed using the SABioscience software and the fold change in gene expression identified.

Table 3.1 summarises the results of the TLR gene arrays from two independent experiments. The results were clustered into three groups according to their fold increase compared to a control PBS challenge. Any change ≤ 1.9 or C_q-value beyond 35 cycles was not considered significant. The majority of genes contained within the array did not show a difference in gene expression in response to the four hour bacterial challenges (Table 3.1, first column). However, variations were observed when the data from the three different challenge experiments were compared. Significantly, neither the *E. coli* K-12 nor NU14 challenges were associated with NF- κ B gene activation although upregulation of IL-8 gene expression was detected (2.95 and 2.07 fold change, respectively). In contrast, the *E. coli* NCTC 10418 challenge was linked with NF- κ B (2.6) and IL-8 gene (25.4) gene activation. Both, K12 and NU14 challenges activated

gene expression of the anti-inflammatory cytokine IL-10 (1.98 and 2.00 fold, respectively), Lymphotoxin A (LTA) (2.41 and 2.22 fold, respectively), and CD14 (2.70 and 2.47 fold, respectively). The NU14 challenge, additionally, induced LY86 and CCL2 gene expression, by 2.13 and 2.30 fold, respectively. Activation of IL-1B (2.16 fold), IL-1A (2.83 fold) and CXCL10 (11.40 fold) were unique to *E. coli* NCTC 10418.

Although the regulation of genes linked to the TLRs was limited the array data confirmed a significant role for NF- κ B signalling in the response of the uroepithelium to bacterial challenge. This was directly obvious from the array data in response to the *E. coli* NCTC 10418 challenge, but indirectly for *E. coli* K-12 and NU14, and suggested only via enhancement of IL-8 gene (NF- κ B responsive) expression. However, overall these data suggested a significant role for NF- κ B signalling in the defence of the UT and justified further focus on this pathway.

Table 3.1 Results of TLR-associated genes array. The genes were clustered into 3 different groups depending on the $\Delta\Delta C_q$ difference to the PBS challenged control. After 4 hours challenge, the order of the genes within the groups is correspondent to its fold increase over the control. ()-Brackets demonstrates average fold increase. N=2 independent experiments

K-12

-1.5<Fold change<1.9 (not significant)	1.9< Fold change<10	Fold change>10
<i>CD80, TOLLIP, IRAK1, ELK1, TIRAP, NFKB2, CSF2, HRAS, MAP2K3, ECSIT, MAP4K4, IRAK2, IRF3, FADD, RIPK2, CASP8, IKBKB, UBE2V1, MAPK8IP3, TAB1, MYD88, TICAM1, SARM1, PRKRA, UBE2N, IRF1, NFRKB, EIF2AK2, CHUK, NFKB1, PELI1, CD86, TRAF6, IL1B, PPARA, JUN, HSPD1, TNFRSF1A, TLR1, REL, TLR6, TLR4, TICAM2, BTK, NR2C2, NFKBIA, MAP3K1, MAP2K4, MAPK8, FOS, MAP3K7, TLR-5, HSPA1A, PTGS2, LY96, HMGB1, TLR3, TBK1, TLR2, NFKBIL1, IL1A, IL2, REL, TLR7, CCL2, TNF, SIGIRR, CXCL10, CSF3, IFNA1, IFNB1, IFNG, TLR10, TLR8, CLEC4E, LY86, TLR9, CD180, IL6</i>	<i>IL10(1.98), IL12A(2.11), LTA(2.41), CD14(2.70), IL8(2.95)</i>	-

A

NU14

-1.5<Fold change<1.9 (not significant)	1.9<Fold change<10	Fold change>10
<i>TOLLIP, CD80, IRAK1, IRF1, TIRAP, MAP2K3, NFKBIL1, SARM1, ELK1, ECSIT, FADD, BTK, JUN, HRAS, IRF3, MAPK8IP3, REL, NFRKB, MAP4K4, TAB1, IRAK2, MYD88, UBE2V1, SIGIRR, PPARA, RIPK2, HSPA1A, TLR3, TICAM1, TLR-5, PRKRA, UBE2N, CSF2, NFKB2, IKBKB, PELI1, TLR1, EIF2AK2, HSPD1, CHUK, NFKB1, NR2C2, FOS, TNFRSF1A, TRAF6, LY96, IL1B, TLR7, NFKBIA, TICAM2, TLR6, MAP2K4, TLR4, CD86, MAPK8, CD180, PTGS2, MAP3K1, CASP8, MAP3K7, IL2, TBK1, HMGB1, CSF3, IFNA1, IFNB1, IFNG, CXCL10, TLR2, IL12A, IL6, IL1A, TLR10, TLR8, CLEC4E, TNF, REL, TLR9</i>	<i>IL10(2.00), IL-8(2.07), LY86 (2.13), LTA (2.22), CCL2 (2.30), CD14 (2.47)</i>	-

B

NCTC 10418

-1.5<Fold change<1.9 (not significant)	1.9<Fold change<10	Fold change>10
<i>CD86, CD80, CCL2, IL2, LY96, TIRAP, TLR-5, BTK, SARM1, TICAM2, PRKRA, SIGIRR, NR2C2, UBE2N, PPARA, ECSIT, NFKB2, FOS, UBE2V1, MYD88, NFKBIL1, MAPK8IP3, TNFRSF1A, HRAS, JUN, TRAF6, MAPK8, NFRKB, IRF3, IRAK1, TAB1, TLR1, FADD, HSPD1, IKBKB, ELK1, MAP4K4, CHUK, MAP2K4, TLR6, REL, EIF2AK2, CASP8, PELI1, HSPA1A, RIPK2, IL10, MAP3K1, CD180, TLR4, MAP3K7, TLR3, TLR9, TICAM1, MAP2K3, NFKB1, HMGB1, TOLLIP, TNF, LTA, IL6, IRAK2, TBK1, CLEC4E, CSF3, IFNA1, IFNB1, LY86, TLR10, TLR8, TLR2, IFNG, IRF1, REL, TLR7, PTGS2, IL12A, CSF2</i>	<i>IL1B (2.16), NFKBIA (2.59), CD14 (2.67), IL1A (2.83)</i>	<i>CXCL10 (14.40), IL-8 (25.42)</i>

C

3.3. NF- κ B ACTIVATION BY LABORATORY *E. COLI* STRAINS

After analysing the early response to three different *E. coli* strains, a more in depth analysis of the innate response was attempted. Furthermore, in addition to the UPEC strain NU14 a second UPEC strain *E. coli* CFT 073, was added to the investigations. Data from previous studies, demonstrated that challenging uroepithelium model with live bacteria was only possible up to eight hours, due to cell death¹³⁷. To address this, RT4 NF- κ B cells were challenged with heat-killed bacteria for up to 24 hours (section 2.14.I).

The RT4 NF- κ B cells were developed by stably transfecting a reporter plasmid into RT4, which contains binding sites for NF- κ B and a luciferase reporter gene. Upon activation of NF- κ B as a transcription factor, luciferase will be produced and quantified by adding a luciferase substrate (luciferin) and measuring the luminescence.

The results of these challenges are shown in Figure 3.2. All vertical-axes show the fold increase in luminescence when compared to the negative control (cells challenged with PBS). One hour following the NCTC 10418 challenge, there was a significant 9.6 ± 2.6 fold increase in NF- κ B activity over the negative control (Fig. 3.2.A). After two hours the NF- κ B activity was 22.0 ± 1.6 with the peak 43.3 ± 2.5 fold increase observed four hours post challenge. After 16 hours, the NF- κ B activity was reduced to 22.0 ± 2.3 . The final measurement (7.5 ± 1.5 fold) at 24 hours was still significantly above the control value (Figure 3.2.A).

In comparison, when RT4 cells were challenged with K-12, significant NF- κ B activity was observed only after four hours of challenge (4.4 ± 0.6 fold increase over the negative control) and this response peaked at 16 hours, (12.3 ± 1.5 fold increase), although this

peak value was four times less than the response observed with NCTC 10418 (Figure 3.2.B). After 24 hours, the NF- κ B response fell to 9.9 ± 1.2 , but as for NCTC 10418 was still above the control value.

Comparable responses were observed following the CFT 073 and NU14 challenges, although the maximum fold increases in NF- κ B activity were greater for CFT 073 (19.8 ± 3.4), than NU14 (7.3 ± 1.0) (Figure 3.2.C and D). As for NCTC 10418, the peak activities measured for CFT 073 were at 4 and 8 hours respectively, but the values determined were mid-way between those of NCTC 10418 and the K-12. Interestingly the highest NF- κ B response to NU14 was measured at 24 hours.

The cytotoxicity was analysed microscopically and the cells did not show morphological changes or signs of cellular death.

Although the general patterns were similar the level of NF- κ B response differed between the four *E. coli* strains. NU14 showed similar results to previous findings, *i.e.* the strain induced a very low NF- κ B response, when compared to the other strains¹³⁷.

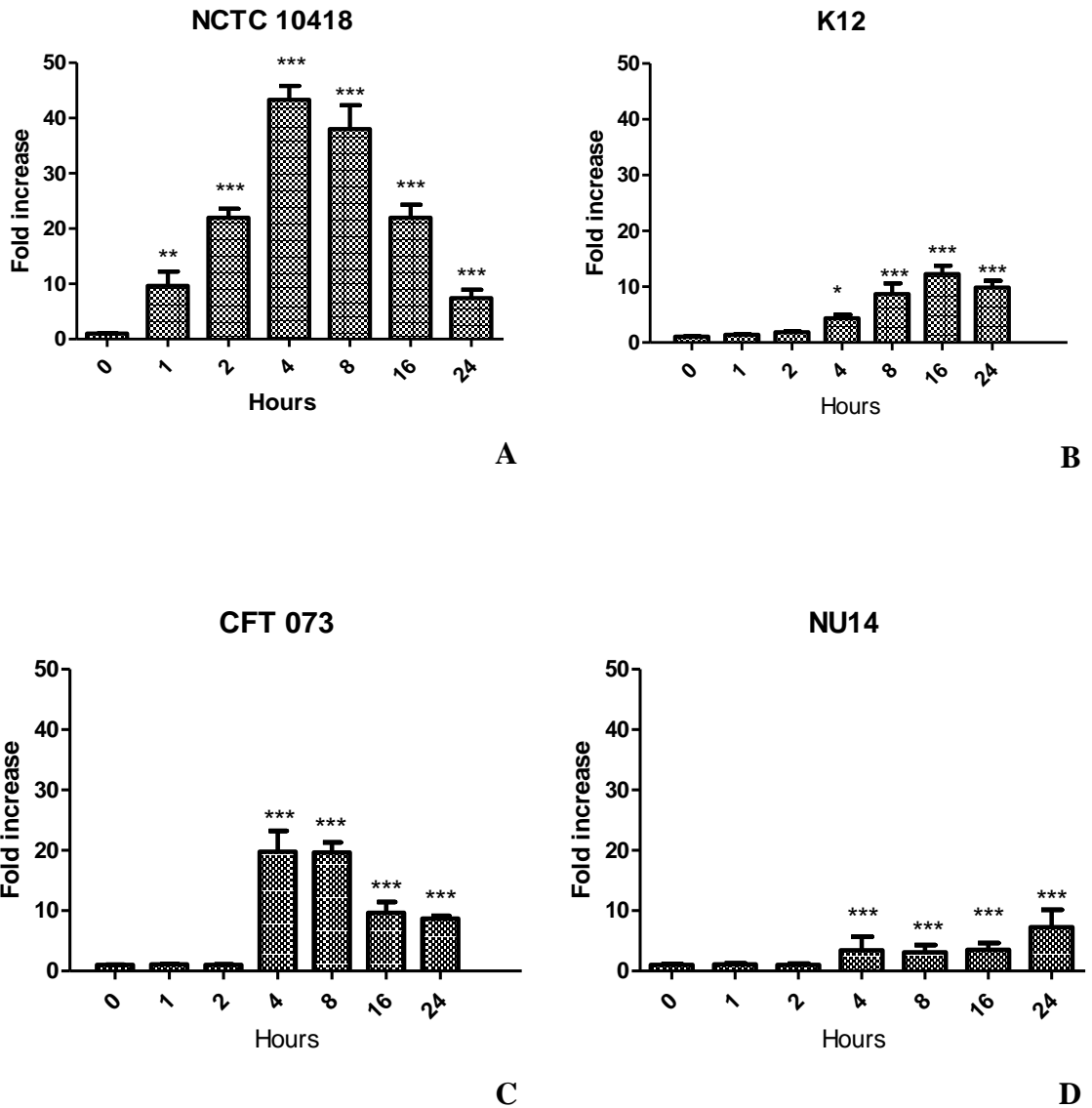


Figure 3.2 NF- κ B Response of RT4 to different laboratory *E. coli* strains using the NF- κ B-luciferase reporter. The different strains were grown to an OD_{600nm} of 0.6 and heat killed by 100 °C for 20 minutes. The CFU/ml was determined and 5×10^4 CFU/ml were added to RT4 NF- κ B reporter cells and luminescence was measured. **(A)** Response to NCTC 10418. **(B)** Response to K-12. **(C)** Response to motile UPEC CFT 073. **(D)** Response to non-motile NU14. The bars are the mean of the fold increase of luciferase activity of challenged cells, when compared to PBS challenged ones. N=9, 3 experiments with 3 replicates. Error bars are \pm standard error of the mean. Statistical significance determined by ANOVA; *= $p < 0.05$, **= $p < 0.01$, ***= $p < 0.001$.

3.4. DETERMINATION OF MOTILITY OF THE LABORATORY STRAINS

To help explain the differences in RT4 NF- κ B responses, the motility of the four *E. coli* strains was analysed, in collaboration with by Dr Philip Aldridge, Newcastle University, as described in section 2.14.IV. The results are presented in Figure 3.3 and show that the NCTC 10418, K12 and CFT073 strains are associated with halos indicative of bacterial motility. The lack of a halo indicated that the NU14 strain was not motile. Although only semi-quantitative these data suggest that the highest NF- κ B activating strain NCTC 10418 was also the strain with the highest motility. It is well established, that the flagella complex is responsible for bacterial motility¹⁴⁶ and flagellin is the extracellular part of the flagella complex^{94,146}. So to specifically investigate the role of motility in the innate response of the urinary tract, flagellin was isolated from *E. coli*, specifically NCTC 10418, and used to challenge RT4 cells.

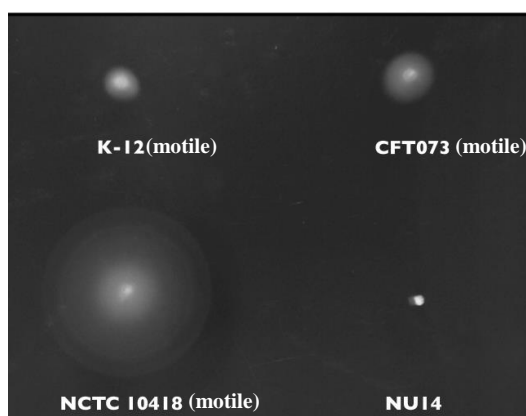


Figure 3.3 Assessing *E. coli*'s motility using a soft agar assay. The four *E. coli* strains were grown on a low percentage agar growth plate (0.3 %) for eight hours. K-12 shows a small halo, comparable to the UPEC CFT 073, while NCTC 10418's halo is larger. These three strains show therefore motility, while NU14 is non-motile. Experiment was performed by Dr Phillip Aldridge (Newcastle University).

3.5. FLAGELLIN ISOLATION FROM *E. COLI* NCTC 10418

Flagellin was isolated using a procedure previously described¹⁴⁶. Briefly, 2 L of an *E. coli* NCTC 10418 culture were grown to an OD₆₀₀ of 0.6 and collected by centrifugation. The flagellin protein was separated by sonication and collected by ultracentrifugation. Two independent flagellin preparations were isolated. Figures 3.4.A and 3.4.E show the results of two independent flagellin isolations.

Figure 3.4.A shows the result of the first isolation with purified flagellin in lane 8. The protein ladder shows that the isolated protein had a molecular weight of approximately 55 kDa. The protein was further purified by size exclusion and Figure 3.4.B shows the result of measuring the absorption at 280 nm of the eluted samples. As no peaks were observed, the elution samples collected were electrophoresed on a 10 % SDS-gel (Figure 3.4.C). No samples were visible, suggesting complete loss of sample. The size exclusion column was verified using 1 mg/ml BSA (Figure 3.4.D) and the peak shown in 3.4.D suggested a fully functional size-exclusion column. However, the lack of pure protein suggested that the size exclusion filtration was not optimal for flagellin. The flagellin isolation was repeated and protein analysed on a 10 % SDS gel (Figure 3.4.E). Again, the main band was 55 kDa (blue arrow, Figure 3.4.E). Different concentrations of BSA (2 mg/ml, 1.5 mg/ml, 1 mg/ml, 0.75 mg/ml and 0.5 mg/ml) were used for qualitative quantification, suggesting a concentration of approximately 0.6 mg/ml. The concentration of the isolated flagellin was determined using a Bradford-Assay and the final concentration was 0.67 mg/ml.

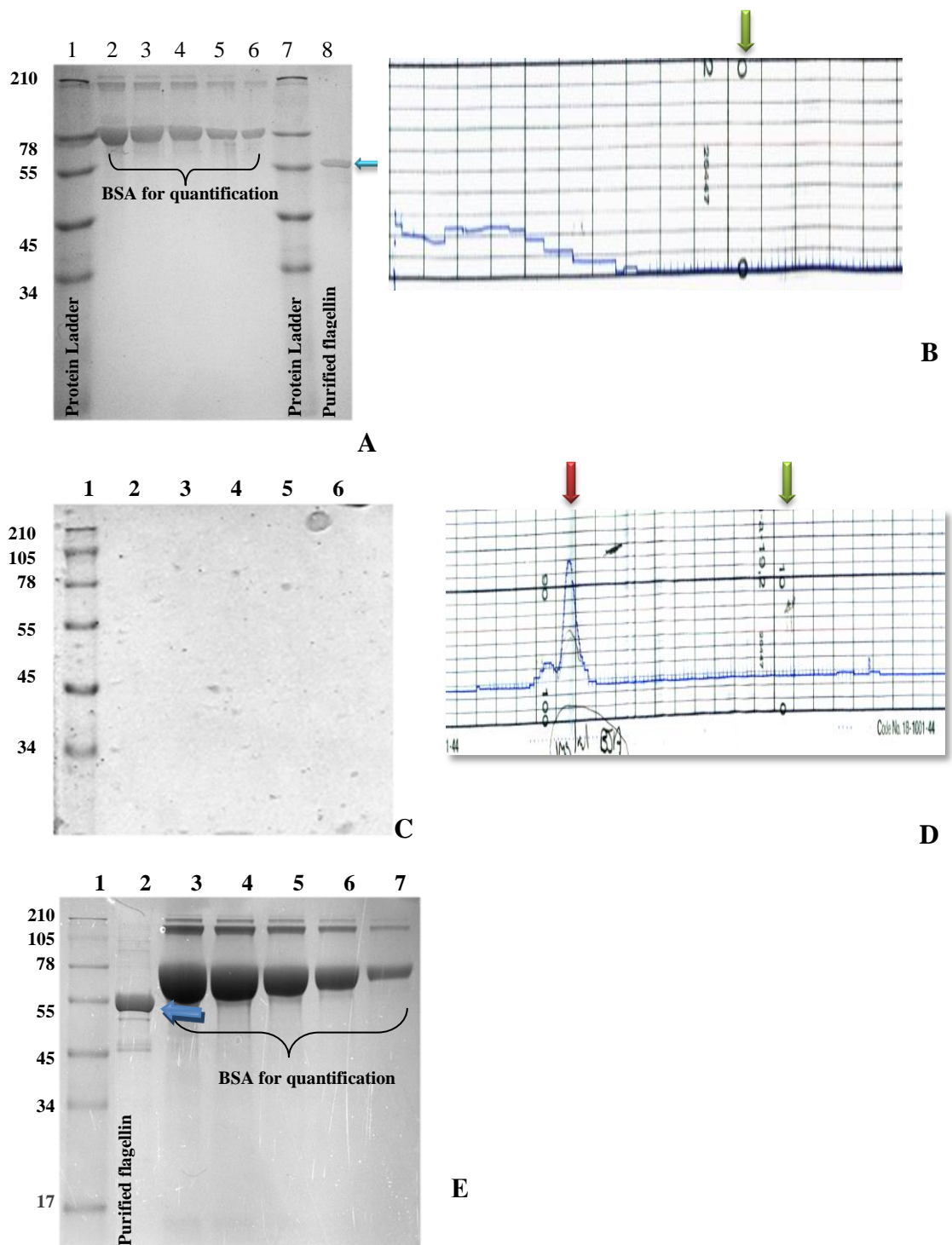


Figure 3.4 Isolation of flagellin from NCTC 10418 (A) The first isolation was separated on a denaturing 10 % Tricine SDS-PAGE. Lane 2-6 BSA standard for protein concentration determination. The ladder is SeeBlue® Plus2 Pre-Stained Standard (Invitrogen, Carlsbad). Blue arrow marks isolated flagellin (B) Absorbance of the eluted samples at 280 nm, after passing a size exclusion column. Green arrow shows area of expected peak (C) Denaturing 10 % Tricine SDS-PAGE to visualise the aliquots. The ladder is SeeBlue® Plus2 Pre-Stained Standard (Invitrogen, Carlsbad). (D) Absorbance of 1 mg/ml BSA (red arrow). Expected area for the flagellin peak is marked by the green arrow. (E) Second isolation of flagellin, the ladder is SeeBlue®. Lane 3-7 BSA standard for protein concentration determination. Blue arrow marks isolated flagellin.

3.6. INNATE IMMUNE RESPONSE OF THE URO-EPITHELIUM TO COMPONENTS OF THE BACTERIAL CELL WALL

The previous results showed that the four *E. coli* strains induced different degrees of NF- κ B signalling and motility, thus flagellin, appeared to be a major factor in the response. Nevertheless, two motile strains, K-12 and CFT 073, caused less NF- κ B activation than NCTC 10418, suggesting that other factors may have contributed. To try and further understand why the strains of *E. coli* showed different responses, the activation of NF- κ B by bacterial membrane molecules was assessed. Flagellin, as well as LPS and peptidoglycan, two additional major PAMPs of the *E. coli* cell wall, were investigated.

1. FLAGELLIN

Flagellin is a protein expressed by the *FliC* gene and is part of the flagella motor responsible for the bacterial mobility⁹⁴. Pilot data indicated that flagellin was able to evoke an NF- κ B response in RT4 cells, but the flagellin used was isolated from *Salmonella typhimurium*¹³⁷. In the following experiments the flagellin isolated from *E. coli* NCTC 10418 was utilised.

First, a timecourse of the NF- κ B response to 250 ng/ml of flagellin was investigated. The media bathing the challenged cells was collected, and the IL-8 concentration was measured. Results are shown in Figure 3.5.A and B, respectively.

A significant increase in NF- κ B activity was observed one hour post challenge (7.4 ± 0.6 fold; $p < 0.01$), but the peak response was measured at four hours (44.9 ± 1.7 fold increase over the negative control). From eight to 16 hours, the NF- κ B activity gradually decreased and at 24 hours was comparable to that measured at one hour.

A significant difference between the IL-8 concentration of the negative control and flagellin challenged samples was initially observed at four hours ($p < 0.001$). Moreover, when compared to the PBS challenge, flagellin induced a 27 fold increase in the mean IL-8 concentration measured at four hours (8263.4 ± 192.3 pg/ml) and a 52 fold increase at 24 hours (23879.0 ± 631.1 pg/ml).

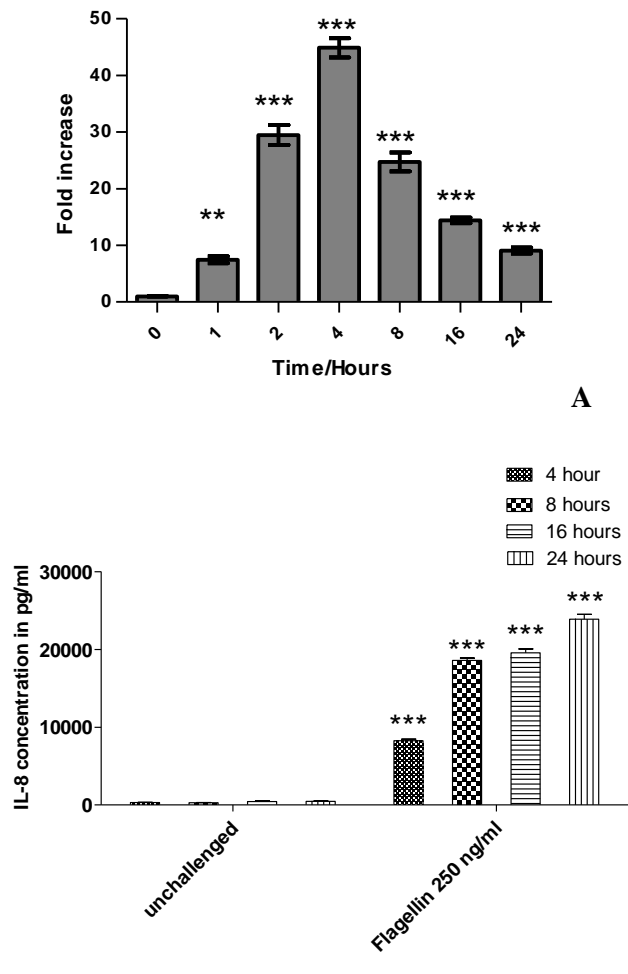


Figure 3.5 NF-κB and IL-8 Response of RT4 uroepithelium to Flagellin isolated from *E. coli*. The RT4 reporter cells were challenged for up to 24 hours using 250 ng/ml of flagellin. The NF-κB activity and IL-8 secretion was measured. **(A)** The RT4 reporter cells were lysed and their luminescence caused by the NF-κB reporter was measured. The fold increase over the negative control was calculated for each replicate. The bars represent the mean and the error bars stand for the standard error of the mean. N=9, 3 experiments with 3 replicates. **(B)** IL-8 concentration the media from three replicates of the challenge above and was measured using a sandwich ELISA (BD OPTEDIA). N=2 using pooled medium of 3 replicates. Statistical significance determined by ANOVA; *= $p < 0.05$, **= $p < 0.01$, ***= $p < 0.001$

These data showed that challenging the RT4 cells with 250 ng/ml of *E. coli* flagellin resulted in a significant increase in NF-κB reporter activity and within one hour of the

challenge. The next experiment investigated whether the NF- κ B response and IL-8 secretion caused by flagellin was concentration dependent. Therefore, flagellin was serially diluted (concentrations from 250 ng/ml to 2.5 fg/ml) and the challenge experiments were repeated. Due to the different concentrations of flagellin being tested only three time points, 4, 8 and 24 hours were analysed. Since 4 hours was associated with increased IL-8 concentrations this time-point was used to avoid natural accumulation of IL-8 in the media. The results are shown in Figure 3.6.A and B.

Flagellin induced a significant NF- κ B response at all time-points at concentrations of 250 pg/ml or higher, although at four hours and a concentration of 25 pg/ml, the NF- κ B response was doubled (2.1 ± 0.4 fold, Fig. 3.6.A). As previously observed with NCTC 10418, NF- κ B activity peaked at four hours post challenge.

Significant increases in IL-8 were detected when the RT4 cells were challenged with 2.5 ng/ml of flagellin or higher (Fig. 3.6.B). Although 250 pg/ml of flagellin caused a significant NF- κ B response, no significant change in the media concentration of IL-8 was detected. However, a trend was noticed (590.5 ± 75.0 pg/ml compared to 317.4 ± 109.6 pg/ml of the cells challenged with PBS).

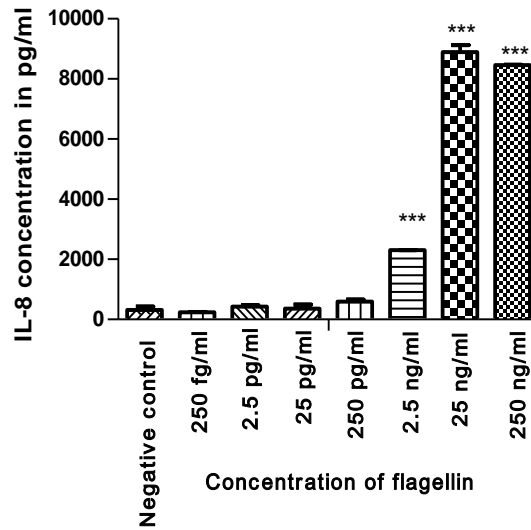
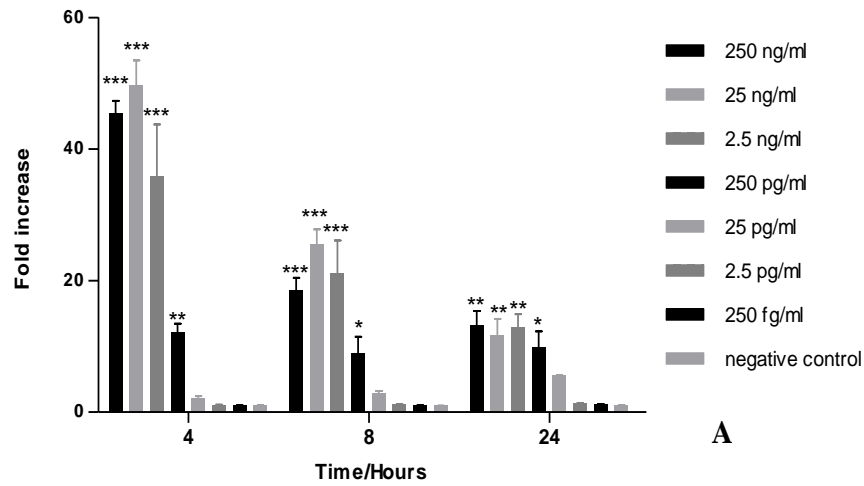


Figure 3.6 NF- κ B and IL-8 response of RT4 to different concentrations of flagellin. (A) RT4 cells are stably transfected with a NF- κ B reporter, were challenged with flagellin isolated from *E. coli* NCTC 10418 at the described concentrations. The NF- κ B response was measured at three different time points (four, eight and 24 hours). The negative control was a PBS challenge. Bars represent the mean with their standard errors. The statistical significance was measured using two way ANOVA with the Bonferroni post hoc Test. N=6, 2 experiments with 3 replicates. **(B)** IL-8 concentration the media from three replicates of the challenge above and was measured using a sandwich ELISA (BD OPTEDIA). N=2, using medium pooled of three replicates. Statistical significance determined by ANOVA; *= $p < 0.05$, **= $p < 0.01$, ***= $p < 0.001$

2. INHIBITION OF NF-κB ACTIVATION BY TLR-5 BLOCKING

A NF-κB response was observed in RT4 cells challenged with flagellin. Flagellin functions via TLR-5¹⁴⁶ and to further explore the importance of TLR-5 in the innate defences of the bladder, the RT4 cells were treated for one hour with a monoclonal antibody specific for TLR-5 before being challenged with 250 ng/ml of flagellin (section 2.14.III). The results of the NF-κB reporter activity data following TLR-5 blocking are shown in Figure 3.7.A. In these experiments NF-κB reporter activity was measured at eight hours rather than four hours to accommodate the IL-8 measurements. Blocking TLR-5 resulted in reduced NF-κB activity from 30.9 ± 1.6 to 22.9 ± 1.4 fold (eight fold difference, $p < 0.001$). A reduction in NF-κB activity was also measured at 16 (four fold difference, $p < 0.001$) and 24 hours (6.6 fold difference, $p < 0.001$) respectively.

The results of IL-8 analyses are shown in Figure 3.7.B. The concentration of IL-8 was 9522.5 ± 55.9 pg/ml after the eight hour flagellin challenge and blocking of TLR-5 resulted in a significant reduction ($p < 0.001$) to 6783.1 ± 37.3 pg/ml. Significant reductions ($p < 0.001$) in IL-8 were also detected at 16 and 24 hours respectively. However, blocking TLR-5 did not reduce either the NF-κB reporter activity or IL-8 concentrations to background (data not shown) suggesting that other components were involved in the NF-κB activation. The flagellin preparation used in the challenge experiments was not purified by gel exclusion thus it was feasible that contaminants including Endotoxin or Lipopolysaccharide (LPS), were playing a role.

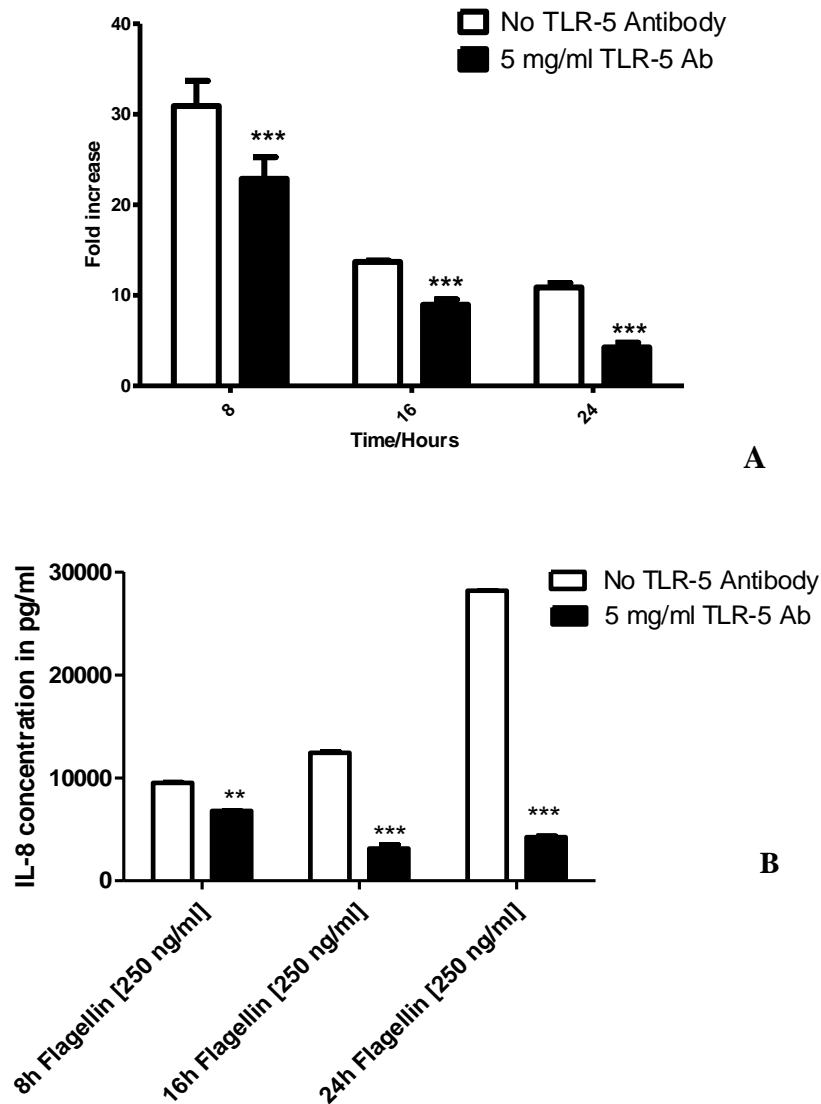


Figure 3.7 Inhibition of innate response to flagellin through TLR-5 blocking in RT4 cells. RT4 cells were challenged with 250 ng/ml of flagellin and preincubated with 5 µg/ml monoclonal TLR-5 specific antibody. (A) The NF-κB activity was measured using a reporter assay (N=9, 3 experiments with 3 replicates) (B) The IL-8 secretion into the bathing media was measured using a sandwich ELISA (N=3, using medium pooled of three replicates). Statistical significance determined by Student's T-test; **=p <0.01, ***=p <0.001

3. LIPOPOLYSACCHARIDES

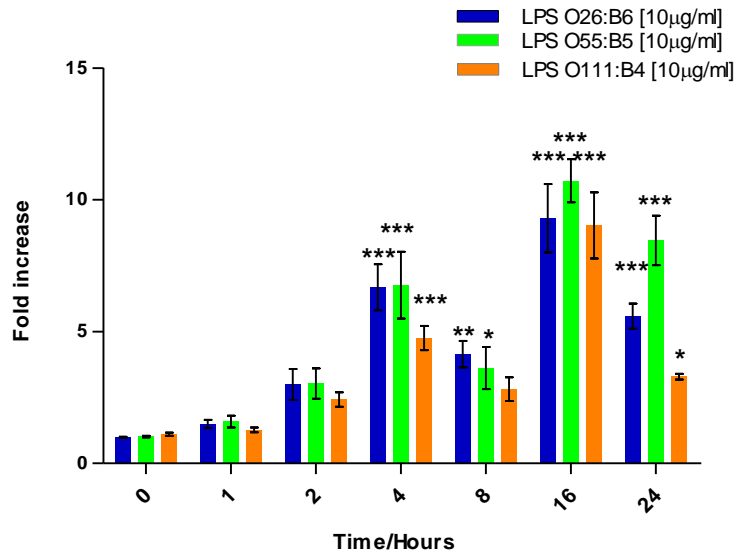
Previous challenge of RT4 cells with LPS, a ligand for TLR-4, failed to induce a NF- κ B response. This suggested that TLR-4, generally considered one of the most important TLRs in pathogen recognition¹⁴⁹, had a reduced function in the defence of the UT¹³⁷. Nonetheless, activation of NF- κ B in the uroepithelium in response to LPS has been described previously¹⁵⁰. Thus the effects of LPS were re-examined, but using 10 μ g/ml (a two fold increase compared to previous experiments) and three different types of LPS (O26:B6, O55:B5 and O111:B4), all isolated from *E. coli*. RT4 NF- κ B reporter cells were challenged for up to 24 hours, and luciferase activity was measured. The results are presented as fold increase over the negative control (PBS challenge) and shown in Figure 3.8.A.

RT4 cells showed no significant change in NF- κ B reporter activity in response to LPS in the first two hours post challenge. However, at four hours, the NF- κ B activity was significantly upregulated and with all three LPS preparations ($p < 0.001$). Following a dip in reporter activity at eight hours, the NF- κ B activity peaked at 16 hours (9.3 \pm 1.3 for LPS O26:B6, 10.7 \pm 0.8 for LPS O55:B5 and 9.0 \pm 1.3) with all three types of LPS causing a significant response ($p < 0.001$).

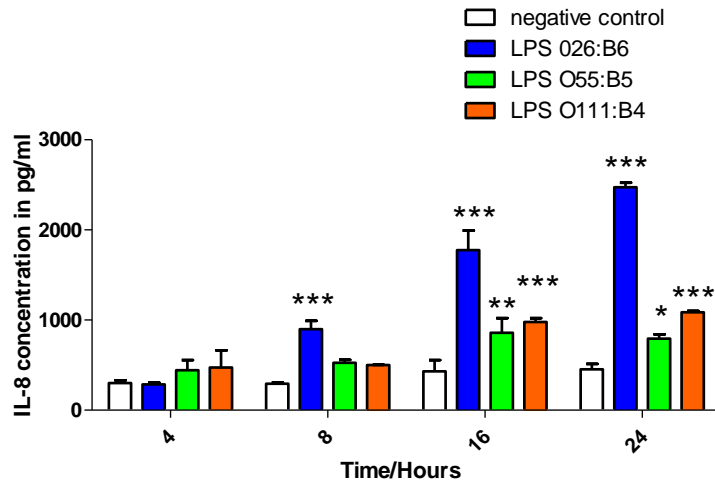
Media bathing the cells were collected at 4, 8, 16 and 24 hours. At each time point, the media was pooled and the IL-8 concentrations measured. The data is shown in Figure 3.8.B.

A significantly increased concentration of IL-8 was measured at 8 hours post challenge, but only in response to LPS O26:B6 (898.2 \pm 93.2 pg/ml, $p < 0.001$). However, at 16 and 24 hours, and consistent with the NF- κ B data all LPS types caused a significant increase in IL-8 ($p < 0.001$ for LPS O26:B6, LPS O111:B4 and $p < 0.01$ LPS O55:B5).

NF- κ B reporter activation associated with LPS was much lower than observed with flagellin. Indeed while flagellin was associated with a mean peak response of 44.9 ± 1.7 fold, LPS induced only a peak response of 10.7 ± 0.8 fold (LPS O55:B5). IL-8 secretion was also reduced when RT4 cells were challenged with LPS compared to flagellin (maximal secretion 2473.6 ± 50.0 for LPS and 23879.0 ± 631.1 pg/ml for flagellin).



A



B

Figure 3.8 Innate immune response of RT4 cells to three different types of *E. coli*'s LPS. (A) NF-κB response to 10 μg/ml of LPS. (N=9, 3 experiments with 3 replicates). (B) Measurement of RT4's IL-8 secretion when challenged with 10 μg/ml LPS (N=3, using medium pooled of three replicates) *= $p < 0.05$; **= $p < 0.01$; ***= $p < 0.001$.

4. PEPTIDOGLYCAN

Peptidoglycan is also part of the *E. coli* cell wall. It is known to induce NF- κ B activity through two receptor families, TLR 2/6 and Nod-Like receptors¹⁵¹. TLR 2/6 recognise the intact peptidoglycan while Nod-Like receptors recognise breakdown products of peptidoglycan^{63,66,151,152}.

Previous research demonstrated the expression of TLR-2 in RT4 cells¹³⁷. TLR-2 functions as a dimer with TLR-6 and amplifying RT4 cDNA using primers specific for the TLR-6 gene resulted in a band with a size comparable to the expected 777 bp (Figure 3.9), which was confirmed as TLR-6 by DNA sequencing.

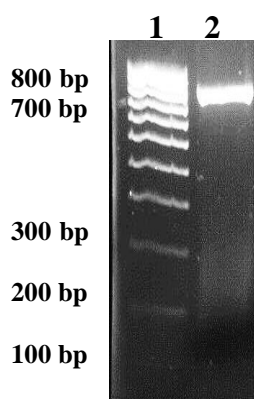


Figure 3.9 Expression of TLR6 in RT4. The first lane shows Hyperladder IV. Second lane shows the amplification of RT4 cDNA using TLR6 specific primers resulting in a band of expected size (777 bp).

Once the expression of TLR-2 and 6 were confirmed the effects of peptidoglycan (10 μ g/ml, maximal concentration recommended by the supplier, Invivogen, USA) on RT4 NF- κ B reporter activity were investigated¹⁵³. As previous, the medium bathing the challenged cells was collected at four, eight, 16 and 24 hours and IL-8 secretion was measured. Results are shown in Figure 3.9.

Peptidoglycan caused a significant increase in NF- κ B reporter activity but only after eight hours of challenge (5.4 ± 1.4 , $p < 0.001$; Fig. 3.10.A). This response stayed stable for up to 16 hours (6.3 ± 0.6 , $p < 0.001$; Fig. 3.10.A). However, the maximal activation of NF- κ B by peptidoglycan was < 7 fold. This response was comparable to that of LPS but much lower than the observed with flagellin. The IL-8 concentrations measured in the media suggested an increase in IL-8 in response to PG, particularly at 16 and 24 hours, but these data were not statistically significant compared to control (Fig. 3.10.B).

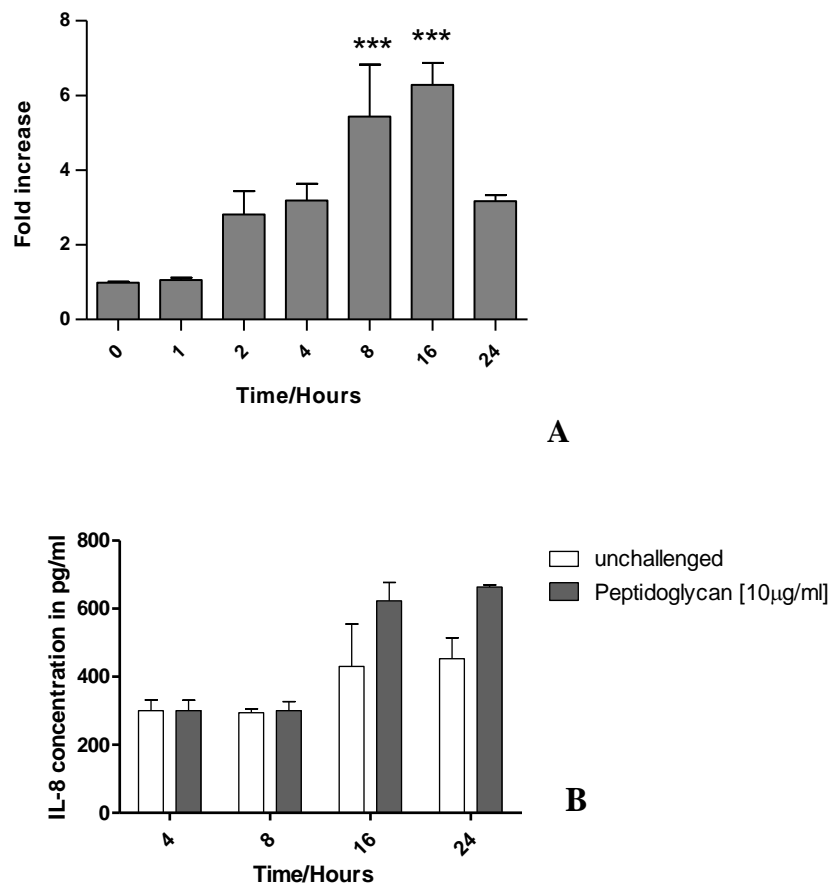


Figure 3.10 Innate immune response of RT4 cells to 10 μ g/ml of *E. coli*'s peptidoglycan. (A) NF- κ B response of RT4 cells (N=9, 3 experiments with 3 replicates. *=P<0.001). (B) Concentration of IL-8 secreted into the medium bathing the challenged cells of A). N=3 using medium pooled from 3 replicates**

3.7. NF-KB AND IL-8 RESPONSE TO CLINICAL ISOLATES.

From these data flagellin appeared to be the major activator of innate immunity in RT-4 cells, thus linking bacterial motility to activation of the host innate response. With this in mind it could be predicted that clinical strains associated with UTI are able to avoid the host defences by their reduced motility. This was investigated further utilising clinical isolates of patients suffering infections of the urinary tract.

1. DETERMINING THE MOTILITY OF CLINICAL ISOLATES OF UPEC STRAINS

A collection of 24 clinical isolates related to patients with UTI was kindly provided by Dr Kathy Walton (Freeman Hospital, Newcastle upon Tyne, UK). Of these, eight clinical isolates were associated with asymptomatic bacteriuria, nine isolates with acute cystitis, four isolates with pyelonephritis and three with bacteraemia. All bacteria were clinically identified as *E. coli* following microbiological analyses at the Microbiology Laboratories, Freeman Hospital, Newcastle upon Tyne. Bacterial motility was determined by Dr Christopher Birchall and Dr Philip Aldridge (Newcastle University). The results are shown in Figure 3.11 and summarised in Table 3.2.

Of the clinical isolates with a defined patient history 50 %, *i.e.* 12/24 were motile. Interestingly, the majority of motile isolates were related to symptomatic urinary tract infections, *i.e.* cystitis (six out of nine) and pyelonephritis (three out of four). In the asymptomatic bacteriuria group only two isolates out of eight were motile. The isolates collected from the bacteraemia patients contained two motile and one non-motile strains. In brief, those strains with the highest motility were associated with large halos, although halo sizes were variable. The most motile strains (biggest halo) were observed

in the cystitis group, followed by the pyelonephritis strains and asymptomatic bacteriuria group. The motile bacteraemia strain formed a small halo.

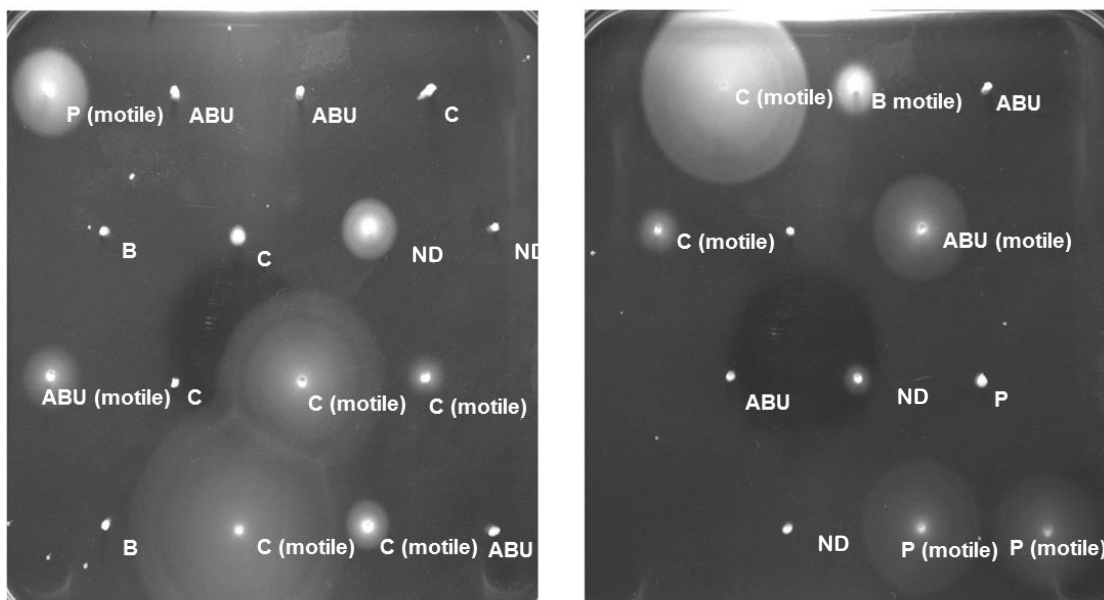


Figure 3.11 Motility of the clinical UPEC Strains. Motility was determined using a soft agar using 0.3 % Bactoagar. The bacteria were seeded in the centre of each puncture and allowed to grow for eight hours at 37 °C. Motile bacteria are seen by their halo like shape. The abbreviations are C= Acute Cystitis, ABU=asymptomatic bacteriurea, P=Pyelonephritis and B=bacteraemia, ND=strains of *E. coli* without defined clinical pathology. Experiment performed by Dr Christopher Birchall and Dr Phillip Aldridge.

Table 3.2 Motility of clinical UPEC strains.

Clinical picture	Total	Motile	Non-motile
Asymptomatic Bacteriuria	8	2	6
Cystitis	9	6	3
Pyelonephritis	4	3	1
Bacteraemia	3	2	1

2. INNATE IMMUNE RESPONSE OF THE URO-EPITHELIUM TO CLINICAL ISOLATES OF UPEC

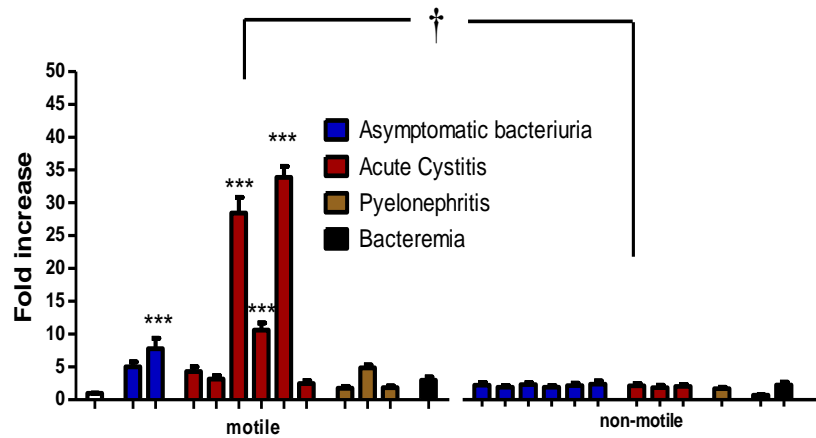
The clinical isolates were also investigated for their ability to trigger a NF- κ B response. The clinical strains were grown to an OD_{600nm} of 0.6, heat killed (100 °C for 20 minutes) and used to challenge RT4 - NF- κ B reporter cells grown on 96 wells plates. The cells were challenged for four, eight and 24 hours using 5x10⁴ CFU/ml of each clinical strain

or PBS. Media from each 24 hour challenge was collected and the IL-8 concentrations measured. The results of the NF- κ B activation of each clinical isolate are shown in Figure 3.12.

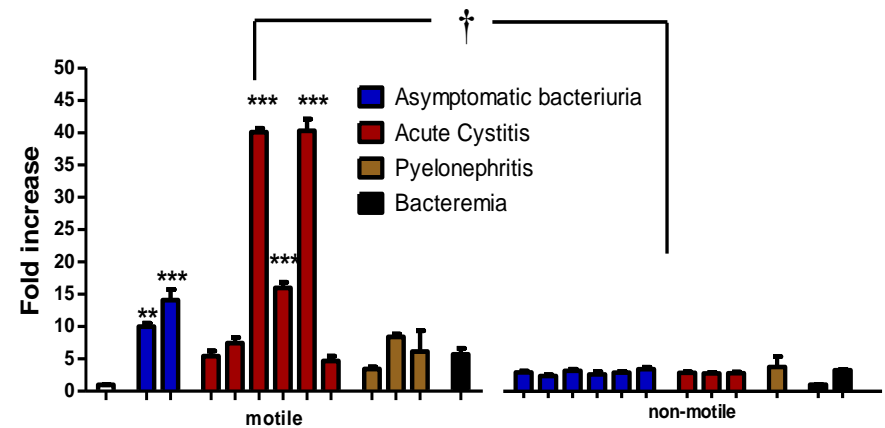
The strains were sub grouped into motile or non-motile and the mean NF- κ B activation of the motile strains was found to be significantly higher than that of non-motile strains at all three time points ($p < 0.05$ for four and eight hours; $p < 0.01$ for 24 hours). Surprisingly, the IL-8 concentrations failed to show a significant difference between motile and non-motile clinical isolates ($p = 0.054$).

At four hours, only four motile strains caused a statistically significant difference in NF- κ B reporter activation ($P < 0.001$). Three of the four, were isolated from patients suffering symptomatic cystitis and they were also the strains with the largest halos in the motility assay (Fig. 3.11). The other motile strain that caused a significant response was from a patient suffering from asymptomatic bacteriuria. None of the non-motile strains activated NF- κ B significantly.

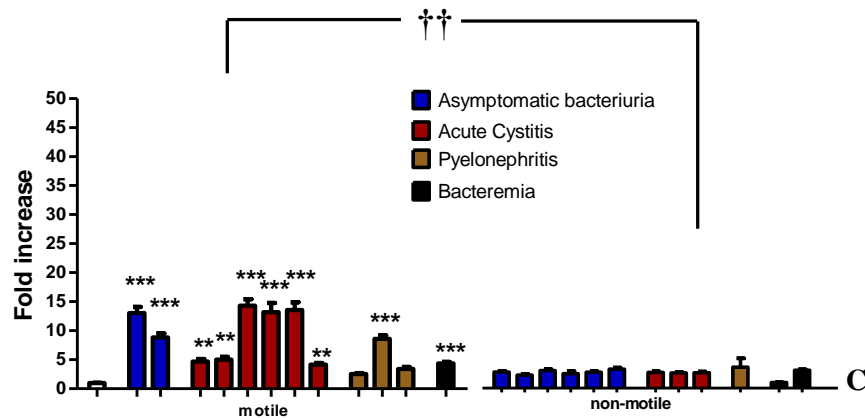
At eight hours, one motile strain of the asymptomatic group was also found to cause significant NF- κ B reporter activity ($p < 0.01$, Fig. 3.12.B). At the final time point, 24 hours, all but two motile strains showed significant activation of NF- κ B ($p < 0.001$ or $p < 0.01$). The strains that did not activate NF- κ B were both from the pyelonephritis group.



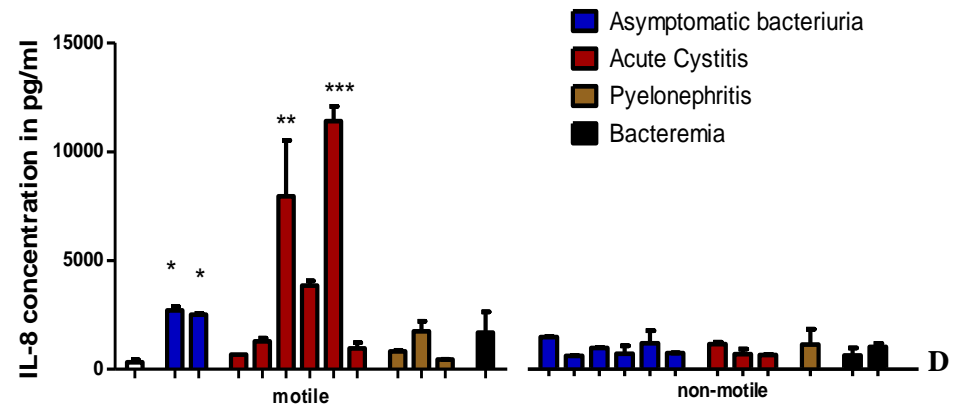
A



B



C



D

Figure 3.12 Innate Immune Response of RT4 to clinical UPEC isolates. 5×10^4 CFU/ml of the clinical isolates were added to RT4 NF- κ B reporter cells. The bars represent fold increase of luciferase activity of challenged cells over PBS challenged ones (N=6, 2 experiments with 3 repeats each). (A) Luminescence was measured after four hours. (B) Luminescence was measured after eight hours. (C) Luminescence was measured after 24 hours. (D) The IL-8 concentration was measured on the pooled media of RT4 cells challenged for 24 hours (N=2, medium pooled from 3 replicates). Statistical significance between negative control (white bar) and clinical isolates was determined by two-way ANOVA with a Bonferroni post hoc test; *= $p < 0.05$, **= $p < 0.01$, ***= $p < 0.001$. Statistical significance between motile and non-motile was determined by analysing the means using a Student's T-test; †= $p < 0.05$ and ††= $p < 0.01$.

3. INNATE IMMUNE RESPONSE TO FLAGELLIN ISOLATED FROM CLINICAL STRAINS

Twelve clinical bacterial isolates associated with UTIs were motile and activated a NF- κ B signalling response, but it was noted that the intensities of the responses differed between isolates. To investigate this further, flagellin from 11 of the clinical strains was isolated (Dr Christopher Birchall and Dr Philip Aldridge) and used to challenge RT4-NF- κ B reporter cells. Typical results relating to the flagellin isolations are shown in Figure 3.13.A, where five motile strains were used as a flagellin source. A non-motile strain was used as control, hence the absence of a flagellin protein band. Flagellin protein bands shown in lanes 2, 5 and 6 migrate as a single band, while the flagellin isolations shown in lanes 4 and 7 migrate as multiple bands, with flagellin probably being the largest of the protein bands at 50 kDa and 60 kDa, respectively. The isolated flagellins ranged in size from 45 kDa to 75 kDa.

The purified flagellins were used to challenge the RT4-NF- κ B-luciferase cells and the resulting fold increases in NF- κ B signalling ranged between 30.4 ± 1.8 and 46.1 ± 2.5 (Figure 3.13.B). However, there were no statistical differences identified between the responses induced by the different flagellins. These data indicated that flagellin itself could not explain the differences in NF- κ B signalling induced by the different clinical isolates.

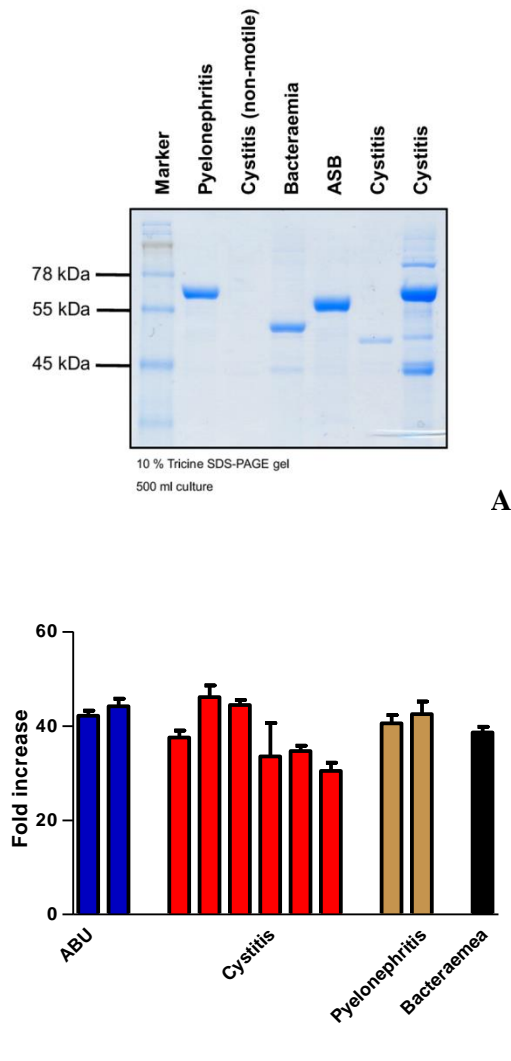


Figure 3.13 Isolation of flagellin from clinical isolates and NF-κB response of RT4 cells to purified flagellin. (A) Example of purified flagellin electrophoresed on a 10 % Tricine SDS-PAGE. **(B)** NF-κB response of RT4 reporter cells when challenged with 250 ng/ml of flagellin. The challenge was performed for four hours (N=6, 2 experiments with 3 replicates).

3.8. INNATE IMMUNE RESPONSE TO CLINICAL STRAINS ISOLATED OF PATIENTS CARRYING TLR-5(C1174T) SNP

The previous data showed that many clinical isolates associated with UTI are motile, have flagella and induce a NF-κB response in bladder epithelial cells, presumably via TLR-5. Thus for infection to occur either the bacteria are able to inhibit signalling pathways downstream of NF-κB or the host is unable to recognise the motile bacteria. To explore the latter and in collaboration with Mr Ased Ali, Newcastle University, a group of patients suffering from recurrent UTI and carrying a C1174T SNP in their

TLR-5 gene was identified⁸⁹. The mutation results in an early stop codon, resulting in the synthesis of a truncated TLR-5 receptor and the reduced ability of the host epithelium to recognise flagellin¹⁵⁴. Such patients were recruited to investigate the role of the mutation in the innate defences of the urinary tract. Urine was collected from three SNP patients during an UTI, the bacteria isolated and used to challenge the RT4 NF- κ B reporter cells. Gram staining of the bacteria isolate identified only gram negative species and analysis of colony growth did not suggested difference between the colonies. Urine IL-8 concentrations were measured using a sandwich ELISA.

1. INNATE IMMUNE RESPONSE OF RT4-NF-KB TO BACTERIA ISOLATED FROM URINE OF TLR-5(C1174T) CARRIERS

The bacterial strains were grown in LB-broth to an OD₆₀₀ of 0.6, the CFU/ml was determined and the bacteria heat killed (100 °C for 20 minutes). RT4 NF- κ B reporter cells were infected with 5×10^4 CFU/ml and the NF- κ B activity was measured, as a fold increase over PBS challenged cells. The results are shown in Figure 3.14:

The bacteria significantly activated NF- κ B signalling as early as two hours following challenge, with fold increases ranging from 28.1 ± 1.4 to 34.2 ± 5.8 ($p < 0.001$), and a peak response observed at four hours. At eight hours the signalling response was reduced but was still above control values and, moreover, this response was maintained up to the final time-point of 24 hours. These data indicated that the bacteria collected from the TLR-5 SNP patients elicited a 'normal' NF- κ B signalling response in RT4 cells and that infection was probably due to the defect in the host TLR-5 receptor resulting in reduced NF- κ B signalling and reduced innate defences.

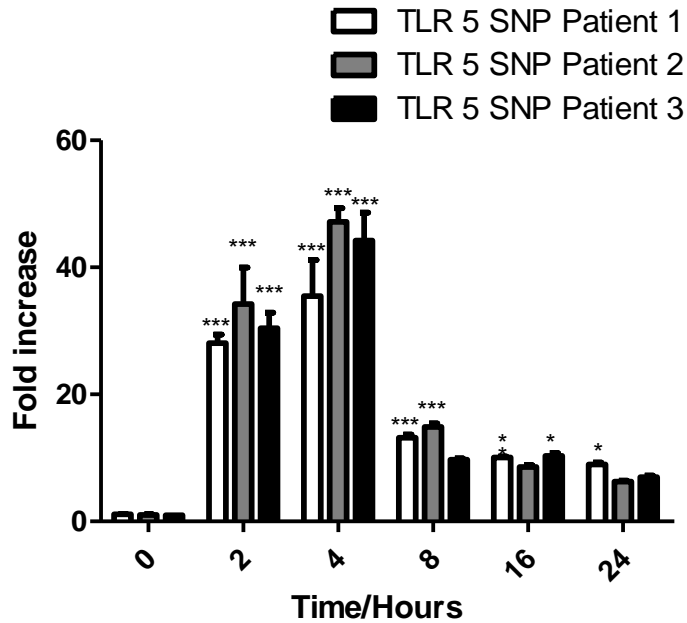


Figure 3.14 NF- κ B response of RT4 cells to bacteria isolated from patients carrying TLR-C1174T. RT4 reporter cells were incubated with 5×10^4 CFU/ml of heat killed bacteria isolated from urine. Error bars represent standard error of the mean and statistical significance was determined by ANOVA; *= $p < 0.05$, **= $p < 0.01$, ***= $p < 0.001$. (N=6, 2 experiments with 3 replicates each)

2. INHIBITION OF INNATE IMMUNE RESPONSE BY TLR-5 BLOCKING

To mimic the effects of the SNP, RT4 cells were treated with antibody to TLR-5 and the cells were challenged for 24 hours with the bacterial clinical isolates. The medium bathing the cells was collected and analysed for IL-8, which allowed downstream signalling effects of the SNP to be reported. The results are shown in Figure 3.15.

Challenging RT4 cells with 250 ng/ml of flagellin resulted in IL-8 mean concentration of 12429.5 ± 130.4 pg/ml. Blocking TLR-5 resulted in a significant reduction in IL-8 synthesis to 3130.7 ± 372.7 pg/ml (4 fold, $p < 0.001$). The three bacterial clinical isolates induced a mean IL-8 concentration of 20349.4 ± 1080.8 pg/ml for strain 1 (strain of patient 1) 19771.7 ± 465.9 pg/ml for strain 2 (strain of patient 2) and 23181.9 ± 745.4 pg/ml for strain 3 (strain of patient 3). Treating the cells with the TLR-5 antibody

significantly reduced ($p < 0.001$) the IL-8 concentrations for all challenges- 10.7 fold reduction for strain 1, 12.8 fold reduction for strain 2 and 15.9 fold reduction for strain 3. These data confirmed the importance of the host innate defences in the recognition and clearance of bacteria associated with UTI. To further verify these findings, the urine IL-8 concentrations of patients carrying the SNP and with active UTI were compared to those of normal controls also having an infection.

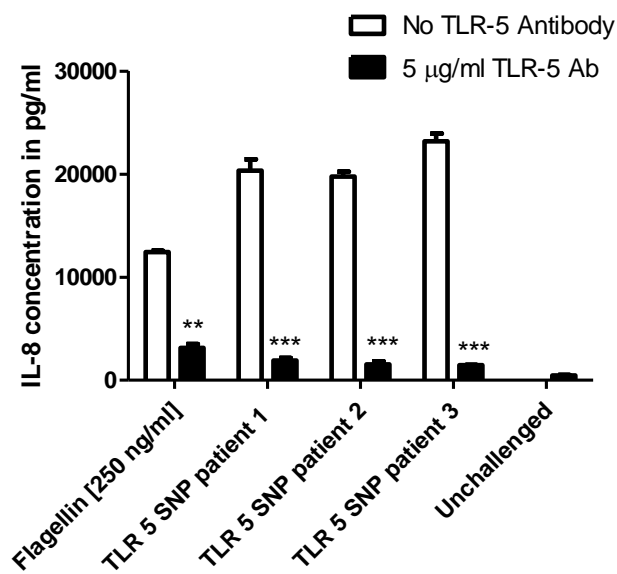


Figure 3.15 Inhibition of innate immune response to SNP-Bacteria by blocking TLR-5. RT4 cells were challenged with 5×10^4 CFU/ml of TLR-5 SNP bacteria in the presence or absence of 5 µg/ml of blocking TLR-5 specific antibody. Flagellin was used a positive control. RT4 cells were additionally incubated with the blocking antibody only. Media bathing the cells was used to measure the IL-8 secretion (N=2, using pooled media from 3 replicates each). Statistical significance was investigated using a Student's T-test; **= $p < 0.01$, ***= $p < 0.001$

3. IL-8 RESPONSE IN URINE OF PATIENTS WITH A URINARY TRACT INFECTION

Figure 3.16 shows the group of TLR-5 SNP patients suffering from a UTI had a mean IL-8 urine concentration of 117.8 ± 64.2 pg/ml, which was significantly reduced ($p < 0.05$)

compared to the mean urine concentration of patients carrying wild-type TLR-5 (705.1±302.3 pg/ml) although these data were not normalised to creatinine.

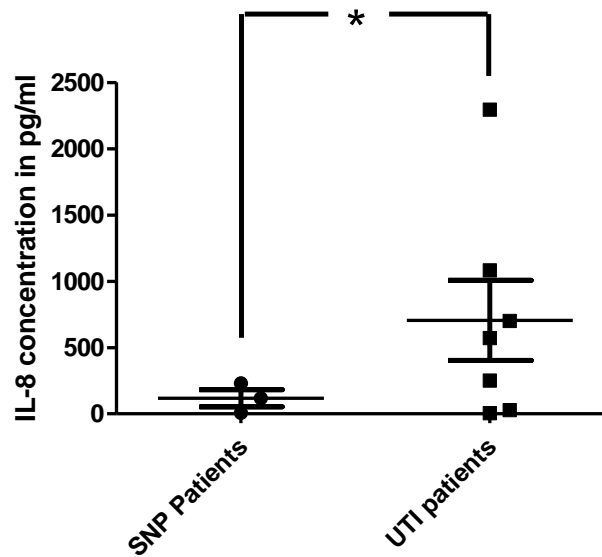


Figure 3.16 Measurement of IL-8 concentration in Urine from patients suffering a UTI. Measurement performed using a sandwich ELISA. Urine samples of UTI patients were grouped according to the presence of the C1174T SNP in the TLR-5 gene (N=3 for SNP Carriers and N=7 for normal TLR-5 gene carriers). Statistical significance was measured using a Student's T-test. *=p<0.05.

These data suggest that the TLR-5 SNP patients failed to recognise motile flagellated pathogens and this has predisposed them to recurrent UTI. It is worth noting that a number of the non-TLR-5 SNP patients also failed to induce IL-8. This may have been due to other genetic factors such as SNPs in the promoter regions of the IL-8 gene reducing gene expression and protein synthesis¹⁵⁵.

3.9. DISCUSSION

This Chapter focussed on the significance of bacterial PAMPs and cell surface TLRs in the innate defence of the uroepithelium from microbial assault.

To analyse the early innate immune response in detail a qPCR gene array comprising genes associated with TLR signalling was utilised. RNA was isolated from RT4 cells modelling the uroepithelium challenged with three different *E. coli* strains, including NU14 associated with infection of the UT²⁴. The results were generally disappointing with the majority of genes not showing differential expression. In reality the majority of genes on the array plate were more linked to the functioning of professional APC and adaptive immune cells than epithelia, which may explain their lack of activation in the experimental system used, *i.e.* RT4 cells. Another explanation for the limited data from the plates could be that the time point of four hours was too early to capture significant differential gene expression. Nonetheless, this time point was selected based on pilot data that indicated significant NF- κ B signalling in RT4 cells challenged with *E. coli*¹³⁷ and was further supported by the NCTC 10418 array data (Table 3.1).

The genes that were upregulated, however, showed a unique response of RT4 cells to each of the *E. coli* strains used K12, NCTC10418 and NU14. The strains were chosen according to their motile characteristics (K-12 and NCTC 10418 are motile strains¹³⁷) and their pathological background (NU14 is a UPEC isolated from a cystitis event). While only two genes were upregulated in all three challenges - CD14, encoding a protein involved in LPS recognition and IL-8, regulated by NF- κ B and encoding a chemoattractant for neutrophils, the latter result indicated the importance of NF- κ B signalling in the innate defences of the uroepithelium.

To further investigate the signalling responses RT4 NF- κ B reporter cells were used and all bacteria used in the challenge of the cells were heat killed to prevent cell cytotoxicity caused by the bacterial overgrowth¹³⁷. An initial concern with this approach was that bacterial cell lysis released antigens, which epithelial cells *in vivo* would not normally be exposed to. However, bacterial cell lysis does occur in the bladder as a result of natural bacterial death and the action of antimicrobial agents including AMPs and lysozyme. Moreover, by killing the bacteria the number of challenge time-points was increased (up to 24 hours), experimental variation was reduced as all the bacterial cells were grown to OD₆₀₀ of 0.6 and the challenges were all performed using the same numbers of bacterial cells.

The NCTC 10418 strain, which was the most motile, induced the highest NF- κ B response in the RT4 reporter cells (43 fold). In fact the signalling response was twice that of CFT 073 (20 fold), a laboratory strain originating from a patient with pyelonephritis¹⁴⁷. The maximal NF- κ B response to the non-motile UPEC strain NU14 was also very weak (7 fold), supporting the pathogenic capabilities of the latter two strains to overcome the host defences. In addition these data indicate the significance of bacterial motility in the ability of the host to recognise potential pathogens. In fact, it could be argued that the lack of motility of the UPEC strain NU14 allows it to 'hide' from the host innate defences. Yet, the motility theory is not straightforward as CFT 073 is motile and induces an innate response via NF- κ B signalling, but is associated with UTI. CFT 073, however, has developed a method by which it can manipulate the host response. In 2008, Cirl and colleagues showed that CFT 073 secreted a protein that mimics the TIR domain of TLR³⁷. The authors named this protein TcpC (TIR-domain containing protein of *E. coli*), and demonstrated its ability to prevent the attachment of the adaptor protein MyD88 by sequestering it³⁷. This adaptation may explain the

reduced NF- κ B signalling response observed in the RT4 cells but further challenge experiments using CFT 073 strains in which the TcpC protein is either mutated or deleted are required.

Bacterial motility is linked to flagellin which is the ligand for TLR-5^{94,146}. Flagellin (250 pg/ml) purified from *E. coli* induced a significant NF- κ B response in RT4 cells as early as four hours and the response was, 34 times greater than that observed with LPS (10 μ g/ml) or peptidoglycan (10 μ g/ml). Flagellin was also associated with effector IL-8 concentrations ten times greater than those detected following LPS challenge and 200 times those associated with peptidoglycan. These data indicated that TLR-5 is a pivotal receptor in the defence of the uroepithelium and this was confirmed by experiments using a TLR-5 blocking monoclonal antibody. Analogous results were also reported using primary cells by Smith et al, in 2011¹⁵⁶, where flagellin induced strong IL-6 and IL-8 responses, but only in proliferating uroepithelium¹⁵⁶.

The response to LPS was investigated to control for LPS contamination of the flagellin preparation. Initial experiments to purify the *E. coli* flagellin used a size exclusion column but this resulted in a catastrophic loss of sample (Fig. 3.4B). Thus flagellin was prepared and used without the size exclusion step, *i.e.* fine purification, so contamination of the flagellin stocks with LPS could not be excluded. Potential LPS contamination of flagellin was not considered a problem as during previous research, the TLR-4 ligands LPS and Lipid A failed to evoke an NF- κ B response¹³⁷. However, other investigators have reported LPS to induce an innate response in bladder cells¹⁵⁰. Thus LPS challenges of RT4 cells were performed up to 24 hours, and compared to previous experiments, using an increased concentration, *i.e.* 10 μ g/ml. The results revealed that LPS induced a NF- κ B signalling response but the maximum response was <10 fold and at 16 hours post challenge. This compared to the flagellin response which

was 7 fold at one hour and maximum, *i.e.* 45 fold at 4 hours. These data indicated that LPS is less important in the induction of an innate response in the bladder although interestingly NU14 is known to have a mechanism, using the *waaL* gene, by which it manipulates its outer LPS to evade a host response³⁶. It is worth noting that Smith *et al.* (2011), using 1 µg/ml did not detect any innate immune response of the uroepithelia to LPS. The findings reported here therefore indicate that higher concentrations of LPS are needed to evoke an uroepithelial innate immune response and supported previous findings that in the defence of the human uroepithelium TLR4 is less important than TLR-5. When RT4 cells were challenged with peptidoglycan, a TLR-2 ligand, NF-κB signalling was again detected but the response was weak and comparable to that of LPS. These data again suggested that TLR-2, like TLR4, is of reduced importance in the defence of the UT.

The PAMPs used, *i.e.* flagellin, LPS and Peptidoglycan did not induce microscopically visible cytotoxic effects in RT4 cells. Nonetheless, an assessment of the cytotoxicity of the challenges must be performed in future research using a cell viability assay, *e.g.* MTT assay.

As TLR-5 appeared to be a key UT defence factor it was predicted that clinical strains associated with UTI may avoid the host defences by adopting reduced motility. To explore this further the motility and NF-κB activating ability of 24 clinical isolates, defined as *E. coli* by standard clinical methodology, were investigated. However, 12/24 strains were motile and ten of those induced NF-κB signalling, although the NF-κB signalling responses of the motile strains were quite variable. Induction of NF-κB signalling was surprising but as statistical analysis of the effector IL-8 concentrations failed to show significance, the data could be interpreted to support bacterial

mechanisms functioning to inhibit signalling pathways downstream of NF- κ B. This requires further investigation.

Conversely UTIs may result from motile, NF- κ B activating bacteria infecting subjects characterised by defects in their host innate defences, including non-functioning TLR receptors. It is known that people suffering from a TLR-5 C1174T SNP are more prone to recurrent urinary tract infections⁸⁹. In fact, bacteria isolates collected from the urine of such patients during an infection and used to challenge RT4 cells resulted in NF- κ B activation and IL-8 synthesis. These observations support the premise that a functional TLR-5 is key in protecting the uroepithelium from infection.

This chapter highlights the importance of bacterial motility, flagellin and TLR-5 in the recognition of potential pathogens by the uroepithelium. Activation of TLR-5 is known to result in IL-8 synthesis and the recruitment of APCs, and neutrophils, but for rapid bacterial clearance host agents able to kill the microbes are essential. One such agent is human β -Defensin 2 (h β D-2), and this was shown by a colleague, Mr Ased Ali (Newcastle University), to protect the uroepithelium from bacterial infection¹⁵⁷. The following chapter focuses on the development of an h β D-2 specific reporter to investigate h β D-2 gene regulation.

CHAPTER FOUR

Human β -Defensin 2 Reporter

4.1. INTRODUCTION

In the previous chapter, the interactions between pathogen and host were investigated in cells modelling the urinary tract. These data determined a pivotal role for TLR-5 in the recognition of motile bacteria and the resulting activation of the transcription factor NF- κ B. Impaired recognition, as a consequence of a SNP in the TLR-5 gene or by pathogen inhibition of cell signalling, resulted in a deficient NF- κ B and thus innate immune response as evidenced by reduced IL-8 concentrations and h β D-2 secretion¹⁵⁷. It is proposed that this impaired response increases the risk of recurrent (r)UTI in susceptible women. Restoring a normal h β D-2 response in such subjects could therefore help prevent or help treat rUTIs.

Based on this premise, the investigations in this Chapter focussed on exploring the mechanisms, in addition to NF- κ B, involved in regulating h β D-2 expression. To achieve this a bioinformatics approach was used to identify putative transcription factor binding sites in the 5'- non-translated promoter region and a h β D-2 reporter system was engineered to examine whether such sites could be exploited to activate h β D-2 expression.

Based on the bioinformatics data the roles of hormones and nutritional factors, specifically, oestrogen, resveratrol and vitamin D in the induction of h β D-2 were investigated using RT4 bladder and VK-2E6/E7 vaginal cells. In addition, h β D-2 induction was investigated using Zymosan, a fungal cell wall preparation alone and in combination with oestrogen, resveratrol and Vitamin D.

4.2. TRANSCRIPTION FACTOR BINDING SITES IN THE 5' UTR OF hβD-2

Previous work has shown that hβD-2 is synthesised in response to infection of the urogenital tract and that a reduction in hβD-2 increases the chance of infection with flagellated *E. coli* strains^{158,159}. Hence, an understanding of hβD-2 expression is necessary for the design of future therapies directed at its enhancement. Thus the 5' non-translated region of the hβD-2 or DEFB4 gene was investigated for potential transcription factor (TF) binding sites using bioinformatics. For this, the sequence of 2030 bp preceding the 5' start codon of the DEFB4 gene was obtained from the genome database GRCh37.p10 and analysed using the PROMO software¹⁶⁰. The resulting TF binding sites found during this investigation are shown in Figure 4.1:

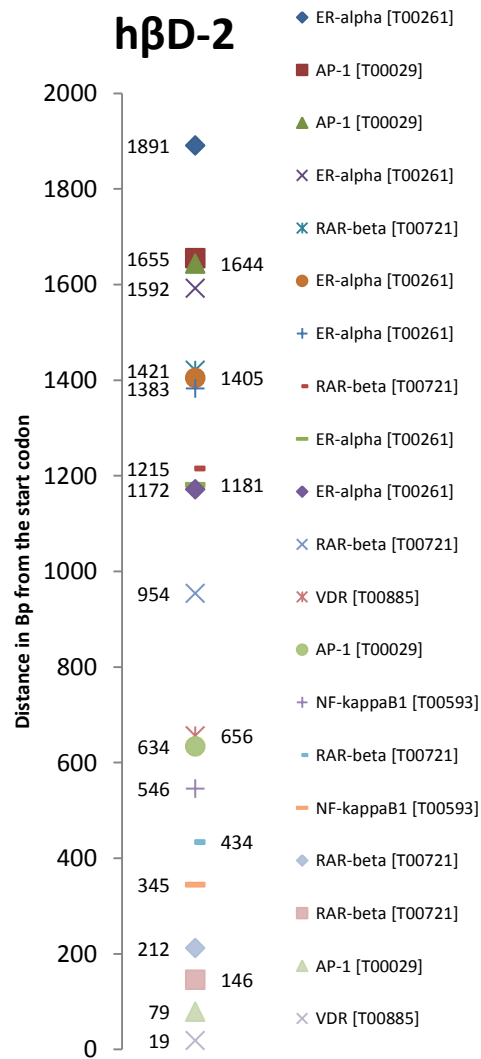


Figure 4.1 Transcription factor binding site search in the 5-UTR of the *hβD-2* gene using the Bioinformatics software PROMO. Transcription factors included in the investigation were NF-κB, Activator Protein 1 (AP-1), Vitamin D receptor (VDR), Retanoic Acid Receptor (RAR-beta) and Oestrogen Receptor (ER-alpha). The transcription factors in the legend are sorted by their proximity to the start codon (0). For details see materials & methods section 2.19.I

Data mining of TF binding sites of the *hβD-2* 5' untranslated region (Fig. 4.1) identified two NF-κB binding sites , 345 and 546 bp respectively from the start codon of the *h-βD-2* gene. Four AP-1 binding sites were also detected at positions 79, 634, 1644 and 1655 bp respectively. Adjacent to the start codon with a distance of 19 bp was the Vitamin D Receptor (VDR) transcription factor binding site (Fig. 4.1). A further VDR binding site was detected at 656 bp from the start codon. A total of six binding sites were found for Retinoic Acid Receptor-beta (RAR-beta) at 146, 212, 434, 954, 1215 and 1421 bp from

the start codon; Oestrogen Receptor- alpha (ER- α) also had a total of six binding sites 1172, 1181, 1383, 1405, 1592 and 1891 bp from the start codon.

These data show that in addition to NF- κ B, a number of other transcription factors are present in the 5' non-translated region of the DEFB4 gene. Moreover, the presence of the ER- α and VDR elements raised the potential of exploiting vitamin D or oestrogen therapy to enhance h β D-2 expression and help prevent or treat UTIs. The roles and importance of such TF binding sites in the functioning of the urogenital epithelium in relation to h β D-2 expression were therefore investigated using a reporter gene assay. For this assay, 2030 bp of the 5' non-translated region of h β D-2 were fused to a reporter gene, transfected into either RT4 bladder cells or VK-2 E6/E7 vaginal cells and challenged with *E. coli*, bacterial PAMPs and reagents including oestrogen and vitamin D. The aim was to identify potential agents that activated and /or enhanced h β D-2 expression in the urogenital tract.

4.3. CONSTRUCTION OF REPORTER PLASMID USING GFP REPORTER

In order to engineer the reporter plasmid, 2030 bp of DNA 5' to the start of the DEFB4 gene was amplified as described in section 2.5.V.

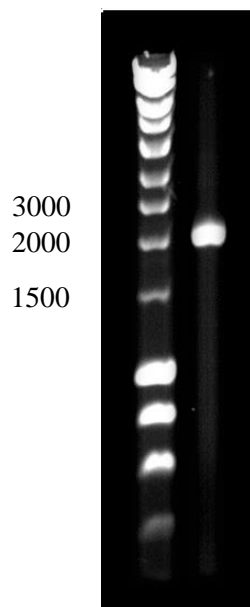


Figure 4.2 Amplification of a 2030 bp region 5'UTR of the DEFB4 gene. Lane 1, the marker Hyperladder I. Lane 2 shows the amplification of the 2030 bp region using KOD-polymerase. DNA was separated on a 0.8 % agarose gel.

The amplification resulted in a band of the expected size, *i.e.* 2000 bp (Fig. 4.2, lane 2). This was cloned into the pGlow TOPO vector as described in section 2.12.II. The presence and orientation of the insert in the plasmid was confirmed by using unique EcoRI and KpnI restriction sites, determined using SerialCloning 2.5 Software, in the insert (Fig. 4.3).

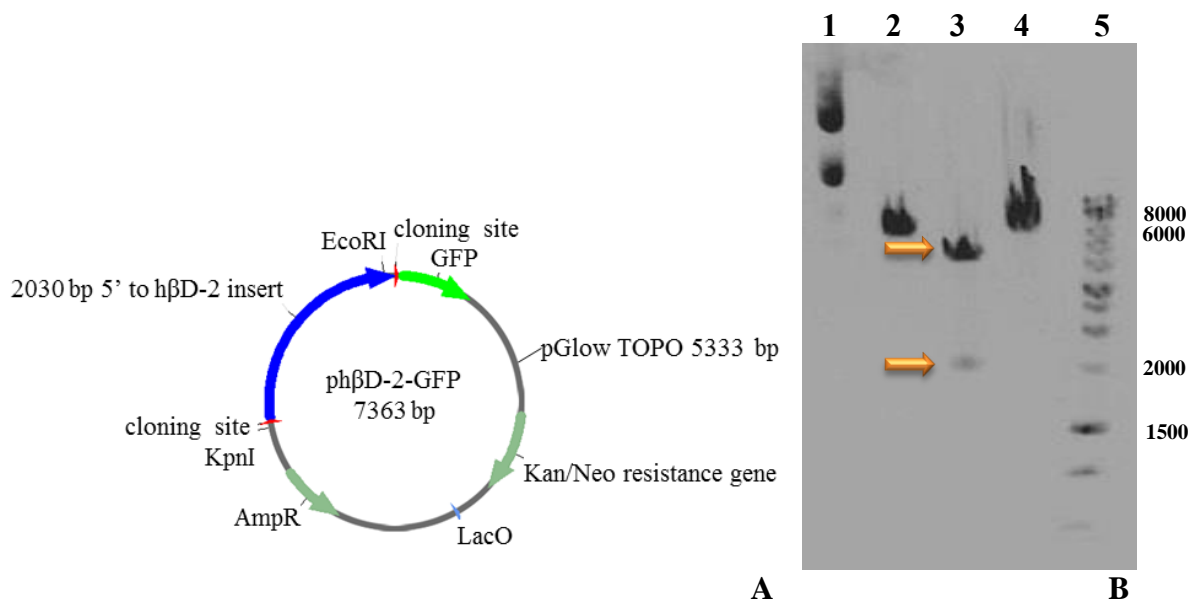
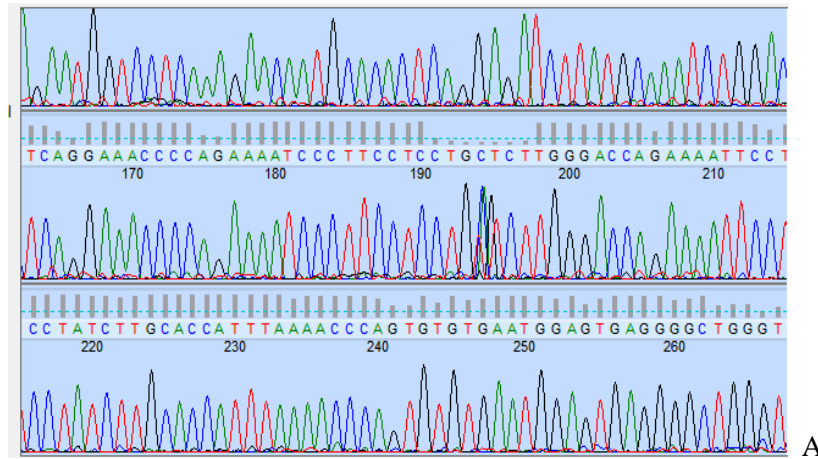
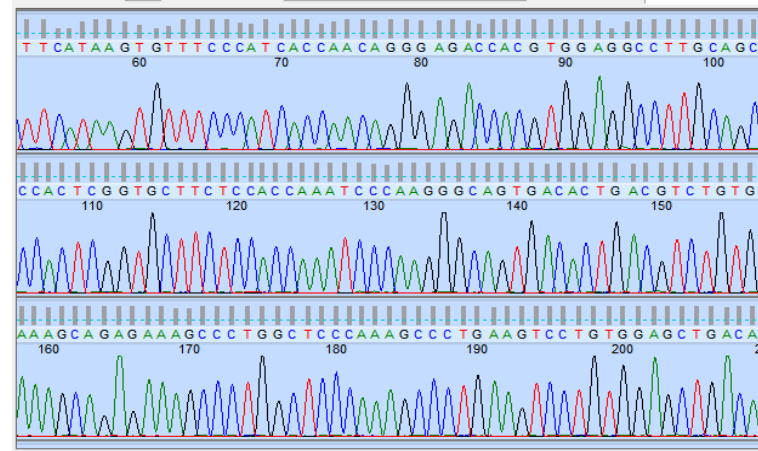


Figure 4.3 Engineering ph β D-2-GFP Reporter. (A) Schematic view of plasmid after ligation with the restriction sites for Plasmid containing the first 2030 bp of the 5' region of the DEFB4 gene. (B) Cloning of the 5' UTR into pGlow TOPO. The first lane is the undigested plasmid. The second lane shows the plasmids after ligation linearised with Eco RI, the third with Eco RI and Kpn I. The orange arrows show the products of expected size. The fourth lane shows Kpn I digestion of the plasmid after the ligation. The ladder is 1 kBp (lane 5, Promega). DNA was separated on a 0.8 % agarose gel.

The predicted plasmid, following cloning of the promoter region and highlighting the unique EcoR1 and Kpn1 restriction sites, is shown in Fig.4.3.A. Linearisation of the plasmid was achieved using either EcoRI or KpnI, and the linearised plasmid DNA migrated at approximately 7500 bp, which related to the expected size of 7363 bp (Lanes 2 and 4, Fig.4.3.B). The enzymatic restriction with EcoRI and KpnI simultaneously resulted in the expected two bands of approximately 5500 and 2000 bp, which agreed with the expected sizes of 5395 bp and 1968 bp respectively (lane3). These data indicated that the cDNA insert was the h β D-2 5' region and was cloned in the correct orientation. DNA sequencing (GENEVISION, Newcastle, UK) confirmed the presence and orientation of the insert (Fig. 4.4).



A



B

Score	Expect	Identities	Gaps	Strand
1886 bits(1021)	0.0	1089/1117(97%)	24/1117(2%)	Plus/Plus
Query 43	AGCATTTCGTGGGGTGCCTGGCAGGACATGTGCATGGCGAGGCAGGTTCATCAGCAGCAAG	102		
Sbjct 15	AGCATTTCGTGGGGTGCCTGGCAGGACATGTGCATGGCGAGGCAGGTTCATCAGCAGCAAG	74		
Query 103	TGAGAGCTGCCTCTTACTTTCTAAAGGTGACATAGCAAATATACAAAAAAAAAATAATAA	162		
Sbjct 75	TGAGAGCTGCCTCTTACTTTCTAAAGGTGACATAGCAAATATACAAAAAAAAAATAATAA	134		
Query 163	ATTATTAATTTAGGTAGAGCACATAAAGGCTTTAATTCATATTCATTTCTCTGTATGCT	222		
Sbjct 135	ATTATTAATTTAGGTAGAGCACATAAAGGCTTTAATTCATATTCATTTCTCTGTATGCT	194		
Query 223	TTCTTCACCAGGAAGAAATAGTTTTAGTGTGAGGAAATGAATGAGTGTGCCCTCAATTC	282		
Sbjct 195	TTCTTCACCAGGAAGAAATAGTTTTAGTGTGAGGAAATGAATGAGTGTGCCCTCAATTC	254		
Query 283	AGCCTGCTCAACACACAAGGAACAAAGCCCTGACAATCAGAGTGACTCCCTGGTGACTA	342		
Sbjct 255	AGCCTGCTCAACACACAAGGAACAAAGCCCTGACAATCAGAGTGACTCCCTGGTGACTA	314		
Query 343	AGCTCCAGTCTGGATGCATATTTGTTTAGCAGTCTGACAGCATCTGACCCAGCCCTCT	402		
Sbjct 315	AGCTCCAGTCTGGATGCATATTTGTTTAGCAGTCTGACAGCATCTGACCCAGCCCTCT	374		

C

Score	Expect	Identities	Gaps	Strand
1742 bits(943)	0.0	962/970(99%)	5/970(0%)	Plus/Plus
Query 1061	CCAGAGACCTCACACAGCCCTGAAAACATGGGGCTCCCTTCATAAGTGTTCATCCATCACCA	1120		
Sbjct 16	CCAGAGACCTCACACAGCCCTG-AAACATGGGGCTCCCTTCATAAGTGTTCATCCATCACCA	74		
Query 1121	ACAGGGAGACCACGTGGAGGCCTTCAGCCCCACTCGGTGCTTCTCCACCAATCCCAAG	1180		
Sbjct 75	ACAGGGAGACCACGTGGAGGCCTTCAGCCCCACTCGGTGCTTCTCCACCAATCCCAAG	134		
Query 1181	GGCAGTGACGCTGACGTCTGTGGAAGCAGAGAAAGCCCTGGCTCCCAAGCCCTGAAGT	1240		
Sbjct 135	GGCAGTGACACTGACGTCTGTGGAAGCAGAGAAAGCCCTGGCTCCCAAGCCCTGAAGT	194		
Query 1241	CCTGTGGAGCTGACATTCCTGAGTGACGGTGTGAATGGAAGGAACCTAAGTGCAGGTTGG	1300		
Sbjct 195	CCTGTGGAGCTGACATTCCTGAGTGACGGTGTGAATGGAAGGAACCTAAGTGC-GGTGG	253		
Query 1301	TAGGCCACCTCCTGGCCAGGCCTGGGTGAACCTGAGGGGACACATGTAGTCACAAATCC	1360		
Sbjct 254	TAGGCCACCTCCTGGCCAGGCCTGGGTGAACCTGAGGGGACACATGTAGTCACAAATCC	313		
Query 1361	CATCCTCCCAATTCCTTCTCAGAGGAAGGAAGTGGGCATCCATCTGCCCATCTCTCTC	1420		
Sbjct 314	CATCCTCCCAATTCCTTCTCAGAGGAAGGAAGTGGGCATCCATCTGCCTCATCTCTCTC	373		

D

Figure 4.4 Confirmation of engineered ph β D-2-GFP Reporter by sequencing and alignment. (A and C) Sequencing using the forward primer at position 1: (A) Plasmid was sequenced by Genevision UK. (B) Sequence was aligned with predicted sequence using BLAST alignment tool. (B and D) Sequencing using a forward primer from position 1000. (C) Plasmid was sequenced by Genevision UK. (D) Sequence was aligned with predicted sequence using BLAST alignment tool (<http://blast.ncbi.nlm.nih.gov/BlastAlign.cgi>).

In fact, aligning the cloned sequences to the predicted sequence found in the RefSeq Genome database (<http://www.ncbi.nlm.nih.gov/refseq/>) showed 97 % identity. The plasmid was considered optimal and therefore the next step was the optimisation of its transfection into RT4 and VK-2 E6/E7 cells modelling the urogenital tract.

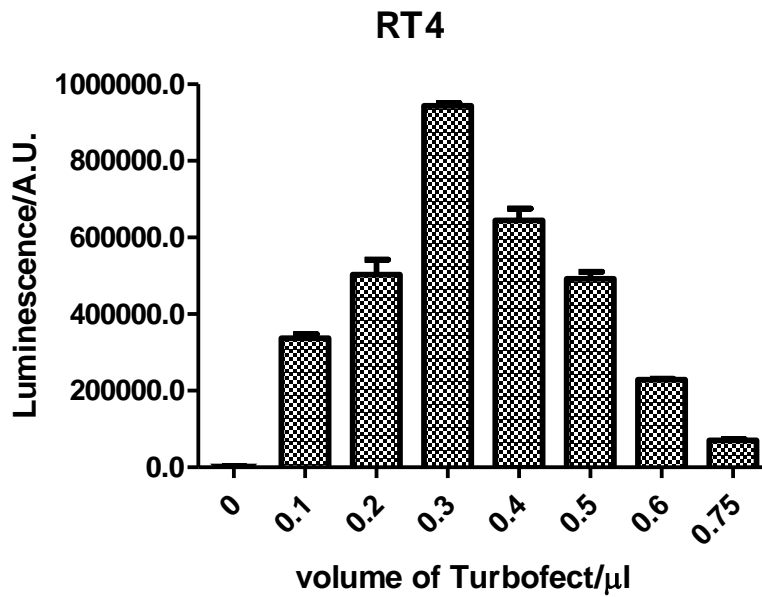
1. TRANSFECTION OPTIMISATION OF RT4 AND VK-2 E6/E7 CELLS

The transfection conditions of the RT4 and VK-2 E6/E7 cells were optimised to achieve maximum transfection efficiency. For this, transfections a reporter plasmid with a strong promoter (CMV) and a luciferase reporter was used (pGL4.51, Promega, UK). For RT4 cell transfections the transfection reagent TurboFect was utilised while for VK-2 E6/E7 cells Attractene transfection agent was used. Attractene was used because no transfection was achieved when TurboFect was used to transfect the VK-2 E6/E7 cells (data not shown). The concentrations of DNA-transfection reagent are shown in Table 4.1:

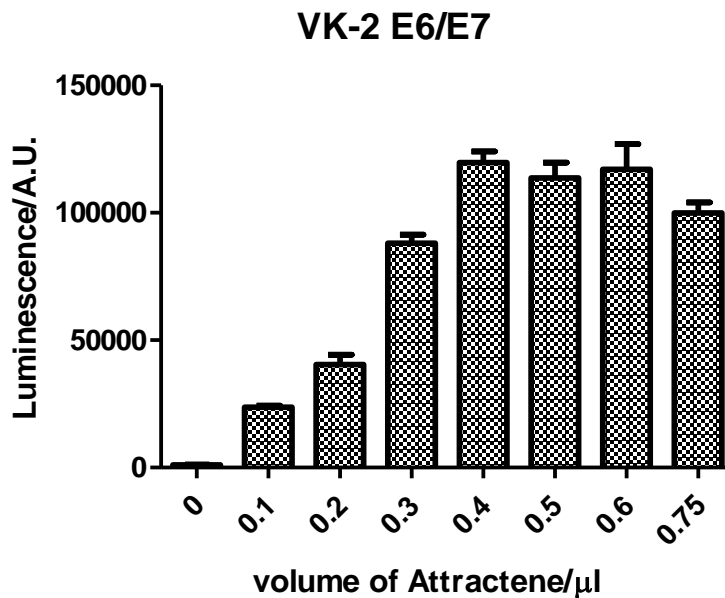
Table 4.1: Concentration of DNA-Transfection Reagent Mixture

Volume of trans- fection reagent/ μ l	TurboFect	Attractene
	Amount of DNA/ng	Amount of DNA/ng
0	0	0
0.1	50	27
0.2	100	54
0.3	150	81
0.4	200	108
0.5	250	135
0.6	300	162
0.75	375	202.5

The results of the transfection optimisation are shown in Figure 4.5:



A



B

Figure 4.5 Optimisation of transfection using CMV-Luciferase reporter plasmid. (A) Optimising transfection in RT4 cells using TurboFect transfection reagent (Thermo Scientific). **(B)** Optimisation of transfection in VK-2 E6/E7 cells using Attractene (QIAGEN). Values shown on the x-axis represent the volume of transfection reagent used. Reporter plasmid was CMV-Luc. N=6, 2 experiments with 3 replicates

As shown in Figure 4.5.A, the concentration of TurboFect achieving the highest transfection efficiency in RT4 was 0.3 μ l. Indeed, at volumes higher than 0.5 ml, cell cytotoxicity was observed and reporter activity, *i.e.* luminescence was reduced. In

accordance with this, the optimal volume for transfecting RT4 was determined as 0.3 μ l of TurboFect-DNA.

VK-2 E6/E7 cells transfected with 0.4 μ l to 0.75 μ l of Attractene-DNA mix showed a similar response with luminescence of 119631 ± 4409 A.U. for 0.4 μ l vs. 99979 ± 4127 A.U. for 0.75 μ l (Fig. 4.5.B). Moreover, no cell cytotoxicity was observed when the cells were observed under the microscope. Therefore, 0.4 μ l Attractene-DNA was used as the optimal concentration for transfection of VK-2 E6/E7 cells.

4.4. VALIDATION OF PHBD2-GFP REPORTER GENE

Next, a pilot experiment using the optimal concentration of the transfection reagent-DNA mix and RT4 cells was performed. To control that the optimised concentration for the transfection is suitable for a GFP assay, the cells were transfected with a positive control reporter containing a GFP reporter (CMV-GFP, SABiosciences) and the ph β D-2-GFP reporter, as described in section 2.11.II. The latter cells challenged with flagellin or the *E. coli* strain NCTC 10418 for up to 16 hours. NCTC 10418 and flagellin were chosen as they induced the highest NF- κ B activity in RT4. Fluorescence was detected using a fluorescent microscope (EVOS FL) and the results of the images taken are shown in Figure 4.6:

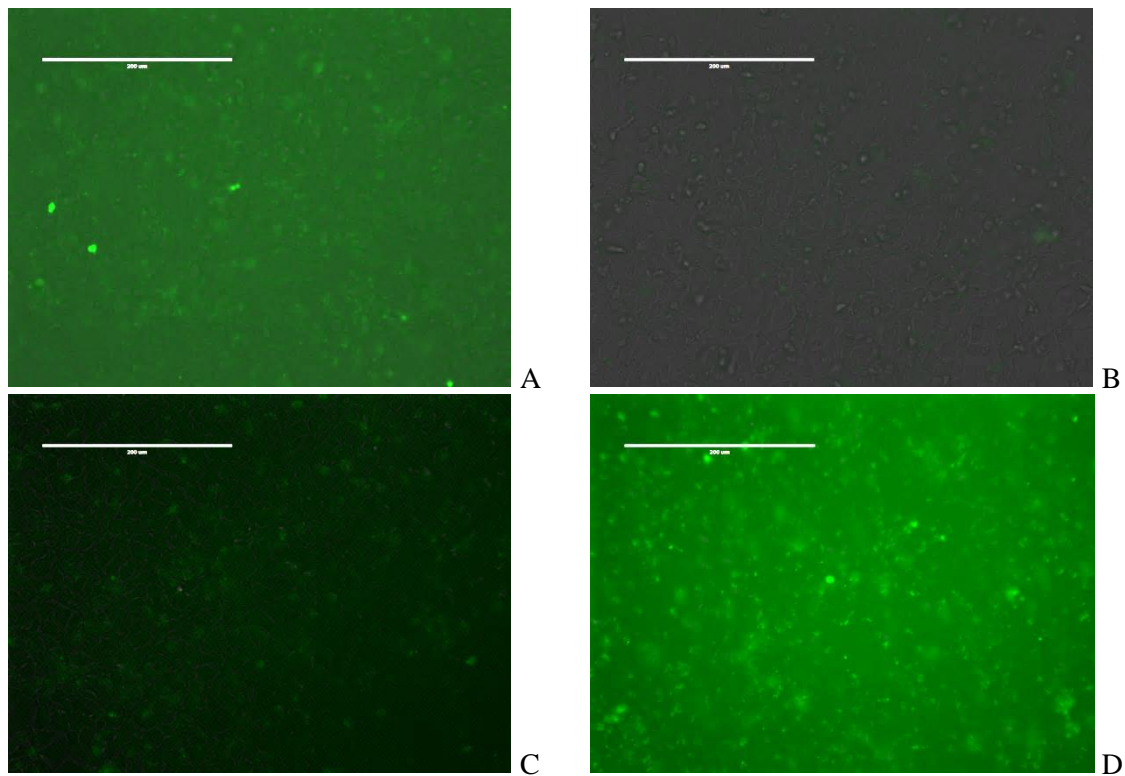


Figure 4.6 Validation of ph β D-2-GFP using fluorescent microscopy RT4 cells were transfected with control reporter (A, CMV-GFP, SABiosciences) or with ph β D-2-GFP reporter (B-D). (B) RT4 cells challenged with PBS, (C) 250 ng/ml flagellin, (D) 5×10^4 CFU/ml of NCTC 10418. Images taken using an EVOS FL microscope and, 100 x magnification. Bars represent 200 μ m

Transfection of the positive control (Fig. 4.6.A) resulted in fluorescence indicating that the RT4 cells were successfully transfected with the optimised concentration. The ph β D-2-GFP transfected RT4 cells incubated with PBS did not show fluorescence (Fig. 4.6.B), but did fluoresce when either flagellin or bacteria (NCTC 10418) were added to the cells (Fig. 4.6.C and D).

The transfections appeared to work but the observations were subjective; the aim was now to develop a quantitative reporter gene assay to investigate the activation of the h β D-2 gene. Quantitation of the fluorescence was achieved using a BMG Omega FluoStar fluorometer. RT4 cells were transfected as described previously and challenged with flagellin and NCTC 10418 for up to 16 hours. In addition, TNF- α , a known endogenous activator of h β D-2¹⁶¹, is functioning as a positive control and was

added to the challenges. The fluorescence was measured and the results of the transfected cells are shown Figure 4.7:

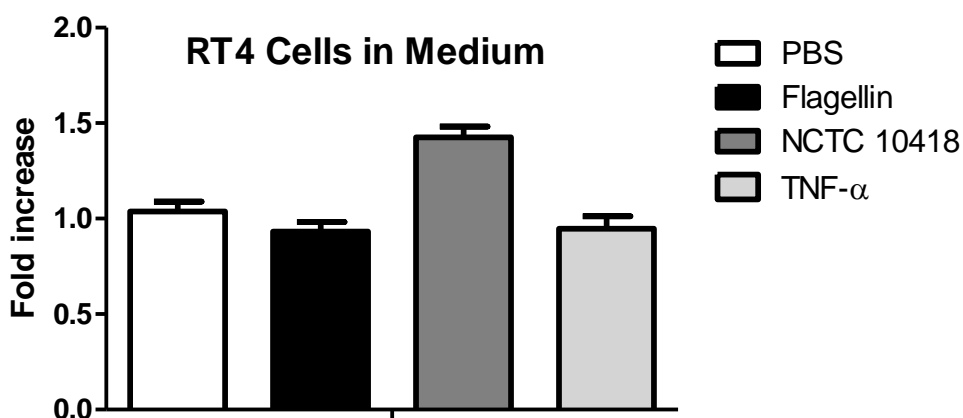


Figure 4.7 ph β D-2-GFP Reporter Activity in Challenged RT4 Cells. RT4 cells were transfected with the ph β D-2 reporter plasmid and challenged with the endogenous h β D-2 inducer TNF- α [20 ng/ml], bacterial flagellin [250 ng/ml], NCTC 10418 [5×10^4 CFU/ml] or PBS for 16 hours. Fluorescence of transfected and challenged RT4 cells was measured in RT4 medium. N=12, 4 experiments with 3 replicates each.

These data indicated that challenging RT4 cells transfected with the ph β D-2-GFP reporter plasmid did not result in any measurable increase in fluorescence with any of the reagents shown previously to induce h β D-2 gene expression. To address the possibility of auto-fluorescence of the media masking the reporter activity, the fluorescence of transfected RT4 cells was measured in PBS and the result is shown in Figure 4.8:

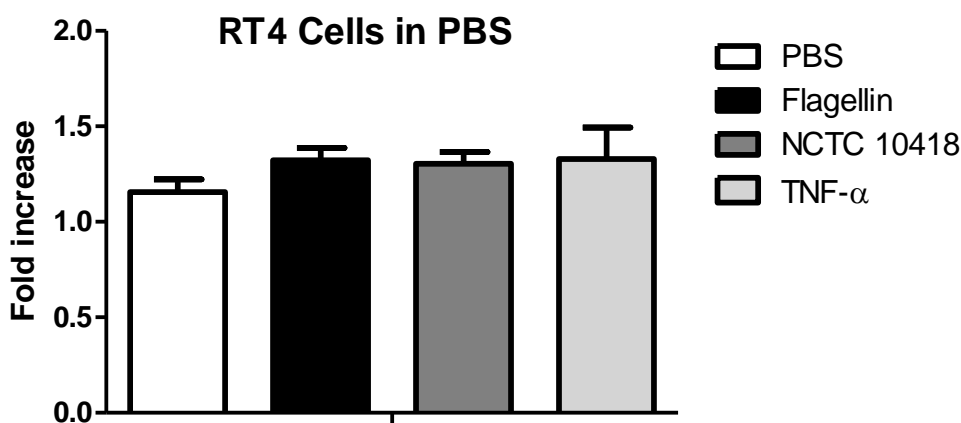


Figure 4.8 phβD-2-GFP reporter activities in challenged RT4 cells maintained in PBS. RT4 cells were transfected with the phβD-2 reporter plasmid and challenged with the endogenous hβD-2 inducer TNF-α [20 ng/ml], bacterial flagellin [250 ng/ml], NCTC 10418 [5x10⁴ CFU/ml] or PBS for 16 hours. The medium was washed off twice and replaced by PBS. Fluorescence of transfected and challenged RT4 cells was measured in PBS solution. N=12, 4 experiments with 3 replicates.

Changing the media to PBS did not cause an effect on the fluorescence measurement, suggesting that the phβD-2-GFP reporter as a tool to investigate the hβD-2 5' region for TF activity was too insensitive due to the cellular autofluorescence. Therefore an alternative reporter system was investigated.

4.5. CONSTRUCTION OF REPORTER PLASMID USING LUCIFERASE REPORTER VECTOR

Luciferase has the advantage, when compared to GFP, that it circumvents any problems due to cell, eukaryote and prokaryote, auto-fluorescence. The luciferase vector chosen was pGL 4.10 luciferase and the 2032 bp 5' non-translated region preceding the hβD-2 gene was ligated into pGL 4.10 as described in section 2.12.II using KpnI and HindIII restriction sites. Cloning results are shown in Figure 4.9:

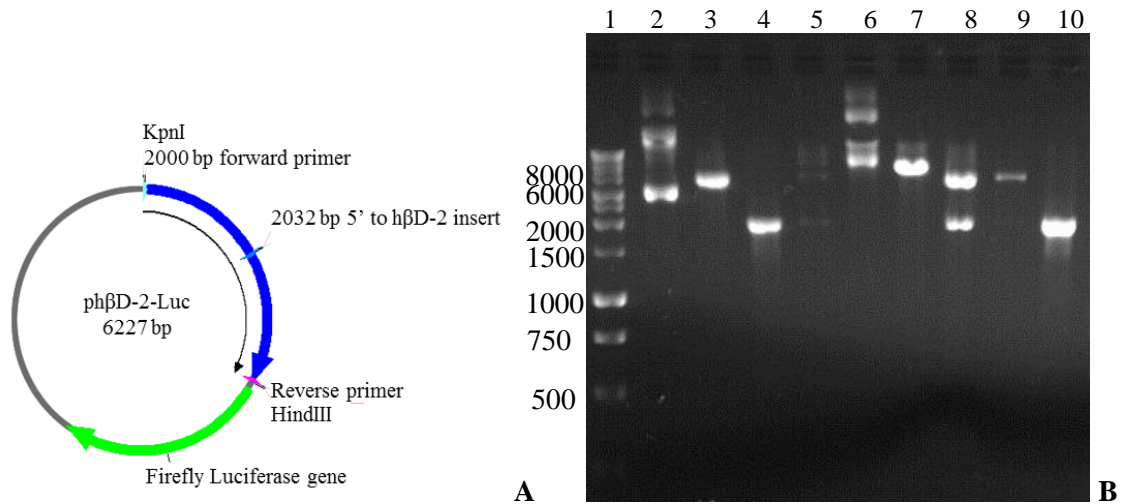
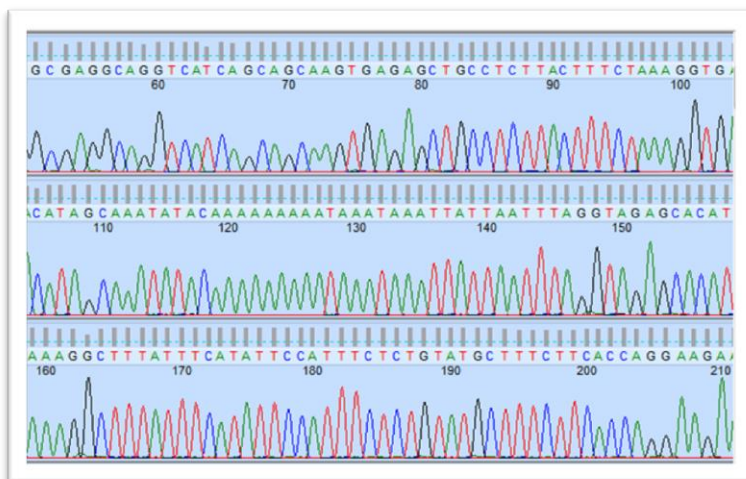
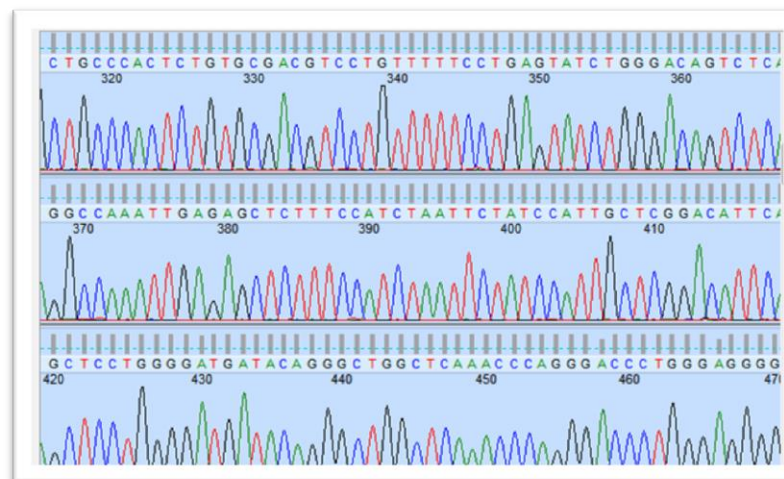


Fig. 4.9 Engineering of the ph β D-2-Luc Reporter. (A) Schematic view of ph β D-2-Luc using Serial cloner v2.5. 2032 bp insert of the 5' non-translated region of the h β D-2 gene is depicted in blue. The luciferase gene is shown in green. The plasmid has a size of 6227 bp after ligation. Plasmid engineering was simulated using Serial Cloner 2.5. (B) Engineering of the reporter gene using the pGL4.10 vector. The gel shows: 1 kbp marker (Promega UK, lane 1), pGL4.10 after purification (lane 2), pGL4.10 after double digestion using KpnI and HindIII (lane 3), the insert after double digestion using KpnI and HindIII (lane 4), ligation of the insert and pGL4.10 creating ph β D-2-Luc (lane 5), ph β D-2-Luc (insert + pGL 4.10) after transformation and purification (lane 6), plasmid linearised after Kpn I digestion (lane 7), insert verification of insert presence using Kpn I and Hind III (lane 8), linearisation of the ph β D-2-Luc plasmid with HindIII (lane 9) and PCR product using ph β D-2 primers and the plasmid as template (lane 10). DNA separated on 1 % Agarose gel.

Lane 3 shows the linear pGL4.10 vector following restriction with KpnI and HindIII (4191 bp). Lane 4, shows the h β D-2 insert migrating at approximately 2 kbp consistent with expected size of 2032 bp. Lane 7 shows the KpnI linearised ph β D-2-Luc plasmid migrating at approximately 6 kbp consistent with an expected size of 6227 bp (4191 bp for the pGL4.10 plus 2032 bp insert). A KpnI and HindIII double digestion of the ph β D-2-Luc plasmid resulted in the expected two bands with 2032 bp and 4187 bp (lane 8). Using the ph β D-2-Luc plasmid as a template for a PCR and using the insert primers (Table 2.1) also resulted in a band of the expected size (2032 bp, lane 10). Plasmid authenticity was confirmed by DNA sequencing (Fig. 4.10):



A



B

Range 1: 15 to 1108 [Graphics](#) ▼ Next Match ▲ Previous

Score	Expect	Identities	Gaps	Strand
1801 bits(975)	0.0	1075/1118(96%)	28/1118(2%)	Plus/Plus
Query 52	AGCATTTCGTGGGGTGGTGGCAGGACATGTGCATGGTGAGGCAGGTCAICAGCAGCAAG	111		
Sbjct 15	AGCATTTCGTGGGGTGTGGCAGGACATGTGCATGGCGAGGCAGGTCAICAGCAGCAAG	74		
Query 112	TGAGAGCTGCCCTCTACTTTCTAAAGGIGACATAGCAAGTATACaaaaaa---aaaTAA	168		
Sbjct 75	TGAGAGCTGCCTCTTACTTTCTAAAGGTGACATAGCAAATATACAAAAAAAAATAAATAA	134		
Query 169	AATATTAATTTAGGCAGAGCACATAAAGGCTTTATTTTCATATCCATTTCTCTGTATGCT	228		
Sbjct 135	ATTATTAATTTAGGTAGAGCACATAAAGGCTTTATTTTCATATCCATTTCTCTGTATGCT	194		
Query 229	TTCTTCACCAGGAAGAAATAGTTTTAGTGTGAGAAIGAAIGAGTCTGCCCTCAATTC	288		
Sbjct 195	TTCTTCACCAGGAAGAAATAGTTTTAGTGTGAGAAIGAAIGAGTCTGCCCTCAATTC	254		
Query 289	AGCCTGCTCAGCACACAAGGAACAAAGCCCTGACAAICAGAGTGACTCCCTGGTGACTA	348		
Sbjct 255	AGCCTGCTCAGCACACAAGGAACAAAGCCCTGACAAICAGAGTGACTCCCTGGTGACTA	314		

C

Range 1: 8 to 1264 [Graphics](#) ▼ Next Match ▲ Previous

Score	Expect	Identities	Gaps	Strand
2087 bits(1130)	0.0	1238/1284(96%)	31/1284(2%)	Plus/Minus
Query 724	ATAT-CGITACCA-GCTTCCTTTAAATCCACCTCTGGCCTGCCAGGAATCAGGGTTCCTTC	781		
Sbjct 1264	ATATGCG-TACAACGCTTCCTTGAATTCACCTTTAGC-TG-C-GG-ATCA-GG-TC-TC	1213		
Query 782	AGAACCTGACATTTTAAATGAAGAGGTCAGGCAGGTTCATGAGGAAAGCCTCATTGTCCCC	841		
Sbjct 1212	CGAA-CTGACATTTT-AATGAAGA-GTCAGCCAGGTTCATGAGGAAAGC-TCATGT-CCC	1158		
Query 842	ATGTCCTGTCTACTGCTGCACCCCTGAGACATCACAGACATGGA-CACTGGGGCCTGCTT	900		
Sbjct 1157	ATGTTTCGGTCA-TGCTGCA-CCCTGAGACATCACAGACATGGAACACT-GGGCTTGC-I	1102		
Query 901	GTTTCTCAAATGCCCTTAGATCGAAAGAGGGAGGAACAGGATGAATGCCACTCATTTT	960		
Sbjct 1101	GTTTCTCAAATGCC--TAGATCGAAAGAGGGAGGAACAGGATGAATGCCACTCATTT-	1045		
Query 961	CCCAAGAAAGGCCCTCTCCTGAGTGCCTGGGATGGGGCTCTGICCATTGCTGGGGCCGC	1020		

D

Figure 4.10 Confirmation of engineered ph β D-2-Luc Reporter by sequencing and alignment. Purified ph β D-2-Luc plasmid was sequenced by Genevision. (A) Sequencing of the ph β D-2-Luc plasmid using the forward primer and (B) reverse primer (B) BLAST alignment of (A) with predicted sequence. (C) BLAST alignment of sequence obtained from (A) with predicted sequence. (D) BLAST alignment of sequence obtained from (B) with predicted sequence.

Indeed sequencing using forward and reverse primers confirmed a high identity between the plasmid sequence and the predicted sequence (96 %, Fig. 4.10.B and Fig. 4.10.D).

The plasmid was therefore used to transfect RT4 cells.

4.6. CHALLENGING RT4 CELLS TRANSFECTED WITH PHBD-2-LUC

RT4 cells were, using new ph β D-2-Luc reporter construct, transiently transfected and challenged with the known h β D-2 inducers flagellin, NCTC 10418 and TNF- α . The results are presented in Fig. 4.11 with data presented as fold increase in h β D-2 expression compared to PBS challenge:

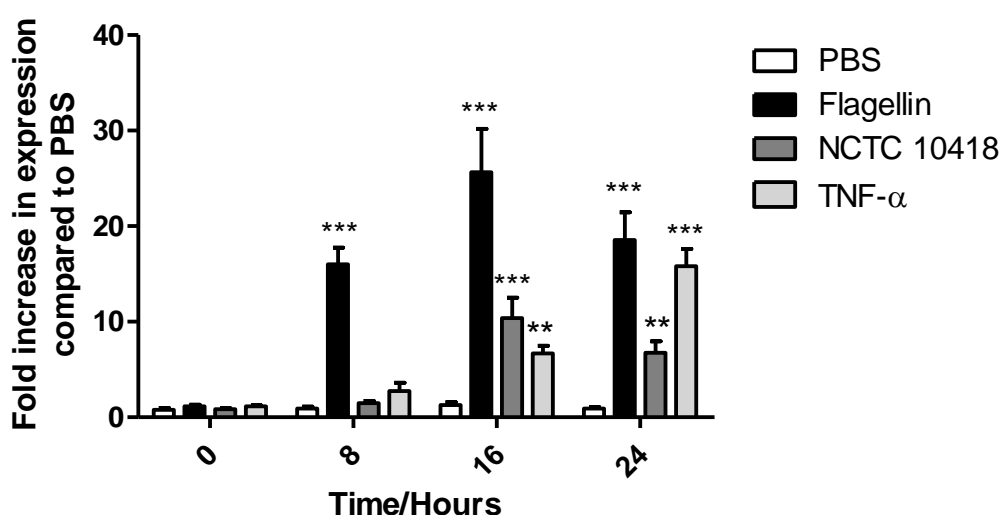


Figure 4.11 Validating ph β D-2-Luc reporter activity in RT4. After 16 hours of transfection, the cells were challenged with PBS, flagellin [250 ng/ml], NCTC 10418 [5×10^4 CFU/ml] or TNF- α [20 ng/ml]. The luminescence was measured at 0, 8, 16 and 24 hours. Results are shown as fold-increase over PBS challenged RT4 cells N=6, 2 experiments with 3 replicates **p<0.01; ***p<0.001.

When compared to the PBS challenge, the highest response was observed when the RT4 cells were challenged with flagellin, and at all three time points examined, *i.e.* 8, 16 and 24 hours. The response to flagellin peaked at 16 hours (25.7 ± 4.5 , p<0.001), which was consistent with h β D-2 gene expression data (Mr A. Ali, personal communication and presented data¹⁵⁸). Furthermore, the responses to NCTC 10418 and TNF- α were

significant at 16 and 24 hours when compared to the PBS challenge. These data indicated the ph β D-2-Luc reporter system was functionally active and from these data 16 hours was chosen as the optimal time point to measure luciferase activity.

4.7. INVESTIGATING THE PH β D-2-LUC REPORTER RESPONSE OF RT4 CELLS USING THE MOTILE NCTC 10418 AND BACTERIAL COMPONENTS

To further investigate h β D-2 gene regulation the RT4 cells were transiently transfected with the reporter and challenged up to 16 hours with a selection of PAMPS including LPS and peptidoglycan. The results are shown in Figure 4.12.

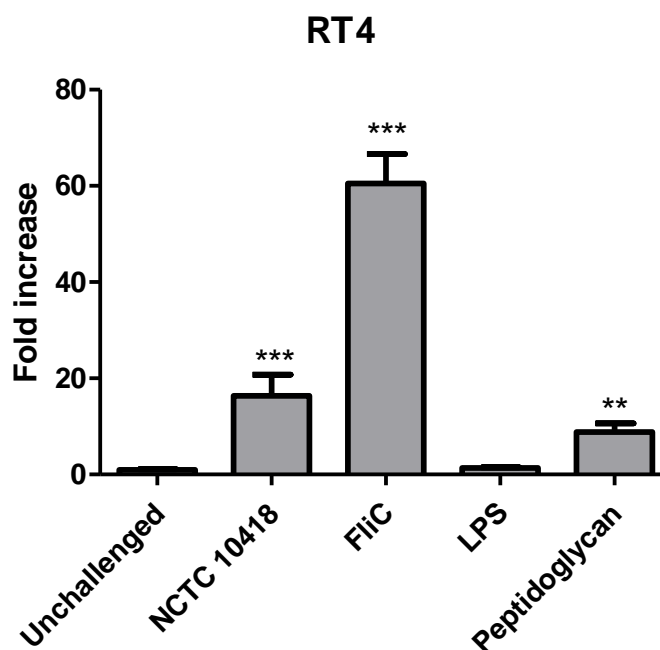


Figure 4.12 ph β D-2-Luc response to *E. coli* strain NCTC 10418 or bacterial PAMPs. RT4 cells were transfected with ph β D-2-Luc. After 16 hours, the transfected RT4 cells were challenged for 16 hours with PBS, *E. coli* NCTC 10418 [5×10^4 CFU/ml], Flagellin [250 ng/ml], LPS [10 μ g/ml], or Peptidoglycan [10 μ g/ml] N=6, 2 experiments with 3 replicates. **p<0.01; ***p<0.001.

As observed previously, the transfected RT4 cells showed a significant response (p<0.001) to flagellin (60.5 \pm 6.6 fold) and NCTC 10418 (16.4 \pm 4.4 fold) when compared to PBS. LPS did not induce a response from the ph β D-2-Luc reporter (1.4 \pm 0.1),

although upregulation was identified following peptidoglycan treatment (8.8 ± 1.8 fold increase). However, the response to peptidoglycan was reduced by two and seven fold respectively compared to NCTC 10418 and flagellin.

These data confirmed gene expression observations and showed that flagellin, activated h β D-2 presumably functioning through TLR-5 and NF- κ B signalling. The ph β D-2-Luc reporter was therefore used to investigate the effects of further treatments on h β D-2 expression in conjunction with or independent of flagellin.

4.8. ENHANCING PHBD-2-LUC REPORTER RESPONSE USING IMMUNOMODULATORY TREATMENT IN RT4 CELLS

1. ZYMOSAN ENHANCES PHBD-2-LUC REPORTER ACTIVITY

Zymosan is a β -1,3 glucan, found in fungal cell walls, and known to activate NF- κ B¹⁶². Using the reporter construct the effects of Zymosan on the flagellin response was investigated. To achieve this RT4 cells were transfected with the ph β D-2-Luc reporter and challenged with either flagellin, or Zymosan or a combination of both. The results of the challenges are shown in Figure 4.13:

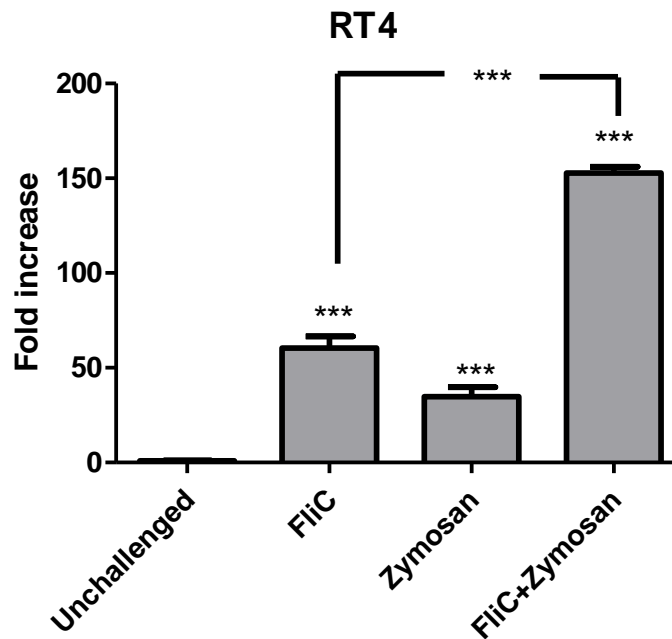


Figure 4.13. Enhancing hβD-2 response to flagellin using Zymosan in RT4. RT4 cells transfected with phβD-2-Luc were challenged for 16 hours with flagellin [250 ng/ml], Zymosan [50 μg/ml] or a combination of both N=6, 2 experiments with 3 replicates. ***p<0.001.

The flagellin challenge resulted in a fold increase of 60.5±6.6. When compared to flagellin, the response of the RT4 cells to Zymosan was reduced by approximately two-fold (34.8±5.0). However, the hβD-2 response to flagellin plus Zymosan challenge was significantly higher (p<0.001) when compared to that of flagellin or Zymosan alone (152.8±3.4 fold increase). These data suggest that Zymosan is also an activator of hβD-2 expression and moreover, significantly enhances the hβD-2 response to flagellin.

2. FURTHER ENHANCEMENT OF HBD-2 REPORTER ACTIVITY USING CALCITRIOL

Bioinformatics analyses identified a number of different TF binding sites in 5' region of hβD-2 gene including two VDR at 19 bp and 656 bp respectively. To explore the functioning of such sites RT4 cells were incubated for 16 hours with 10 nM 1,25 dihydroxycholecalciferol, also named calcitriol, the active form of Vitamin D, before transfection with the phβD-2-Luc reporter and challenge with LPS, PG, flagellin,

Zymosan as well as flagellin in combination with Zymosan. The results of the challenge are presented in Figure 4.14:

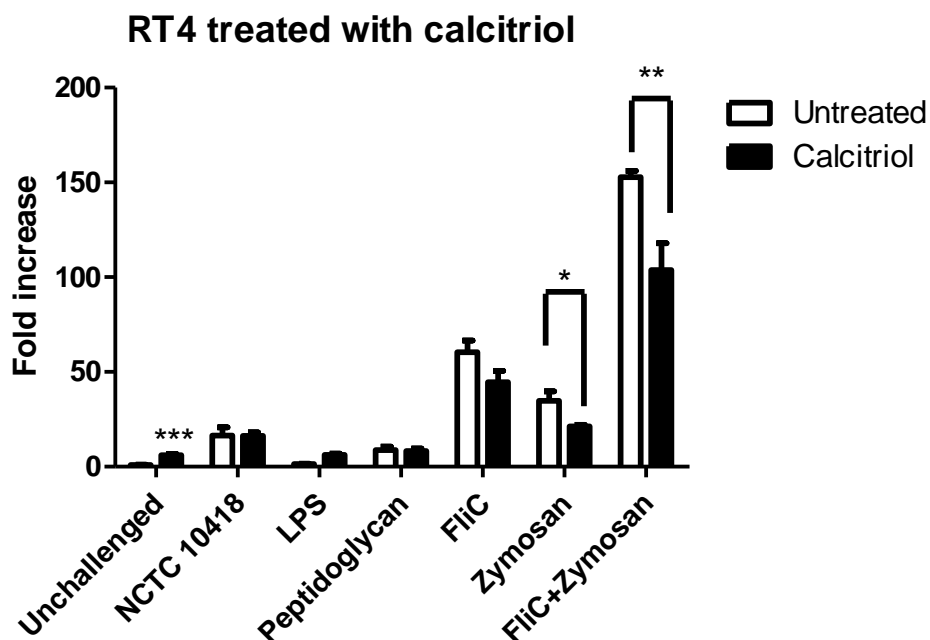


Figure 4.14 phβD-2-Luc Response enhancement in RT4 cells by the presence of calcitriol. RT4 cells were grown in medium supplemented with calcitriol [10 nM] or in normal medium (untreated). The RT4 cells were transfected and challenged with NCTC 10418 or PAMPs for 16 hours N=6, 2 experiments with 3 replicates. * $p < 0.05$, ** $p < 0.01$; *** $p < 0.001$.

Treatment with vitamin D induced a significant increase in hβD-2 in the unchallenged cells (6.0 ± 0.8 calcitriol treated vs. 1.0 ± 0.1 without calcitriol). Vitamin D had no effects on hβD-2 regulation when the cells were challenged with either LPS, peptidoglycan or NCTC 10418. In contrast, when calcitriol supplemented RT4 cells were challenged with flagellin there was the suggestion of a reduced hβD-2 response (44.6 ± 6.0 calcitriol treated vs. 60.5 ± 6.1 untreated). Moreover, when the calcitriol supplemented cells were challenged with either Zymosan or Zymosan and flagellin the responses were reduced significantly (21.2 ± 0.8 calcitriol + Zymosan treated vs. 34.8 ± 5.0 untreated, $p < 0.05$) and (103.8 ± 14.1 calcitriol + flagellin + Zymosan treated vs. 151.8 ± 3.4 untreated, $p < 0.01$).

These data suggested that calcitriol is a h β D-2 inducer in the absence of bacterial challenge. However, in the presence of bacteria or PAMPs it appeared to suppress the h β D-2 response.

3. CYTOTOXIC EFFECT OF OESTROGEN OR RESVERATROL TREATMENT ON RT4 CELLS

Bioinformatics analyses also identified six ER- α in the 5' region of h β D-2 gene. Oestrogen is a known regulator of immunity (reviewed by Nadkarni *et al.*, 2013¹⁶³). To explore the functioning of the ER- α sites in h β D-2 gene regulation, RT4 cells were grown in 17 β -oestradiol [4 nM] before being transfected with ph β D-2-Luc and challenged as described in section 4.8.II. The results of the challenges are shown in Figure 4.15:

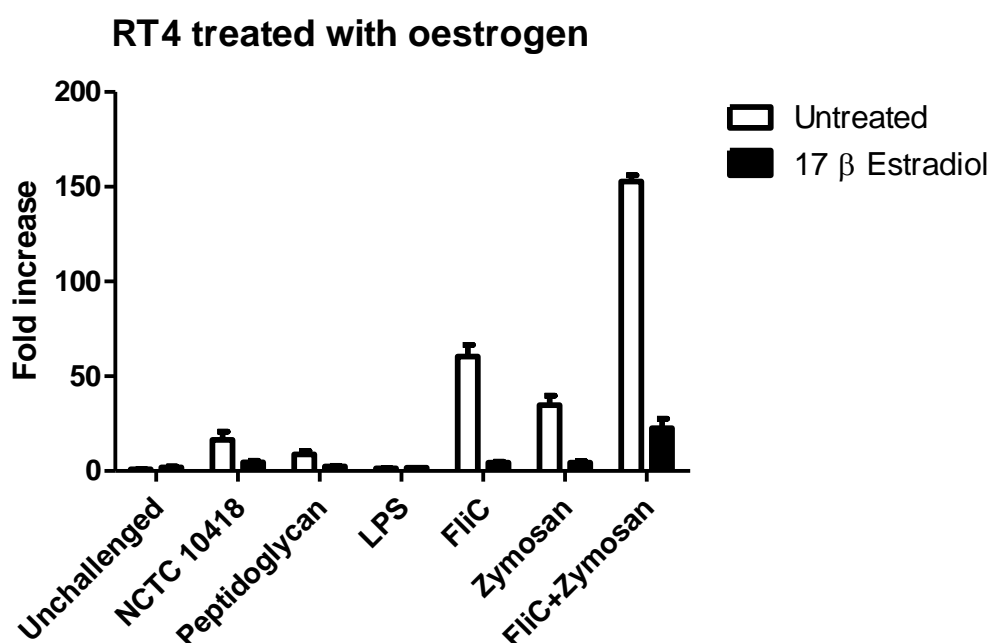


Figure 4.15 Cytotoxic effect of 17 β -oestradiol. RT4 cells were grown in medium supplemented with 17 β -oestradiol [4 nM] or in normal medium (untreated). The RT4 cells were transfected and challenged with NCTC 10418 or PAMPs for 16 hours. No statistical analysis was performed due to the observed cytotoxicity. N=6, 2 experiments with 3 replicates

In the absence of 17 β -oestradiol the responses were as previously reported. However, the h β D-2 responses in the presence of 17 β -oestradiol were much reduced. When the

transfected cells were observed under the microscope cell death was evident thus explaining the data. Therefore it appeared that the transfection agent was killing the oestrogen treated cells suggesting that the data observed was due to cytotoxic rather than physiological effects.

Resveratrol is a polyphenol produced by plants, *e.g.* grapes. It is found at high concentrations in red wine ranging from >1-12.3mg/l¹⁶⁴ and known to act through the receptors ER- α and ER- β ¹⁶⁵. Hence, it was considered as an alternative to oestrogen treatment. Cells were grown in resveratrol at concentrations ranging from 1 to 50 μ M. However, microscopic observations showed that resveratrol was highly cytotoxic to RT4 cells, and hence, transfection of resveratrol treated cells was not possible.

4.9. INVESTIGATING PH β D-2-LUC REPORTER RESPONSE IN VK-2 E6/E7 VAGINAL EPITHELIUM

As mentioned in the introduction to this thesis, the route of a urinary tract infection in women is via the vagina. Since UPEC is present in the vagina before it infects the urinary tract¹⁸ enhancing the innate immunity of the vagina through increasing h β D-2 expression could be a mechanism of preventing or treating urinary tract infections. Therefore, the reporter gene was used to investigate the expression of h β D-2 in VK-2 E6/E7 cells used as a model of the vaginal epithelium.

VK-2 E6/E7 cells were transfected with ph β D-2-Luc using the optimised concentration of attractene described in Fig. 4.5, and challenged with *E. coli* NCTC 10418 or bacterial PAMPs. The results of the ph β D-2-Luc response are shown in Figure 4.16:

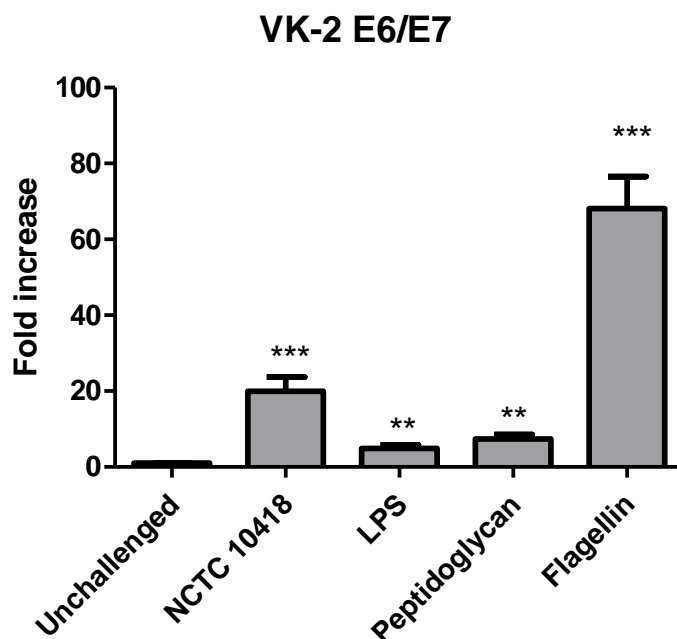


Figure 4.16 $h\beta D-2$ -Luc response in VK-2 E6/E7 transfected with reporter construct and challenged with *E. coli* NCTC 10418 or bacterial PAMPs. VK-2 E6/E7 were transfected with $h\beta D-2$ -Luc and challenged for 16 hours with 5×10^4 CFU/ml of *E. coli* NCTC 10418, LPS [10 μ g/ml], peptidoglycan [10 μ g/ml], flagellin [250 ng/ml] N=6, 2 experiments with 3 replicates, ** $p < 0.01$; *** $p < 0.001$.

NCTC 10418 induced a significant 19.9 ± 3.8 fold increase ($p < 0.001$) in $h\beta D-2$ reporter activity compared to cells challenged with PBS alone. The response to LPS or peptidoglycan was also significantly increased ($p < 0.01$), with a 4.9 ± 0.9 fold increase for LPS and 7.4 ± 1.2 fold increase for peptidoglycan. As with the RT4 cells, the maximal response to a bacterial compound was measured, when VK-2 E6/E7 cells were challenged with flagellin (68.1 ± 8.5 fold increase, $p < 0.001$).

1. ZYMOSAN ENHANCES OF PHBD-2-LUC REPORTER RESPONSE IN VK-2 E6/E7

Whether the $h\beta D-2$ response to flagellin could be enhanced by Zymosan was also investigated in VK-2 E6/E7 cells. For this, $h\beta D-2$ -Luc transfected VK-2 E6/E7 cells were challenged with Zymosan in either the absence or presence of flagellin and the results are shown in Figure 4.17:

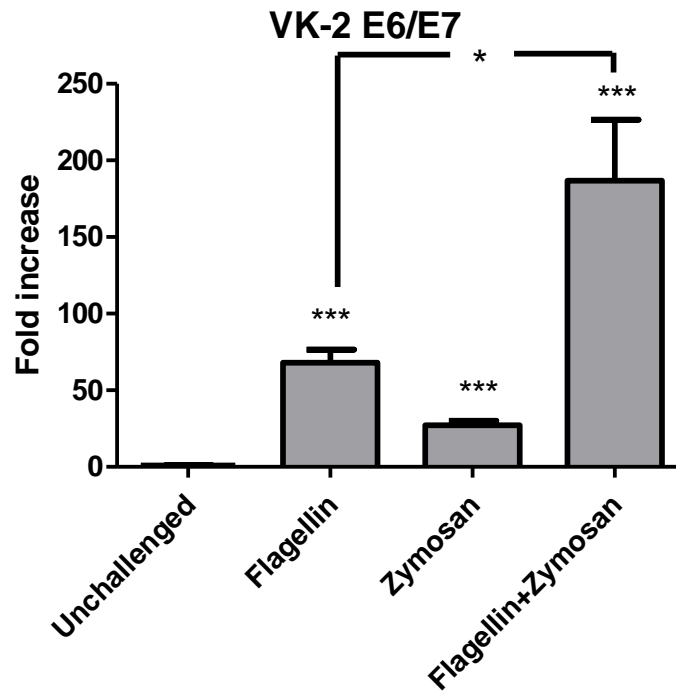


Figure 4.17 Enhancing the hβD-2 response in VK-2 E6/E7 to flagellin with Zymosan. VK-2 E6/E7 cells were transfected with phβD-2-Luc and challenged with flagellin [250 ng/ml], Zymosan [50 μg/ml] or the combination of flagellin and Zymosan for 16 hours N=6, 2 experiments with 3 replicates. *p<0.05, ***p<0.001.

As observed with RT4 cells Zymosan induced a significant increase (p<0.001) in the hβD-2 response in VK-2 E6/E7 cells (27.2±2.9). Again, similar to that observed in RT4 cells, the response to flagellin was higher (68.1± 8.5 fold for flagellin vs. 27.2±2.9 fold for Zymosan,). Moreover, the combination of flagellin and Zymosan induced a significantly higher hβD-2 response when compared to flagellin alone (189.7±39.8 for the combined challenge, p<0.05).

2. FURTHER ENHANCEMENT OF PHBD-2-LUC RESPONSE UPON CALCITRIOL TREATMENT

The effects of calcitriol treatment on the hβD-2 response in VK-2 E6/E7 were investigated. Like the RT4 cells, the VK-2 E6/E7 cells were grown in 10 nM calcitriol and challenged as described before. The results are shown in Figure 4.18:

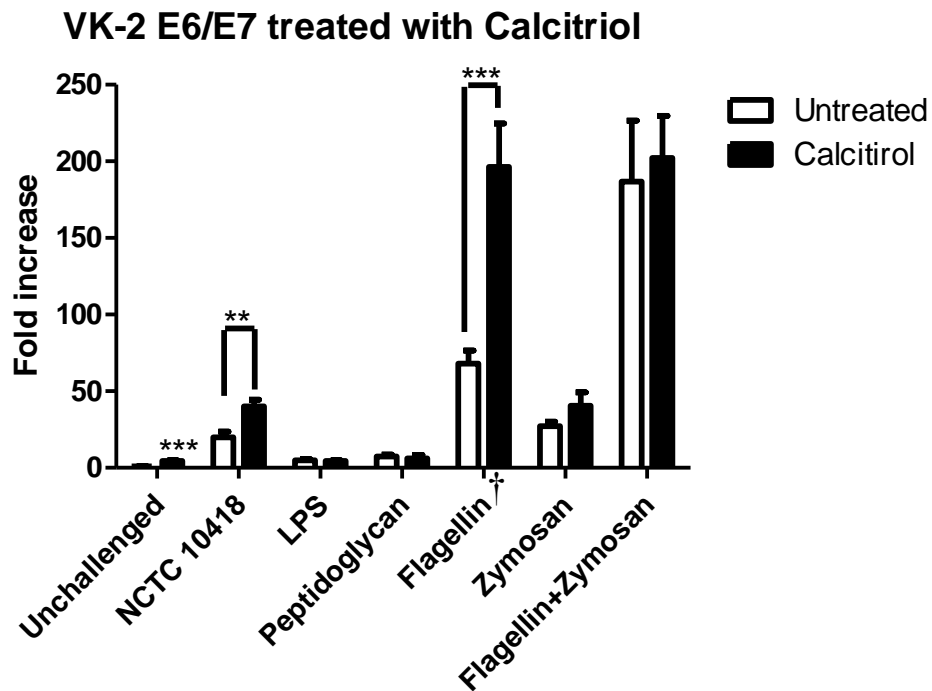


Figure 4.18 hβD-2 response enhancement in VK-2 E6/E7 to *E. coli* NCTC 10418 and PAMPs after calcitriol treatment. VK-2 E6/E7 were grown in 10 nM calcitriol and transfected with phβD-2-Luc, before being challenged for 16 hours with 5×10^4 CFU/ml of *E. coli* NCTC 10418, LPS [10 μg/ml], peptidoglycan [10 μg/ml], flagellin [250 ng/ml], Zymosan [50 μg/ml] or the combination of flagellin and Zymosan. † Two outliers were removed from the calcitriol treated and flagellin challenged VK-2 E6/E7 cells N=6, 2 experiments with 3 replicates **p<0.01, ***p<0.001.

Calcitriol treatment alone induced a significant reporter response in the VK-2 E6/E7 cells (4.4 ± 0.5 fold compared to 1.0 ± 0.1 fold). The reporter response to NCTC 10418 was also significantly increased when VK-2 E6/E7 cells were treated with calcitriol (40.1 ± 4.3 vs. 19.9 ± 3.8 , $p < 0.01$). In addition, there was the suggestion of an enhanced response to flagellin in the calcitriol treated cells but this was not statistically significant. However, when two low outlying data points (34.10 from the first experiment and 41.14 from the second experiment) were excluded from the data set the data was statistically significant (196.3 ± 28.3 fold compared to 68.1 ± 8.5). The responses to LPS and Peptidoglycan were not altered by the calcitriol treatment.

This section demonstrated the ability of calcitriol to activate the hβD-2 response and enhance the response of the vaginal epithelium to motile bacteria and flagellin.

3. ENHANCEMENT OF PHBD-2-LUC REPORTER RESPONSE THROUGH OESTROGEN TREATMENT

Oestrogen dependent immunomodulation of the h β D-2 reporter was also investigated in VK-2 E6/E7 cells. VK-2 E6/E7 cells were grown in 17 β -oestradiol and challenged with the compounds described previously as well as with *E. coli* NCTC 10418. The results are shown in Figure 4.19:

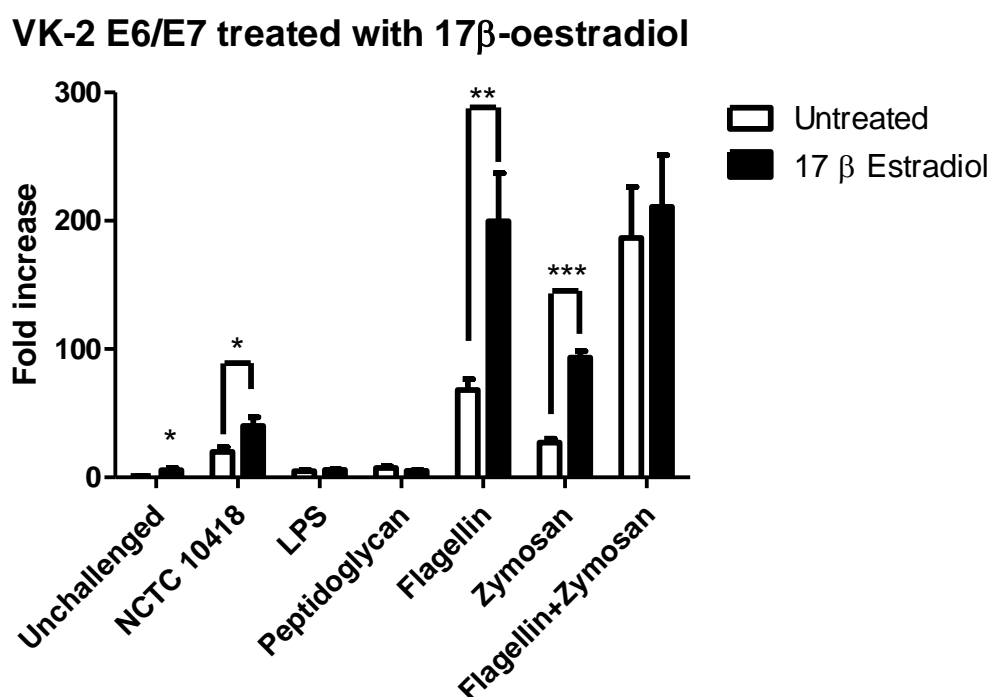


Figure 4.19 Enhancing the response to flagellin using 17 β -oestradiol. VK-2 E6/E7 were grown in the presence of 17 β -oestradiol and transfected with ph β D-2-Luc and challenged for 16 hours with 5×10^4 CFU/ml of *E. coli* NCTC 10418, LPS [10 μ g/ml], peptidoglycan [10 μ g/ml], flagellin [250 ng/ml], Zymosan [50 μ g/ml] or the combination of flagellin and Zymosan N=6, 2 experiments with 3 replicates. * $p < 0.05$, ** $p < 0.01$; *** $p < 0.001$.

The cytotoxic effects of 17 β -oestradiol seen in the RT4 cells were not observed in the VK-2 E6/E7 after 16 hours of transfection. Moreover, 17 β -oestradiol treatment induced a 5.7 ± 1.7 fold increase ($p < 0.05$) in reporter activity compared to the untreated cells (1.0 ± 0.1). Furthermore, flagellin challenged VK-2 E6/E7 cells pre-treated with oestrogen induced a significantly higher reporter response (68.1 ± 8.4 vs. 199.5 ± 37.7 , $p < 0.01$). Similarly, the response to NCTC 10418 was also doubled when VK-2 E6/E7 were pre-treated with oestrogen (19.9 ± 3.8 fold vs. 40.2 ± 6.6 for oestrogen treated,

p<0.05). The hβD-2 response to a Zymosan challenge was also significantly higher when cells were treated with oestrogen (93.3±5.0 vs. 27.2±2.9, p<0.001). Interestingly, no statistically significant difference was observed when a combination of flagellin and Zymosan was used (186.7±39.8 vs. 210.9±40.2 for oestrogen treated). Also, no difference was observed in relation to either the LPS or peptidoglycan challenges. These data supported oestrogen potentiating the hβD-2 response to motile bacteria, flagellin and Zymosan but not to LPS or peptidoglycan.

4. RESVERATROL HAS AN AMBIVALENT EFFECT ON THE PHBD-2-LUC ACTIVITY

Resveratrol, an oestrogen mimic, has been described as having immunomodulatory effects¹⁶⁵. To explore the effects of resveratrol, VK-2 E6/E7 cells were cultured in 100µM resveratrol (concentration chosen after personal communication with Dr Claire Townes Newcastle University) and challenged as described previously. The results are shown in Figure 4.20:

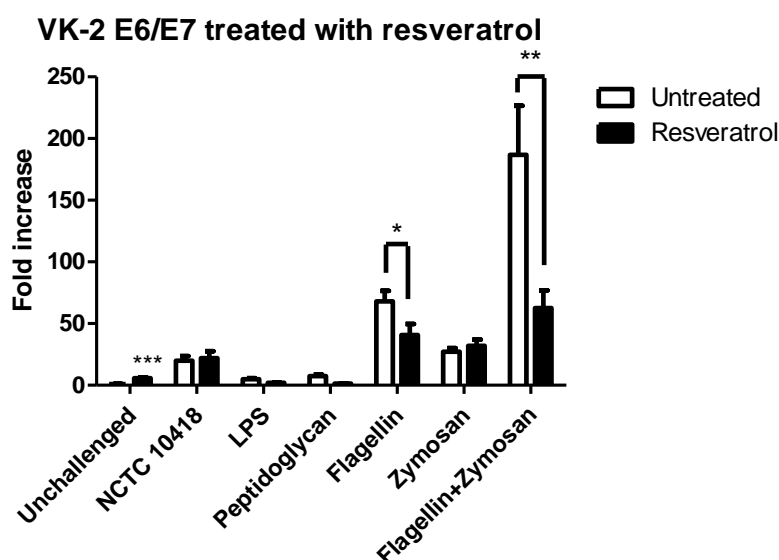
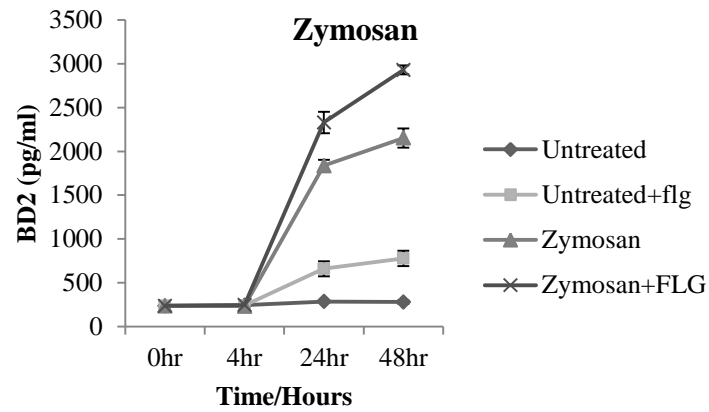


Figure 4.20 hβD-2 response in VK-2 E6/E7 to *E. coli* NCTC 10418 and PAMPs after resveratrol treatment. VK-2 E6/E7 were grown in 100 µM resveratrol and transfected with phβD-2-Luc, before being challenged for 16 hours with 5x10⁴ CFU/ml of *E. coli* NCTC 10418, LPS [10 µg/ml], peptidoglycan [10 µg/ml], flagellin [250 ng/ml], Zymosan [50 µg/ml] or the combination of flagellin and Zymosan. N=6, 2 experiments with 3 replicates.*p<0.05, **p<0.01; ***p<0.001.

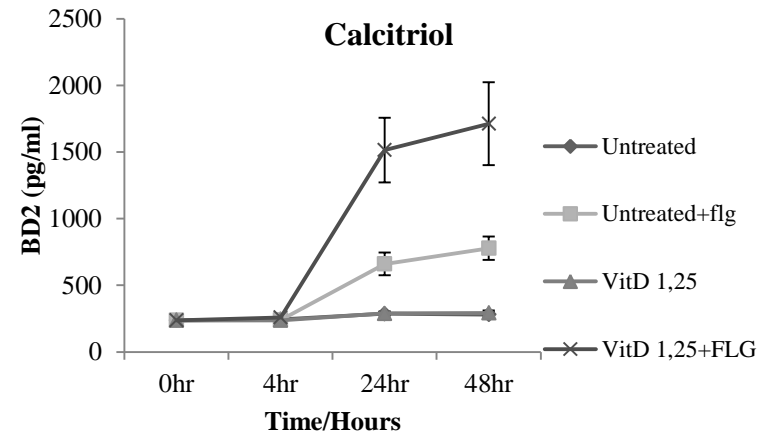
As observed with 17β -estradiol, resveratrol induced an h β D-2 response in the unchallenged VK-2 E6/E7 cells (5.7 ± 0.7 fold vs 1.0 ± 0.1 fold, $p<0.001$). Again and similar to the 17β -oestradiol data, resveratrol did not significantly affect the responses to peptidoglycan or LPS. Additionally, no effects were observed when VK-2 E6/E7 cells treated with resveratrol were challenged with Zymosan or with NCTC 10418. However, in contrast to the 17β -oestradiol data, reduced reporter activity was observed in the VK-2 E6/E7 cells treated with resveratrol and challenged with flagellin (68.1 ± 8.5 for untreated cells vs. 40.7 ± 8.9 for resveratrol treated cells, $p<0.05$) or flagellin in combination with Zymosan (186.7 ± 39.8 for untreated cells vs. 62.7 ± 14.4 for resveratrol treated cells, $p<0.01$).

4.10. COMPARISON OF THE PHBD-2-LUC REPORTER ACTIVITY WITH THE HBD-2 PROTEIN SECRETION USING AN ELISA

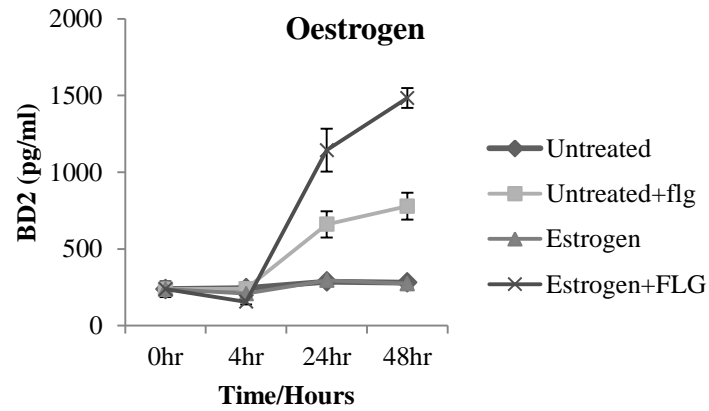
The findings using the h β D-2 reporter showed that it was possible to enhance the h β D-2 response by treating VK-2 E6/E7 cells with calcitriol and oestrogen. In contrast, the data suggested that the oestrogen mimic resveratrol reduced the induction of the h β D-2 reporter. Hence, these findings needed confirmation via h β D-2 peptide measurements. Such analyses were performed by Dr Claire Townes, ICaMB, Newcastle University; the concentrations of h β D-2 in the media of the VK-2 E6/E7 cells treated with calcitriol, 17β -oestradiol and resveratrol plus/minus challenge with flagellin and Zymosan were measured by ELISA (Leinco #B428). The results of the h β D-2 peptide concentrations are shown in Figure 4.21:



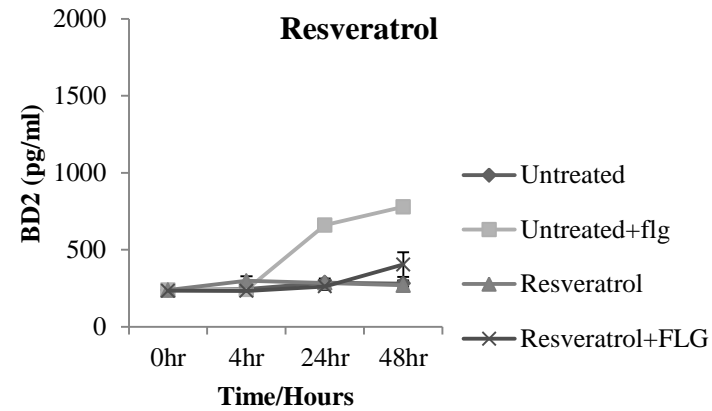
A



B



C



D

Figure 4.21 Enhancement of h β D-2 peptide secretion in VK-2 E6/E7. VK-2 E6/E7 cells were treated with flagellin [250 ng/ml]. Additionally, VK-2 E6/E7 cells were treated with Zymosan [50 μ g/ml], calcitriol [10nM], oestrogen (17 β -oestradiol) [4 nM] or resveratrol [100 μ M]. The protein was collected at each time point and measured using a h β D-2 specific sandwich ELISA (Leinco #B428). The experiments were performed by Dr Claire Townes. N=6, 2 experiments with 3 replicates

As expected challenging VK-2 E6/E7 cells with flagellin was linked with increased concentrations of the h β D-2 peptide. Moreover, challenging with flagellin and Zymosan enhanced the h β D-2 peptide concentration further. However, in contrast to the findings of ph β D-2-Luc reporter were the h β D-2 peptide concentrations observed when the VK-2 E6/E7 cells were challenged with Zymosan. Essentially, the h β D-2 reporter activity following Zymosan treatment was reduced when compared to that of flagellin treatment (Section 4.9.I), but the peptide measurements did not reflect this (Fig. 4.21.A).

Calcitriol and 17 β -oestradiol treatments also showed a difference in h β D-2 peptide concentrations in comparison to the ph β D-2-Luc reporter activities. The ph β D-2-Luc reporter was activated by calcitriol, 17 β -oestradiol and resveratrol treatments (Fig. 4.18, 4.19 and 4.20). This induction, however, was not observed in the h β D-2 concentrations measured. However, the induction of the ph β D-2-Luc reporter was low (4.4, 5.7 and 5.7 fold), hence, it was feasible that h β D-2 synthesis was increased but the levels were below the sensitivity of the ELISA and thus not detectable. In support, increased peptide levels were detected when flagellin was added to the calcitriol, 17 β -oestradiol treated VK-2 E6/E7 cells (Fig. 4.21.B and C), and reduced when challenged with flagellin in the presence of resveratrol (Fig. 4.21.D) reflecting the data obtained using the ph β D-2-Luc reporter.

In conclusion, the ph β D-2-Luc reporter findings were in general supported by the h β D-2 peptide measurements.

4.11. DISCUSSION

The data presented in Chapter 3 showed NF-kB activation in RT cells in response to bacterial and flagellin challenges. NF-kB activation is linked to IL-8 and h β D-2

synthesis, the latter of which is a potent bacterial killing agent. The data also showed that when the NF- κ B response was reduced, through TLR-5 blocking, the host innate response was diminished. In parallel colleagues have shown that this truncated host response involves reduced synthesis of anti-bacterial factors including h β D-2. Human β D-2 has been shown to kill gram negative bacteria including *E. coli*¹⁶⁶ thus the regulation of the h β D-2 gene in the urogenital tract is of immunological and therapeutic interest. This Chapter through the construction and use of a h β D-2 reporter and *in vitro* systems modelling the urogenital tissues focussed therefore on exploring the regulation of the h β D-2 (DEFB4) gene.

Two kbp of UTR sequence 5' to the start of the h β D-2 gene was cloned and analysed. This fragment size was chosen following bioinformatic analyses using PROMO software, which revealed a number of TF binding sites including those for NF- κ B, AP-1, VDR, RAR and ER alpha (Fig. 4.1). Two NF- κ B binding sites were identified at positions 345 and 546. NF- κ B binding sites have been identified by other groups but in contrast to our findings, were located at positions 199-208^{167,168} and at positions 564, 175, 165¹⁶⁹.

Nonetheless, the positions found by the groups Vora *et al.* (2004) and Wada *et al.* (2001) have to be viewed critically, since the database used to map the positions was AF071216 (last release 2000)^{168,170}, while the current database (used in this investigation) was GRCh37.p10 (last version 31.08.2012). Interestingly, performing a BLAST analysis of the primers used in the construction of their reporter (Fw- 5'-GGCTCGAGGGCTCGGACATCAGCACCAAA-3' and Rv- 5'-AAAAGCTTAGGAGCTGAGTCTGGGGAGGA-3')¹⁶⁸, using the current genome reference data base (GRCh37.p10), showed a product of 2088 bp rather than 2111 bp and located 24 bp away from the start codon, indicating the differences in the genome

databases. Wang *et al.* (2003) did not state the database, or the primers used to engineer their wild type h β D-2 promoter reporter¹⁶⁹. Hence, an assessment of their NF- κ B binding sites was not possible.

A further discrepancy related to the VDR binding sites. Two were identified in this bioinformatics analyses, one adjacent to the DEFB 4 gene (19 bp 5' to the start codon) and one at position 656 bp, which conflicted with the one VDR binding site reported by Wang *et al.*, (2004) at position 1231 bp¹⁷¹. Wang *et al.*, do not state which database was used. Using BLAST alignment of the primers used to construct the promoter reporter with the current database (GRCh37.p10) showed a product of 1287 bp, located at 14 bp before the DEFB4 gene. Wang *et al.* (2004), however, state that their promoter reporter construct starts 23 bp before the start codon and is 1266 or 1225 bp long¹⁷¹, indicating differences between the current database version and the one used in their investigation. Therefore, a direct comparison of the binding position is not possible.

The initial h β D-2 reporter construct was engineered using pGlow TOPO, which contains a GFP reporter. The advantage of the GFP system was that it allowed reporter, *i.e.* GFP measurements to be done without killing the cells, thus increasing the number of time-points analysed. This was in comparison to the luciferase system that required cell death to measure reporter activity, and restricted the number of time-points. However, while the GFP system worked reasonably successfully as visualised via microscopy, quantitation of the data was not possible due to a combination of cell autofluorescence and the limited sensitivity of plate reader. Thus for the h β D-2 reporter experiments the pGL4.10 luciferase system was adopted.

Previous work had shown that RT4 cells challenged with flagellin resulted in the upregulation of h β D-2 expression¹⁵⁸. Experiments in which RT4 cells were transfected

with the p β D-2-Luc reporter and similarly challenged mirrored these findings (Fig. 4.11) and the reporter system was therefore adopted as a valid tool to investigate h β D-2 induction. With this knowledge it was clear that the reporter data also supported another finding, namely that LPS did not cause a h β D-2 response in RT4 cells, again highlighting the importance of flagella in initiating the host uroepithelial innate response.

Bioinformatics indicated VDR and ER binding sites located in the h β D-2 5'UTR, which suggested potential roles for the steroids Vitamin D, namely 1,25 (OH)₂ dihydroxycholecalciferol, also called calcitriol, and oestrogen in h β D-2 gene regulation. Surprisingly, investigation of a h β D-2 induction in RT4 using oestrogen (17 β -oestradiol) and resveratrol an oestrogen mimic was not possible. In fact, transfection of the 17 β -oestradiol treated cells with TurboFect resulted consistently in cell death suggesting the transfection reagent, under the conditions studied, was cytotoxic. As no product information was available to confirm this observation or help address the problem, no further experiments were attempted. In hindsight a potential solution to this issue was to remove the 17 β -oestradiol during the actual transfection procedure but to supplement the transfection media with 17 β -oestradiol during the challenges. In contrast to RT4, challenging VK-2 E6/E7 cells with oestrogen was possible and resulted in a higher h β D-2 response to flagellin and to Zymosan but not to the combination of flagellin and Zymosan. It appears that the response to a combination of flagellin and Zymosan is the maximal response, unable of any further increase.

Resveratrol also caused problems in that it actually killed RT4 cell growth. RT4 cells died within hours after addition of resveratrol (1 to 50 μ M) and even lowering the concentration to 1 μ M still caused cell death. These observations were in contrast to reports in the literature, particularly one study, which reported that incubating bladder

cells in low doses of resveratrol (0.1 to 20 μ M) protected against oxidative stress, although the cells used in cited study were ECV 304 and not RT4¹⁷². An explanation for the observed cell death of RT4 cells may relate to the anti-carcinogenic activity of resveratrol. In fact numerous cell lines, such as breast (MCF-7) and ovarian (A2780) cancer cell lines, as well as the bladder tumour cell line T24, interestingly from which ECV 304 cells were derived, have been shown to be killed by resveratrol¹⁷³⁻¹⁷⁵. Cytotoxic effects in T24 cells were reported at 50 μ M and higher concentrations as early as 24 hours post treatment¹⁷³. A future possibility is to repeat the experiments but using polydatin, a natural precursor of resveratrol, as it has been described as a h β D-2 inducer in keratinocytes¹⁷⁶.

On the other hand, in VK-2 E6/E7 cells resveratrol induced a trend towards lowering the h β D-2 response, which can be explained by its ability to inhibit NF-kB activation^{173,177}. Interestingly, although lowering the h β D-2 response, resveratrol by itself induced h β D-2. It could hence, be used as a preventive agent. However, Zymosan and oestrogen induced a higher response when challenged with flagellin, which was the aim of this investigation.

The induction of h β D-2 by Zymosan reported in this thesis was novel and to the best of knowledge has not been shown before in the uroepithelium or indeed in epithelia. To date, the only literature suggesting Zymosan as a NF-kB activator in vaginal epithelium was that of Pivarcsi *et al.* (2005)¹⁷⁸. The authors, using PK2 E6/E7 vaginal cells derived from a post-menopausal subject and a Zymosan concentration of 10 μ g/ml, reported Zymosan to induce IL-8 but interestingly not h β D-2. In view of the data reported in this thesis the lack of h β D-2 detection was surprising but may relate to the concentration of Zymosan used by Pivarcsi *et al.* (2005), which was five times less than that used in this study, *i.e.* 50 μ g/ml.

Importantly, however, in this study the h β D-2 response to flagellin was significantly enhanced in bladder and vaginal cells (2.5 and 2.8 fold) in the presence of Zymosan, and the *in vitro* reporter data demonstrate a potential therapeutic role for Zymosan in controlling UTIs. In fact these data suggest that Zymosan can function as a potential protective agent in the urogenital tract and the therapeutic potential of Zymosan will be investigated further in Chapter 6.

Vitamin D (25-vitamin D₃ and calcitriol) treatment has been shown *in vitro* to induce the expression of the cathelicidin gene hCAP-18 in the UT¹⁷⁹. Identification of putative VDR elements in 5'UTR of h β D-2 gene endorsed the experiments investigating the effects of the active metabolite of Vitamin D, *i.e.* calcitriol (1,25 dihydroxycholecalciferol) on h β D-2 gene regulation. The RT4 data was surprising. Vitamin D treatment enhanced h β D-2 expression in unchallenged cells but the presence of either flagellin, Zymosan, or flagellin plus Zymosan appeared to inhibit gene expression. The absence of peptide data however, makes it difficult to comment further and these experiments need to be repeated with ELISAs performed concurrently. In contrast, the h β D-2 gene expression data relating to the VK-2 E6/E7 cells treated with vitamin D was supported by peptide data and indicated a role for vitamin D in enhancing the h β D-2 response. The literature also supports this, with h β D-2 expression upregulated in keratinocytes treated with calcitriol¹⁷¹. They showed that the induction of h β D-2 by IL-1 was significantly upregulated when primary keratinocytes and cell lines were treated with calcitriol¹⁷¹. Vitamin D is therefore a good therapeutic candidate as it can be administered topically or supplemented nutritionally.

The data mining revealed multiple binding sites for all transcription factors. The contribution of each TF binding site could be analysed by introducing mutation in those positions by site directed mutagenesis. The mutation would also clarify if the

differences noticed between the here reported binding sites and the ones published in the literature are indeed due to the changes in the sequenced Genome data bases.

Overall these data suggest that Zymosan, Vitamin D as well as Oestrogen can enhance hβD-2 gene expression and synthesis in VK-2 E6/E7 cells and therefore can be considered as potential targets in future therapeutic strategies.

CHAPTER FIVE

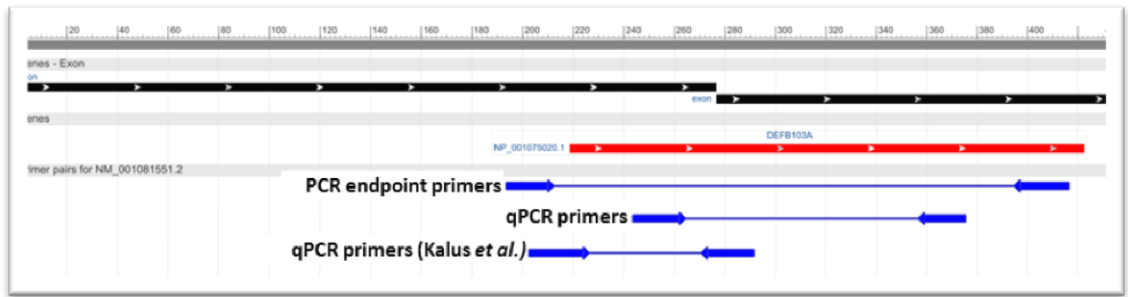
Investigating Human β -Defensin 3 in the Urogenital Tract

5.1. INTRODUCTION

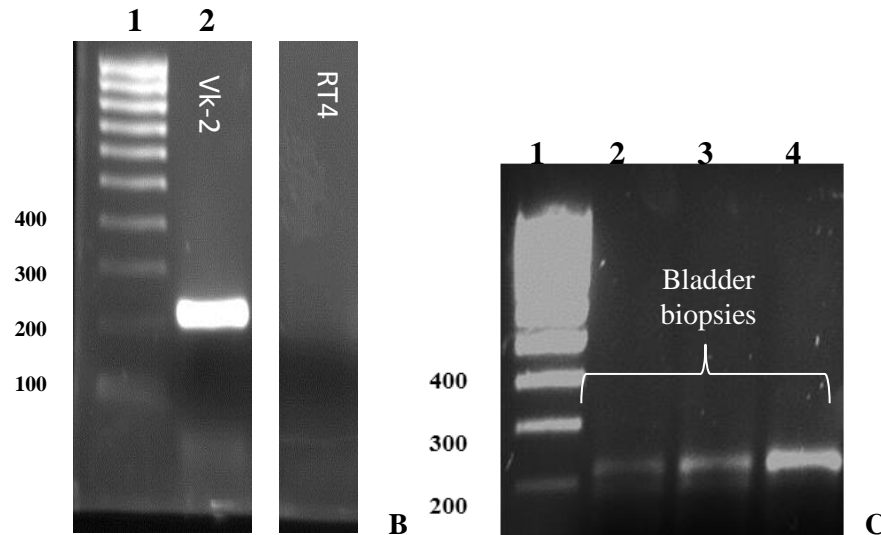
The Defensin h β D-2 is induced in the urogenital tract of the host in response to and to help fight infection. Human β D-2 is however, a salt sensitive antimicrobial peptide, which has a reduced antimicrobial activity in physiological salt concentrations, hence its killing activities are probably limited to the epithelial layer⁵. Another member of the Defensin family, h β D-3, which is known to possess potent microbial killing properties, including against *E. coli*, is not salt sensitive, thus enabling bacterial killing in elevated salt environments such as that of urine¹⁸⁰. The antimicrobial activity of h β D-3 could also be complementary to the h β D-2 activity, as h β D-3 has also a potent antimicrobial activity against gram positive bacteria¹⁸⁰. Hence, this chapter aimed to investigate h β D-3 expression in the urogenital tract *in vitro* by using the cell lines RT4 and VK-2 E6/E7.

5.2. DETECTION OF HBD-3 EXPRESSION IN THE UROGENITAL TRACT

First, the expression of h β D-3 was analysed in VK-2 E6/E7 and RT4 cells, as well as in three bladder biopsies, using endpoint RT-PCR. The expected size of the h β D-3 PCR product was 224 bp and the results are shown in Figure 5.1:



A



B

C

Figure 5.1 Detection of h β D-3 expression in VK-2 E6/E7 vagina and RT4 bladder epithelium. (A) Binding sites of the end-point and quantitative primers in the DEF103 gene. (B-C) Product of the PCR amplification using the end-point primers. The cDNA of VK-2 E6/E7, RT4 and bladder biopsies were amplified using 30 cycles. The expected size of the PCR product is 224 bp. (B) Left hand side (LHS) Lane 1 shows Hyperladder IV, lane 2 the amplification product using VK-2 E6/E7 cDNA and right hand side (RHS) using cDNA of RT4. (C) Lane 1 shows Hyperladder IV. Lane 2-4 show bands indicative for the amplification of h β D-3 in bladder biopsies. DNA was separated on a 2 % Agarose TBE gel.

A cDNA band of approximately 220 bp (expected size was 224 bp) and shown in Fig. 5.1.B (LHS panel), suggested that h β D-3 was constitutively expressed in VK-2 E6/E7 cells. In contrast, no cDNA band was detected when RNA isolated from the RT4 cells was analysed suggesting that h β D-3 was not expressed constitutively in RT4 bladder cells (Fig. 5.1.B: RHS panel), although interestingly, h β D-3 was detected in the bladder biopsies of three different donors (Fig. 5.1.C). It is known that h β D-3 is upregulated in many tissues upon bacterial challenge^{181,182}. The expression of h β D-3 was therefore investigated after challenging the VK-2 E6/E7 and RT4 cell lines with bacteria and bacterial components. To facilitate this, a qPCR assay was developed to quantitate h β D-3 expression.

5.3. DEVELOPMENT OF HBD-3 ASSAYS

1. QUANTITATIVE GENE EXPRESSION MEASUREMENTS USING A PCR ASSAY

I. ENGINEERING A h β D-3 CALIBRATOR PLASMID

A quantitative h β D-3 PCR assay, using SYBR green was developed. The efficiency and limit of detection of the reaction must be determined using a positive control¹⁴⁴. To achieve this, the 220 bp DNA band encoding h β D-3, shown in Fig. 5.1.B, lane 2 was excised and inserted into a pGem-T easy vector, as described in Section 2.3. Successful cloning was confirmed by restriction digest, PCR and DNA sequencing. The results are shown in Figure 5.2:

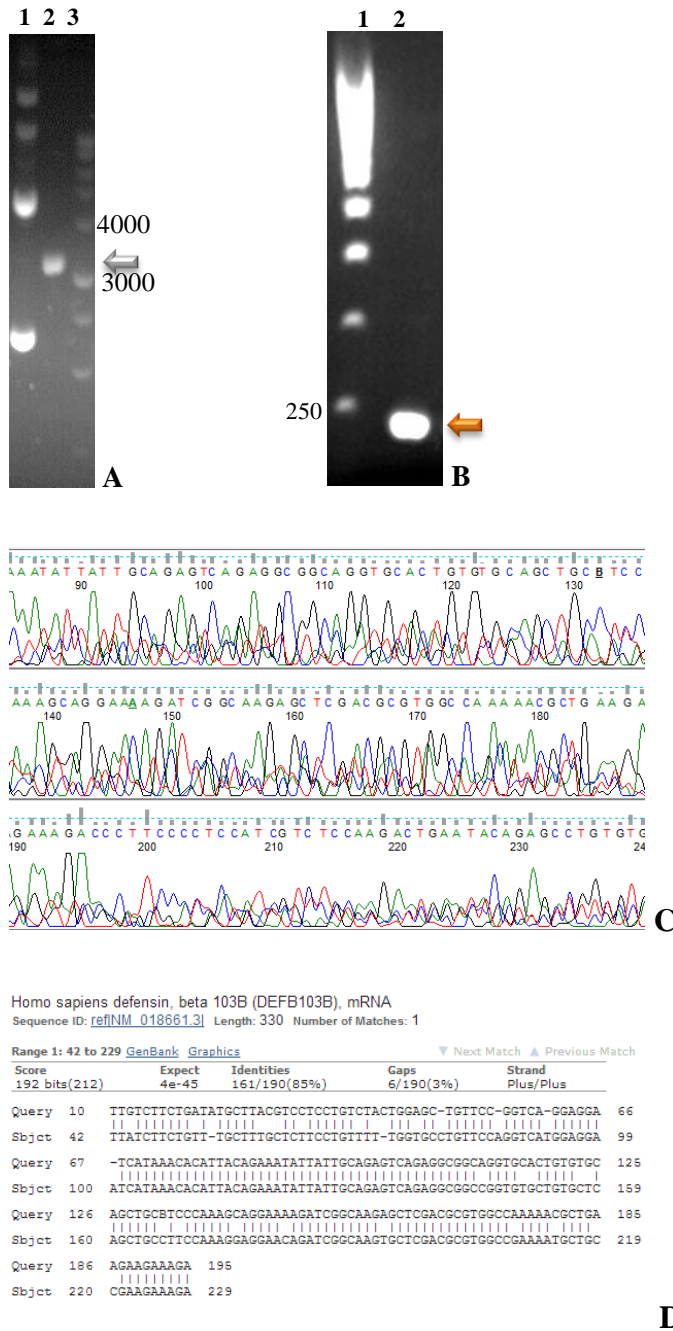


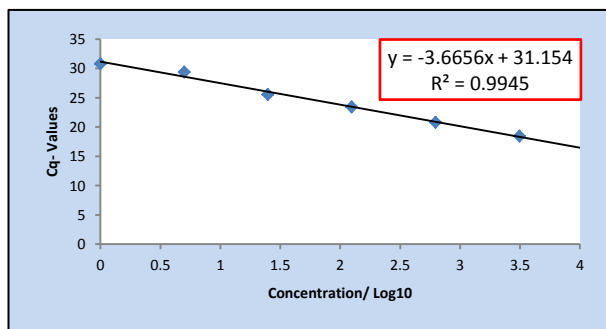
Figure 5.2 Engineering a pGem-T-easy plasmid containing part of the hβD-3 gene. (A) pGem-T-easy after ligation with hβD-3 product from Fig. 5.1. Lane 1 shows isolated plasmid. Lane 2 shows the result of digesting the plasmid with Eco RV, a cutting site found only in the hβD-3 gene. Lane 3 is the marker (Hyperladder IV). (B) Lane 1 shows the marker (Hyperladder I). Lane 2 Amplification using hβD-3 endpoint primer and the isolated plasmid to confirm the presence of the insert. (C) Sequencing result was used to perform a BLAST search. (D) Result of the blast search.

The engineered hβD-3 plasmid was successfully isolated and verified by linearisation with Eco RV (Fig. 5.2A lane 2), which provided a unique cutting site in the sequence of the hβD-3 insert and resulted in a band of approximately 3.2 kbp (predicted 3239 bp).

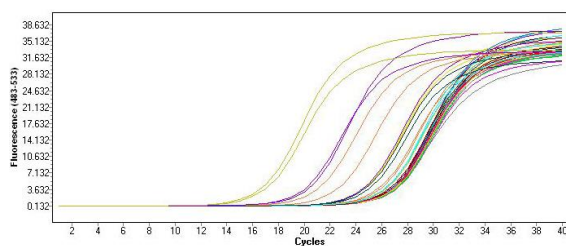
The plasmid was used as a template for PCR using the hβD-3 endpoint primers and resulted in a band of approximately 220 bp (expected size 224 bp, Fig. 5.2.B, lane 2, orange arrow). The hβD-3 plasmid insert was sequenced by GeneVision (Newcastle, UK) with the results of the BLAST search (Fig. 5.2.C) confirming its authenticity (Fig. 5.2.D.). This plasmid was utilised in the development of the hβD-3 qPCR assay.

II. ESTABLISHING A WORKING STANDARD CURVE

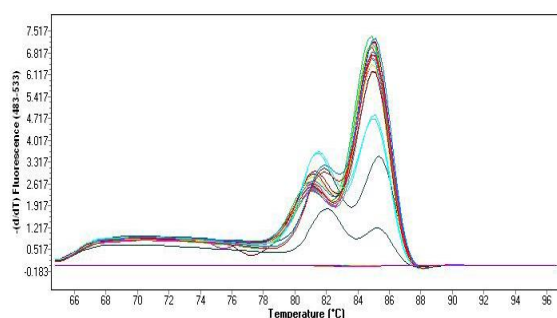
The optimal efficiency of a PCR reaction is 2, meaning that the amount of the amplicon is doubled at each reaction cycle. Since many factors can impact on the efficiency, including primer binding, ion concentration and the actual PCR instrument itself, the efficiency of the reaction had to be established. Reaction efficiency was calculated using the threshold value (C_q) obtained from a dilution series of the hβD-3-pGemT easy plasmid. A standard was therefore created by diluting the calibrator plasmid 10^{-3} to 10^{-12} times. The qPCR amplification was carried out using a Lightcycler 480 (see section 2.5.VII), and the standard curve data is shown in Figure 5.3:



A



B



C

Figure 5.3 First trial for a standard curve determination. (A) Standard curve formation using the C_q -value and concentration of h β D-3 template. The slope of -3.67 and the Y-intercept of 31.15 were used to determine the efficiency. (B) Amplification curves of h β D-3-pGemT-easy. (C) Analysis of the dissociation curve of the qPCR assay with two peaks (at 81.5 °C and 85.5 °C).

The resulting C_q values, calculated by the LightCycler 480 software (Roche Applied Science, UK) and the concentration of the h β D-3 template were plotted in a XY-diagram (Fig. 5.3.A). The C_q values could only be defined over a magnitude of 10^4 . The y-intercept and slope, and the correlation coefficient R^2 of the standard curve were calculated using Excel (Microsoft Office 2010, Fig. 3.5.A, red rectangle). The PCR efficiency was calculated using the formula proposed by the MIQE-committee¹⁴⁴:

$$Efficiency/\% = (10^{-\frac{1}{slope}} - 1) * 100$$

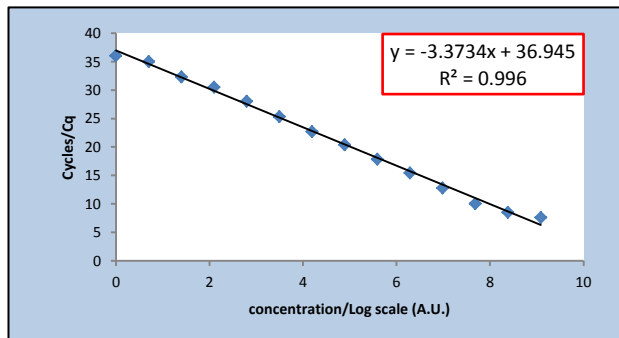
The standard curve shows a slope of -3.6656, hence the efficiency is:

$$Efficiency = (10^{-\frac{1}{-3.6656}} - 1) * 100 = 87.4 \%$$

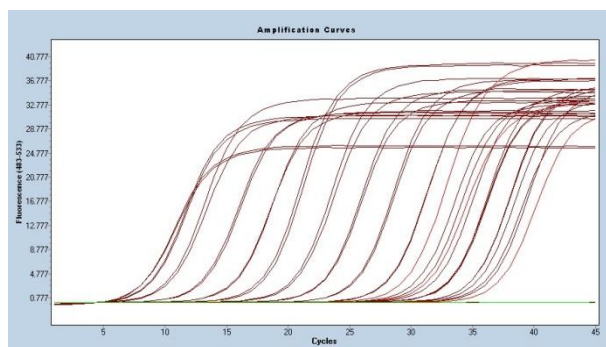
The calculated efficiency was 87.4 %. For the assay to be valid the PCR efficiency must lie between 95 and 105 %, and have a correlation coefficient between 0.9 and 1.0¹⁸³. In view of these requirements the data generated was a concern; the results meant that, with each amplification cycle, a 12.6 % error chance was introduced into the quantitation of the gene expression.

Furthermore, the analysis of the amplification curve showed a positive result even for the negative control (Figure 5.3.B) at C_q of 28 cycles, indicating contamination with the plasmid. Finally, the disassociation curve showed more than one peak suggesting the presence of two amplification products. To verify if the plasmid was contaminated with foreign DNA, the engineering of the hβD-3-reporter plasmid was repeated (data not shown). The results were reproducible, strongly suggesting that the primers themselves were inadequate since they were creating two products.

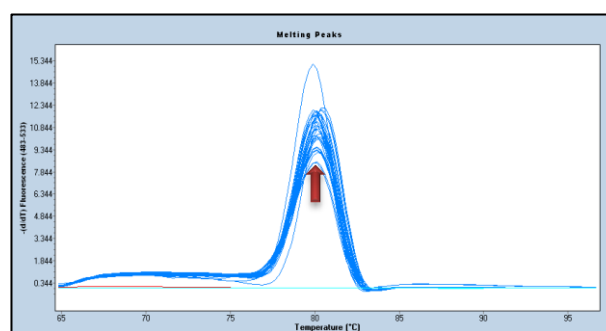
Primer sequences used in the second qPCR assay were obtained from the literature¹⁸⁴. Their binding sites are shown in Fig. 5.1.A (qPCR primer Kalus *et al.*) and are located within the sequence of the amplification product used to engineer the hβD-3 reporter plasmid. Hence, the previous hβD-3 template was serially diluted five-fold, amplified using the new qPCR primers and the results are shown in Figure 5.4:



A



B



C

Figure 5.4 Second trial for a standard curve determination. (A) Standard curve using C_q value and arbitrary concentration of hβD-3-template. (B) Analysis of amplification curve. Red lines are the hβD-3 templates at different concentration. Green line represents the negative control. (C) Disassociation curve of PCR products. Arrow indicates the peak. Light blue line represents the negative control.

The standard curve was plotted in a XY diagram using the C_q -values, calculated by the LightCycler 480 software, on the y-axis and the arbitrary concentration of the hβD-3 template on the x-axis (Fig. 5.4.A). The PCR efficiency was again calculated using the formula proposed by the MIQE-committee:

$$Efficiency/\% = (10^{-\frac{1}{slope}} - 1) * 100$$

The trendline shows a slope of -3.3734, therefore the efficiency is:

$$Efficiency = (10^{-\frac{1}{-3.3734}} - 1) * 100 = 97.9 \%$$

For this hβD-3 assay, the calculated efficiency of 97.9 % and the correlation coefficient of 0.996 were acceptable. The theoretical detection limit of the qPCR assay was extrapolated to 36.9 cycles. Nonetheless, C_q -values beyond 35 cycles were considered to be replication of random products (personal communication Dr Alison Howard, Newcastle University) and considered as such in subsequent analyses.

Amplification and disassociation curve analysis were performed. The amplification curve showed no increase in fluorescence for the negative control (Fig. 5.4.B, green line) and the disassociation curve identified only one amplified product (Fig.5.4.C). All amplicons showed the same peak, T_m at ~81 °C (red arrow on dark blue curve, Figure 5.4.C). The negative control did not show a peak (light blue line, Figure 5.4.C). The assay was considered successful and adopted for use.

To support the molecular analyses and data an ELISA to measure hβD-3 peptide concentration was also developed.

2. DEVELOPMENT OF A HBD-3 ELISA

Two ELISA methods were explored: the first was a simple indirect ELISA and the second was a sandwich ELISA.

I. INDIRECT ELISA SPECIFIC FOR HBD-3

To measure the concentration of h β D-3 peptide an indirect ELISA, the simplest form of ELISA, was developed. Three different concentrations of h β D-3 specific antibody, ranging from 0.5 to 2 μ g/ml, were used and a standard curve was constructed using synthetic h β D-3 ranging from 10 to 500 ng/ml. The results are shown in Figure 5.5 and Table 5.1:

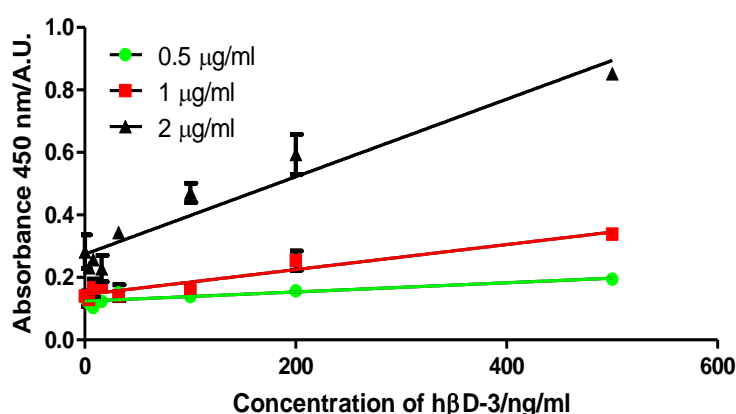


Fig. 5.5 Determination of a h β D-3 peptide standard curve using indirect ELISA. Synthetic h β D-3 was incubated over night at 4°C and the concentration measured using monoclonal h β D-3 antibody (N=2).

Table 5.1 Linear regression analysis of the standard curve determined by indirect ELISA

Concentration of antibody	Slope	Y-Intercept	R ²
0.5 mg/ml	0.0001470 \pm 0.00003190	0.1240 \pm 0.006192	0.6026
1 mg/ml	0.0004006 \pm 0.00004076	0.1449 \pm 0.007910	0.8734
2 mg/ml	0.001241 \pm 0.0001019	0.2739 \pm 0.01978	0.9136

The linear regression analysis showed that a standard curve with a R²>0.9 only occurred when a concentration of 2 μ g/ml primary antibody was used. However, at this concentration they intercept the Y-axis at an absorbance of 0.27 \pm 0.01 indicated a high

background (Tab. 5.1, Y-Intercept). Therefore, the indirect ELISA was considered inadequate to measure the concentration of hβD-3 peptide and development switched to a more complex sandwich ELISA.

II. DEVELOPMENT OF A SANDWICH ELISA SPECIFIC FOR HBD-3

Through the use of two antibodies rather than one a sandwich ELISA has superior sensitivity and a higher specificity. The first antibody, used in the previous assay as detection antibody, was immobilised in a 96 wells plate and captures the hβD-3 from solution while a new second antibody is used for detection of the captured hβD-3.

The antibodies used in the sandwich assay were first optimised using synthetic hβD-3. The sensitivity of the hβD-3 sandwich ELISA was much higher than that of the indirect ELISA. In fact, trying to determine a standard curve using the same concentration of synthetic hβD-3 as in the indirect ELISA (500 ng/ml- 31.25 ng/ml) caused an absorbance value at 450 nm beyond 4.0 (data not shown), making a concentration depending absorbance reading impossible. Therefore, the concentration of the synthetic hβD-3 was reduced to 1000 pg/ml and serially diluted to 31.25 pg/ml. The results of the hβD-3 sandwich ELISA optimisation using the lower concentration of hβD-3 are shown in Figure 5.6 and Table 5.2:

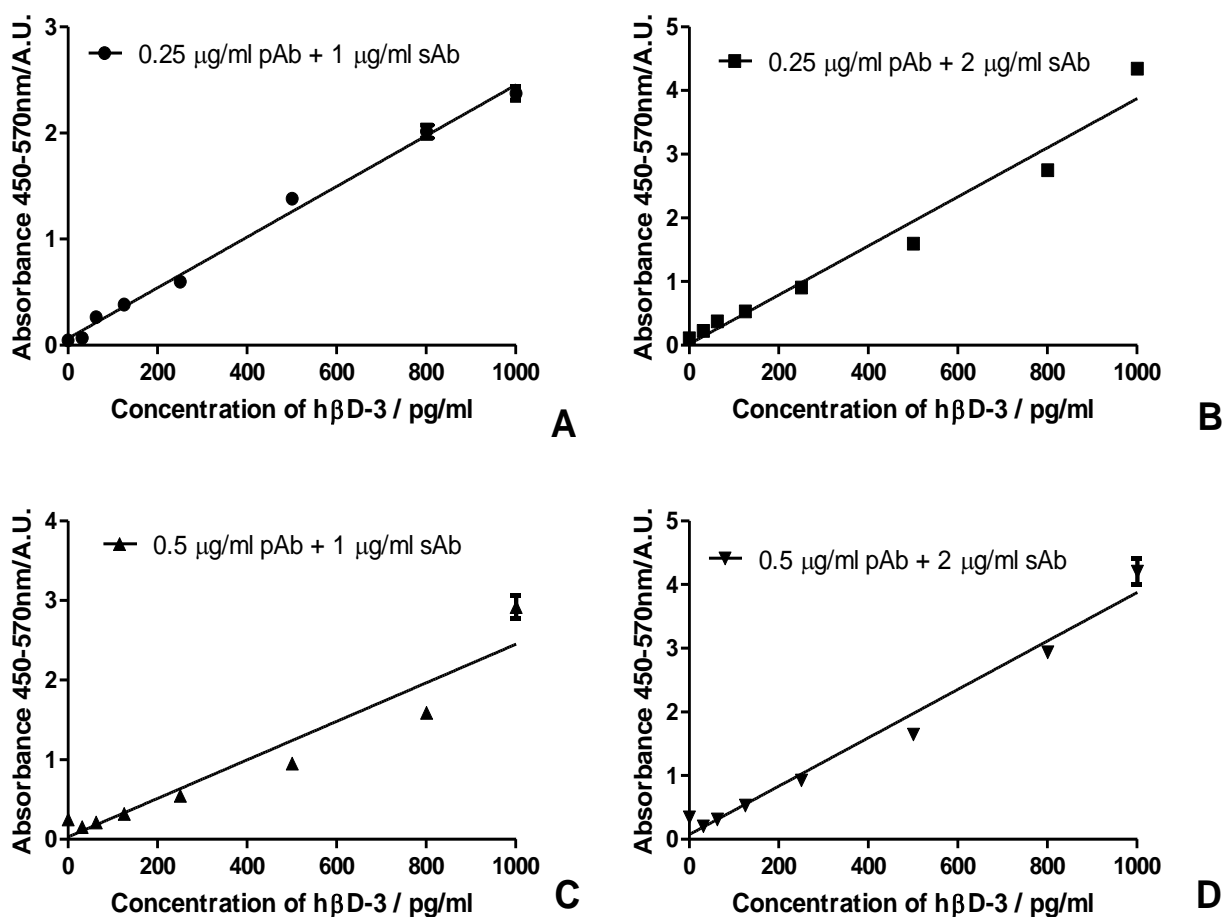


Figure 5.6 Determination of a hβD-3 specific standard curve using a sandwich ELISA. The capture antibody was used at 0.25 μg/ml (A and B) or at 0.5 μg/ml (C and D). The secondary detection antibody was used at a concentration of 1 μg/ml (A and C) or at 2 μg/ml (B and D). The concentration of synthetic hβD-3 varied between 31.25 and 1000 pg/ml. Absorbance was measured at 450 nm and corrected at 570 nm.

Table 5.2 Linear regression analysis of the standard curve resulted by a sandwich ELISA

Concentration of the antibodies	Slope	Y-intercept	R ²
0.25 μg/ml pAb & 1 μg/ml sAb	0.002389 ± 0.00005008	0.06479 ± 0.02487	0.9904
0.25 μg/ml pAb & 2 μg/ml sAb	0.003855 ± 0.0001523	0.01980 ± 0.07561	0.9668
0.5 μg/ml pAb & 1 μg/ml sAb	0.002422 ± 0.0001584	0.03015 ± 0.07864	0.914
0.5 μg/ml pAb & 1 μg/ml sAb	0.003802 ± 0.0001373	0.07545 ± 0.06821	0.9721

Linear regression analyses showed that all combinations of primary and secondary antibodies resulted in a coefficient of determination $R^2 > 0.9$ (Table 5.2), indicating a linear correlation between the absorbance measured and the concentration of hβD-3.

The highest coefficient of determination R^2 , was measured for the lowest concentration of primary and secondary antibody (0.25 $\mu\text{g/ml}$ and 1 $\mu\text{g/ml}$, respectively; Table 5.2, $R^2=0.9904$). Additionally, the Y-intercept, which determines the unspecific binding of the antibodies was 0.07 ± 0.03 , indicating very low levels of unspecific bindings. Hence, these antibody concentrations were adopted as the working concentrations. The sandwich ELISA assay was considered optimised to measure the secretion of h β D-3.

With the qPCR and ELISA assays established the h β D-3 responses of the epithelial cells modelling the urogenital tract, to bacterial challenge, were investigated.

5.4. RT4 HBD-3 RESPONSE TO *E. COLI* CHALLENGE

The *E. coli* strains NCTC 10418 (motile) and NU14 (non-motile) were used to challenge RT4 cells. Both strains were heat killed and RT4 cells were challenged up to 24 hours with 10^5 CFU/ml bacteria. The results are shown in Figure 5.7:

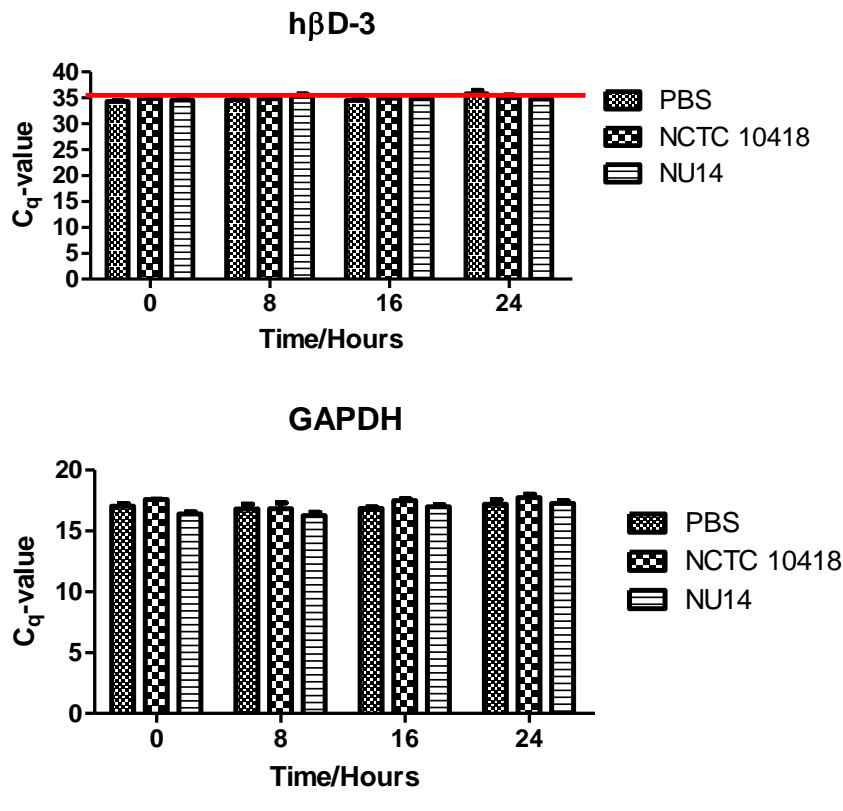


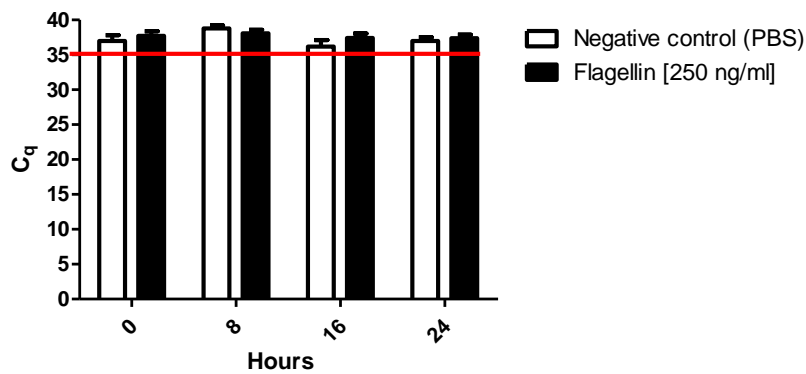
Figure 5.7 Expression of hβD-3 in RT4 challenged with *E. coli* strains. (A) The expression of hβD-3 was quantified in RNA isolated from RT4 cells challenged with 10⁵ CFU/ml for up to 24 hours. The Y-axis represents the C_q-value calculated by the Lightcycler 480 Software. (B) C_q-value of the reference gene GAPDH. Bars represent the mean with their standard error as error bars. N=6, 2 experiments with 3 replicates

Results of the quantitative PCR (the limit of detection is marked by the red line) indicated that very low or no expression was detected in RT4 cells at 0 hours (C_q 34±0.2 for PBS, C_q 35±0.5 for NCTC 10418, C_q 35±0.2 for NU14, Fig. 5.7.A), and these data concurred with end-point PCR results shown in Fig. 5.1.B. Following challenge with *E. coli* strains NCTC 10418 and NU14 no upregulation of hβD-3 expression at either 8 (C_q 35±0.2 for PBS, C_q 35±0.4 for NCTC 10418, C_q 35±0.5 for NU14, Fig. 5.7.A), 16 (C_q 34±0.5 for PBS, C_q 35±0.2 for NCTC 10418, C_q 35±0.3 for NU14, Fig. 5.7.A) or 24 hours (C_q 36±0.7 for PBS, C_q 35±0.5 for NCTC 10418, C_q 35±0.3 for NU14, Fig. 5.7.A) was detected. The presence of RNA was verified using GAPDH as the reference gene and GAPDH was expressed at the expected levels (personal communication Dr Alison Howard, Newcastle University), with a C_q-value of ≤ 18 cycles (Fig. 5.7.B), confirming

that the mRNA was successfully reverse transcribed. Overall these data indicated that the h β D-3 gene was not expressed in RT4 cells either constitutively or following bacterial challenge.

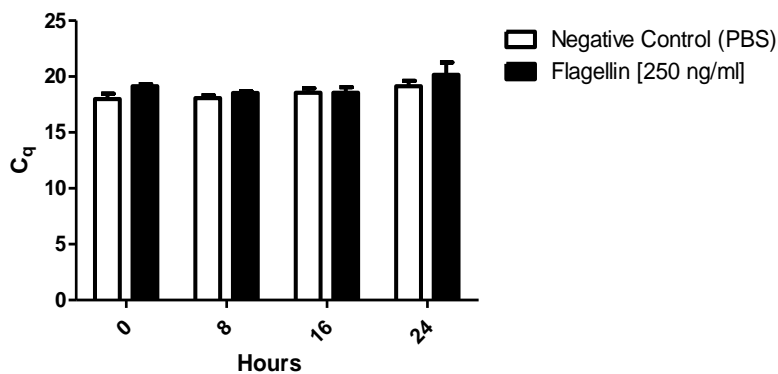
Next, the PAMP associated with the highest immune response, *i.e.* flagellin, was used to investigate if h β D-3 gene expression was induced when a high concentration of a purified bacterial compound was used. RT4 cells were challenged with 250 ng/ml of flagellin for up to 24 hours and the results of h β D-3 expression are shown in Figure 5.8:

RT4 challenged with Flagellin- hβD-3



A

RT4 challenged with Flagellin- GAPDH



B

Figure 5.8. Expression of hβD-3 in RT4 cells challenged with flagellin. RT4 cells were challenged with 250 ng/ml of flagellin isolated from *E. coli*. The RNA was reverse transcribed and the gene expression for (A) hβD-3 and (B) GAPDH was measured using qPCR. N=6, 2 experiments with 3 replicates. Red line shows the limit of detection according to MIQE.

The results (Fig. 5.8.A & B) were comparable to previous. Essentially, no expression of hβD-3 was detected in the RT4 cells as all C_q -values were ≥ 35 cycles (Fig. 5.8.A). The mRNA reverse transcription was successful as demonstrated by C_q -values of the GAPDH reference gene ($C_q \geq 18$ cycles, except 24 hours with C_q -value of 19 ± 0.4 for PBS and 20 ± 1.1 for flagellin, Fig. 5.8.B). Therefore, it was concluded that RT4 does not express hβD-3 constitutively or following challenge with either *E. coli* or the bacterial component flagellin.

5.5. VK-2 E6/E7 HBD-3 RESPONSE TO *E. COLI* CHALLENGE

As mentioned in the introduction and in section 4.9, the vaginal epithelium plays a major role in regulating the colonisation of UPEC by inducing h β D-2 activation and secretion. The expression of h β D-3 was therefore analysed in VK-2 E6/E7 cells to explore potential roles for h β D-3 in the vaginal innate defences. VK-2 E6/E7 cells were challenged for up to 24 hours using 5×10^4 CFU/ml of bacteria. Human β D-3 gene expression and peptide synthesis were quantitated as previously described (sections 5.3.1 and 5.3.2.II). The results of the h β D-3 expression were normalised using GAPDH expression and are shown in Figure 5.9:

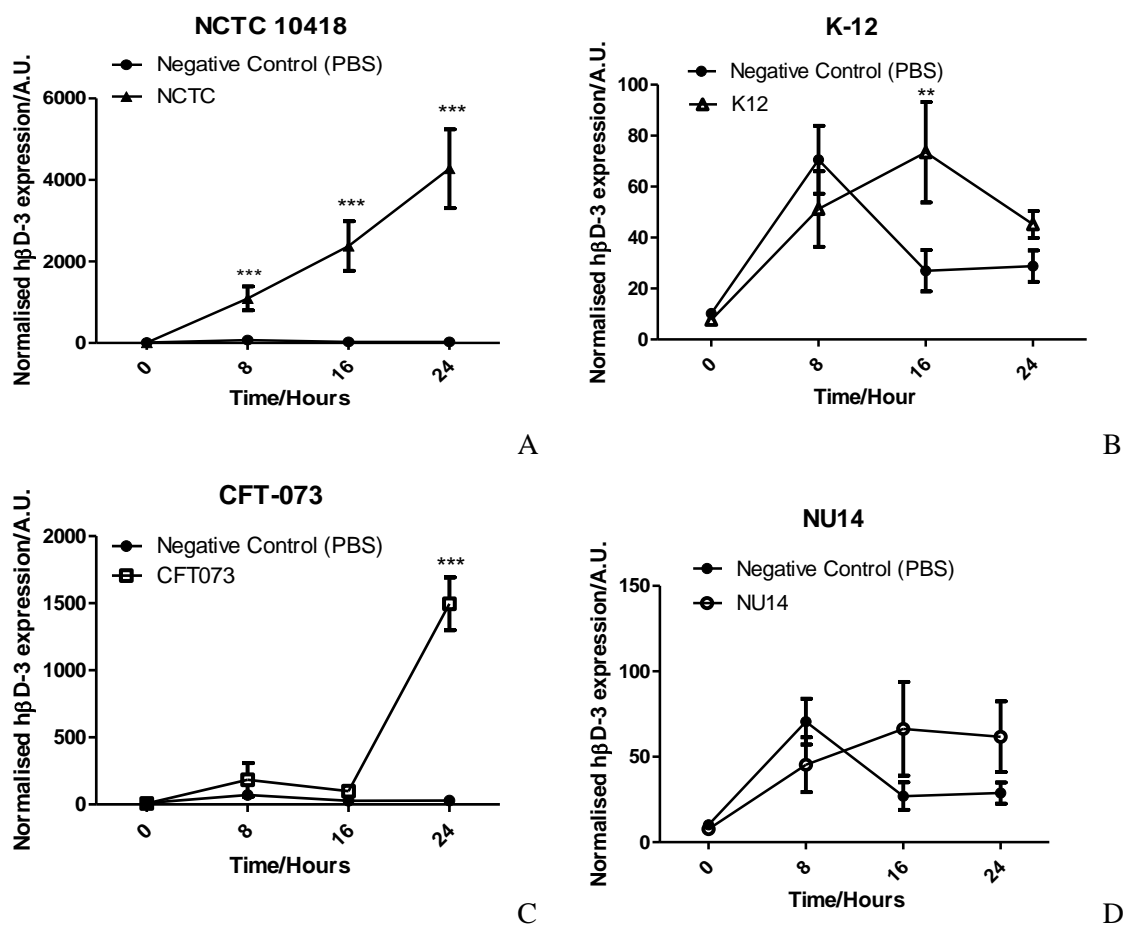


Figure 5.9: Quantification of hβD-3 expression in VK-2 E6/E7 challenged with *E. coli* strains using qPCR. VK-2 E6/E7 challenged with PBS and 5×10^4 CFU/ml of (A) Motile NCTC 10418 (N=9, 3 experiments with 3 replicates), limit of the Y-axis is set to 6000. (B) Motile K-12 (N=6, 2 experiments with 3 replicates), limit of the Y-axis is set to 100. (C) Motile CFT 073 (N= 6, 2 experiments with 3 replicates), limit of the Y-axis is set to 2000. (D) Non-motile NU14, limit of the Y-axis is set to 150. (N=6, 2 experiments with 3 replicates). Y-Axis represent the fold increase of hβD-3 expression normalised using GAPDH shown in arbitrary units (A.U.) and using the Pfaffl method¹⁸⁵. Statistical significance was investigated using ANOVA and a Bonferroni post hoc test. **= $p < 0.01$, ***= $p < 0.001$.

In these experiments the *E. coli* strains, K-12 and CFT 073, in addition to NCTC 10418 and NU-14 were used. They were added because K-12 is a standard laboratory *E. coli* strain with moderate motility and CFT 073 is a motile UPEC. The results are shown as fold increase (compared to the 0 hour time point) using the Pfaffl method¹⁸⁵. As shown in Figure 5.9.A, the NCTC 10418 challenge of VK-2 E6/E7 resulted in a significantly higher expression of hβD-3 when compared to the negative control (PBS), and the

increase was detected from the first time-point, *i.e.* eight hours post challenge (518.5 ± 139.2 for NCTC 10418 challenged cells vs. 70.5 ± 13.4 , $p < 0.001$).

The expression of h β D-3 increased with time and the highest value was measured at the final time point, *i.e.* 24 hours (4275.6 ± 969.3 for NCTC 10418 and 26.8 ± 6.2 for PBS).

In contrast, K-12 showed significant upregulation of h β D-3 only at 16 hours of challenge (Fig. 5.9.B; $p < 0.01$). Furthermore, h β D-3 induction in VK-2 E6/E7 cells by K-12 was reduced by 32 fold when compared to NCTC 10418 (73.5 ± 19.7 , Fig. 5.9.B vs 2379.3 ± 606.1 , Fig. 5.9.A). Note that the scale of the Y-axis in Fig. 5.9.A is 2000 while in Fig. 5.9.B is only 100 for presentation purposes.

The motile UPEC CFT 073 did not affect h β D-3 expression for the first 16 hours of challenge (Fig. 5.9.C), but at 24 hours, the expression of h β D-3 was significantly increased (1496.0 ± 196.5 for CFT 073 vs. 28.7 ± 6.2 for PBS; $p < 0.001$). Nonetheless, the h β D-3 response induced by CFT 073 (Fig. 5.9.C) at 24 hours was 2.7 fold lower than the response seen for NCTC 10418 (Fig. 5.9.A).

The non-motile UPEC NU14 did not induce h β D-3 expression at any time point measured (Fig. 5.9.D).

From these results it can be concluded that the two strains with a higher motility, NCTC 10418 and CFT 073, induced the strongest h β D-3 expression at 24 hours. The strain with the lowest motility, K-12, also induced the lowest expression of h β D-3 and the non-motile strain failed to induce a h β D-3 response.

In order to validate these findings, hβD-3 peptide concentrations were measured in the media bathing the VK-2 E6/E7 cells challenged with the four *E. coli* strains, using the sandwich ELISA. The results are shown in Figure 5.10:

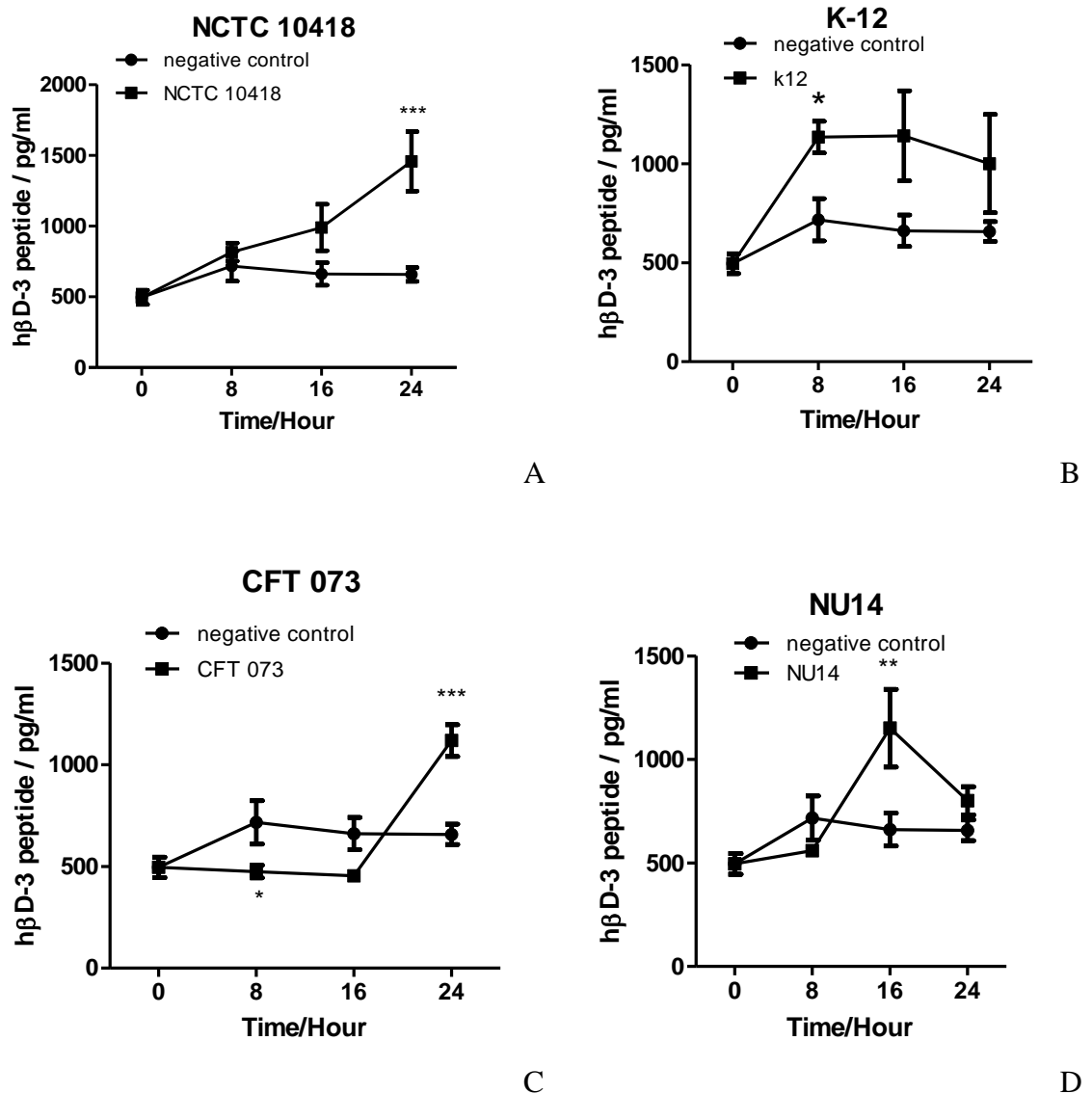


Figure 5.10 hβD-3 secretion of VK-2 E6/E7 upon challenge with *E. coli* strains. VK-2 E6/E7 was challenged with 5×10^4 CFU/ml with (A) NCTC 10418, (B) K-12, (C) CFT 073 and (D) NU14. N=2, using media pooled of 3 replicates. Human βD-3 concentration was measured using the developed sandwich ELISA. Statistical significance was investigated using ANOVA with a Bonferroni post hoc test. *=p<0.05, **=p<0.01, ***=p<0.001.

Supporting the molecular data, the NCTC 10418 challenge was associated with a significantly higher hβD-3 concentration in the media bathing the VK-2 E6/E7 cells after 24 hours of challenge than that of the PBS challenged cells (Fig. 5.10.A,

1456.9±209.7 pg/ml for NCTC 10418, 657.9±49.7 pg/ml for PBS). The challenge with K-12 also suggested induction of hβD-3 synthesis, however, statistical significance could only be determined at 8 hours due to the large variations within the individual measurements (Fig. 5.10.B, 1141.0±227.8 pg/ml at 16 hours and 1000.6±248.1 pg/ml at 24 hours, p<0.05). The ELISA data suggested that challenge with the motile UPEC CFT 073 inhibited hβD-3 secretion up to 8 hours (Fig. 5.10.C, p<0.05), but as with the mRNA expression, the hβD-3 concentrations were significantly increased at 24 hours (Fig. 5.10.C, 1119.2±77.8 pg/ml for CFT 073 vs. 657.9±50.0 pg/ml for PBS, p<0.001). NU14 challenged VK-2 E6/E7 cells showed no significant difference in hβD-3 concentrations at 8 hours (559.0±15.4 pg/ml for NU14 vs. 717.5±106.6 pg/ml for PBS). This was comparable to the 8 hour CFT 073 effects (Fig. 5.10.C, 474.8±31.3 pg/ml for CFT 073 at 8 hours). However, contradicting the mRNA data, the NU14 challenge was associated with significantly elevated hβD-3 concentrations at 16 hours (Fig. 5.10.D, 1150.8±187.7 pg/ml for NU14 vs. 661.68±79.5 pg/ml for PBS, p<0.01).

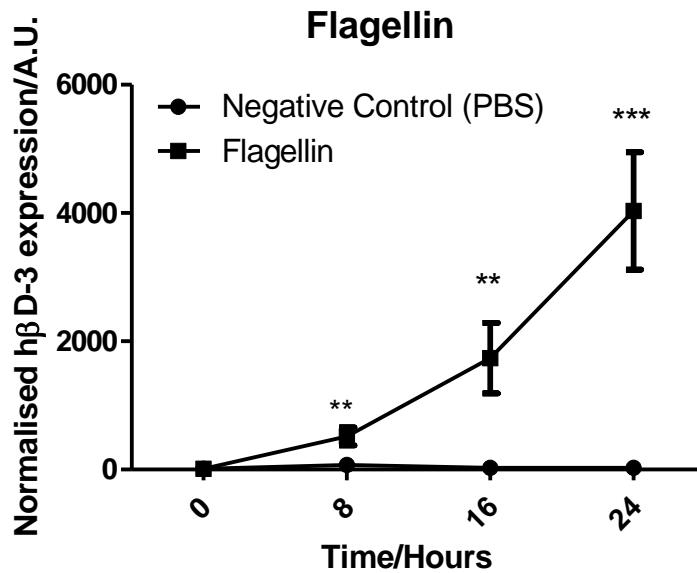
Apart from one time point of the NU14 challenge, all peptide findings mirrored the gene expression data. Interestingly, the highest hβD-3 expression and peptide concentrations were associated with the two highly motile strains NCTC 10418 and CFT 073 at 24 hours post challenge. Moreover, both UPEC strains, CFT 073 and NU14, showed a tendency to reduce hβD-3 expression and synthesis for up to 8 hours of challenge. The measurements of hβD-3 secreted by VK-2 E6/E7 when challenged with K-12 did not result in consistent data and therefore, need to be evaluated with caution.

Concluding, challenges with the motile strains caused a higher hβD-3 response and therefore, the role of flagellin was further investigated. Additionally, components of the bacterial cell wall including LPS and peptidoglycan, which may have contaminated the flagellin preparation were also tested.

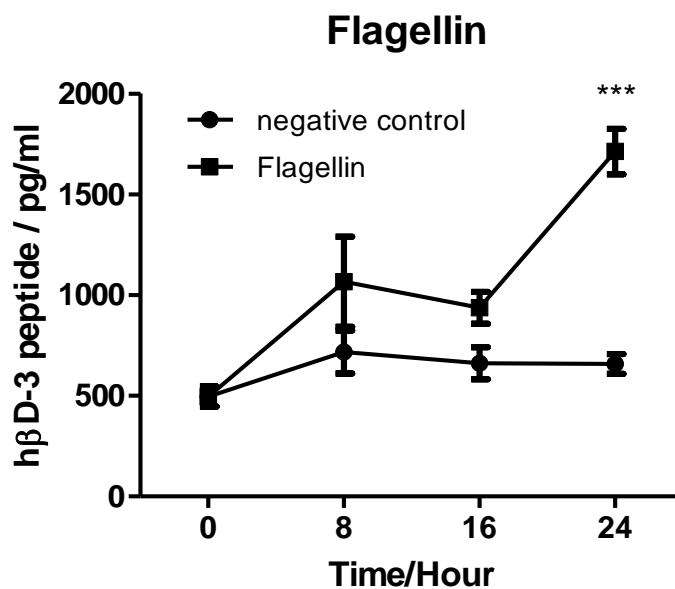
5.6. HBD-3 REGULATION IN VK-2 E6/E7 CHALLENGED WITH COMPOUNDS OF THE BACTERIAL CELL WALL

1. FLAGELLIN

Flagellin isolated from *E. coli* (see section 3.5) was used to challenge the VK-2 E6/E7 cells. The h β D-3 expression was measured using qPCR and the concentration of the peptide in the media bathing the cells was determined by ELISA. The results are shown in Figure 5.11:



A



B

Figure 5.11 hβD-3 response of VK-2 E6/E7 cells to flagellin. VK-2 E6/E7 cells were challenged with 250 ng/ml for up to 24 hours. (A) Quantitation of hβD-3 mRNA expression using qPCR. The expression was normalised against GAPDH. (N=9, 3 experiments with 3 replicates). (B) Media of PBS or flagellin challenged VK-2 E6/E7 cells was collected and hβD-3 secretion was measured using sandwich ELISA (N=6, 2 experiments with 3 replicates). Statistical significance was investigated using ANOVA and a Bonferroni post hoc test. **= $p < 0.01$, ***= $p < 0.001$.

Flagellin induced a hβD-3 response at the mRNA level as early as 8 hours after challenge (Fig. 5.11.A, 518.5 ± 139.2 for flagellin vs. 70.5 ± 13.4 for PBS, $p < 0.01$). The response increased with time and the highest response was measured at the final time

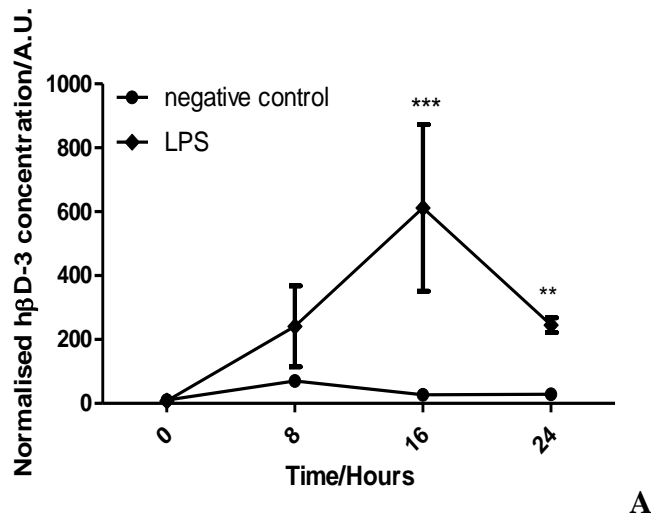
point, *i.e.* 24 hours after challenge (4032.2 ± 915.4 compared to PBS control of 28.8 ± 6.2 ; $p < 0.001$). This response was similar to that observed for NCTC 10418 (Fig. 5.9.A, 4275.6 ± 969.3).

Human β D-3 peptide concentrations were also significantly increased at 24 hours after flagellin challenge (Fig. 5.11.B, 1712.9 ± 112.6 pg/ml for flagellin vs. 657.9 ± 49.73 pg/ml for PBS, $p < 0.001$). Again, this value was comparable to the concentrations measured when VK-2 E6/E7 cells were challenged with the highly motile NCTC 10418 strain (Fig. 5.9.B. 1456.9 ± 209.7 pg/ml).

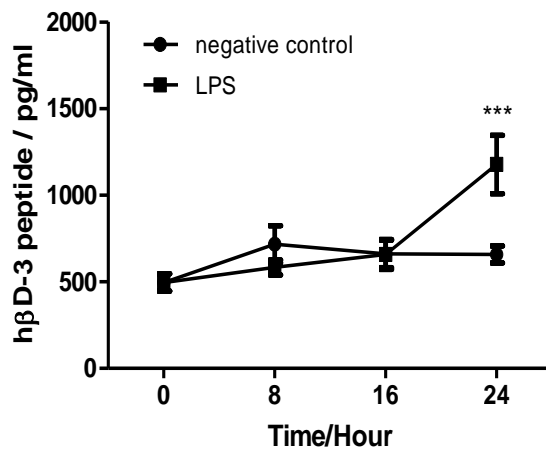
In conclusion, the highest induction of h β D-3 expression and secretion in the VK-2 E6/E7 cells following bacterial challenge was observed using the motile *E. coli* strain NCTC 10418. Flagellin (250 ng/ml), the component responsible for bacterial motility, also induced comparable levels of h β D-3 expression and synthesis.

2. LIPOPOLYSACCHARIDES (LPS)

LPS was the first of the two bacterial cell wall components that were used to investigate h β D-3 gene regulation. To allow comparisons to previous experiments the VK-2 E6/E7 cells were challenged with 10 μ g/ml of LPS for up to 24 hours. RNA was collected for gene expression analyses and the cell bathing media was analysed for h β D-3 peptide concentrations. The results are shown in Figure 5.12:



A



B

Figure 5.12 hβD-3 response of VK-2 E6/E7 cells challenged with LPS. VK-2 E6/E7 cells were challenged using 10 μg/ml of LPS isolated from *E. coli*. **(A)** mRNA expression of hβD-3 was measured using RT-qPCR. The expression was normalised against GAPDH. **(B)** media of PBS or LPS challenged VK-2 E6/E7 cells was collected and hβD-3 concentration was determined using sandwich ELISA (N=2). Statistical significance was investigated using ANOVA and a Bonferroni post hoc test. **= $p < 0.01$, ***= $p < 0.001$.

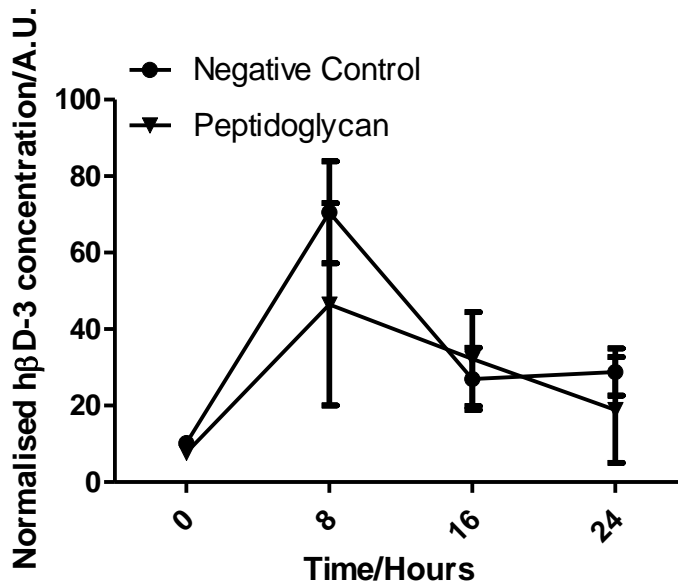
LPS in contrast to flagellin, did not induce hβD-3 significant mRNA up-regulation at 8 hours after challenge (Fig. 5.12.A, 241.4 ± 126.8 for LPS vs. 70.5 ± 13.4 for PBS), although arguably there was a suggestion of upregulation masked by the large error bars associated with this time point. Significant upregulation was measured at 16 hours after challenge, which also represented the peak of hβD-3 expression (Fig.5.12.A, 612.2 ± 260.8 for LPS vs. 27.0 ± 8.1 for PBS, $p < 0.001$). The final 24 hour time point,

values showed a reduction in hβD-3 expression, although the mean value determined was still statistically significantly higher than that measured for the PBS challenged cells (Fig.5.12.A 245.3±22.8 for LPS vs. 28.8±6.2 for PBS, p<0.01).

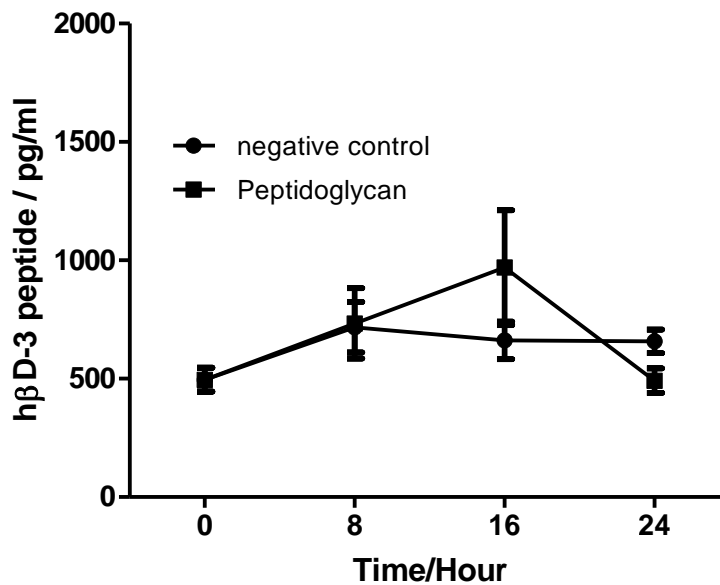
The hβD-3 peptide concentrations following LPS challenge were significant at 24 hours (Fig. 5.12.B, 1177.5±168.8 pg/ml for LPS compared to 657.9±49.7 pg/ml for PBS, p<0.001. These data indicate that the hβD-3 response to LPS was reduced when compared to those observed for the motile bacteria NCTC 10418 and for flagellin.

3. PEPTIDOGLYCAN

VK-2 E6/E7 cells were challenged with the same concentration of PG as LPS. Human βD-3 gene expression and peptide responses were measured and the results are shown in Figure 5.13:



A



B

Figure 5.13: hβD-3 response to Peptidoglycan in VK-2 E6/E7. VK-2 E6/E7 cells were challenged using 10 μg/ml of peptidoglycan isolated from *E. coli*. (A) Messenger RNA expression of hβD-3 was measured using RT-qPCR. The expression was normalised against GAPDH. (B) Media of PBS or peptidoglycan challenged VK-2 E6/E7 cells was collected and hβD-3 concentration was determined using sandwich ELISA (N=2). Statistical significance was investigated using ANOVA and a Bonferroni post hoc test. *= $p < 0.05$, **= $p < 0.01$, ***= $p < 0.001$.

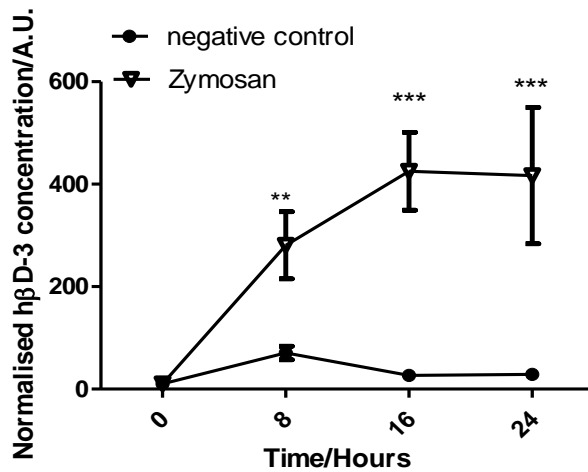
Peptidoglycan did not induce any significant changes in hβD-3 expression or peptide concentrations (Fig. 5.13.A and B). Although the data suggested increased hβD-3 peptide levels at 16 hours post challenge, the statistical analysis did not show any significant differences when the data were compared to the negative control (Figure

5.13.B, 969.375 ± 242.5 pg/ml for peptidoglycan and 661.7 ± 79.5 pg/ml for PBS). Summarising, these data suggested peptidoglycan did not activate either h β D-3 expression or synthesis.

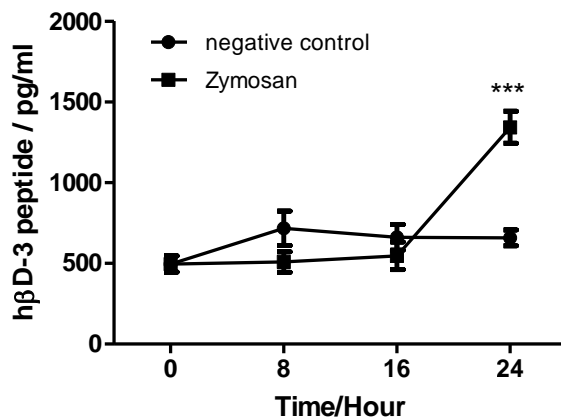
In conclusion, h β D-3 expression and synthesis was induced in vaginal cells following a bacterial challenge that modelled infection. Flagellin was linked with a marked h β D-3 response suggesting that microbial motility plays a key role in the h β D-3 induction in vaginal epithelia. Human β D-3 activation by LPS was also observed but using a similar concentration, peptidoglycan failed to induce a h β D-3 response altogether.

5.7. ALTERNATIVE ACTIVATION OF HBD-3 USING FUNGAL CELL WALL COMPONENT ZYMOBAN

As reported in Chapter 4, Zymosan activated h β D-2 reporter activity in the bladder (section 4.8.I) as well as vaginal epithelia (section 4.9.I), highlighting a potential role for Zymosan in protecting against bacterial infection and recurrent UTI. Therefore, it was also investigated whether Zymosan could induce a h β D-3 response in VK-2 E6/E7 cells, by challenging the cells with 50 μ g/ml of Zymosan. Human β D-3 gene expression and peptide were measured using qPCR and ELISA. The results are shown in Figure 5.14:



A



B

Figure 5.14 hβD-3 response in VK-2 E6/E7 challenged with Zymosan. VK-2 E6/E7 cells were challenged up to 24 hours using 50 μg/ml of Zymosan. **(A)** mRNA expression of hβD-3 was measured using RT-qPCR. The expression was normalised against GAPDH. **(B)** media of PBS or Zymosan challenged VK-2 E6/E7 cells was collected and hβD-3 concentration was determined using sandwich ELISA (n=3). Statistical significance was investigated using ANOVA and a Bonferroni post hoc test. **= $p < 0.01$, ***= $p < 0.001$.

Zymosan induced a significant hβD-3 mRNA response in VK-2 E6/E7 as early as 8 hours (Fig. 5.14.A, 280.8 ± 65.7 for Zymosan vs. 70.5 ± 13.4 for PBS, $p < 0.01$). The response was significant ($p < 0.001$) at the following time points up to 24 hours. Zymosan also induced a significant increase in hβD-3 peptide concentrations but only at 24 hours after challenge (Fig. 5.14.B, 1342.9 ± 99.1 for Zymosan vs. 657.9 ± 49.7 for PBS, $p < 0.001$). Although the hβD-3 mRNA response was four fold lower when compared to either the motile strain NCTC 10418 or flagellin, the peptide

concentrations were comparable (1342.4±99.1 pg/ml vs 1456.9±209.7 pg/ml and 1712.9±112.6, respectively).

5.8. DISCUSSION

Work presented in the previous chapter indicated that hβD-2 was induced in the urogenital tract in response to infection and as such was an important factor in the innate defences of such tissues. This Chapter explored whether another member of the Defensin family, namely hβD-3, also played a role in such defences. Such investigations were motivated by studies published in the literature that supported hβD-3 gene induction and synthesis in infected tissues¹⁸⁶. Moreover, physiologically hβD-3 is probably important in urogenital defences as unlike hβD-2, it is salt insensitive^{180,187}, which means that its bacterial killing activities can continue in urine regardless of fluctuating sodium concentrations associated with fluid intake.

The studies first necessitated the development of new qPCR and ELISA assays. Using primer sequences reported previously¹⁸⁴, the qPCR assay established in the laboratory fulfilled the required MIQE standards. In addition, the development of a sandwich ELISA allowed quantification of hβD-3 in the picogram range as its sensitivity was 1000 fold increased compared to that of the indirect ELISA, due to a reduction in the background absorbance (Figs 5.5 & 5.6).

To perform the experiments *in vitro* cell models were required. Despite the development and use of sensitive molecular and peptide assays neither hβD-3 expression nor peptide synthesis was detected in RT4 cells either constitutively or after challenging with *E. coli* strains mimicking an UTI. This result was in direct contrast to the findings in the bladder biopsies. Interestingly, Lüthje *et al.* (2013), also showed that although hβD-3 was present in exfoliated cells in urine, the cell lines 5637 and the telomerase-

immortalized normal human urothelial cell line (TERT-NHUC) did not express h β D-3¹⁸⁸. Additionally, the investigation showed that postmenopausal women had significantly less h β D-3 expression in the exfoliated cells when compared to premenopausal ones¹⁸⁸, suggesting an direct or indirect effect of oestrogen on the induction of h β D-3 in the urinary tract. Sørensen *et al.* (2005), also showed that in skin, h β D-3 induction is TGF- α and EGFR dependent¹⁸⁹. TGF- α is known to be induced in MDA-MB-231 breast cancer cells in an ER- α dependent fashion¹⁹⁰. Hence, the absence of h β D-3 in the uroepithelium cell lines was probably a consequence of required cofactors not being present in the *in vitro* environment. Experiments stimulating RT4 cells with TGF- α and EGF in addition to challenges should be performed to validate this hypothesis.

In contrast to the RT4 observations, h β D-3 expression and peptide was detected in VK-2 E6/E7 cells. Furthermore, expression was constitutive, which if translated to the *in vivo* situation suggests that h β D-3 functions as a constant innate defence mechanism functioning to control microbial numbers in the vaginal tissues. In the VK-2 E6/E7 cell model the presence of h β D-3 can be explained by the presence of EGF in the culture medium. Challenging the vaginal cells with *E. coli*, including two UPEC strains, also resulted in an increased h β D-3 response. These data thus supported a significant role for h β D-3 in vaginal epithelial defences. A publication by Mitchel *et al.*, (2013) also supports the importance of h β D-3 in the vaginal environment, as lower levels of h β D-3 were associated with increased levels of bacterial vaginosis in pregnant women¹⁹¹.

Human β D-3 induction is via an AP-1 dependent pathway, and is thus independent of NF- κ B^{186,192}. However, the h β D-3 induction profiles in response to bacteria and flagellin challenges were comparable to the observations described in chapter three. The h β D-3 gene response to the NCTC 10418 challenge was ‘early’ and occurred within 8

hours, while the response to CFT 073, a motile strain associated with UTIs, was delayed until 24 hours. Similar to previous findings NU14 failed to induce a h β D-3 response completely. Taken together these data suggest that the UPEC strains have adapted to inhibit Defensin gene expression, *i.e.* host innate defences, thus allowing them to colonise the vaginal tissues. The observations relating to CFT 073 can be explained, since the protein that inhibits NF- κ B activation, TcpC, might also be involved in the inhibition of h β D-3. Indeed the signalling cascades initiated by MyD88, which is inhibited by TcpC, also result in the MAP kinase dependent activation of AP-1⁹⁶, thus increasing the virulence potential of TcpC⁺ UPEC. The ability of flagellin to cause induction of h β D-3 was also observed by Scharf *et al.* (2010), but in lung epithelia¹⁸⁶, further supporting h β D-3 induction by motile bacteria, in this case *Legionella pneumophila*.

The data in this Chapter indicated that similar to h β D-2 induction, motility rather than bacterial cell wall components such as LPS and peptidoglycan, plays a key role in the activation of h β D-3 (Figure 5.11). Challenging VK-2 E6/E7 with LPS did result in the upregulation of h β D-3 gene expression and synthesis, but expression was reduced by 2.8 fold, when compared to that measured for flagellin and peptide concentrations by 31 %. These data therefore suggest that the recognition of bacterial motility by the host is essential in the defence of the vaginal tissues.

Peptidoglycan (PG) treatment did not induce expression of h β D-3. The PG findings, however, contradict the work of Dusio *et al.* (2011)¹⁹³. These investigators were able to detect an increase in h β D-3 when VK-2 E6/E7 cells were challenged with peptidoglycan for 18 hours¹⁹³. A potential explanation for the conflicting results may be simple, for example, contamination of the peptidoglycan used by Dusio *et al.* (2011) with LPS.

As described in chapter three, TLR-5 is an important host factor in the recognition of potential uropathogens. Research in Newcastle has shown that TLR-5 activation results in NF- κ B signalling, h β D-2 synthesis and microbial killing¹⁵⁷. The flagellin challenge data presented in this Chapter also support the importance of TLR-5 in the induction of h β D-3 expression and synthesis in vaginal epithelia although it cannot be excluded that LPS, functioning presumably via TLR4, may also play a significant role¹⁹⁴.

The data presented in Chapter 4 indicated that the fungal β -1,3 glucan Zymosan could also activate h β D-2 gene expression and synthesis, presumably by a TLR-5 independent mechanism. Zymosan also activated the expression and synthesis of h β D-3 and this, to our knowledge, is the first description of this observation. Zymosan is known to act through a TLR-2 pathway, which classically, is the receptor through which PG signals^{195,196}. This was interesting as challenging the VK-2 E6/E7 cells with PG did not induce a h β D-3 response (Fig. 5.12). These data did nonetheless suggest that Zymosan is an inducer of the innate response through Defensin synthesis and understanding its mechanism of induction may provide a potential therapeutic avenue that can be exploited in the treatment of UTIs.

The next Chapter focuses on investigating the receptor associated with the Zymosan recognition.

CHAPTER SIX

The Dectin-1 Receptor in the Urogenital Tract

6.1. INTRODUCTION

Chapter three highlighted the importance of bacterial motility in urinary tract infections. From the host's perspective, TLR-5 was identified as a key defence factor in protecting the urogenital epithelium from potential infections with activation associated with the synthesis of effectors including IL-8 (Section 3.6.1) and h β D-2¹⁵⁸. However, data presented in Chapter four indicated that when either RT4 or VK-2 E6/E7 cells transfected with the h β D-2 reporter were challenged with Zymosan, not known as a TLR-5 ligand, reporter activity was induced, which translated to h β D-2 synthesis. In addition the Chapter five results also showed that Zymosan also induced h β D-3 expression and secretion in VK-2 E6/E7 cells. These data indicated that Zymosan is recognised by cells of the urogenital tract resulting, presumably, in an innate response involving Defensin expression, synthesis and microbial killing.

Zymosan is a β -1,3 glucan found in the fungal cell wall¹⁹⁷. It is known to activate the host's innate immune response in macrophages and dendritic cells through TLR-2/TLR-6 and Dectin-1, a calcium independent C-type lectin^{196,197}, signalling. There are reports of Dectin-1 being expressed in lung and in skin epithelia, however, there is no current evidence for the receptor being expressed in the urogenital tract^{75,198}. This is perhaps surprising, as the vagina is a common area for fungal infections¹⁹⁹.

This chapter explores the expression, localisation and activation of the Dectin-1 receptor in the urogenital epithelia with aim of identifying alternative host signalling pathways that could be exploited to help protect against UTI.

6.2. THE NF-KB RESPONSE TO FUNGAL ZYMOBAN

Previous data showed that Zymosan was able to induce h β D-2 reporter activation and secretion (Figures 4.13, 4.17 and 4.20) and that h β D-2 is NF- κ B dependent; to verify that Zymosan can activate NF- κ B, RT4 NF- κ B cells (used in chapter three), and VK-2 E6/E7 cells, transiently transfected with a NF- κ B-GFP reporter (section 2.11; Figure 6.1), were challenged with 50 μ g/ml Zymosan.

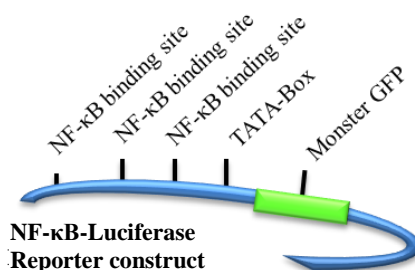


Figure 6.1 Reporter construct used to measure NF- κ B activity in VK-2 E6/E7. The reporter contains diverse NF- κ B binding sites, which when activated induce the expression of a modified version of GFP (MonsterGFP). The fluorescence of transfected cells was measured using the filters 480nm for excitation and 530nm for emission.

1. ZYMOBAN INDUCES NF-KB ACTIVATION IN RT4 AND VK-2 E6/E7

RT4 and VK-2 E6/E7 cell lines were challenged for up to 24 hours using 50 μ g/ml of Zymosan. NF- κ B activation, via luciferase and GFP activities, was measured every eight hours and the results represent the findings of two independent experiments. NF- κ B activity of cells challenged with Zymosan was determined as a fold increase over the NF- κ B activity of PBS challenged cells. The results are shown in in Figure 6.2:

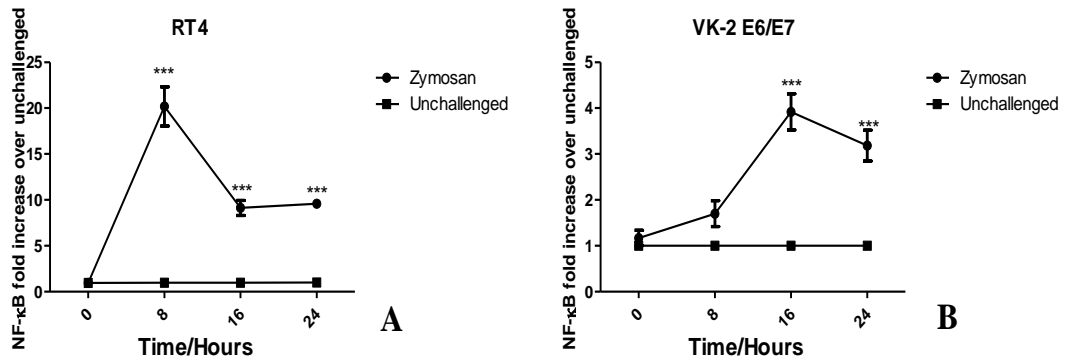


Figure 6.2 NF-κB activity of RT4 or VK-2 E6/E7 challenged with Zymosan. The cell lines were challenged with 50 µg/ml of Zymosan for eight, 16 and 24 hours. **(A)** NF-κB activity of RT4 cells was measured using a NF-κB-Luciferase reporter. **(B)** NF-κB activity of VK-2 E6/E7 cells measured using a NF-κB-GFP reporter. N=6, 2 experiments with 3 replicates, *** p<0.001

The NF-κB response of the RT4 cells challenged with 50ug/ml of Zymosan peaked at eight hours with a significant increase of 20.2±2.1 fold over the PBS negative (unchallenged) control (p<0.001, Fig. 6.2.A.). After 16 hours of challenge the response was reduced, 9.1±0.8 fold, but still significantly increased compared to the negative control (p<0.001, Fig. 6.2.A). The NF-κB response remained elevated, 9.6±0.4 fold, at 24 hours (p<0.001). These data indicated that Zymosan was able to induce a NF-κB response in RT4 cells modelling the bladder epithelium.

In VK-2 E6/E7 cells, the first significant response to Zymosan was identified at a later time-point, *i.e.* after 16 hours of challenge, when the NF-κB activity was increased by 3.9±0.4 fold (p<0.001) compared to the negative control (PBS challenge). This response continued for up to 24 hours, with the fold increase measured as 3.2±0.3 (p<0.001, Fig. 6.2.B).

The fold increases detected in RT4 and VK-2 E6/E7 were not directly comparable due to the different reporter systems. However, it can be concluded from the data that Zymosan induced NF-kB reporter activity in both cell lines. A downstream effect of this NF-kB activation was analysed by investigating the secretion of IL-8.

2. ZYMOBAN INDUCES IL-8 SECRETION IN RT4 AND VK-2 E6/E7

To achieve this the media bathing the RT4 and VK-2 E6/E7 cells challenged with either PBS or Zymosan were collected, pooled where appropriate and analysed for IL-8 using a sandwich ELISA. The results are shown in Figure 6.3:

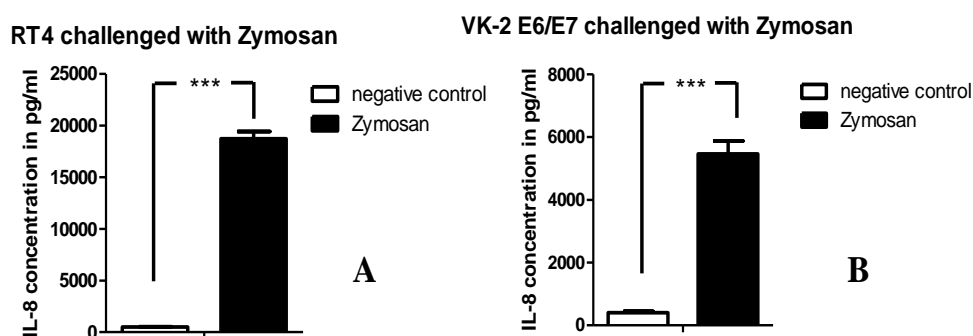


Figure 6.3 IL-8 secretion of urogenital epithelial cell lines when challenged with Zymosan. The secretion was measured using Sandwich ELISA. IL-8 secretion into the pooled medium bathing challenged (A) RT4 uroepithelium and (B) VK-2 E6/E7 vaginal epithelium. N=2, using pooled medium of three replicates. *** p<0.001.

The background concentration of IL-8 in RT4 cells was 503.0 ± 22.5 pg/ml (Fig. 6.3.A), but when the cells were challenged with Zymosan, a significant 37 fold increase ($p < 0.001$), to 18740.7 ± 697.8 pg/ml (Fig. 6.3.A) was observed. In VK-2 E6/E7 cells, the background IL-8 concentration was lower and recorded as 403.9 ± 39.0 pg/ml. Following challenge with Zymosan, a significant ($p < 0.001$), 13.5 fold increase to 5462.5 ± 411.7 pg/ml of IL-8 (Fig. 6.3.B) was observed. Interestingly, the increase in IL-8 concentration in RT4 cells following challenge was three times that of the VK-2 E6/E7 cells.

Summarising, Zymosan challenge of RT4 and VK-2 E6/E7 cells induced NF- κ B activation and increased IL-8 synthesis. As mentioned in Chapter 1, in macrophages and dendritic cells, Zymosan functions through TLR-2/6 and Dectin-1 signalling

mechanisms. TLR-2 expression had been shown previously in RT4 cells, thus the role of TLR-2 in the recognition of Zymosan was investigated¹³⁷.

6.3. INVESTIGATING THE ROLE OF TLR-2 IN THE RECOGNITION OF ZYMOBAN

To achieve this investigations were performed using monoclonal antibodies that blocked TLR-2 signalling. Thus the RT4 containing the NF- κ B luciferase reporter cells were preincubated with a TLR-2 specific monoclonal antibody (10 μ g/ml, Invivogen, USA) before being challenged with Zymosan (50 μ g/ml) for eight hours. The results are shown in Figure 6.4:

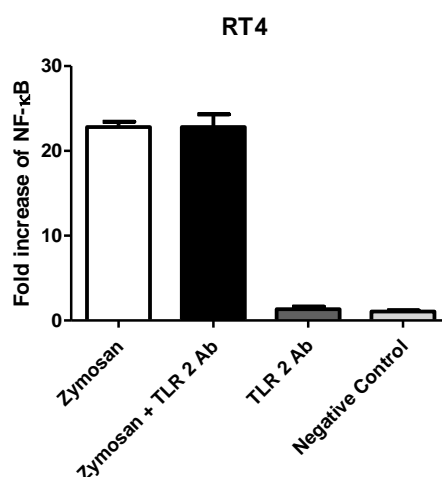


Figure 6.4 NF- κ B activation in RT4 cells challenged with Zymosan after blocking TLR-2. TLR-2 was blocked by preincubating RT4 reporter cells with 10 μ g/ml of monoclonal anti-TLR-2 antibody, before challenging with 50 μ g/ml of Zymosan for eight hours. N=6, 2 experiments with 3 replicates.

Zymosan induced a NF- κ B response of 22.8 ± 0.6 fold. Furthermore, challenging RT4 cells with Zymosan in the presence of TLR-2 blocking antibody induced an equivalent response (Fig. 6.4, 22.8 ± 1.5 fold activation). However, the antibody itself did not induce a NF- κ B response, as the response was comparable to that of PBS control (1.3 ± 0.3 and 1.1 ± 0.1 fold, respectively).

Thus blocking TLR-2 in RT4 cells did not affect NF- κ B activation by Zymosan, suggesting that in bladder cells TLR-2 is not involved in Zymosan recognition.

6.4. DETECTION OF MULTIPLE ISOFORMS OF DECTIN-1 IN RT4 AND VK-2 E6/E7

In macrophages and dendritic cells Dectin-1 also functions as a β -1,3 Glucan receptor. Eight isoforms of Dectin-1 have been identified and these as well as the CLEC7A gene, encoding the Dectin-1 receptor, are shown in Figure 6.5:

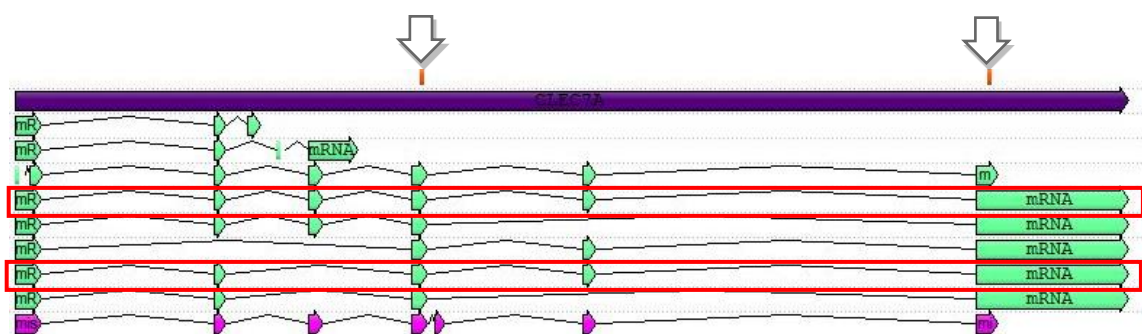
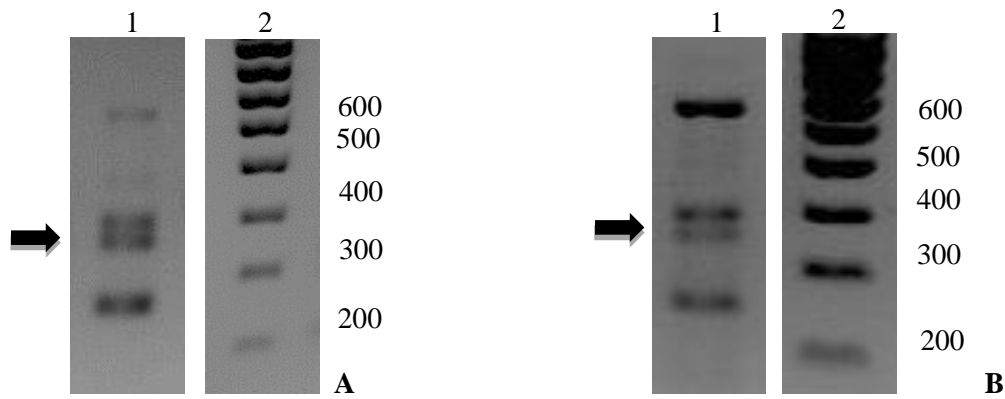


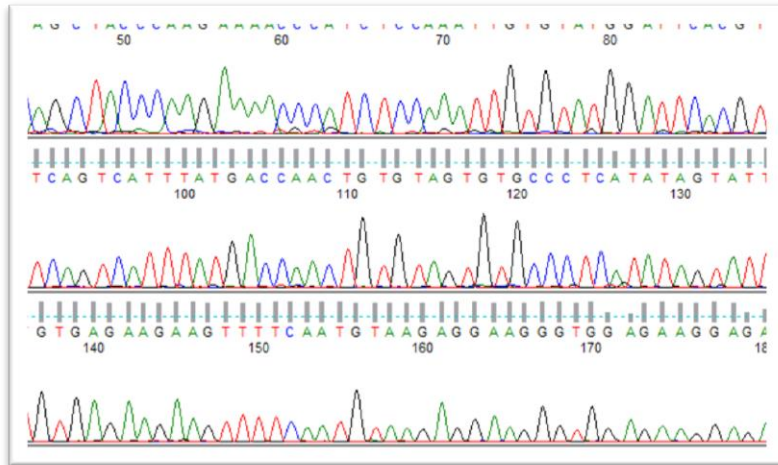
Figure 6.5 The Dectin-1 gene with its different known and predicted isoforms. The primers used for the PCR are in the first line, coloured in orange and marked with white arrows. The CLEC7A gene is shown in the second lane and coloured in purple. The known isoforms are coloured in green and shown in lanes 3 to 10. Isoforms with a functional recognition domain are in the red rectangles. The predicted sequence XR_242899.1 is shown in pink. The diagram was constructed using UGENE software and locus NC_000012.

The expression of CLEC7 was investigated in the urogenital RT4 and VK-2 E6/E7 cell models. To achieve this, mRNA from the cell lines was reverse transcribed and analysed by RT-PCR using specific primers to the Dectin-1 receptor (Table 2.2). The primer pair covered all functional isoforms of Dectin-1 (Figure 6.5, white arrows). The expected product size was 330 bp for the isoforms 1, 2 and 5, and 211 for the isoforms 3 and 4. The results of the RT-PCR are shown in Figure 6.6:

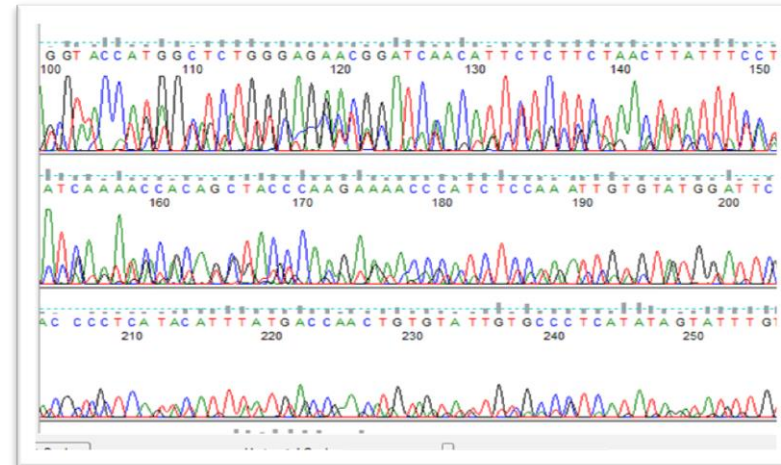


6.6 Expression of Dectin-1 in urogenital epithelial cell lines. First lane shows the amplification using Dectin-1 specific primers. Lane 2 shows the DNA ladder Hyperladder IV. The expression of Dectin-1 was investigated using RT-PCR in **(A)** RT4 bladder cells and in **(B)** VK-2 E6/E7 vaginal cells.

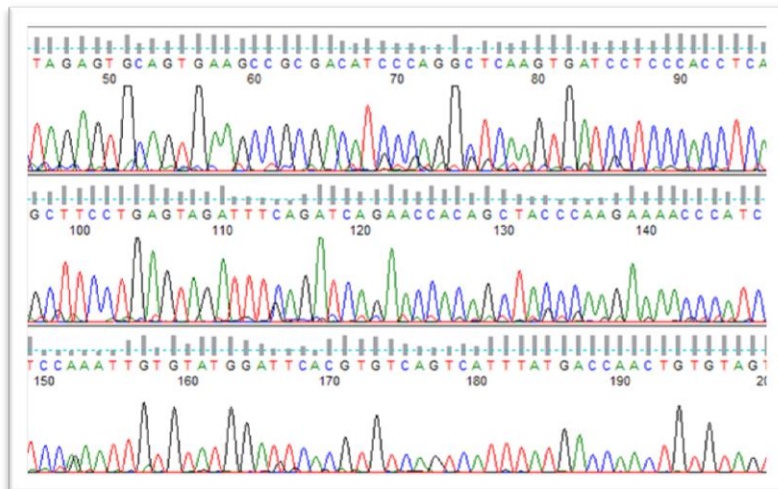
A similar cDNA banding pattern for Dectin-1 expression was observed for each of the two cell lines. Multiple bands were detected and included the expected band of 330 bp (Figure 6.6. bold arrow). Additionally, bands relating to the 211 bp, 417 bp and 580 bp isoforms were observed, supporting the expression of different isoforms. The bands were isolated using a PCR purification kit (section 2.7), identified by DNA sequencing (Genevision, UK) (Figure 6.7 & Appendix) and BLAST analyses was used to identify different isoforms.



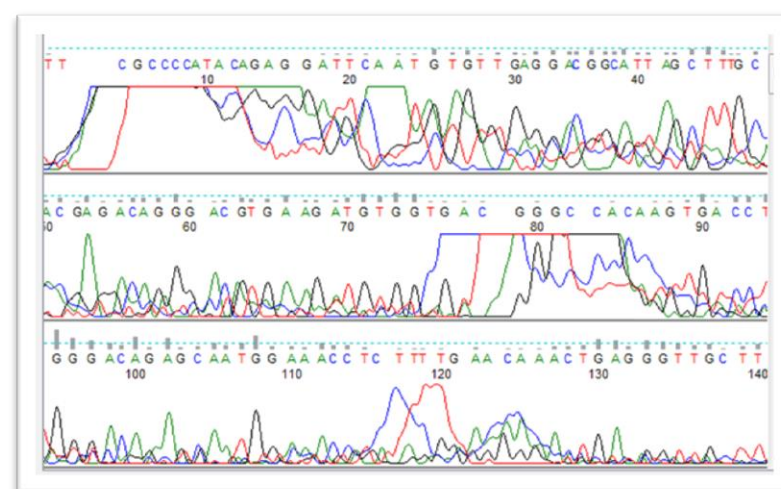
A



B



C



D

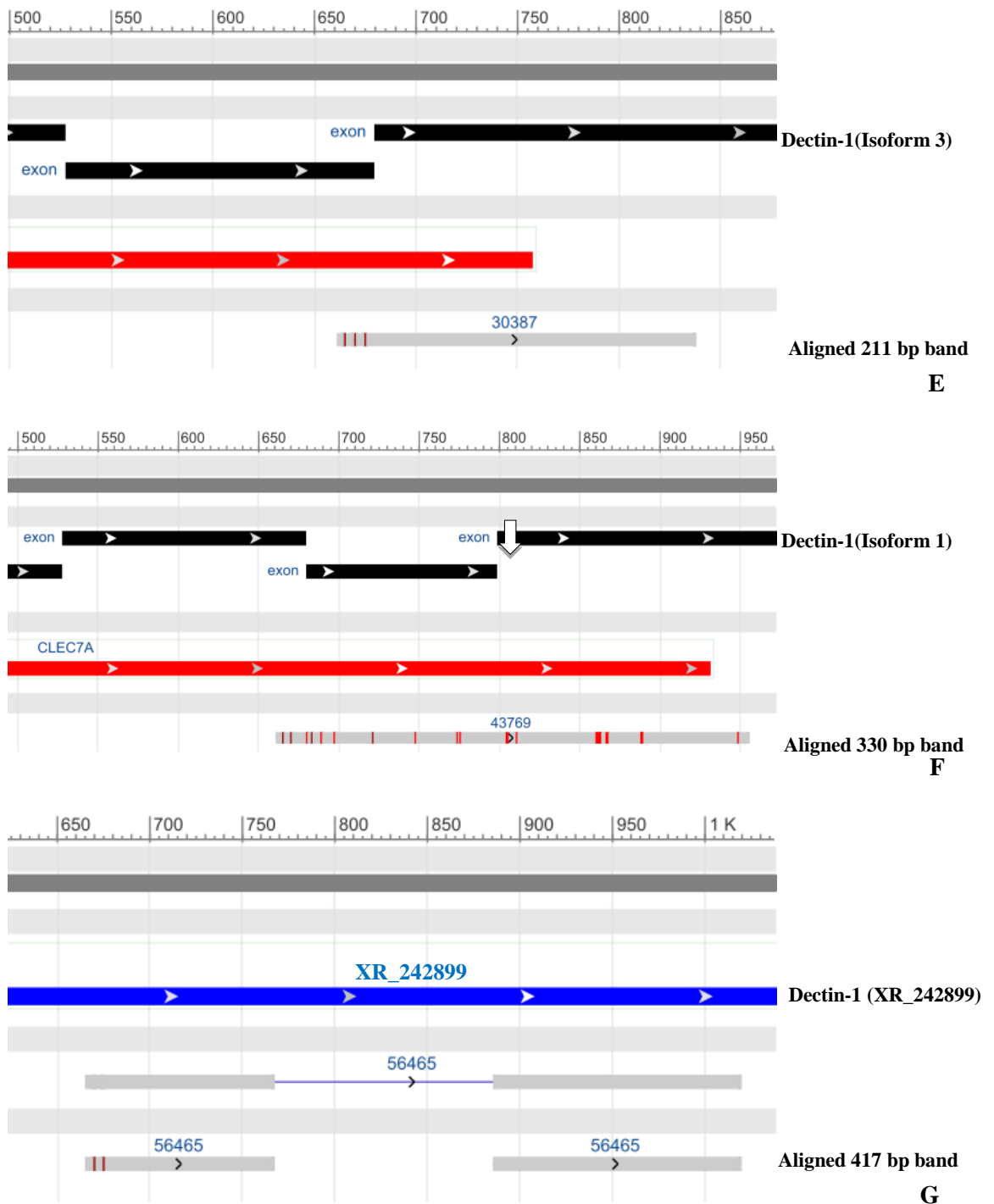


Figure 6.7 Sequencing and BLAST results for the bands from the Dectin-1 PCR, performed using RT4 mRNA. (A) Sequencing result of the 210 bp band of RT4. (B) Sequencing result of the 330 bp product of RT4. (C) Sequencing of the 400 bp band. (D) Sequencing result of the 580 bp band. (E) BLAST alignment of the sequence of the 210 bp band with isoform 3. (F) BLAST alignment of the sequence of the 330 bp band with isoform 1. White arrow highlights exon 5. (G) BLAST alignment of the sequence of the 410 bp band with predicted Dectin-1 isoform XR_242899.

The 211 bp cDNA band related to isoforms 3 or 4 of the CLEC7A gene, which lack exon 5 (Fig. 6.7.E). The 330 bp band related to the isoforms 1, 2 or 5 as it contained a sequence encoding the fifth exon (Fig. 6.7.F). Additionally, the band at 417 bp was

identified as a predicted sequence with the assertion number XR_242899.1 (Fig. 6.7.G). The BLAST search using the sequence of the 580 bp fragment, which, admittedly, was very poor quality (Fig. 6.7D), did not result in any matches to the CLEC7A gene. All findings were confirmed in both cell lines RT4 and VK-2 E6/E7.

These molecular data therefore indicated the expression and synthesis of at least three different isoforms of the Dectin-1 (CLEC7A) gene in RT4 and VK-2 E6/E7 cells.

6.5. DECTIN-1 DETECTION USING FLOW CYTOMETRY

To confirm the synthesis of Dectin-1 protein the cells, and in this study the focus was VK-2 E6/E7 cells, were stained with a monoclonal antibody specific for Dectin-1 (MAB 1859, R & D Biosystem) and analysed by flow cytometry. In addition, to observe any effects of a microbial challenge on Dectin-1 expression the VK-2 E6/E7 cells were challenged with Zymosan, flagellin, motile *E. coli* NCTC 10418 and LPS for 18 hours before Dectin-1 analyses. Fluorescent cell sorting was performed using a FACSCalibur flowcytometer as described in section 2.17. The results of the flow cytometry analyses are shown in Figure 6.8:

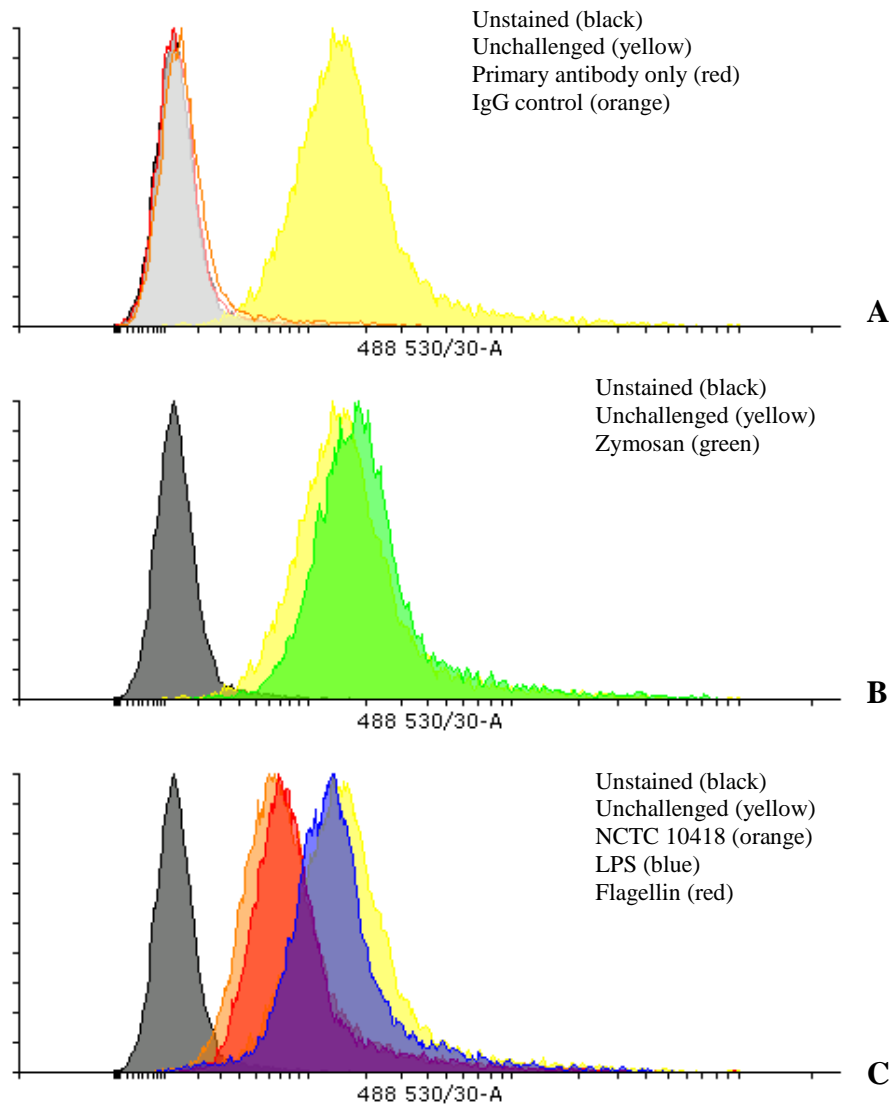


Figure 6.8 Determining the cell surface presence and concentration of Dectin-1 using flow cytometry. VK-2 E6/E7 cells were challenged for 16 hours with PBS, NCTC 10418 [5×10^4 CFU/ml], Flagellin [250ng/ml], Zymosan [50 μ g/ml] or LPS [10 μ g/ml], before being stained for Dectin-1 using a monoclonal anti-Dectin-1 antibody [2.5 μ g/ 10^6 cells] and a secondary antibody labelled with Alexa 488[1/500]. (A) VK-2 E6/E7 cells stained using IgG2b control antibody [2.5 μ g/ 10^6 cells] (orange histogram), unstained (black histogram), only stained with primary antibody (red histogram) or stained with primary and secondary antibody (yellow histogram). (B) VK-2 E6/E7 cells unchallenged (PBS, yellow histogram) or challenged with Zymosan (green histogram). (C) VK-2 E6/E7 challenged with NCTC 10418 (orange histogram) or flagellin (red histogram) or LPS (blue histogram) and stained with primary and secondary antibody. N=1, 10000 events were measured. FACS analyses were performed on a FACSCanto II (BD Biosystems)

The control staining (Fig. 6.8.A) showed that non-specific binding of the antibody was minimal with unstained and IgG stained cells shown as the grey and orange peaks respectively. Dectin-1 stained VK-2 E6/E7 cells are shown by the yellow peak and in fact staining for Dectin-1 with the primary and secondary antibody shifted the fluorescence by 100 fold. Challenging the VK-2 E6/E7 cells with Zymosan for 18 hours

(Fig. 6.8.B, green curve), shifted the Dectin-1 staining peak to the right suggesting a higher number of Dectin-1 receptors on the cell surface. In contrast, challenging VK-2 E6/E7 cells with motile bacteria or flagellin shifted the peak to the left (Fig. 6.8.C, orange and red), suggesting a reduction in the surface concentration of Dectin-1 receptors. LPS also caused a reduction in the cell surface concentration of Dectin-1 receptors (Fig. 6.8.C blue curve), but the effects of LPS were reduced when compared to those observed with the motile bacteria and flagellin.

These data relate to one experiment and indicated Dectin-1 receptors were synthesised by VK-2 E6/E7 cells. Additionally, Zymosan challenge increased the numbers of receptors but in contrast flagellin, motile bacteria and LPS challenge reduced the numbers of receptors. This experiment was repeated twice more and the results are shown in Figure 6.9:

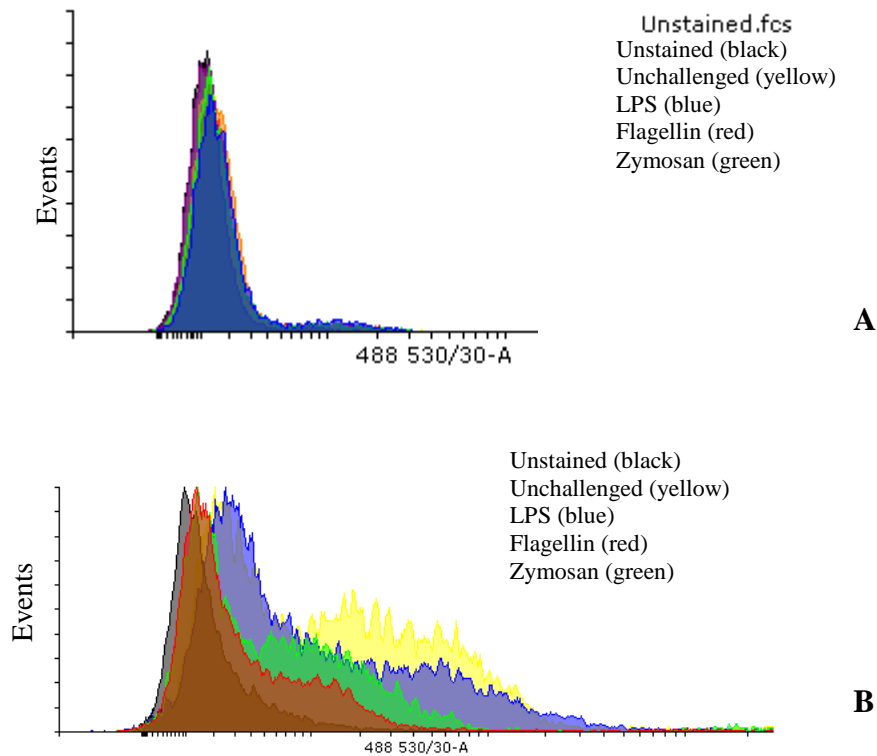


Figure 6.9 Repetition of the cell surface concentration determination of Dectin-1 using flow cytometry. The challenges and stainings were repeated. **(A)** Second repetition of the FACS experiment, VK-2 E6/E7 were not stained (black curve), stained with primary and secondary antibody after challenging with PBS (yellow histogram), Zymosan (green histogram), flagellin (red histogram), LPS (blue histogram). **(B)** Third repetition of the FACS experiment. VK-2 E6/E7 were not stained (black curve), stained with primary and secondary antibody after challenging with PBS (yellow histogram). Zymosan (green histogram), flagellin (red histogram), LPS (blue histogram). 10000 events were measured. FACS analyses were performed on a FACSCanto II (BD Biosystems)

Disappointingly, the distinct peaks supportive of Dectin-1 staining and peak shifts following Zymosan, flagellin and LPS challenge were not reproduced. In Figure 6.9.A, no Dectin-1 staining was observed and in Figure 6.9.B while there was a suggestion of Dectin-1 staining (yellow) and peak shifts (blue and green) the peaks were very broad and thus the data unreliable. Thus the original data shown in Fig. 6.8 could not be reproduced. One explanation for the different results was the loss or destruction of receptors due to the proteolytic activity of the trypsin used to harvest the cells. The flow cytometry results were therefore deemed untrustworthy and a new approach was adopted in which the harvesting of the cells was not necessary.

6.6. DETECTION OF DECTIN-1 IN UROGENITAL CELL LINES USING IMMUNOCYTOCHEMISTRY

Immunocytochemistry was therefore employed to detect Dectin-1 receptors. To achieve this RT4 and VK-2 E6/E7 cells were cultured on cover slips, fixed and stained for Dectin-1 and cell nuclei as described in section 2.18. To ensure that only a limited permeabilisation and hence mainly cell surface epitopes were available, the fixation was performed using paraformaldehyde rather than methanol. The results of the cell staining are shown in Figure 6.10.A and B:

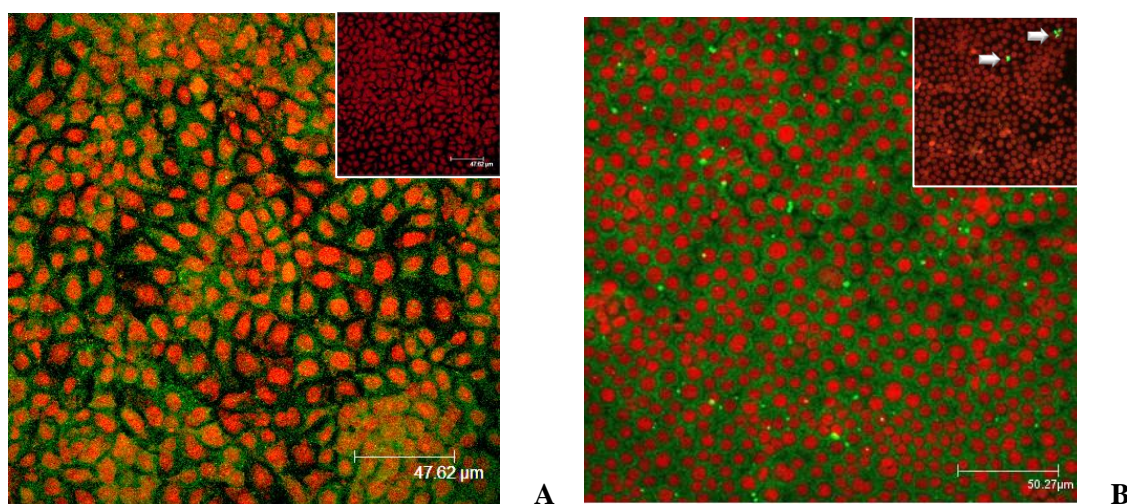


Figure 6.10 Detection of Dectin-1 in the urogenital tract using fluorescent microscopy. RT4 cells were stained using a Dectin-1 specific antibody (A) or using a non-specific IgG control (inlet). VK-2 E6/E7 cells were stained using a Dectin-1 specific antibody (B) or using a non-specific IgG control (inlet). White arrows show non-specific staining. All counter stainings were done using nucleic acid specific PI. Images were taken using Nikon Eclipse Ti and 100 x magnification.

The green staining shown in Figure 6.10.A and B, was indicative of Dectin-1 staining and was supported by the negative IgG control data (Fig. 6.10 inlets). To confirm specificity of the Dectin-1 antibody, the antibody was mixed with an excess of recombinant Dectin-1 for 1h and used to stain the VK-2 E6/E7 cells. Non-absorbed antibody was used as the positive control. Results are shown in Figure 6.11.:

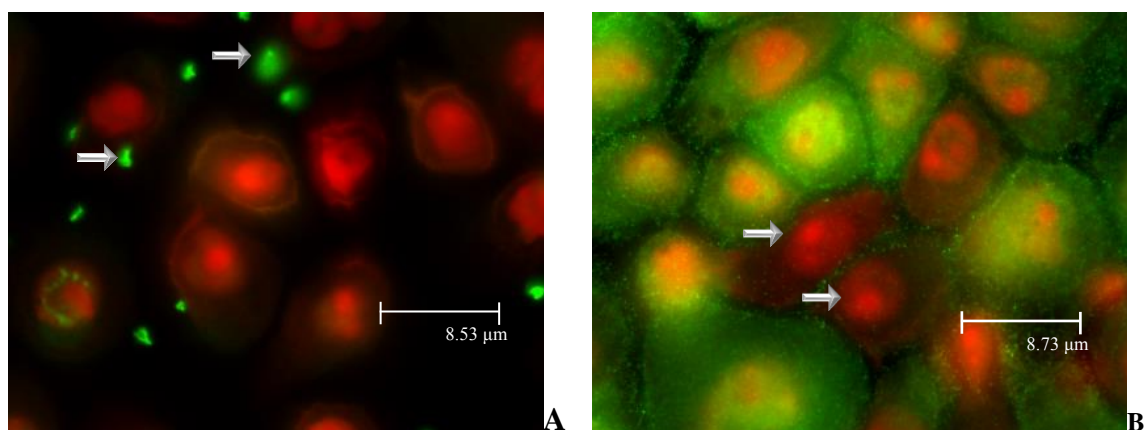


Figure 6.11 Dectin-1 Antibody specificity control using recombinant Dectin-1. (A) The Dectin-1 antibody was preincubated with recombinant Dectin-1 and used to stain VK-2 E6/E7. White arrows highlight fluorescent spots. (B) Positive control using untreated Dectin-1 antibody. White arrows highlight unstained cells. All counterstainings were done using nucleic acid specific PI. Images were taken using Nikon Eclipse Ti and 600 x magnification.

When pre-incubated with recombinant Dectin-1 the antibody did not bind to the cells (Fig. 6.11.A) and only red staining, associated with nuclear staining, was observed. Hence, these results confirmed that the antibody was specific for Dectin-1. The fluorescent spots marked by the white arrows in Fig. 6.11.A did not co-localise with cells and were probably antibody-recombinant Dectin-1 complexes, which were not removed during the wash steps. In contrast, the staining in Figure 6.11.B. which used unabsorbed antibody confirmed the earlier data, showing green fluorescence and indicative of Dectin-1 receptor staining. Interestingly, two cells in Figure 6.11.B marked with white arrows appear not to have stained for Dectin-1.

6.7. LOCALISATION OF DECTIN-1 USING CONFOCAL MICROSCOPY

The cellular localisation of Dectin-1 was further analysed using confocal microscopy. RT4 and VK-2 E6/E7 cells were cultured on cover slips, fixed using paraformaldehyde and stained as described in section 2.18. Confocal images were taken on a Nikon A1R microscope at the Bioimaging Unit (Newcastle University) and the results are shown in Figure 6.12:

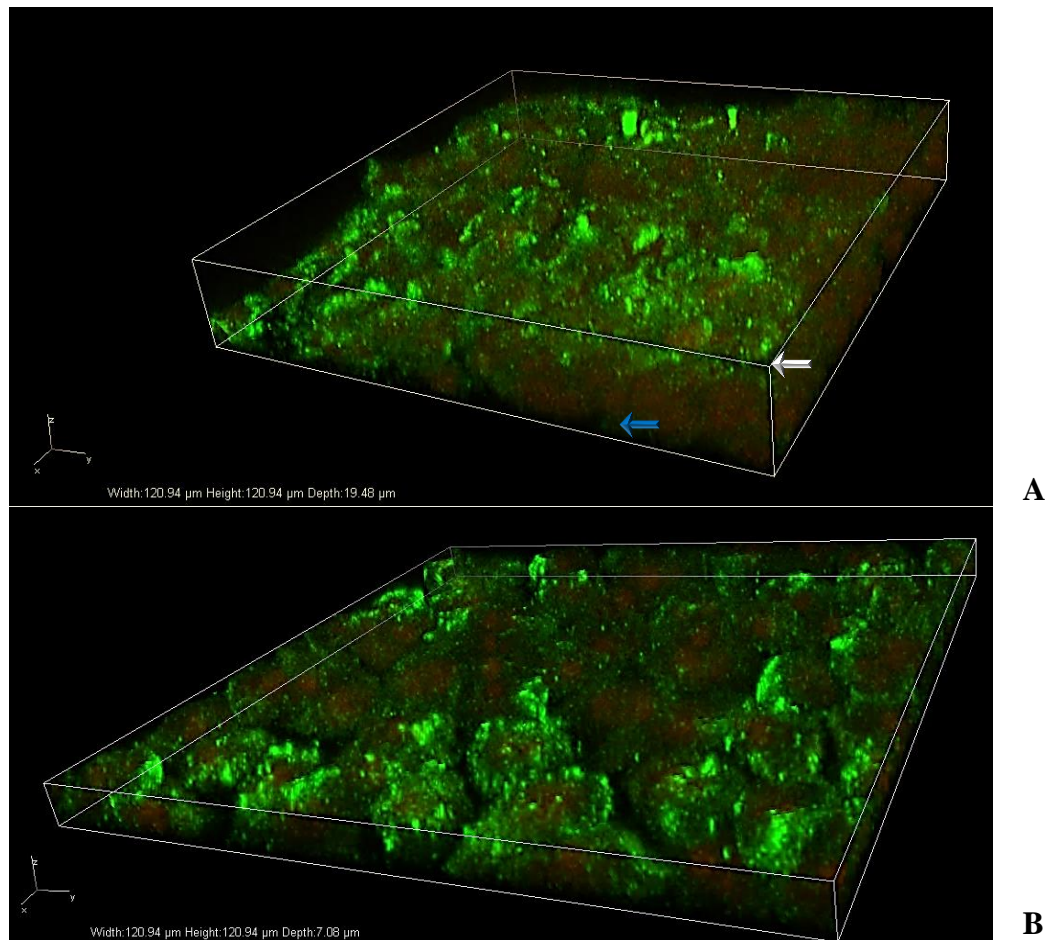


Figure 6.12 Cellular Localisation of Dectin-1 using confocal microscopy. (A) RT4 cells were stained for Dectin-1 (green staining) and for DNA (red) using PI. White arrow indicates the fluorescent staining, X-axis and Y-axis are 120.94 μm long, Z-axis is 19.48 μm long. **(B)** Dectin-1 stained VK-2 E6/E7 cells. Red staining is the nucleus using PI. X-axis and Y-axis are 120.94 μm long, while Z-axis is 7.08 μm long. All images were taken using Nikon A1R microscope and 400 x magnification

Confocal imaging suggested that in RT4 cells, the Dectin-1 staining was stronger on the apical membrane (White arrow, Figure 6.12.A). The staining of the lower basal regions was much fainter (compare area highlighted by white arrow to that of blue arrow, Fig. 6.12.A). These data were suggestive of the receptor in RT4 cells being located apically.

In VK-2 E6/E7 cells, a similar pattern was observed with strong outer membrane staining supportive of Dectin-1 receptors although faint intracellular staining (Fig. 6.12.B) was also identified suggestive of intracellular located receptors or background fluorescence.

Overall the ICC data confirmed the presence of Dectin-1 receptors in RT4 and VK-2 E6/E7 cells supportive of their presence in the urogenital tissues.

6.8. ACTIVATION OF THE DECTIN-1 RECEPTOR IN VAGINAL EPITHELIA

Further *in vitro* investigations relating to Dectin-1 focussed on the VK-2 E6/E7 vaginal cells. The rationale for this decision was that uropathogenic bacteria, in order to colonise the bladder, need to first evade the defences of the vaginal epithelium and thus understanding the vaginal innate defences, and their triggers, may underpin the development of future antimicrobial therapies.

Firstly, Dectin-1 receptor localisation in untreated cells was compared to that in cells challenged with 50 µg/ml of Zymosan for 24 hours. The results are shown in Figure 6.13:

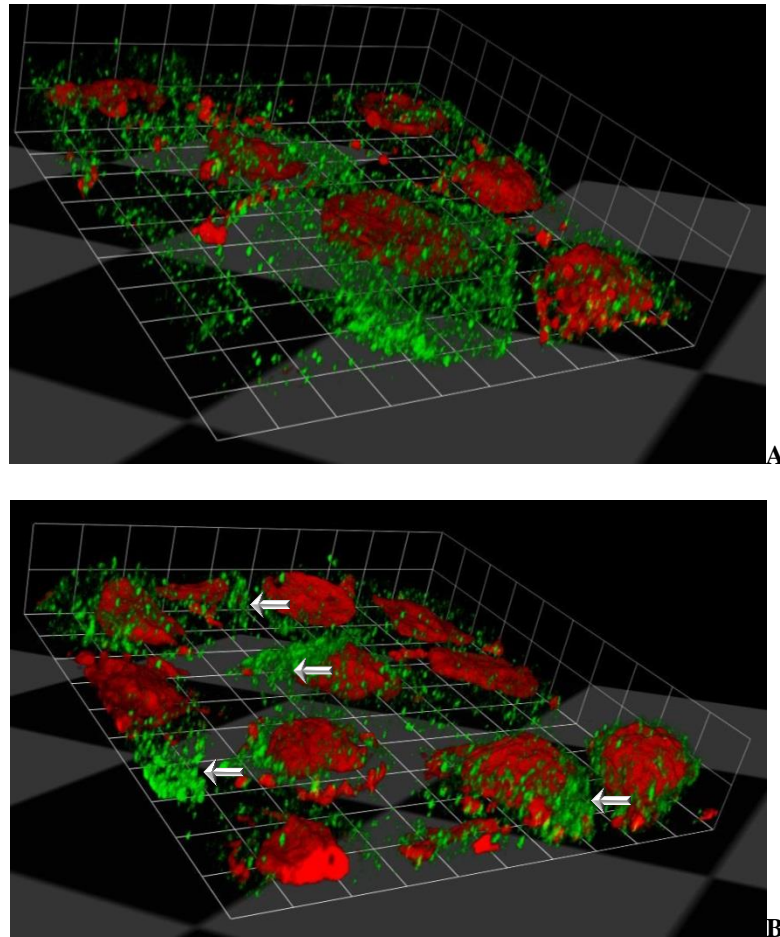


Figure 6.13 Clustering of Dectin-1 in VK-2 E6/E7 when challenged with Zymosan. Cells were challenged with (A) PBS or (B) 50 µg/ml of Zymosan for 24 hours, before being fixed using 4 % paraformaldehyde and stained for Dectin-1. DNA in the nucleus was stained red using Propidium iodine. Images were taken with Leica TCS SP2 microscope and 630x magnification with oil immersion. Squares represent 5 µm.

Confirming previous observations (Figure 6.12.B) the Dectin-1 receptor was localised, randomly, to the outer membrane of the VK-2 E6/E7 cells (Fig. 6.13.A). However, receptor localisation changed dramatically when the cells were challenged with Zymosan with Dectin-1 immuno-staining concentrated in clusters (Fig. 6.13.B and clusters marked with white arrows). Following ligand binding, Dectin-1 receptors form homodimers and homopolymers, which may explain the observed clusters. Homodimer formation is necessary to activate and phosphorylate the adaptor protein SYK⁷⁶, thus the clustering response observed suggested activation of a Dectin-1 responsive signalling response. The presence and phosphorylation of SYK were investigated in the Zymosan challenged VK-2 E6/E7 cells.

6.9. PHOSPHORYLATION OF SYK ADAPTOR PROTEIN

In macrophages, the phosphorylation of SYK occurs within 60 minutes of a Zymosan challenge²⁰⁰. Using this knowledge, VK-2 E6/E7 cells were challenged for 15, 30, 45 minutes, 1.5 and 2.5 hours with Zymosan (50 µg/ml) and western analyses were used to investigate the phosphorylation of SYK (section 2.15). The results of the western blot are shown in Figure 6.14:

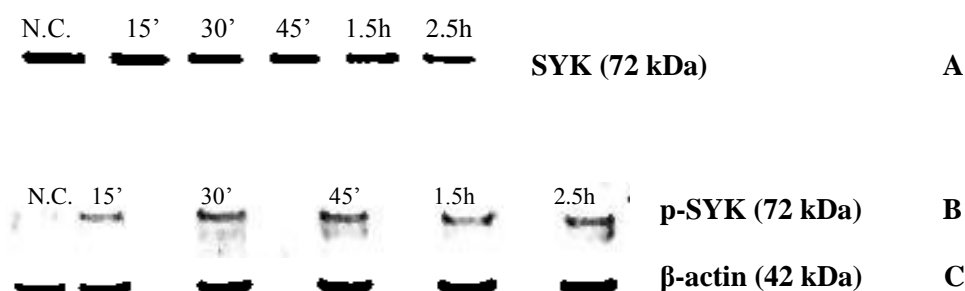


Figure 6.14 Detection of SYK and phosphorylated SYK by Western Blot. (A) Total SYK was measured in VK-2 E6/E7 cells challenged with 50 µg/ml of Zymosan from 15 minutes to 2.5 hours, N.C.= not challenged. (B) Phosphorylated of SYK after challenging VK-2 E6/E7 with Zymosan (C) Protein loading control using β-actin. Western blot performed using Li-Cor Odyssey.

The adaptor protein SYK, with a weight of 72 kDa was detected in all samples (Fig. 6.14.A). The signalling cascade is initiated by the phosphorylation of SYK, therefore, a western blot was performed using an antibody which specifically recognises the phosphorylated form of SYK. As seen in Figure 6.14.B, SYK was not phosphorylated in unchallenged (NC) VK-2 E6/E7 cells. Following challenge with Zymosan, the adaptor molecule was phosphorylated within 15 minutes as shown by a 72 kDa band. The band appeared strongest between 30 to 45 minutes, but these data suggested that phosphorylated material was still present up to 2.5 hours. β-actin showed a band at the expected size of 42 kDa and showed no significant differences in protein loading between the lanes (Fig. 6.14.C).

The presence of Dectin-1 receptor and phosphorylation of SYK in VK-2 E6/E7 cells in response to Zymosan provides strong evidence for a physiological role for this receptor in the defence of vaginal epithelium.

6.10. DECTIN-1 IN PRIMARY VAGINAL EPITHELIA

VK-2 E6/E7 cells represent *in vitro* cell models of the vaginal epithelium; to confirm Dectin-1 expression *in vivo*, vaginal epithelial cells were expanded from vaginal biopsies and analysed by ICC for Dectin-1 immunoreactivity. Vaginal tissue biopsies were obtained under ethical consent from patients undergoing surgery at the Royal Victoria Infirmary, Newcastle upon Tyne (see section 2.2.IV). Epithelium-layers were isolated from the tissue using dispase and trypsin as described in section 2.2.III. Primary cultures were successfully expanded from six donor biopsies. Of these, four were passaged at least three times. Figure 6.15 shows microscopic images of one of the four cell lines:

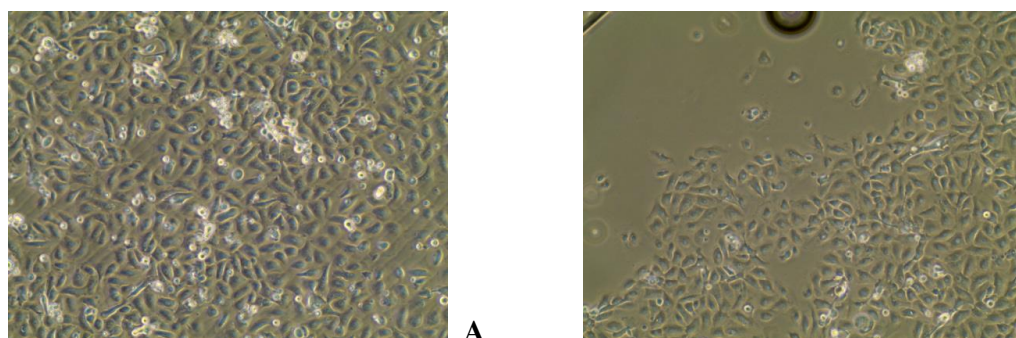


Figure 6.15 Primary vaginal epithelium. (A) Confluent grow of vaginal cells after seeding epithelial layer in a six well-plate. (B) Vaginal cells were grown on cover slips for immunocytochemistry. Images taken using AMG Evos XL Core Microscope and 100x magnification.

Primary epithelial vaginal cells were cultured on 6 well plates, as well as methanol sterilised 10mm diameter glass cover slips (Figure 6.15). Cells attained confluence after two weeks on a six well plate (Figure 6.15.A) and after one week on 10mm diameter cover slips. Primary cells on the cover slips were used for immunocytochemistry.

To prove the epithelial characteristics of the cells they were stained with C11 antibody from Leico Biosystems (Section 2.18). This antibody recognises cytokeratins 4, 5, 6, 8, 10, 13 and 18 and acts as a marker for epithelial cells^{138,201-203}. The result of the cytokeratin staining for four different primary vaginal cell lines is shown in Figure 6.16:

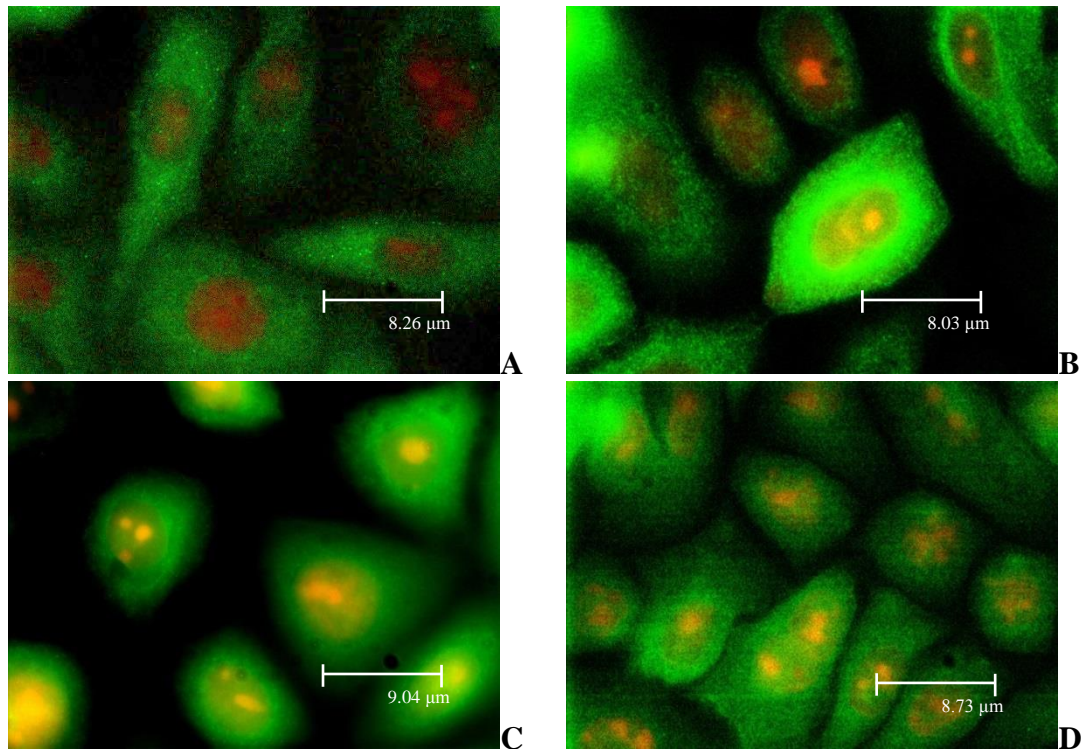


Figure 6.16 Control for epithelial cell marker cytokeratin using C11- antibody. (A-D) Four primary vagina cells were permeabilised according to the manufacturer's instruction and stained using NCL-C11 antibody. Nucleic acid was stained using PI. All images were taken using Nikon Eclipse Ti and 600 x magnification.

All primary cell lines showed a positive staining for cytokeratin as seen by the intense green staining (Fig. 6.16). The staining pattern also supported the presence of only one type of cells, *i.e.* epithelial cells. The negative control data are shown in Figure 6.17; only the nuclei were visible supporting the specificity of the NCL-11 antibody.

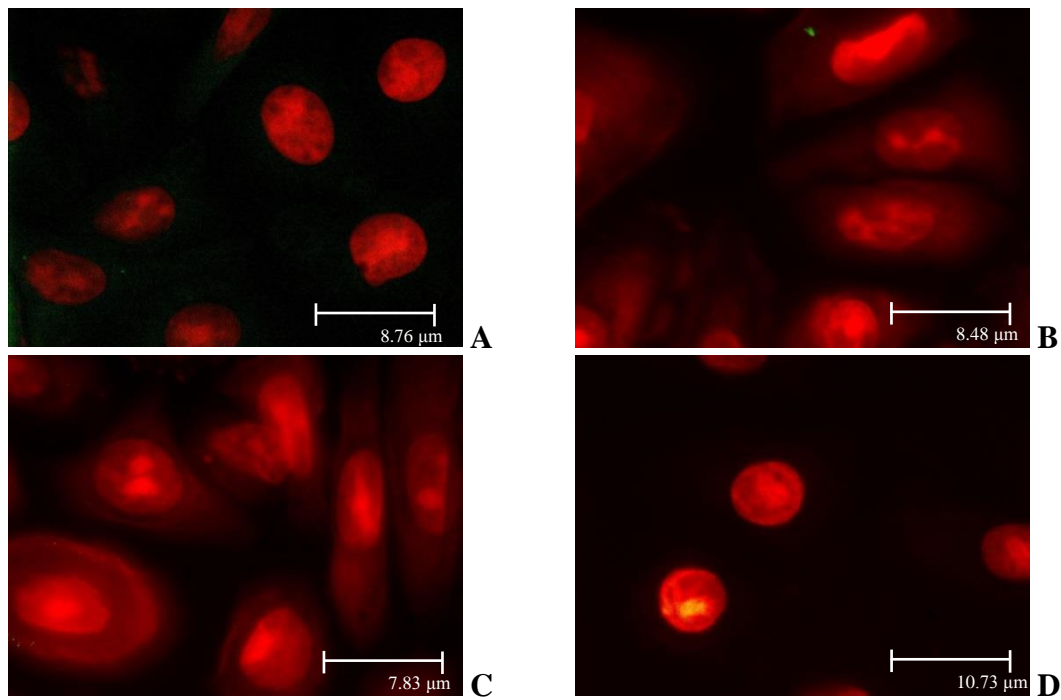


Figure 6.17 Control for unspecific binding in the primary vaginal cultures. Immunostaining was performed using non-specific IgG. Nucleic acid was stained using PI. All images were taken using Nikon Eclipse Ti and 600 x magnification.

Having confirmed the expanded vaginal primary cells as being epithelial, the presence of Dectin-1 was investigated using the Dectin-1 antibody. The results of the immune staining are shown in Figure 6.18:

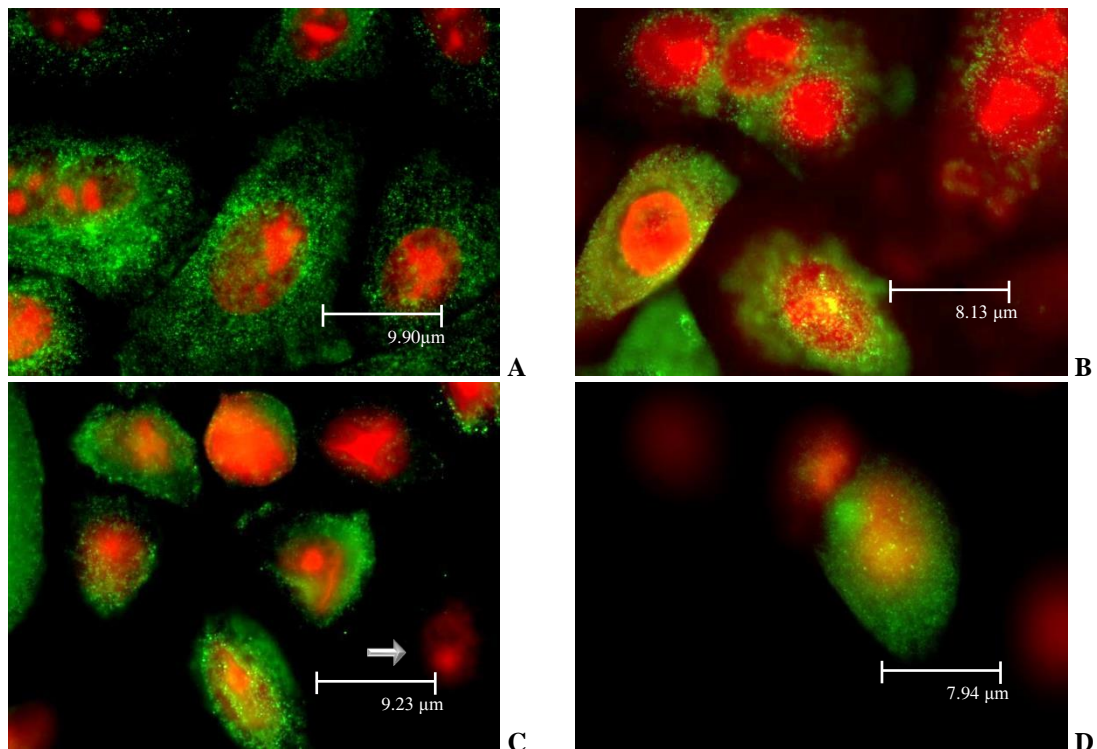


Figure 6.18. Immunostaining of Dectin-1 in Primary Vaginal Epithelia. (A-D) The four primary cell lines were stained for Dectin-1 using immunocytochemistry. Nucleic acid was stained using PI. All images were taken using Nikon Eclipse Ti and 600 x magnification.

Fluorescence confirmed Dectin-1 production in the cells expanded from four different biopsies (Fig. 6.18). Moreover, the Dectin-1 staining was dispersed over each cell and the pattern similar to that observed in the unchallenged VK-2 E6/E7 cells (Fig. 6.18.A-D).

These data confirmed the presence of the Dectin-1 receptor in the urogenital epithelia and *in vitro* experiments using VK-2 E6/E7 cells supported its activation by Zymosan.

6.11. DECTIN-1 ACTIVITY IN THE ABSENCE OF TLR-5

These data thus supported exploitation of the Dectin-1 receptor as a mechanism to boost the innate defences of patients carrying the C1174T TLR-5 SNP. However, interplay between Dectin-1 and TLRs, specifically 2 and 6, has been shown previously¹⁶². To explore any mechanistic links between Dectin-1 and TLR-5 Zymosan challenge experiments were performed in the absence of TLR-5. Essentially, RT4 and VK-2

E6/E7 cells were treated with monoclonal antibody to block TLR-5, simulating the TLR-5 C1174T SNP, challenged with Zymosan and the activation of NF- κ B investigated using NF- κ B reporter assays. The results are shown in Figure 6.19:

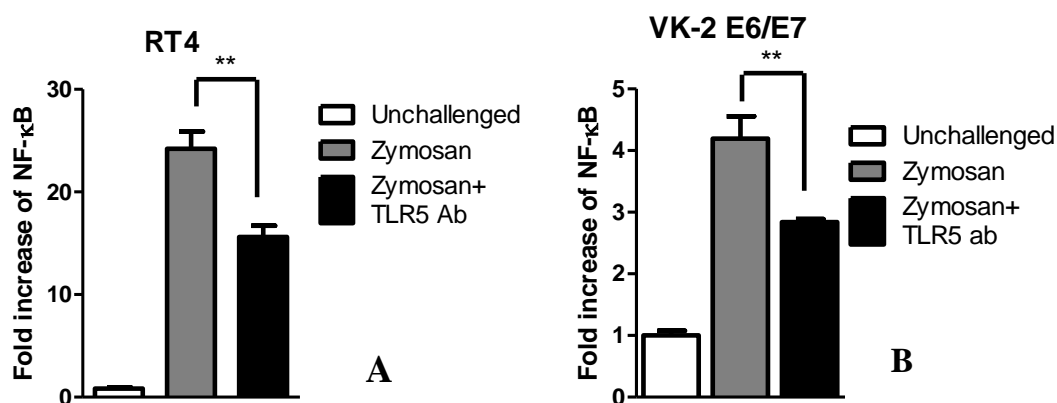


Figure 6.19 Inhibition of Zymosan induced NF- κ B activation by blocking TLR-5. (A) RT4 NF- κ B reporter cells or (B) VK-2 E6/E7 transiently transfected with NF- κ B-GFP reporter were treated with TLR-5 blocking Ab and challenged with Zymosan [50 μ g/ml] in the presence or not of a blocking TLR-5 Ab [10 μ g/ml] (8 hours for RT4 and 16 hours for VK-2 E6/E7). N=6, 2 experiments with 3 replicates each, **p<0.01.

Zymosan induced a 24.2 ± 1.7 fold increase in NF- κ B activity in RT4 when compared to the NF- κ B activity of PBS challenged RT4 (Fig. 6.19.A). The treatment with the TLR-5 blocking antibody resulted in a significant decrease in NF- κ B activation to 15.6 ± 1.1 (Fig. 6.19.A, p<0.01). Similar results were observed in VK-2 E6/E7 (Fig. 6.19B) with Zymosan inducing a 4.2 ± 0.4 fold increase in NF- κ B activity which, following treatment with a TLR-5 blocking antibody, was significantly reduced to 2.8 ± 0.1 , p<0.01). These data suggested a mechanistic relationship between the Dectin-1 and TLR-5 receptors.

6.12. COLOCALISATION OF TLR-5 AND DECTIN-1 USING IMMUNOCYTOCHEMISTRY

To further explore the relationship between TLR-5 and Dectin-1, VK-2 E6/E7 cells were challenged with Zymosan and flagellin and stained for TLR-5 and Dectin-1. The aim was to investigate whether there was colocalisation of the TLR-5 and Dectin-1

receptors following ligand binding. The results of the immunostaining are shown in Figure 6.20:

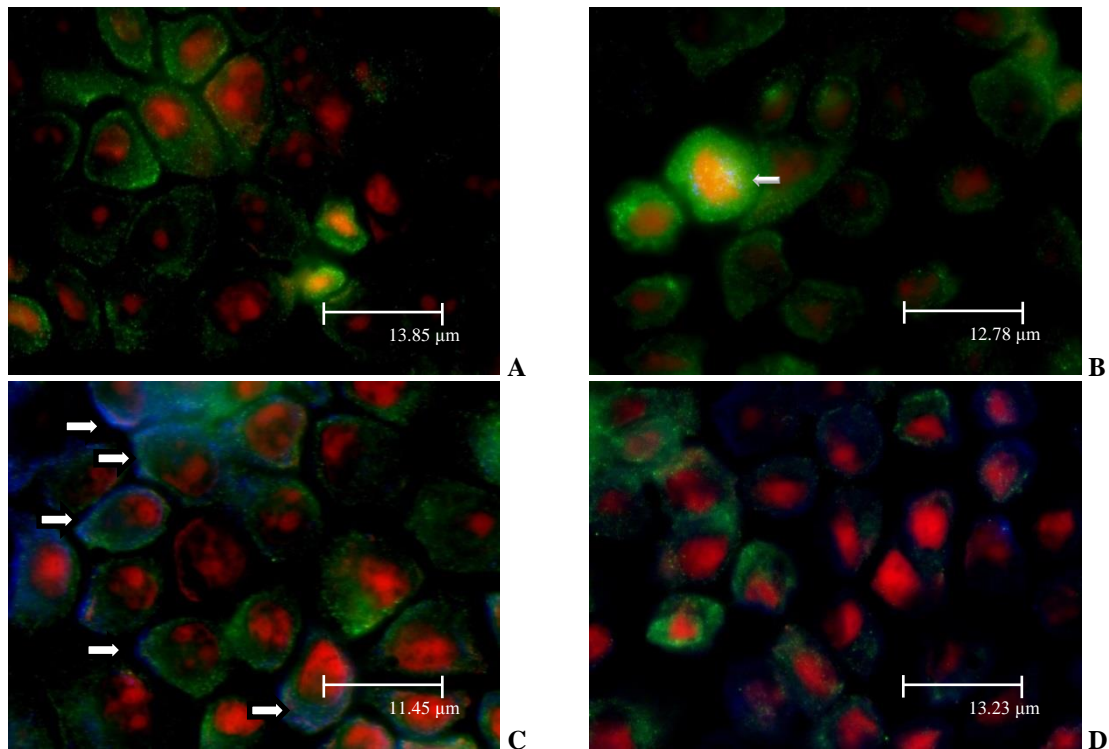


Figure 6.20 Dual immunostaining VK-2 E6/E7 for TLR-5 and Dectin-1. VK-2 E6/E7 cells were stained with anti-TLR-5 antibody [10 $\mu\text{g/ml}$] (recognised by reporter-antibody labelled with Alexa350, blue colour) and Anti-Dectin-1 antibody [10 $\mu\text{g/ml}$] (recognised by reporter-antibody labelled with Alexa480, green colour). (A) Staining of unchallenged cells. (B) VK-2 E6/E7 cells challenged for 16 hours with Zymosan [50 $\mu\text{g/ml}$]. (C) VK-2 E6/E7 cells challenged for 16 hours with flagellin [250 ng/ml]. (D) VK-2 E6/E7 cells challenged for 16 hours with flagellin [250 ng/ml] and Zymosan [50 $\mu\text{g/ml}$]. Images taken using a Leica TCS SP2 microscope and 400 x magnification

Figure 6.20 shows the dual immunostaining data for TLR-5 and Dectin-1 proteins in VK-2 E6/E7 cells. TLR-5 antibody staining was recognised by a secondary detection antibody labelled with alexa350 that stained blue, while the primary Dectin-1 antibody was recognised by a secondary detection antibody linked to alexa480 and stained green. No blue colour was observed following staining of the cells with TLR-5 (6.20.A), indicating either no TLR-5 protein was present on the cells or that the staining had not worked. However, green staining was observed consistent with the presence of the Dectin-1 receptor. Panel B shows the immunostaining after the VK-2 E6/E7 cells were challenged with Zymosan. Again while no staining supporting the presence of TLR-5

receptors was detected, immunostaining supportive of Dectin-1 receptors was evident. The VK-2 E6/E7 cells were also challenged with flagellin and the results are shown in panel C. In this case blue staining as well as green was observed indicative of TLR-5 as well as Dectin-1. Moreover, there was the suggestion of receptor co-localisation (white arrows). Although TLR-5 and Dectin-1 immunostaining were observed in cells challenged with Zymosan and flagellin (Panel D), the staining was poor thus credible analyses of the data was not possible.

6.13. DISCUSSION

This chapter investigated the presence of the Dectin-1 receptor in vaginal and bladder epithelia and its activation by the fungal β -1,3 glucan, known commercially as Zymosan.

Zymosan was shown to induce NF- κ B activity in RT4 and VK-2 E6/E7 cells, which resulted in IL-8 secretion. These data indicated that Zymosan challenge (mimicking a fungal infection) of the urogenital epithelia, induced an innate response, which functioned via a NF- κ B signalling pathway. In 1999 Steele *et al.*, from research using naive mice recognised that in the genital tract, the vaginal epithelial cells were important in defending against fungal, specifically *Candida albicans*, infection²⁰⁴. Two years later, the group using vaginal epithelial cells harvested from women by vaginal lavage showed human cells to inhibit *C. albicans* growth and suggested the functioning of an innate host defence mechanism, although the authors were not able to define the actual mechanisms¹⁹⁹. The data presented in this Chapter together with the findings of section 4.8.I and 4.9.I, in which Zymosan was shown to activate h β D-2 expression and synthesis in RT4 and VK-2 E6/E7 cells, and the results of section 5.7, in which Zymosan induced h β D-3 expression and synthesis, suggest that the mechanism involves

the production of Defensins, and that these antimicrobial molecules play significant roles in protecting the host epithelium against fungal infections.

To further understand the signalling mechanisms, the receptor(s) involved in Zymosan recognition in the urogenital epithelium needed to be identified. Zymosan has been shown to activate the host innate immune response in macrophages and dendritic cells through TLR-2¹⁹⁶, but experiments in RT4 cells in which TLR-2 signalling was blocked did not result in a lowering of the NF- κ B response. Acknowledging that the experiments were not repeated in VK-2 E6/E7 cells these data did suggest that the TLR-2 receptor was either not involved or played a minimal role in Zymosan recognition by urogenital cells. Thus as TLR-2 did not respond to Zymosan an alternative receptor was investigated.

It has been shown in oral epithelial cells that their anti-fungal activity is destroyed by periodic acid treatment, indicating that surface carbohydrates play a role in detecting potential fungal pathogens²⁰⁵. Furthermore it is well established that in macrophages the main receptor for fungal detection is the calcium independent C-type lectin named CLEC7A or Dectin-1⁷³. In 2001, Wilment *et al.*, showed that the Dectin-1 receptor has eight different isoforms of which only six contain the Carbohydrate Recognition Domain (CRD) and that only two of them are able to bind Zymosan and are therefore functional⁷². Molecular analyses of RT4 and VK-2 E6/E7 RNA using primers designed to detect isoforms containing the CRD of the Dectin-1 gene resulted in several bands, and sequencing revealed that at least two known isoforms of Dectin-1 were expressed.

These isoforms related to functional receptors as when the DNA sequences were translated they encoded CRD. These data thus supported the synthesis of functional Dectin-1 receptors in RT4 and VK-2 E6/E7 cells. This was further supported by the NF-

kB and IL-8 responses observed following Zymosan challenge, but additional challenge experiments using antibodies to block Dectin-1 receptor functioning would allow confirmation. The molecular analyses (Fig. 6.6) also identified a third cDNA band that showed significant identity to the predicted sequence XR-242899.1. This suggested the expression of a third isoform containing an additional exon extending the CRD peptide sequence. The actual roles of the different isoforms are not known and such understanding will require further experimental analyses initially using siRNA technology.

The presence of the Dectin-1 receptor protein in RT4 and VK-2 E6/E7 cells was investigated using flow cytometry. Initial data was exciting, indicating the presence of the receptor, receptor induction in response to Zymosan and down-regulation in response to flagellin and motile bacteria (Fig. 6.8). However, the results were not reproducible and this was attributed to harvesting the cells before FACS analyses by trypsinisation. It has been shown previously that trypsin reduces cell surface receptors²⁰⁶, so the technique was considered inappropriate and the data unreliable.

To address these problems the cells were cultured on cover slips and using immunocytochemistry, the presence of the Dectin-1 receptor on the cell surface was confirmed (Figures 6.10 and 6.11). Dectin-1 staining for RT4 showed cell membrane specific staining (Fig. 6.10) comparable to that seen in skin keratinocytes (de Koning *et al.*, Fig. S1)¹⁹⁸. De Koning and colleagues identified the presence of Dectin-1 in keratinocytes and showed the receptors to be upregulated in psoriasis indicating a role in the chronic inflamed skin¹⁹⁸. However, in contrast to the data reported using vaginal and bladder cells, Zymosan failed to induce a cytokine or antimicrobial peptide response¹⁹⁸.

Increasing the magnification supported membrane staining indicating the presence of Dectin-1 receptors on the VK-2 E6/E7 cell surface (Fig. 6.11.B). The localisation of Dectin-1 on the surface of the RT4 and VK-2 E6/E7 cells was further analysed using confocal microscopy. Localisation of the Dectin-1 staining on RT4 was apical, which suggests Dectin-1 expression on the lumen side of the epithelium. Analyses of VK-2 E6/E7 images supported staining throughout the cell layer.

In addition to the analyses of the immortalised cells, primary vaginal epithelia cultures were investigated for Dectin-1 immunostaining. Epithelial cells from four different vaginal biopsies were expanded successfully showing vaginal epithelial morphology comparable to that published previously¹³⁸ and cytokeratin staining consistent with epithelia^{202,207}. These cells also stained positively for Dectin-1, supporting the presence of the receptor *in vivo*. However, immunohistological investigations should also be performed on bladder and vaginal biopsies to confirm these findings.

Immunocytochemical (ICC) analyses of vaginal VK-2 E6/E7 cells was attempted to explore the cellular localisation of Dectin-1 before and after challenging with Zymosan, and the images showed the formation of cluster structures (Fig. 6.13). It has been reported previously that Zymosan induces dimerisation of Dectin-1²⁰⁸. It was feasible therefore that the areas with higher Dectin-1 concentrations comprised Dectin-1 dimers. Receptor clustering and NF- κ B activation provided strong evidence for functional Dectin-1 receptors and functionality was supported by experiments showing phosphorylation of the Dectin-1 adaptor molecule SYK in response to Zymosan. However, a pivotal experiment to confirm Dectin-1 requires the receptor to be blocked and the Zymosan challenges repeated.

Activation of the Zymosan-Dectin-1 signalling pathway resulted in NF- κ B activity, IL-8 and Defensin synthesis. Thus this pathway represents an alternative signaling system to induce Defensin activity that could be exploited therapeutically in women with rUTI and TLR-5 SNP C1174T (R392STOP). However, interaction of TLR-5 with Dectin-1 has been described before, although mainly as a synergistic effect¹⁹⁸. Interestingly my work showed that blocking the TLR-5 receptor reduced the NF- κ B activating capacity of Zymosan in RT4 and in VK-2 E6/E7 cells. A similar observation was reported using murine macrophages, where the absence of MyD88 abolished TNF- α secretion⁷⁶. Together these data indicate a functional relationship between the Dectin-1 and TLR-5 receptors either at level of receptors themselves or via signalling molecules.

To pursue this further co-localisation of the receptors was investigated by ICC following challenge of VK-2 E6/E7 cells with Zymosan. This experiment was performed only once, therefore the data has be interpreted with caution. However, from the immunostaining data there was a suggestion of co-localisation between the Dectin-1 and TLR-5 receptors (6.20.C). This was exciting as it supported the biochemical data where antibody blocking of TLR-5 and challenging with Zymosan resulted in reduced NF- κ B signalling. However, the challenge experiments and ICC analyses need to be repeated before any conclusions can be made. If co-localistion is not confirmed then further experiments exploring the synergistic effects of Dectin-1 and TLR-5 will be focussed at the adaptor molecule level.

In summary, these data showed the synthesis of Dectin-1 in urogenital epithelia and functioning of receptor in response to Zymosan. Although not proven these data also hint of functional interactions between Dectin-1 and TLR-5.

CHAPTER 7

Final Discussion

7.1. LIMITATIONS OF THE INVESTIGATION

In Chapter 4 limitations of a GFP reporter system were shown. The autofluorescence of the RT4 cells inhibited the detection of the fluorescence of the reporter construct. Swenson *et al.* (2007) and others, showed that many tissues have autofluorescence and that GFP should only be used as a reporter for highly expressed genes due to its diverse limitations^{209,210}. The solution was to change the reporter to luciferase as RT4 cells do not contain auto-luminescence. Nonetheless, using the luciferase reporter system had its limitations: the transfection efficiency was normalised across the plates using the positive control and negative control. This however did not measure variances between single wells transfection efficiencies. A solution would be to use second reporter with a stable expression, perform a simultaneous transfection of both reporter constructs (gene of interest and normalisation plasmid), *e.g.* the Dual-Luciferase system (Promega, UK) and normalise the result from each well using the normaliser plasmid, or to stably transfect the RT4 cells with the reporter. The reporter construct used in chapter 3 was stably transfected into the urothelial cell line RT4. Therefore, there was no variance between the wells due to variable transfection efficiency.

The gene expression could alternatively be measured using quantitative PCR and the protein secretion could be measured using ELISA or Western blot. Analyses of transcription factor binding sites could be done using electromobility shift assays.

The TLR-array used in the third chapter of this thesis and the qPCR assay used in Chapter 5 are based on SYBR-green detection of gene expression using predesigned primers. These primers are not publicly available and must therefore verified further using qPCR primers for the specific genes. SYBR green intercalates with double stranded DNA, changing its fluorescent characteristics and can therefore be used for

quantification of DNA. However, the binding of SYBR green to double stranded DNA is nonspecific. The results when using this method have to be analysed carefully, as nonspecific primer dimers or nonspecific amplification of DNA would be reported as false positives. Additional information is necessary in order to validate findings with SYBR green. Analyses of the melting curves give information about the presence of multiple products with different melting temperatures. Additionally, the products of the qPCR could be send to sequencing and the obtained sequence could then be compared to predicted sequence. An alternative for the SYBR green detection method is the Taqman technology: The reporter is directly attached to the primer, ensuring a high specificity and reducing the risk of false positive quantitation of gene expression.

The results in Chapter 3 revealed that flagellin is the main bacterial PAMP recognised by TLR-5. Nonetheless, it is known that TLR-tolerance can be achieved by continuous stimulation of the TLRs^{211,212}. The tolerance of TLR-5 was not investigated and should be part of the future investigations.

7.2. FUTURE WORK AND FINAL HYPOTHESIS

The literature published to date has identified the importance of TLR-4 in the defence of the urinary tract against infection. Overall, however, such research has focussed on using the rodent as the *in vivo* model^{82,213}. Using an *in vitro* cell line of human origin to model the uroepithelium, the research presented in Chapter 3 of this thesis supported TLR-5 rather than TLR-4 as the key host factor in the uroepithelial detection of microbes. TLR-5 functions following activation by flagellin, which is part of the flagella structure and involved in microbial motility. The cytotoxic effect of the PAMP challenges is not known. To address this, the viability of RT4 cells needs to be analysed using a MTT assay while challenging the cells with flagellin, LPS or peptidoglycan.

Additionally, the synergistic effect of the activation of multiple TLRs should be investigated by challenging with a combination of the PAMPs. As mentioned before, experiments using repetitive challenges could address the question of TLR tolerance in the urogenital epithelia.

It was proposed that UPEC strains could avoid detection by the host defences through a reduction in flagellin and hence reduced motility. However, this was not the case, as 12/24 clinical isolates examined were found to be motile and activated NF- κ B signalling, as well as IL-8 synthesis in RT4 bladder cells. However, the signalling responses were reduced compared to those of the motile *E. coli* strain NCTC10418 suggesting bacterial mechanisms functioning to inhibit signalling pathways downstream of NF- κ B. This area is one of further research in the laboratory in collaboration with Dr Philip Aldridge, Newcastle University. Additional clinical isolates of UPEC are being collected, the motility as well as the presence and function of immune inhibitory proteins, e.g. TcpC will be investigated.

Focussing on the host rather than the bacteria, it was evident that the impaired recognition of bacterial motility increased a person's vulnerability to recurrent UTI (rUTI)⁸⁹. Indeed, bacteria isolated from TLR-5 SNP C1174T carriers suffering from rUTIs were able to induce a NF- κ B response in RT4 cells, which was comparable to that of NCTC 10418. These findings suggest that the truncated TLR-5 receptor resulting from the SNP was significant (if not the actual cause) in their susceptibility to UTI. The fact that the isolated bacteria were motile, induced NF- κ B signalling and IL-8 synthesis meant that the use of agents boosting the innate defences of such patients could present an alternative treatment to that of antibiotics. Concerning the bacteria isolated from the urine of TLR-5 SNP patients: A Gram staining revealed only gram negative strains.

Future investigations should identify the bacterial species in the urine using 16S rRNA and fatty acid methyl ester analyses.

With this in mind, research focussed on exploring host defence factors and their potential augmentation *in vitro*. A colleague, Mr Ased Ali, showed that h β D-2 synthesised by the urogenital epithelia was able to kill *E. coli* and thus a key host factor in the UT¹⁵⁷. Hence, a reporter assay containing 2000 bp of h β D-2 5'UTR sequence was engineered to explore potential agents that could boost h β D-2 expression and synthesis. 17 β -oestradiol was found to be a potent inducer of reporter activity in VK-2 E6/E7 cells suggesting that oestrogen plays a role in the genital innate defences. In fact, oestrogen treatment has been used to prevent rUTI in postmenopausal women and analysing nine studies in which oestrogen was used, Perrotta *et al.* (2008), concluded that it is only effective if applied topically to the vagina⁴. The data presented in this thesis provides a mechanism by which oestrogen functions to help protect the UT, *i.e.* enhancing h β D-2 concentrations. Based on these data and that of Mr Ali, a project investigating the roles of oestrogen in the urogenital defences of women including post-menopausal women has been funded and a significant focus of the study is to examine h β D-2 expression in vaginal tissues and peptide concentrations in urine.

Interestingly, resveratrol, chemically related to oestrogen enhanced h β D-2 reporter activity in absence of infection but actually inhibited h β D-2 expression in the presence of flagellin. As discussed in Chapter 4, these data can only be explained if resveratrol induces h β D-2 gene regulation via a mechanism independent of NF-kB. Experiments in which the h β D-2 reporter is transfected into VK-2 E6/E7 cells, NF-kB signalling is inhibited, and the cells are treated with resveratrol will answer this conundrum.

To investigate if differences in the position of transcription factor binding sites of the *DEFB4* gene is due to the different databases used, mutations abrogating the transcription factor binding site will be introduced by site directed mutagenesis. Additionally, the binding sites for the transcription factors AP-1 and retinoic acid receptor (RAR) were found and may be alternatives for the here investigated transcription factors.

As Defensins are potent microbial killing agents, the role of another Defensin, h β D-3, in the defence of the urogenital tract was explored. Human β D-3 was targeted as its expression was detected in bladder biopsies from three different donors and reported in exfoliated uroepithelium¹⁸⁸. The data presented in Chapter 5 shows that h β D-3 expression in the bladder could not be modelled *in vitro* as the RT4 cells did not express the gene either constitutively or in response to infection. Whether this was due to the absence of required co-factors in the growth medium, as argued, requires further investigation. Such investigations will be performed by culturing the RT4 cells in the presence of the growth factors EGF and TGF- α and measuring h β D-3 expression.

VK-2 E6/E7 cells were routinely cultured in the presence of EGF, and h β D-3 expression was detected. Moreover, h β D-3 expression was upregulated in response to infection. Similar to the findings in Chapter 3, the motile strains NCTC 10418 and CFT 073 induced the strongest h β D-3 response. Investigations using TLR ligands, again showed that flagellin induced the highest response, followed by LPS. Peptidoglycan failed to cause a response altogether, but another potential TLR-2 ligand, Zymosan, did induce h β D-3 gene upregulation and increased peptide secretion.

Blocking the TLR-2 receptor and challenging RT4 cells with Zymosan, a β 1,3-glucan found in the fungal cell wall, still activated NF- κ B signalling, suggesting that TLR-2

was not involved in Zymosan recognition. Research in Chapter 6 led to the discovery of the Dectin-1 receptor, an alternative receptor for Zymosan found in macrophages²¹⁴, in both RT4 and VK-2 E6/E7 epithelial cell lines. Moreover, receptor functionality was proven in VK-2 E6/E7 cells by challenging them with Zymosan and observing (i) the activation of NF- κ B and IL-8 secretion, (ii) clustering of the Dectin-1 receptor on the cell surface and (iii) the phosphorylation of its adaptor molecule SYK. Additional experiments to confirm the importance of Dectin-1 in the recognition of Zymosan are (i) challenging VK-2 E6/E7 and RT4 cells, while blocking Dectin-1 with a specific antibody and (ii) inhibiting the expression of Dectin-1 using the siRNA method.

These data were novel and furthermore as Zymosan was shown to enhance h β D-2 and h β D-3 expression *in vitro* it provided the source of a potential therapeutic agent that could be used to treat the TLR-5SNP patients. However, experiments blocking TLR-5 in both RT4 and VK-2 E6/E7 cell lines reduced the NF- κ B response to Zymosan and a pilot experiment using VK-2 E6/E7 cells hinted at co-localisation of the TLR-5 and Dectin-1 receptors challenged with flagellin. These data suggested potential TLR-5/Dectin-1 receptor interactions and future experiments will determine the mechanisms with the focus being on ICC to determine structural relationships and signalling inhibitor experiments to explore shared adaptor molecules. If a structural relationship is proven this would suggest that TLR-5, to date known to function as a homodimer can also function as a heterodimer in the innate defences.

In conclusion, the original hypothesis was confirmed and magnified therefore being:

Host recognition of bacterial motility is pivotal for an innate immune response in the urinary tract and this response can be enhanced by Zymosan, a ligand of the novel urogenital receptor Dectin-1.

References

- 1 NPC/NHS. Urinary tract infection. *MeReC Bulletin* **6**, 1-7 (1995).
- 2 Foxman, B. The epidemiology of urinary tract infection. *Nature reviews. Urology* **7**, 653-660, doi:10.1038/nrurol.2010.190 (2010).
- 3 Rosen, D. A., Hooton, T. M., Stamm, W. E., Humphrey, P. A. & Hultgren, S. J. Detection of intracellular bacterial communities in human urinary tract infection. *PLoS medicine* **4**, e329, doi:10.1371/journal.pmed.0040329 (2007).
- 4 Perrotta, C., Aznar, M., Mejia, R., Albert, X. & Ng, C. W. Oestrogens for preventing recurrent urinary tract infection in postmenopausal women. *Obstetrics and gynecology* **112**, 689-690, doi:10.1097/AOG.0b013e318185f7a5 (2008).
- 5 Bachmann, B. J. Pedigrees of some mutant strains of *Escherichia coli* K-12. *Bacteriological reviews* **36**, 525-557 (1972).
- 6 Raz, R. & Stamm, W. E. A controlled trial of intravaginal estriol in postmenopausal women with recurrent urinary tract infections. *The New England journal of medicine* **329**, 753-756, doi:10.1056/NEJM199309093291102 (1993).
- 7 Huttner, K. M., Brezinski-Caliguri, D. J., Mahoney, M. M. & Diamond, G. Antimicrobial peptide expression is developmentally regulated in the ovine gastrointestinal tract. *The Journal of nutrition* **128**, 297S-299S (1998).
- 8 Czaja, C. A., Scholes, D., Hooton, T. M. & Stamm, W. E. Population-based epidemiologic analysis of acute pyelonephritis. *Clinical infectious diseases : an official publication of the Infectious Diseases Society of America* **45**, 273-280, doi:10.1086/519268 (2007).
- 9 Colgan, R., Williams, M. & Johnson, J. R. Diagnosis and treatment of acute pyelonephritis in women. *American family physician* **84**, 519-526 (2011).
- 10 Grabe, M. *et al.* Guidelines on Urological Infections. *European Association of Urology* (2009).
- 11 Davey, M. S. *et al.* Failure to detect production of IL-10 by activated human neutrophils. *Nature immunology* **12**, 1017-1018; author reply 1018-1020, doi:10.1038/ni.2111 (2011).
- 12 Gallo, R. L. *et al.* Identification of CRAMP, a cathelin-related antimicrobial peptide expressed in the embryonic and adult mouse. *The Journal of biological chemistry* **272**, 13088-13093 (1997).

- 13 Hooton, T. M. *et al.* A prospective study of asymptomatic bacteriuria in sexually active young women. *The New England journal of medicine* **343**, 992-997, doi:10.1056/NEJM200010053431402 (2000).
- 14 AKHTAR, A. J., ANDREWS, G. R., CAIRD, F. I. & FALLON, R. J. URINARY TRACT INFECTION IN THE ELDERLY: A POPULATION STUDY. *Age and Ageing* **1**, 48-54, doi:10.1093/ageing/1.1.48 (1972).
- 15 Hooton, T. M. *et al.* A prospective study of risk factors for symptomatic urinary tract infection in young women. *The New England journal of medicine* **335**, 468-474, doi:10.1056/NEJM199608153350703 (1996).
- 16 Merguerian, P. A., Sverrisson, E. F., Herz, D. B. & McQuiston, L. T. Urinary tract infections in children: recommendations for antibiotic prophylaxis and evaluation. An evidence-based approach. *Current urology reports* **11**, 98-108, doi:10.1007/s11934-010-0095-7 (2010).
- 17 Moore, K. N., Day, R. A. & Albers, M. Pathogenesis of urinary tract infections: a review. *Journal of clinical nursing* **11**, 568-574 (2002).
- 18 Foxman, B. *et al.* Uropathogenic *Escherichia coli* are more likely than commensal *E. coli* to be shared between heterosexual sex partners. *American journal of epidemiology* **156**, 1133-1140 (2002).
- 19 Kaper, J. B., Nataro, J. P. & Mobley, H. L. Pathogenic *Escherichia coli*. *Nature reviews. Microbiology* **2**, 123-140, doi:10.1038/nrmicro818 (2004).
- 20 Lane, M. C., Alteri, C. J., Smith, S. N. & Mobley, H. L. Expression of flagella is coincident with uropathogenic *Escherichia coli* ascension to the upper urinary tract. *Proceedings of the National Academy of Sciences of the United States of America* **104**, 16669-16674, doi:10.1073/pnas.0607898104 (2007).
- 21 Lane, M. C., Simms, A. N. & Mobley, H. L. complex interplay between type 1 fimbrial expression and flagellum-mediated motility of uropathogenic *Escherichia coli*. *Journal of bacteriology* **189**, 5523-5533, doi:10.1128/JB.00434-07 (2007).
- 22 Stamm, W. E. Catheter-associated urinary tract infections: epidemiology, pathogenesis, and prevention. *The American journal of medicine* **91**, 65S-71S (1991).
- 23 Johnson, J. R. Virulence factors in *Escherichia coli* urinary tract infection. *Clinical microbiology reviews* **4**, 80-128 (1991).
- 24 Hultgren, S. J., Schwan, W. R., Schaeffer, A. J. & Duncan, J. L. Regulation of production of type 1 pili among urinary tract isolates of *Escherichia coli*. *Infect Immun* **54**, 613-620 (1986).

- 25 Wiles, T. J., Kulesus, R. R. & Mulvey, M. A. Origins and virulence mechanisms of uropathogenic *Escherichia coli*. *Experimental and molecular pathology* **85**, 11-19, doi:10.1016/j.yexmp.2008.03.007 (2008).
- 26 Garcia, E. C., Brumbaugh, A. R. & Mobley, H. L. Redundancy and specificity of *Escherichia coli* iron acquisition systems during urinary tract infection. *Infect Immun* **79**, 1225-1235, doi:10.1128/IAI.01222-10 (2011).
- 27 Henderson, J. P. *et al.* Quantitative metabolomics reveals an epigenetic blueprint for iron acquisition in uropathogenic *Escherichia coli*. *PLoS pathogens* **5**, e1000305, doi:10.1371/journal.ppat.1000305 (2009).
- 28 Connell, I. *et al.* Type 1 fimbrial expression enhances *Escherichia coli* virulence for the urinary tract. *Proceedings of the National Academy of Sciences of the United States of America* **93**, 9827-9832 (1996).
- 29 Lane, M. C. & Mobley, H. L. Role of P-fimbrial-mediated adherence in pyelonephritis and persistence of uropathogenic *Escherichia coli* (UPEC) in the mammalian kidney. *Kidney international* **72**, 19-25, doi:10.1038/sj.ki.5002230 (2007).
- 30 Wullt, B. *et al.* P fimbriae enhance the early establishment of *Escherichia coli* in the human urinary tract. *Molecular microbiology* **38**, 456-464 (2000).
- 31 Tiba, M. R., Yano, T. & Leite Dda, S. Genotypic characterization of virulence factors in *Escherichia coli* strains from patients with cystitis. *Revista do Instituto de Medicina Tropical de Sao Paulo* **50**, 255-260 (2008).
- 32 Gunther, N. W. t. *et al.* Assessment of virulence of uropathogenic *Escherichia coli* type 1 fimbrial mutants in which the invertible element is phase-locked on or off. *Infect Immun* **70**, 3344-3354 (2002).
- 33 Schilling, J. D., Mulvey, M. A. & Hultgren, S. J. Structure and function of *Escherichia coli* type 1 pili: new insight into the pathogenesis of urinary tract infections. *The Journal of infectious diseases* **183 Suppl 1**, S36-40, doi:10.1086/318855 (2001).
- 34 Thumbikat, P. *et al.* Bacteria-induced uroplakin signaling mediates bladder response to infection. *PLoS pathogens* **5**, e1000415, doi:10.1371/journal.ppat.1000415 (2009).
- 35 Laestadius, A., Richter-Dahlfors, A. & Aperia, A. Dual effects of *Escherichia coli* alpha-hemolysin on rat renal proximal tubule cells. *Kidney international* **62**, 2035-2042, doi:10.1046/j.1523-1755.2002.00661.x (2002).
- 36 Billips, B. K., Schaeffer, A. J. & Klumpp, D. J. Molecular basis of uropathogenic *Escherichia coli* evasion of the innate immune response in the bladder. *Infect Immun* **76**, 3891-3900, doi:10.1128/IAI.00069-08 (2008).

- 37 Cirl, C. *et al.* Subversion of Toll-like receptor signaling by a unique family of bacterial Toll/interleukin-1 receptor domain-containing proteins. *Nature medicine* **14**, 399-406, doi:10.1038/nm1734 (2008).
- 38 Hull, R. A. *et al.* Role of type 1 fimbria- and P fimbria-specific adherence in colonization of the neurogenic human bladder by Escherichia coli. *Infect Immun* **70**, 6481-6484 (2002).
- 39 Kerenyi, M. *et al.* Occurrence of hlyA and sheA genes in extraintestinal Escherichia coli strains. *Journal of clinical microbiology* **43**, 2965-2968, doi:10.1128/JCM.43.6.2965-2968.2005 (2005).
- 40 Marrs, C. F. *et al.* Variations in 10 putative uropathogen virulence genes among urinary, faecal and peri-urethral Escherichia coli. *Journal of medical microbiology* **51**, 138-142 (2002).
- 41 Ferry, S. A., Holm, S. E., Stenlund, H., Lundholm, R. & Monsen, T. J. The natural course of uncomplicated lower urinary tract infection in women illustrated by a randomized placebo controlled study. *Scandinavian journal of infectious diseases* **36**, 296-301 (2004).
- 42 Christmas, T. J. & Bottazzo, G. F. Abnormal urothelial HLA-DR expression in interstitial cystitis. *Clinical and experimental immunology* **87**, 450-454 (1992).
- 43 Thumbikat, P., Waltenbaugh, C., Schaeffer, A. J. & Klumpp, D. J. Antigen-specific responses accelerate bacterial clearance in the bladder. *Journal of immunology* **176**, 3080-3086 (2006).
- 44 Hopkins, W. J., James, L. J., Balish, E. & Uehling, D. T. Congenital immunodeficiencies in mice increase susceptibility to urinary tract infection. *J Urol* **149**, 922-925 (1993).
- 45 Engel, D. *et al.* Tumor necrosis factor alpha- and inducible nitric oxide synthase-producing dendritic cells are rapidly recruited to the bladder in urinary tract infection but are dispensable for bacterial clearance. *Infect Immun* **74**, 6100-6107, doi:10.1128/IAI.00881-06 (2006).
- 46 Engel, D. R. *et al.* CCR2 mediates homeostatic and inflammatory release of Gr1(high) monocytes from the bone marrow, but is dispensable for bladder infiltration in bacterial urinary tract infection. *Journal of immunology* **181**, 5579-5586 (2008).
- 47 Mian, M. F., Lauzon, N. M., Andrews, D. W., Lichty, B. D. & Ashkar, A. A. FimH can directly activate human and murine natural killer cells via TLR4. *Molecular therapy : the journal of the American Society of Gene Therapy* **18**, 1379-1388, doi:10.1038/mt.2010.75 (2010).
- 48 Agace, W. W., Hedges, S. R., Ceska, M. & Svanborg, C. Interleukin-8 and the neutrophil response to mucosal gram-negative infection. *The Journal of clinical investigation* **92**, 780-785, doi:10.1172/JCI116650 (1993).

- 49 Agace, W. W. The role of the epithelial cell in Escherichia coli induced neutrophil migration into the urinary tract. *The European respiratory journal : official journal of the European Society for Clinical Respiratory Physiology* **9**, 1713-1728 (1996).
- 50 Baggiolini, M., Walz, A. & Kunkel, S. L. Neutrophil-activating peptide-1/interleukin 8, a novel cytokine that activates neutrophils. *The Journal of clinical investigation* **84**, 1045-1049, doi:10.1172/JCI114265 (1989).
- 51 Haraoka, M. *et al.* Neutrophil recruitment and resistance to urinary tract infection. *The Journal of infectious diseases* **180**, 1220-1229, doi:10.1086/315006 (1999).
- 52 Mantovani, A., Cassatella, M. A., Costantini, C. & Jaillon, S. Neutrophils in the activation and regulation of innate and adaptive immunity. *Nature reviews. Immunology* **11**, 519-531, doi:10.1038/nri3024 (2011).
- 53 Amulic, B., Cazalet, C., Hayes, G. L., Metzler, K. D. & Zychlinsky, A. Neutrophil function: from mechanisms to disease. *Annual review of immunology* **30**, 459-489, doi:10.1146/annurev-immunol-020711-074942 (2012).
- 54 Tortora, G. J. & Grabowski, S. R. *Principles of anatomy and physiology*. 10th edn, (John Wiley & Sons, 2003).
- 55 Sivick, K. E. & Mobley, H. L. Waging war against uropathogenic Escherichia coli: winning back the urinary tract. *Infect Immun* **78**, 568-585, doi:10.1128/IAI.01000-09 (2010).
- 56 Song, J. & Abraham, S. N. TLR-mediated immune responses in the urinary tract. *Current opinion in microbiology* **11**, 66-73, doi:10.1016/j.mib.2007.12.001 (2008).
- 57 Tanaka, S. T. *et al.* Endodermal Origin of Bladder Trigone Inferred From Mesenchymal-Epithelial Interaction. *The Journal of Urology* **183**, 386-391 (2010).
- 58 Lewis, S. A. Everything you wanted to know about the bladder epithelium but were afraid to ask. *American journal of physiology. Renal physiology* **278**, F867-874 (2000).
- 59 Apodaca, G. The uroepithelium: not just a passive barrier. *Traffic* **5**, 117-128, doi:10.1046/j.1600-0854.2003.00156.x (2004).
- 60 Khandelwal, P., Abraham, S. N. & Apodaca, G. Cell biology and physiology of the uroepithelium. *American journal of physiology. Renal physiology* **297**, F1477-1501, doi:10.1152/ajprenal.00327.2009 (2009).
- 61 Varley, C. L. *et al.* PPARgamma-regulated tight junction development during human urothelial cytodifferentiation. *Journal of cellular physiology* **208**, 407-417, doi:10.1002/jcp.20676 (2006).

- 62 Acharya, P. *et al.* Distribution of the tight junction proteins ZO-1, occludin, and claudin-4, -8, and -12 in bladder epithelium. *American journal of physiology. Renal physiology* **287**, F305-318, doi:10.1152/ajprenal.00341.2003 (2004).
- 63 Akira, S., Uematsu, S. & Takeuchi, O. Pathogen recognition and innate immunity. *Cell* **124**, 783-801, doi:10.1016/j.cell.2006.02.015 (2006).
- 64 Imaizumi, T. *et al.* Upregulation of retinoic acid-inducible gene-I in T24 urinary bladder carcinoma cells stimulated with interferon-gamma. *The Tohoku journal of experimental medicine* **203**, 313-318 (2004).
- 65 Kawai, T. & Akira, S. The role of pattern-recognition receptors in innate immunity: update on Toll-like receptors. *Nature immunology* **11**, 373-384, doi:10.1038/ni.1863 (2010).
- 66 Chamaillard, M. *et al.* An essential role for NOD1 in host recognition of bacterial peptidoglycan containing diaminopimelic acid. *Nature immunology* **4**, 702-707, doi:10.1038/ni945 (2003).
- 67 Inohara, N. *et al.* Host recognition of bacterial muramyl dipeptide mediated through NOD2. Implications for Crohn's disease. *The Journal of biological chemistry* **278**, 5509-5512, doi:10.1074/jbc.C200673200 (2003).
- 68 Huysamen, C. & Brown, G. D. The fungal pattern recognition receptor, Dectin-1, and the associated cluster of C-type lectin-like receptors. *FEMS microbiology letters* **290**, 121-128, doi:10.1111/j.1574-6968.2008.01418.x (2009).
- 69 Shematek, E. M., Braatz, J. A. & Cabib, E. Biosynthesis of the yeast cell wall. I. Preparation and properties of beta-(1 leads to 3)glucan synthetase. *The Journal of biological chemistry* **255**, 888-894 (1980).
- 70 Brown, G. D. Dectin-1: a signalling non-TLR pattern-recognition receptor. *Nature reviews. Immunology* **6**, 33-43, doi:10.1038/nri1745 (2006).
- 71 Willment, J. A. *et al.* Dectin-1 expression and function are enhanced on alternatively activated and GM-CSF-treated macrophages and are negatively regulated by IL-10, dexamethasone, and lipopolysaccharide. *Journal of immunology* **171**, 4569-4573 (2003).
- 72 Willment, J. A., Gordon, S. & Brown, G. D. Characterization of the human beta -glucan receptor and its alternatively spliced isoforms. *The Journal of biological chemistry* **276**, 43818-43823, doi:10.1074/jbc.M107715200 (2001).
- 73 Brown, G. D. *et al.* Dectin-1 is a major beta-glucan receptor on macrophages. *The Journal of experimental medicine* **196**, 407-412 (2002).

- 74 Lee, H. M. *et al.* Innate immune responses to *Mycobacterium ulcerans* via toll-like receptors and dectin-1 in human keratinocytes. *Cellular microbiology* **11**, 678-692, doi:10.1111/j.1462-5822.2009.01285.x (2009).
- 75 Lee, H.-M., Yuk, J.-M., Shin, D.-M. & Jo, E.-K. Dectin-1 is Inducible and Plays an Essential Role for Mycobacteria-Induced Innate Immune Responses in Airway Epithelial Cells. *J Clin Immunol* **29**, 795-805, doi:10.1007/s10875-009-9319-3 (2009).
- 76 Rogers, N. C. *et al.* Syk-dependent cytokine induction by Dectin-1 reveals a novel pattern recognition pathway for C type lectins. *Immunity* **22**, 507-517, doi:10.1016/j.immuni.2005.03.004 (2005).
- 77 Calugaru, A. *et al.* Recognition and modulation of Dectin-1 and TLR-2 receptors by curdlan derivatives and purified natural extracts. *Roumanian archives of microbiology and immunology* **68**, 119-124 (2009).
- 78 Uehara, A., Fujimoto, Y., Fukase, K. & Takada, H. Various human epithelial cells express functional Toll-like receptors, NOD1 and NOD2 to produce anti-microbial peptides, but not proinflammatory cytokines. *Mol Immunol* **44**, 3100-3111, doi:10.1016/j.molimm.2007.02.007 (2007).
- 79 Takeuchi, O. & Akira, S. Pattern recognition receptors and inflammation. *Cell* **140**, 805-820, doi:10.1016/j.cell.2010.01.022 (2010).
- 80 Anderson, K. V., Bokla, L. & Nusslein-Volhard, C. Establishment of dorsal-ventral polarity in the *Drosophila* embryo: the induction of polarity by the Toll gene product. *Cell* **42**, 791-798 (1985).
- 81 Hagberg, L. *et al.* Difference in susceptibility to gram-negative urinary tract infection between C3H/HeJ and C3H/HeN mice. *Infection and Immunity* **46**, 839-844 (1984).
- 82 Ashkar, A. A., Mossman, K. L., Coombes, B. K., Gyles, C. L. & Mackenzie, R. FimH adhesin of type 1 fimbriae is a potent inducer of innate antimicrobial responses which requires TLR4 and type 1 interferon signalling. *PLoS pathogens* **4**, e1000233, doi:10.1371/journal.ppat.1000233 (2008).
- 83 Karoly, E. *et al.* Heat shock protein 72 (HSPA1B) gene polymorphism and Toll-like receptor (TLR) 4 mutation are associated with increased risk of urinary tract infection in children. *Pediatric research* **61**, 371-374, doi:10.1203/pdr.0b013e318030d1f4 (2007).
- 84 Ragnarsdottir, B. *et al.* Reduced toll-like receptor 4 expression in children with asymptomatic bacteriuria. *The Journal of infectious diseases* **196**, 475-484, doi:10.1086/518893 (2007).
- 85 Aronson, M., Medalia, O., Amichay, D. & Nativ, O. Endotoxin-induced shedding of viable uroepithelial cells is an antimicrobial defense mechanism. *Infect Immun* **56**, 1615-1617 (1988).

- 86 Song, J., Bishop, B. L., Li, G., Duncan, M. J. & Abraham, S. N. TLR4-initiated and cAMP-mediated abrogation of bacterial invasion of the bladder. *Cell host & microbe* **1**, 287-298, doi:10.1016/j.chom.2007.05.007 (2007).
- 87 Song, J. & Abraham, S. N. Innate and adaptive immune responses in the urinary tract. *European journal of clinical investigation* **38 Suppl 2**, 21-28, doi:10.1111/j.1365-2362.2008.02005.x (2008).
- 88 Hedlund, M. *et al.* P fimbriae-dependent, lipopolysaccharide-independent activation of epithelial cytokine responses. *Molecular microbiology* **33**, 693-703, doi:10.1046/j.1365-2958.1999.01513.x (1999).
- 89 Hawn, T. R. *et al.* Toll-like receptor polymorphisms and susceptibility to urinary tract infections in adult women. *PLoS One* **4**, e5990, doi:10.1371/journal.pone.0005990 (2009).
- 90 Zhang, D. *et al.* A toll-like receptor that prevents infection by uropathogenic bacteria. *Science* **303**, 1522-1526, doi:10.1126/science.1094351 (2004).
- 91 Ragnarsdottir, B. *et al.* TLR- and CXCR1-dependent innate immunity: insights into the genetics of urinary tract infections. *European journal of clinical investigation* **38 Suppl 2**, 12-20, doi:10.1111/j.1365-2362.2008.02004.x (2008).
- 92 Tabel, Y., Berdeli, A. & Mir, S. Association of TLR2 gene Arg753Gln polymorphism with urinary tract infection in children. *International Journal of Immunogenetics* **34**, 399-405, doi:10.1111/j.1744-313X.2007.00709.x (2007).
- 93 Hawn, T. R. *et al.* Genetic variation of the human urinary tract innate immune response and asymptomatic bacteriuria in women. *PLoS One* **4**, e8300, doi:10.1371/journal.pone.0008300 (2009).
- 94 Aldridge, P. & Hughes, K. T. Regulation of flagellar assembly. *Current opinion in microbiology* **5**, 160-165, doi:10.1016/S1369-5274(02)00302-8 (2002).
- 95 Andersen-Nissen, E. *et al.* Cutting edge: Tlr5^{-/-} mice are more susceptible to Escherichia coli urinary tract infection. *Journal of immunology* **178**, 4717-4720 (2007).
- 96 Kawai, T. & Akira, S. TLR signaling. *Cell death and differentiation* **13**, 816-825, doi:10.1038/sj.cdd.4401850 (2006).
- 97 Ali, A. S., Townes, C. L., Hall, J. & Pickard, R. S. Maintaining a sterile urinary tract: the role of antimicrobial peptides. *J Urol* **182**, 21-28, doi:10.1016/j.juro.2009.02.124 (2009).
- 98 Mendez-Samperio, P. The human cathelicidin hCAP18/LL-37: a multifunctional peptide involved in mycobacterial infections. *Peptides* **31**, 1791-1798, doi:10.1016/j.peptides.2010.06.016 (2010).

- 99 Huttner, K. M., Lambeth, M. R., Burkin, H. R., Burkin, D. J. & Broad, T. E. Localization and genomic organization of sheep antimicrobial peptide genes. *Gene* **206**, 85-91 (1998).
- 100 Chromek, M. *et al.* The antimicrobial peptide cathelicidin protects the urinary tract against invasive bacterial infection. *Nature medicine* **12**, 636-641, doi:10.1038/nm1407 (2006).
- 101 Kai-Larsen, Y. *et al.* Uropathogenic *Escherichia coli* modulates immune responses and its curli fimbriae interact with the antimicrobial peptide LL-37. *PLoS pathogens* **6**, e1001010, doi:10.1371/journal.ppat.1001010 (2010).
- 102 Dhople, V., Krukemeyer, A. & Ramamoorthy, A. The human beta-defensin-3, an antibacterial peptide with multiple biological functions. *Biochimica et biophysica acta* **1758**, 1499-1512, doi:10.1016/j.bbamem.2006.07.007 (2006).
- 103 Chen, H. *et al.* Recent advances in the research and development of human defensins. *Peptides* **27**, 931-940, doi:10.1016/j.peptides.2005.08.018 (2006).
- 104 Schröder, J.-M. & Harder, J. Human beta-defensin-2. *The international journal of biochemistry & cell biology* **31**, 645-651, doi:[http://dx.doi.org/10.1016/S1357-2725\(99\)00013-8](http://dx.doi.org/10.1016/S1357-2725(99)00013-8) (1999).
- 105 Schneider, J. J., Unholzer, A., Schaller, M., Schafer-Korting, M. & Korting, H. C. Human defensins. *J Mol Med (Berl)* **83**, 587-595, doi:10.1007/s00109-005-0657-1 (2005).
- 106 Lehrer, R. I. & Ganz, T. Antimicrobial peptides in mammalian and insect host defence. *Current opinion in immunology* **11**, 23-27 (1999).
- 107 Lehrer, R. I. *et al.* Interaction of human defensins with *Escherichia coli*. Mechanism of bactericidal activity. *The Journal of clinical investigation* **84**, 553-561, doi:10.1172/JCI114198 (1989).
- 108 Morrison, G., Kilanowski, F., Davidson, D. & Dorin, J. Characterization of the mouse beta defensin 1, Defb1, mutant mouse model. *Infect Immun* **70**, 3053-3060 (2002).
- 109 Schroeder, B. O. *et al.* Reduction of disulphide bonds unmasks potent antimicrobial activity of human beta-defensin 1. *Nature* **469**, 419-423, doi:10.1038/nature09674 (2011).
- 110 Niyonsaba, F. *et al.* Antimicrobial peptides human beta-defensins stimulate epidermal keratinocyte migration, proliferation and production of proinflammatory cytokines and chemokines. *J Invest Dermatol* **127**, 594-604, doi:10.1038/sj.jid.5700599 (2007).
- 111 Huang, G. T., Zhang, H. B., Kim, D., Liu, L. & Ganz, T. A model for antimicrobial gene therapy: demonstration of human beta-defensin 2 antimicrobial activities in vivo. *Human gene therapy* **13**, 2017-2025, doi:10.1089/10430340260395875 (2002).

- 112 Joly, S., Maze, C., McCray, P. B. & Guthmiller, J. M. Human α -Defensins 2 and 3 Demonstrate Strain-Selective Activity against Oral Microorganisms. *Journal of clinical microbiology* **42**, 1024-1029, doi:10.1128/jcm.42.3.1024-1029.2004 (2004).
- 113 Bals, R. *et al.* Human beta-defensin 2 is a salt-sensitive peptide antibiotic expressed in human lung. *Journal of Clinical Investigation* **102**, 874 (1998).
- 114 Schroder, J. M. & Harder, J. Antimicrobial skin peptides and proteins. *Cellular and molecular life sciences : CMLS* **63**, 469-486, doi:10.1007/s00018-005-5364-0 (2006).
- 115 Nestle, F. O., Kaplan, D. H. & Barker, J. Psoriasis. *New England Journal of Medicine* **361**, 496-509, doi:doi:10.1056/NEJMra0804595 (2009).
- 116 Semple, F. *et al.* Human β - defensin 3 has immunosuppressive activity in vitro and in vivo. *European journal of immunology* **40**, 1073-1078 (2010).
- 117 Hang, L., Wullt, B., Shen, Z., Karpman, D. & Svanborg, C. Cytokine repertoire of epithelial cells lining the human urinary tract. *J Urol* **159**, 2185-2192 (1998).
- 118 Hedges, S. *et al.* Uroepithelial cells are part of a mucosal cytokine network. *Infect Immun* **62**, 2315-2321 (1994).
- 119 Ingersoll, M. A., Kline, K. A., Nielsen, H. V. & Hultgren, S. J. G-CSF induction early in uropathogenic Escherichia coli infection of the urinary tract modulates host immunity. *Cellular microbiology* **10**, 2568-2578, doi:10.1111/j.1462-5822.2008.01230.x (2008).
- 120 Hedges, S., Anderson, P., Lidin-Janson, G., de Man, P. & Svanborg, C. Interleukin-6 response to deliberate colonization of the human urinary tract with gram-negative bacteria. *Infect Immun* **59**, 421-427 (1991).
- 121 Hedges, S., Svensson, M. & Svanborg, C. Interleukin-6 response of epithelial cell lines to bacterial stimulation in vitro. *Infect Immun* **60**, 1295-1301 (1992).
- 122 Li, K., Sacks, S. H. & Sheerin, N. S. The classical complement pathway plays a critical role in the opsonisation of uropathogenic Escherichia coli. *Mol Immunol* **45**, 954-962, doi:10.1016/j.molimm.2007.07.037 (2008).
- 123 Springall, T. *et al.* Epithelial secretion of C3 promotes colonization of the upper urinary tract by Escherichia coli. *Nature medicine* **7**, 801-806, doi:10.1038/89923 (2001).
- 124 Piatti, G., Mannini, A., Balistreri, M. & Schito, A. M. Virulence factors in urinary Escherichia coli strains: phylogenetic background and quinolone and fluoroquinolone resistance. *Journal of clinical microbiology* **46**, 480-487, doi:10.1128/JCM.01488-07 (2008).

- 125 Snow, V., Mottur-Pilson, C. & Gonzales, R. Principles of appropriate antibiotic use for treatment of nonspecific upper respiratory tract infections in adults. *Annals of internal medicine* **134**, 487-489 (2001).
- 126 Uehling, D. T. & Wolf, L. Enhancement of the bladder defense mechanism by immunization. *Invest Urol* **6**, 520-526 (1969).
- 127 O'Hanley, P., Lalonde, G. & Ji, G. Alpha-hemolysin contributes to the pathogenicity of piliated digalactoside-binding *Escherichia coli* in the kidney: efficacy of an alpha-hemolysin vaccine in preventing renal injury in the BALB/c mouse model of pyelonephritis. *Infect Immun* **59**, 1153-1161 (1991).
- 128 O'Hanley, P., Lark, D., Falkow, S. & Schoolnik, G. Molecular basis of *Escherichia coli* colonization of the upper urinary tract in BALB/c mice. Gal-Gal pili immunization prevents *Escherichia coli* pyelonephritis in the BALB/c mouse model of human pyelonephritis. *The Journal of clinical investigation* **75**, 347-360, doi:10.1172/JCI111707 (1985).
- 129 Sivick, K. E. & Mobley, H. L. An "omics" approach to uropathogenic *Escherichia coli* vaccinology. *Trends in microbiology* **17**, 431-432, doi:10.1016/j.tim.2009.07.003 (2009).
- 130 Russo, T. A. *et al.* The Siderophore receptor IroN of extraintestinal pathogenic *Escherichia coli* is a potential vaccine candidate. *Infect Immun* **71**, 7164-7169 (2003).
- 131 Darouiche, R. O. *et al.* Pilot trial of bacterial interference for preventing urinary tract infection. *Urology* **58**, 339-344, doi:[http://dx.doi.org/10.1016/S0090-4295\(01\)01271-7](http://dx.doi.org/10.1016/S0090-4295(01)01271-7) (2001).
- 132 Roos, V., Ulett, G. C., Schembri, M. A. & Klemm, P. The asymptomatic bacteriuria *Escherichia coli* strain 83972 outcompetes uropathogenic *E. coli* strains in human urine. *Infect Immun* **74**, 615-624, doi:10.1128/iai.74.1.615-624.2006 (2006).
- 133 Ferrières, L., Hancock, V. & Klemm, P. Biofilm exclusion of uropathogenic bacteria by selected asymptomatic bacteriuria *Escherichia coli* strains. *Microbiology* **153**, 1711-1719, doi:10.1099/mic.0.2006/004721-0 (2007).
- 134 Avorn, J. *et al.* Reduction of bacteriuria and pyuria after ingestion of cranberry juice. *JAMA : the journal of the American Medical Association* **271**, 751-754 (1994).
- 135 Howell, A. B. & Foxman, B. Cranberry juice and adhesion of antibiotic-resistant uropathogens. *JAMA : the journal of the American Medical Association* **287**, 3082-3083, doi:10.1001/jama.287.23.3077 (2002).
- 136 Jepson, R. G., Williams, G. & Craig, J. C. Cranberries for preventing urinary tract infections. *The Cochrane database of systematic reviews* **10**, CD001321, doi:10.1002/14651858.CD001321.pub5 (2012).

- 137 Lanz, M. *Innate Host Defence in the Urinary Tract* Master of Research in Medical and Molecular Biosciences thesis, Newcastle University, (2010).
- 138 Fichorova, R. N., Rheinwald, J. G. & Anderson, D. J. Generation of papillomavirus-immortalized cell lines from normal human ectocervical, endocervical, and vaginal epithelium that maintain expression of tissue-specific differentiation proteins. *Biology of reproduction* **57**, 847-855 (1997).
- 139 Mullis, K. *et al.* Specific enzymatic amplification of DNA in vitro: the polymerase chain reaction. *Cold Spring Harbor symposia on quantitative biology* **51 Pt 1**, 263-273 (1986).
- 140 Bioline. *BIOTAQ™ DNA Polymerase*, 2013).
- 141 Takagi, M. *et al.* Characterization of DNA polymerase from *Pyrococcus* sp. strain KOD1 and its application to PCR. *Applied and environmental microbiology* **63**, 4504-4510 (1997).
- 142 Nishioka, M. *et al.* Long and accurate PCR with a mixture of KOD DNA polymerase and its exonuclease deficient mutant enzyme. *Journal of biotechnology* **88**, 141-149 (2001).
- 143 Ye, J. *et al.* Primer-BLAST: a tool to design target-specific primers for polymerase chain reaction. *BMC bioinformatics* **13**, 134, doi:10.1186/1471-2105-13-134 (2012).
- 144 Bustin, S. A. *et al.* The MIQE guidelines: minimum information for publication of quantitative real-time PCR experiments. *Clinical chemistry* **55**, 611-622, doi:10.1373/clinchem.2008.112797 (2009).
- 145 Schagger, H. & von Jagow, G. Tricine-sodium dodecyl sulfate-polyacrylamide gel electrophoresis for the separation of proteins in the range from 1 to 100 kDa. *Analytical biochemistry* **166**, 368-379 (1987).
- 146 Smith, K. D. *et al.* Toll-like receptor 5 recognizes a conserved site on flagellin required for protofilament formation and bacterial motility. *Nature immunology* **4**, 1247-1253, doi:10.1038/ni1011 (2003).
- 147 Welch, R. A. *et al.* Extensive mosaic structure revealed by the complete genome sequence of uropathogenic *Escherichia coli*. *Proceedings of the National Academy of Sciences of the United States of America* **99**, 17020-17024, doi:10.1073/pnas.252529799 (2002).
- 148 Akira, S. & Takeda, K. Toll-like receptor signalling. *Nature reviews. Immunology* **4**, 499-511, doi:10.1038/nri1391 (2004).
- 149 Backhed, F., Soderhall, M., Ekman, P., Normark, S. & Richter-Dahlfors, A. Induction of innate immune responses by *Escherichia coli* and purified lipopolysaccharide correlate with organ- and cell-specific expression of Toll-like receptors within the human urinary tract. *Cellular microbiology* **3**, 153-158 (2001).

- 150 Schilling, J. D. *et al.* CD14- and Toll-Like Receptor-Dependent Activation of Bladder Epithelial Cells by Lipopolysaccharide and Type 1 Piliated Escherichia coli. *Infection and Immunity* **71**, 1470-1480, doi:10.1128/iai.71.3.1470-1480.2003 (2003).
- 151 Nakao, Y. *et al.* Surface-expressed TLR6 participates in the recognition of diacylated lipopeptide and peptidoglycan in human cells. *Journal of immunology* **174**, 1566-1573 (2005).
- 152 Girardin, S. E. *et al.* Nod1 detects a unique muropeptide from gram-negative bacterial peptidoglycan. *Science* **300**, 1584-1587, doi:10.1126/science.1084677 (2003).
- 153 Dziarski, R. & Gupta, D. Peptidoglycan recognition in innate immunity. *Journal of endotoxin research* **11**, 304-310, doi:10.1179/096805105X67256 (2005).
- 154 Hawn, T. R. *et al.* A common dominant TLR5 stop codon polymorphism abolishes flagellin signaling and is associated with susceptibility to legionnaires' disease. *The Journal of experimental medicine* **198**, 1563-1572, doi:10.1084/jem.20031220 (2003).
- 155 Sharma, S. A., Tummuru, M. K. R., Blaser, M. J. & Kerr, L. D. Activation of IL-8 Gene Expression by Helicobacter pylori Is Regulated by Transcription Factor Nuclear Factor- κ B in Gastric Epithelial Cells. *The Journal of Immunology* **160**, 2401-2407 (1998).
- 156 Smith, N. J. *et al.* Toll-like receptor responses of normal human urothelial cells to bacterial flagellin and lipopolysaccharide. *J Urol* **186**, 1084-1092, doi:10.1016/j.juro.2011.04.112 (2011).
- 157 Ali, A. S. M. *Are Beta Defensin 1 and Beta Defensin 2 Key Innate Immune Effector Peptides against Urinary Tract Infections in Women* PhD thesis, Newcastle University, (2013).
- 158 Ali, A. S. M., Lanz, M., Townes, C.L., Varley, C.L., Suarez M-Falero, B., Robson, W.A., Southgate, J., Hall, J.2, Pickard, R.S. in *European Association of Urology Annual Meeting* (Paris France, 2012).
- 159 Ali ASM, L. M., Townes CL, Varley C, Suarez M-Falero B, Robson WA, Southgate J, Brown K, Hilton P, Hall J, Pickard RS. Reduced innate beta-defensin-2 response in the bladder and vaginal epithelia increases susceptibility to flagellated E. coli infection. *BJU international* **109** (2012).
- 160 Messeguer, X. *et al.* PROMO: detection of known transcription regulatory elements using species-tailored searches. *Bioinformatics* **18**, 333-334 (2002).
- 161 Harder, J. *et al.* Mucoïd Pseudomonas aeruginosa, TNF-alpha, and IL-1beta, but not IL-6, induce human beta-defensin-2 in respiratory epithelia. *American journal of respiratory cell and molecular biology* **22**, 714-721, doi:10.1165/ajrcmb.22.6.4023 (2000).

- 162 Dennehy, K. M. *et al.* Syk kinase is required for collaborative cytokine production induced through Dectin-1 and Toll-like receptors. *European journal of immunology* **38**, 500-506, doi:10.1002/eji.200737741 (2008).
- 163 Nadkarni, S. & McArthur, S. Oestrogen and immunomodulation: new mechanisms that impact on peripheral and central immunity. *Current Opinion in Pharmacology*, doi:<http://dx.doi.org/10.1016/j.coph.2013.05.007>.
- 164 Goldberg, D. M. *et al.* A Global Survey of Trans-Resveratrol Concentrations in Commercial Wines. *American journal of enology and viticulture* **46**, 159-165 (1995).
- 165 Gusman, J., Malonne, H. & Atassi, G. A reappraisal of the potential chemopreventive and chemotherapeutic properties of resveratrol. *Carcinogenesis* **22**, 1111-1117, doi:10.1093/carcin/22.8.1111 (2001).
- 166 Singh, P. K. *et al.* Production of beta-defensins by human airway epithelia. *Proceedings of the National Academy of Sciences of the United States of America* **95**, 14961-14966 (1998).
- 167 Vora, P. *et al.* β -Defensin-2 Expression Is Regulated by TLR Signaling in Intestinal Epithelial Cells. *The Journal of Immunology* **173**, 5398-5405 (2004).
- 168 Wada, A. *et al.* Helicobacter pylori-mediated transcriptional regulation of the human beta-defensin 2 gene requires NF-kappaB. *Cellular microbiology* **3**, 115-123 (2001).
- 169 Wang, X. *et al.* Airway epithelia regulate expression of human beta-defensin 2 through Toll-like receptor 2. *FASEB journal : official publication of the Federation of American Societies for Experimental Biology* **17**, 1727-1729, doi:10.1096/fj.02-0616fje (2003).
- 170 AF071216 Database information on the EMBL-Bank website, <<http://www.ebi.ac.uk/Tools/dbfetch/expasyfetch?AF071216>> (Last accessed 16.09.2013).
- 171 Wang, T.-T. *et al.* Cutting Edge: 1,25-Dihydroxyvitamin D3 Is a Direct Inducer of Antimicrobial Peptide Gene Expression. *The Journal of Immunology* **173**, 2909-2912 (2004).
- 172 Stocco, B. *et al.* Dose-dependent effect of resveratrol on bladder cancer cells: chemoprevention and oxidative stress. *Maturitas* **72**, 72-78, doi:10.1016/j.maturitas.2012.02.004 (2012).
- 173 Bai, Y. *et al.* Resveratrol induces apoptosis and cell cycle arrest of human T24 bladder cancer cells in vitro and inhibits tumor growth in vivo. *Cancer science* **101**, 488-493, doi:10.1111/j.1349-7006.2009.01415.x (2010).
- 174 Pipari, A. W., Jr. *et al.* Resveratrol-induced autophagocytosis in ovarian cancer cells. *Cancer research* **64**, 696-703 (2004).

- 175 Scarlatti, F., Maffei, R., Beau, I., Codogno, P. & Ghidoni, R. Role of non-canonical Beclin 1-independent autophagy in cell death induced by resveratrol in human breast cancer cells. *Cell death and differentiation* **15**, 1318-1329, doi:10.1038/cdd.2008.51 (2008).
- 176 Ravagnan, G. *et al.* Polydatin, a natural precursor of resveratrol, induces beta-defensin production and reduces inflammatory response. *Inflammation* **36**, 26-34, doi:10.1007/s10753-012-9516-8 (2013).
- 177 Cianciulli, A. *et al.* Modulation of NF- κ B activation by resveratrol in LPS treated human intestinal cells results in downregulation of PGE2 production and COX-2 expression. *Toxicology in Vitro* **26**, 1122-1128, doi:<http://dx.doi.org/10.1016/j.tiv.2012.06.015> (2012).
- 178 Pivarcsi, A. *et al.* Microbial compounds induce the expression of pro-inflammatory cytokines, chemokines and human beta-defensin-2 in vaginal epithelial cells. *Microbes and infection / Institut Pasteur* **7**, 1117-1127, doi:10.1016/j.micinf.2005.03.016 (2005).
- 179 Hertting, O. *et al.* Vitamin D induction of the human antimicrobial Peptide cathelicidin in the urinary bladder. *PLoS One* **5**, e15580, doi:10.1371/journal.pone.0015580 (2010).
- 180 Harder, J., Bartels, J., Christophers, E. & Schroder, J. M. Isolation and characterization of human beta -defensin-3, a novel human inducible peptide antibiotic. *The Journal of biological chemistry* **276**, 5707-5713, doi:10.1074/jbc.M008557200 (2001).
- 181 Ommori, R. *et al.* Selective induction of antimicrobial peptides from keratinocytes by staphylococcal bacteria. *Microb Pathog* **56**, 35-39, doi:10.1016/j.micpath.2012.11.005 (2013).
- 182 Buhimschi, I. A. *et al.* The novel antimicrobial peptide beta3-defensin is produced by the amnion: a possible role of the fetal membranes in innate immunity of the amniotic cavity. *American journal of obstetrics and gynecology* **191**, 1678-1687, doi:10.1016/j.ajog.2004.03.081 (2004).
- 183 Dieffenbach, C. W. & Dveksler, G. S. *PCR primer : a laboratory manual*. 2nd ed. edn, 194-197 (Cold Spring Harbor Laboratory Press ; [Oxford : Lavis Marketing distributor], 2003).
- 184 Kalus, A. A. *et al.* Association of a genetic polymorphism (-44 C/G SNP) in the human DEFB1 gene with expression and inducibility of multiple beta-defensins in gingival keratinocytes. *BMC oral health* **9**, 21, doi:10.1186/1472-6831-9-21 (2009).
- 185 Pfaffl, M. W. A new mathematical model for relative quantification in real-time RT-PCR. *Nucleic acids research* **29**, e45 (2001).
- 186 Scharf, S. *et al.* Legionella pneumophila induces human beta defensin-3 in pulmonary cells. *Respiratory research* **11**, 93, doi:10.1186/1465-9921-11-93 (2010).

- 187 Tomita, T. *et al.* Effect of ions on antibacterial activity of human beta defensin 2. *Microbiol Immunol* **44**, 749-754 (2000).
- 188 Luthje, P. *et al.* Estrogen supports urothelial defense mechanisms. *Science translational medicine* **5**, 190ra180, doi:10.1126/scitranslmed.3005574 (2013).
- 189 Sorensen, O. E. *et al.* Differential regulation of beta-defensin expression in human skin by microbial stimuli. *Journal of immunology* **174**, 4870-4879 (2005).
- 190 MacGregor Schafer, J. *et al.* Estrogen receptor alpha mediated induction of the transforming growth factor alpha gene by estradiol and 4-hydroxytamoxifen in MDA-MB-231 breast cancer cells. *J Steroid Biochem Mol Biol* **78**, 41-50 (2001).
- 191 Mitchell, C., Gottsch, M. L., Liu, C., Fredricks, D. N. & Nelson, D. B. Associations between vaginal bacteria and levels of vaginal defensins in pregnant women. *American journal of obstetrics and gynecology* **208**, 132.e131-132.e137, doi:<http://dx.doi.org/10.1016/j.ajog.2012.11.019> (2013).
- 192 Steubesand, N. *et al.* The expression of the beta-defensins hBD-2 and hBD-3 is differentially regulated by NF-kappaB and MAPK/AP-1 pathways in an in vitro model of *Candida* esophagitis. *BMC Immunol* **10**, 36, doi:10.1186/1471-2172-10-36 (2009).
- 193 Dusio, G. F. *et al.* Stimulation of TLRs by LMW-HA induces self-defense mechanisms in vaginal epithelium. *Immunology and cell biology* **89**, 630-639, doi:10.1038/icb.2010.140 (2011).
- 194 Shuyi, Y. *et al.* Human beta-defensin-3 (hBD-3) upregulated by LPS via epidermal growth factor receptor (EGFR) signaling pathways to enhance lymphatic invasion of oral squamous cell carcinoma. *Oral Surg Oral Med Oral Pathol Oral Radiol Endod* **112**, 616-625, doi:10.1016/j.tripleo.2011.02.053 (2011).
- 195 Schwandner, R., Dziarski, R., Wesche, H., Rothe, M. & Kirschning, C. J. Peptidoglycan- and lipoteichoic acid-induced cell activation is mediated by toll-like receptor 2. *The Journal of biological chemistry* **274**, 17406-17409 (1999).
- 196 Gantner, B. N., Simmons, R. M., Canavera, S. J., Akira, S. & Underhill, D. M. Collaborative induction of inflammatory responses by dectin-1 and Toll-like receptor 2. *The Journal of experimental medicine* **197**, 1107-1117, doi:10.1084/jem.20021787 (2003).
- 197 Palma, A. S. *et al.* Ligands for the beta-glucan receptor, Dectin-1, assigned using "designer" microarrays of oligosaccharide probes (neoglycolipids) generated from glucan polysaccharides. *The Journal of biological chemistry* **281**, 5771-5779, doi:10.1074/jbc.M511461200 (2006).
- 198 de Koning, H. D. *et al.* A comprehensive analysis of pattern recognition receptors in normal and inflamed human epidermis: upregulation of dectin-1 in psoriasis. *J Invest Dermatol* **130**, 2611-2620, doi:10.1038/jid.2010.196 (2010).

- 199 Barousse, M. M., Espinosa, T., Dunlap, K. & Fidel, P. L., Jr. Vaginal epithelial cell anti-Candida albicans activity is associated with protection against symptomatic vaginal candidiasis. *Infect Immun* **73**, 7765-7767, doi:10.1128/IAI.73.11.7765-7767.2005 (2005).
- 200 Shah, V. B. *et al.* β -Glucan Activates Microglia without Inducing Cytokine Production in Dectin-1-Dependent Manner. *The Journal of Immunology* **180**, 2777-2785 (2008).
- 201 Moll, R., Franke, W. W., Volc-Platzer, B. & Krepler, R. Different keratin polypeptides in epidermis and other epithelia of human skin: a specific cytokeratin of molecular weight 46,000 in epithelia of the pilosebaceous tract and basal cell epitheliomas. *The Journal of cell biology* **95**, 285-295 (1982).
- 202 Moll, R., Franke, W. W., Schiller, D. L., Geiger, B. & Krepler, R. The catalog of human cytokeratins: Patterns of expression in normal epithelia, tumors and cultured cells. *Cell* **31**, 11-24, doi:[http://dx.doi.org/10.1016/0092-8674\(82\)90400-7](http://dx.doi.org/10.1016/0092-8674(82)90400-7) (1982).
- 203 Bártek, J. *et al.* A series of 14 new monoclonal antibodies to keratins: Characterization and value in diagnostic histopathology. *The Journal of Pathology* **164**, 215-224, doi:10.1002/path.1711640306 (1991).
- 204 Steele, C., Ozenci, H., Luo, W., Scott, M. & Fidel, P. L., Jr. Growth inhibition of Candida albicans by vaginal cells from naive mice. *Medical mycology : official publication of the International Society for Human and Animal Mycology* **37**, 251-259 (1999).
- 205 Steele, C., Leigh, J., Swoboda, R., Ozenci, H. & Fidel, P. L. Potential Role for a Carbohydrate Moiety in Anti-Candida Activity of Human Oral Epithelial Cells. *Infection and Immunity* **69**, 7091-7099, doi:10.1128/iai.69.11.7091-7099.2001 (2001).
- 206 Corrales, I., Weersink, A. J., Verhoef, J. & van Kessel, K. P. Serum-independent binding of lipopolysaccharide to human monocytes is trypsin sensitive and does not involve CD14. *Immunology* **80**, 84-89 (1993).
- 207 Franke, W. W. *et al.* Diversity of cytokeratins. Differentiation specific expression of cytokeratin polypeptides in epithelial cells and tissues. *Journal of molecular biology* **153**, 933-959 (1981).
- 208 Brown, J. *et al.* Structure of the fungal beta-glucan-binding immune receptor dectin-1: implications for function. *Protein science : a publication of the Protein Society* **16**, 1042-1052, doi:10.1110/ps.072791207 (2007).
- 209 Coralli, C., Cemazar, M., Kanthou, C., Tozer, G. M. & Dachs, G. U. Limitations of the Reporter Green Fluorescent Protein under Simulated Tumor Conditions. *Cancer research* **61**, 4784-4790 (2001).
- 210 Swenson, E. S., Price, J. G., Brazelton, T. & Krause, D. S. Limitations of Green Fluorescent Protein as a Cell Lineage Marker. *STEM CELLS* **25**, 2593-2600, doi:10.1634/stemcells.2007-0241 (2007).

- 211 Yan, Q. *et al.* Nuclear factor- κ B binding motifs specify Toll-like receptor-induced gene repression through an inducible repressosome. *Proceedings of the National Academy of Sciences* **109**, 14140-14145, doi:10.1073/pnas.1119842109 (2012).
- 212 Medvedev, A. E., Sabroe, I., Hasday, J. D. & Vogel, S. N. Invited review: Tolerance to microbial TLR ligands: molecular mechanisms and relevance to disease. *Journal of endotoxin research* **12**, 133-150, doi:10.1177/09680519060120030201 (2006).
- 213 Svanborg Eden, C., Briles, D., Hagberg, L., McGhee, J. & Michalec, S. Genetic factors in host resistance to urinary tract infection. *Infection* **12**, 118-123 (1984).
- 214 Willment, J. A. *et al.* The human beta-glucan receptor is widely expressed and functionally equivalent to murine Dectin-1 on primary cells. *European journal of immunology* **35**, 1539-1547, doi:10.1002/eji.200425725 (2005).

Appendix

A.1. PUBLISHED ABSTRACTS

1. **Bacterial motility and NF- κ B activation by clinical isolates from urinary tract infections.** Lanz M., Birchall C., Ali A.S.M., Walton K., Townes C.L., Lim L.Y., Roushias S., Aldridge P., Pickard R.S., Hall J. *European Urology Supplements* 2013;12:e623

Prize for best abstract non-oncology

2. **Comparison of the motility and NF-KappaB activating properties of clinical isolates associated with urinary tract infections.** M. Lanz, P. Aldridge, C. Birchall, A. Ali, C. Townes, K. Walton, L. Y. Lim, R. S. Pickard, J. Hall. 2013, BAUS Abstracts, *British Journal of Surgery*, 100: 63–70. doi: 10.1002/bjs.9142

Prize for best non-clinical presentation

3. **Local estrogen enhances the innate immune defences of vaginal epithelium by increasing secretion of beta-Defensin-2 antimicrobial peptide.** A.S.M. Ali, T. Stanly, M. Lanz, C.L. Townes, J. Hall, R.S. Pickard. *European Urology Supplements* 2011;10(2):162

4. **Differential Expression & Induction of Defensins in the Human Urogenital Tract.** A.S. Ali, M. Lanz, C.L. Townes, W. Robson, R.S. Pickard and J. Hall. *Proceedings of Physiological Society* 2010; 19, PC149.

A.2. PRESENTATIONS

BAUS Academic Section, Nottingham, January 2012

- **An innate immune response to motile E. coli is exhibited by both bladder and vaginal cells.** B.S. M-Falero, A.S.M. Ali, M. Lanz, C.L. Townes, R.S. Pickard, J. Hall

EAU, Paris, February 2012

- **Release of the anti-microbial peptide beta-Defensin 2 protects against attack by flagellated Escherichia coli in human urothelium.** Ali, A.S.M., Lanz, M., Townes, C.L., Varley, C.L., Suarez M.-Falero, B., Robson, W.A., Southgate, J., Hall, J., Pickard, R.S.

AUA, Atlanta, May 2012

- **Motile Escherichia coli evokes an Innate Immune Response in both Bladder and Vaginal Cells.** Marcelo Lanz, Ased Ali*, Beatriz Suarez M-Falero, Claire Townes, Judith Hall, Robert Pickard.

BAUS, Glasgow, June 2012

- **Reduced innate beta-Defensin-2 response in the bladder and vaginal epithelia increases susceptibility to flagellated E. coli infection.** Ali A.S.M., Lanz M., Townes C.L., Varley C., Suarez-M. Falero B., Robson W.A., Southgate J., Brown K., Hilton P., Hall J., Pickard R.S.

BAUS Academic Section, London, January 2013

- **Comparison of the motility and NF-kappaB activating properties of Clinical Isolates associated with Urinary Tract Infections.** Lanz M., Aldridge P., Birchall C., Ali A., Townes C., Walton K., Lim L.Y., Pickard R.S., Hall J.

EAU, Mailand, March 2013

- **Bacterial Motility and NF-kappaB Activation by Clinical Isolates from Urinary Tract Infections.** Lanz M., Aldridge P., Birchall C., Ali A., Townes C., Walton K., Lim L.Y., Pickard R.S., Hall J.

BAUS, Manchester, June 2013

- **The Dectin-1 Receptor in the Urogenital Tract.** M., Ali A.S.M., Townes C.L., Pickard R.S., Hall J.

SIU, Vancouver, September 2013

- **Dectin-1 – A Novel Activator of Urogenital Innate Immunity.** Lanz M., Ali A.S.M., Townes C.L., Stanton A., Pickard R.S., Hall J.